ABSTRACT

HOBBIE, KRISTEN RENEE. Toward a Molecular Equivalent Dose: Use of the Medaka Fish Model in Comparative Risk Assessment. (Under the direction of Dr. Mac Law.)

Prompt identification of environmental carcinogens is crucial to safeguarding human health. Two-year rodent bioassays are used to determine carcinogenic-risk in humans. Risk estimates are predominantly based on linear extrapolations of high dose tumor data that may not accurately represent risk at environmentally relevant doses. Incorporation of mechanistic data to risk assessment has provided valuable insights into dose-response relationships. Small fish carcinogenicity models are cost-effective alternatives to rodent models. New tools are necessary to aid in the extrapolation of cancer data between species of divergent phylogenies. Demonstration of equivalent molecular and biochemical responses between species will facilitate species-species extrapolations, reduce default assumptions, and validate non-mammalian models in carcinogen risk assessment.

Data provided in this body of work addresses the "molecular equivalent dose" concept in carcinogen risk assessment. In chapter 2, we hypothesized that the molecular dose for rats exposed to the alkylating carcinogen, dimethylnitrosamine (DMN) would be equivalent to the molecular dose for similarly exposed medaka fish. The objective was to determine a dose extrapolation factor using molecular dosimetry data for rats and medaka exposed to the same carcinogen to facilitate future species-species comparisons. For both models, DNA adducts and mutant frequencies (MF) were measured in liver as molecular dose estimates. Adduct concentrations were determined to be similar in magnitude, whereas MFs for DMN-exposed

fish were up to 20x higher than that observed for DMN-exposed rats. Although the adduct data suggested a "one-to-one" extrapolation for DMN-exposed medaka and rats, the mutant frequency (MF) data for fish was remarkably higher than that of rats. An extrapolation coefficient derived from DNA adduct data would not have provided an accurate estimate of DMN's mutagenic potential between these two species.

DMN is used in a rodent model of alcoholic cirrhosis. In rats, morphologic changes of DMN-induced cirrhosis are associated with expression of TGF-β1. In Chapter 3, we hypothesized that DMN-induced hepatopathology in medaka progresses morphologically via similar TGF- β1-dependent mechanisms as that of rats. Our objectives were (1) to determine if DMN induces a similar extent of fibrosis ("phenotype") in medaka as in the rat cirrhosis model and (2) determine if DMN-induced hepatic fibrosis in medaka has a similar TGF-β1 dependence to that observed for rats. Histopathology suggested that DMN-induced fibrosis in medaka was associated with TGF- β1 expression. However, fibrosis in DMN-exposed medaka was significantly less than what occurs in mammalian livers. Despite this difference, medaka may prove useful for studying the underlying molecular mechanisms of DMN-induced hepatotoxicity. Correlation of tumor data with mechanistic data will provide more accurate estimates of risk and demonstration of common biochemical alterations will strengthen the use of fish in risk assessment.

Drinking water disinfection byproducts (DBPs) are an unintended consequence of chemical disinfection with chlorine. Epidemiological studies have suggested an association between cancer in humans and the consumption of DBPs. In chapter 4, we hypothesized that the DBP, dibromonitromethane (DBNM), would be mutagenic in the medaka fish model.

Our objectives were to isolate DNA adducts and determine MFs from livers of DBNM-exposed λ transgenic medaka. ^{32}P-postlabeling did not isolate DBNM adducts from medaka hepatic DNA and MFs in DBNM exposed medaka were statistically no different from that of control fish. These results are contrary to that reported for DBNM *in vitro* with the Salmonella plate-incorporation assay, which classified DBNM as mutagenic. Despite the lack of significant mutant induct in livers of DBNM exposed medaka, interaction of DBNM with sites of initial contact, such as gills and skin, could not be ruled out.

Toward a Molecular Equivalent Dose: Use of the Medaka Model in Comparative Risk Assessment

by
Kristen Renee Hobbie

A dissertation submitted to the Graduate Faculty of
North Carolina State University
in partial fulfillment of the
requirements for the Degree of
Doctor of Philosophy

Comparative Biomedical Sciences

Raleigh, North Carolina

2009

APPROVED BY:

Dr. J. Mac Law Chair of Advisory Committee	Dr. Anthony B. DeAngelo
Dr. David E. Malarkey	Dr. R. Julian Preston
Dr. Richard N. Winn	

DEDICATION

Dedicated to my parents, Karen and Roger, my sister Heather, and my nieces, Olivia “The Big O” and Phoebe “The Phoebe-meister”

BIOGRAPHY

Kristen Renee Hobbie was born in Gresham, Oregon. She spent her early childhood in Mentor, Ohio, and later moved with her family to the city of Richland, in Southwest Michigan. At twelve years of age, she was diagnosed with bone cancer (osteosarcoma). Treatment involved multiple surgeries and a year of chemotherapy. Rather than let the experience discourage her, she worked diligently through high school and undergraduate school at Michigan State University towards a career in medicine. In 1994, she was accepted into MSU's College of Veterinary Medicine. Upon completion of her veterinary medical training, she decided to pursue a specialty in anatomic pathology. After veterinary school, she spent a year learning aquatic animal pathology with Dr. Sal Frasca at the University of Connecticut's diagnostic laboratory, and later transferred to the anatomic training program at North Carolina State University College of Veterinary Medicine. While at NCSU, she was given the opportunity to begin graduate studies in Comparative Biomedical Sciences under the guidance of Dr. Mac Law (NCSU) and Dr. Tony DeAngelo (U.S. Environmental Protection Agency). Through this Ph.D. graduate program, she has found a meaningful way to apply her knowledge of aquatic animals and personal experience with osteosarcoma towards cancer research.

ACKNOWLEDGEMENTS

I would like to thank my advisor, Dr. Mac Law, and my advisory committee for their guidance in the creation and completion of my dissertation research. Their wealth of knowledge has significantly contributed to my education and vastly broadened my professional experiences. Thank you to Dr. Mac Law, Dr. Tony DeAngelo, Dr. Richard Winn, Dr. Leon King, and Dr. Fred Fuller for graciously allowing me the use of their laboratory facilities for my research. A special thank you to Michelle Norris, Michael George, and Steven Kilburn for their valuable technical assistance. They taught me a great deal. Lastly, I would like to extend a heartfelt thanks to my family and friends. I could not have obtained my professional goals without their continued love and support.

TABLE OF CONTENTS

LIST OF TABLES

LIST OF FIGURES

CHAPTER 1: Literature Review

1. Carcinogen Risk Assessment

Thousands of chemicals are registered for use in the United States and new substances are introduced to the U.S. commerce each year. The effects of these substances on human health are often unknown, and yet exposures occur via the manufacture, distribution, and use of these chemicals, and/or through air, water and soil pollutants. (Law, 2001). 1n 1981, Doll and Peto estimated that approximately 80% of human cancers are linked to environmental factors, such as chemical carcinogens (Doll and Peto, 1991; Law, 2001). This number has subsequently been revised; however, environmental carcinogens are still a significant source of exposure in humans (Begg CB, 2001; Clapp R, 2000; Harvard, 1996). Prompt and efficient identification of potential environmental hazards is therefore essential to safeguarding public health. Government agencies, such as the United States Environmental Protection Agency (EPA) and the National Toxicology Program (NTP), are responsible for the identification of potentially hazardous compounds, the assessment of human exposure risk, or establishment of regulatory standards for that particular chemical agent.

The National Academy of Sciences (NAS) defines risk assessment as a process by which scientific data are analyzed to describe the form, dimension, and characteristics of risk, i.e., the likelihood of harm to humans (Patton, 1993). The NAS cancer risk paradigm consists of three related components: hazard identification, dose-response assessment, and exposure assessment (Preston, 2002). Hazard identification *qualitatively* determines whether

the available scientific data describes a causal relationship between an environmental agent and cancer (Patton, 1993; Preston, 2002). Dose-response establishes a *quantitative* relationship between chemical exposure and an observable adverse response (e.g. neoplasia) in existing studies. Exposure assessment utilizes data from the study of known populations in which a dose-response relationship has *previously* been determined to identify and characterize risk in other potentially exposed populations (Patton, 1993).

Due to a general lack of epidemiological data, the link between exposure to a certain chemical and cancer in humans has been determined with chronic (2-year) rodent bioassays (Law, 2001). The chronic bioassay involves determination of the maximally tolerated dose (MTD) of an agent, after which groups of 50 male and female rats and/or mice are given 3-4 doses including the MTD and half-MTD to increase the likelihood of tumor induction (Weisburger and Williams, 1981). Regulatory agencies set their target at a dose producing 1 additional cancer in 10^6 (Meijers, 1997). Rodent tumor data usually generates a dose statistically resulting in an incidence of 10^{-1} (US EPA, 1996). Doses much higher than that encountered by humans in the environment are frequently required for tumor induction in rodents. Extrapolations across five orders of magnitude are often necessary to obtain the virtually safe dose (VSD) for an agent from rodent tumor data (Williams, 2009). The VSD is the dose that would yield an incremental response in lifetime tumor incidence over and above the spontaneous tumor incidence (Portier and Hoel, 1983). High-to-low dose extrapolations of rodent tumor data are based upon a presumed linear dose-response relationship. Comparative data concerning the metabolism, pharmacokinetics, and mechanisms of action

[for a given agent] aid in the correlation of animal data to humans (EPA, 1993). However, regulatory agencies must often rely upon the linear extrapolated dose (LED) to determine risk at low-dose (environmentally-relevant) exposures from data acquired at high, experimental doses (Williams et al., 2009; Patton, 1993; EPA, 1993).

The most commonly used dose-response model is the multistage model for quantal data (i.e. data indicating only the number of animals with cancer), which expresses upper confidence limits on cancer risk as a linear function of dose in the low dose range (EPA report, 1993). In order to protect public health, this method of risk assessment has to incorporate a high degree of conservatism, particularly when there is a lack of scientific data of sufficient specificity and caliber, to better characterize human risk (Golden et al., 1997). It has become increasingly evident, however, that mathematical extrapolations from bioassay tumor data may not be an accurate representation of carcinogenic risk at lower doses, particularly if the dose response to a certain chemical is, in fact, not linear. In addition, two-year bioassays are costly in regards to animal use and time; evaluation of chemicals at low-doses requires more animals to be statistically significant due to the lower incidence of tumors (Williams et al., 2009).

2. Alternative Animal Models: Japanese Medaka

"In 1993, the US Congress instructed the National Institutes of Health to investigate the use of alternative animal models" (Law, 2001). This instruction called for reducing the number of animals used; replacing animals with in vitro tests, chemical reactions, and

computer models; and refining current methods to emphasize relief of pain, maximize information obtained from each animal, and utilize animals lower on the phylogenetic tree (Salem and Katz, 1998, Law, 2001). Fish models are useful as alternative animal models in chemical carcinogenicity testing. Compared with their rodent counterparts, fish species have low husbandry costs and they mature quickly, facilitating reproduction of large quantities [for a given study] (Williams et al., 2003). Fish are sensitive to a wide variety of chemical carcinogens, but have an extremely low incidence of spontaneous neoplasia (<0.5% in most studies) (Law, 1998). Williams et al. (2009) reported a spontaneous tumor incidence of 0.1% for rainbow trout versus 1% for mice. A low spontaneous tumor incidence is particularly important when designing low-dose experiments (Williams et al., 2009). Fish models also provide a means to practically assess health risks from exposure to pollutants in the aquatic environment (Bailey et al., 1996; Carlson et al., 2002; Kiparissis et al., 2003; Law, 2003). Fish species can potentially serve as 1) sentinels to detect the presence of contaminants and the extent of exposure, 2) surrogates that indicate potential human exposure and effects, and 3) predictors of long-term effects on populations or ecosystems (Wolf and Wolfe, 2005; Law, 2001; McCarthy and Shugart, 1990). Recent advances in fish transgenesis (see Winn et al., 2000) have enhanced the utility of fish as indicators of chemical exposure and as non-mammalian models in comparative carcinogenesis. The best-characterized small (aquarium) fish in carcinogenic research is the Japanese medaka (*Oryzias latipes*) (Hawkins et al., 2003; Brown-Peterson et al., 1999; Okihiro and Hinton, 1999; Boorman et al., 1997; Bunton, 1996).

Japanese medaka are a small freshwater killifish native to Japan, Taiwan, and Southeast Asia. Medaka in Japanese means "tiny fish with big eyes" and the name *Oryzias latipes* is derived from their preferred habitat, rice (*Oryza sativa*) fields. Although worthless for commerce (*i.e. too small to eat*), the medaka has emerged as an important animal model in carcinogenic, developmental, and genomic research. The advantages of medaka as a model are that they are small (2.5-3.0 cm in length), hardy, prolific, and highly resistant to disease (Wittbrodt et al., 2001). Medaka are both eurythermal and poikilothermal. They are capable of tolerating a wide range of water temperatures (0-40º C), as well as salinities, and their bodies fluctuate with changes in ambient temperature (Rotchell et al., 2008; Shima et al., 2004). Medaka embryogenesis is temperature dependent and development can be slowed or arrested if embryos are exposed to temperatures as low as 4 ºC. The life span of medaka is also sensitive to temperature; medaka maintained at 27 ºC live for ~1 year versus five years when maintained outdoors [in Japan] (Shima et al., 2004). In addition, tumorigenesis, DNA synthesis and cell division are increased in medaka when carcinogen initiation and grow-out occur at higher temperatures (25-27 ºC) (Rotchell et al., 2008; Okihiro et al., 1999). Medaka's basic metabolic machinery, with regards to Phase I and Phase II metabolism, is similar to that in mammals. Cytochrome P450 (CYP2E1)-like activity and glutathione-S-transferase (GST) activity have both been demonstrated in medaka exposed to 3-chloro-4-(dichloromethyl)-5-hydroxy-2[5H]-furanone (MX) (Geter et al., 2003). Medaka also carry homologues to many mammalian genes linked to DNA repair such as AlkB, Apex 1, Mgmt, Mre11a, Msh2, and XPA (Broussard et al., 2009). O^6-methylguanine DNA

methyltransferase (Mgmt) activity in livers of medaka exposed to the alkylating carcinogen, dimethylnitrosamine, was found to be comparable to that of mouse values for Mgmt (Nakatsuru et al., 1987).

For all the aforementioned reasons, the medaka fish has become the preeminent model for large scale carcinogenicity testing and is ideal for defining the dose-response curve for genotoxic carcinogens at lower, more environmentally relevant exposure concentrations (Law, 2003). To better define the medaka model of hepatocarcinogenesis, Okihiro and Hinton (1999) used the medaka model to assess the progression and fate of hepatic neoplasia following aqueous exposure to the genotoxic carcinogen, diethylnitrosamine (DEN). They determined that neoplastic progression followed divergent pathways depending on the length of exposure differences suggesting that dedifferentiation of initiated hepatocytes and/or multipotent hepatic stem cells may play a role in medaka hepatocarcinogenesis. In Brown-Peterson et al. (1999), DEN-exposed medaka were used to investigate the relationships of carcinogen exposure and cell proliferation in multi-stage carcinogenesis. Their study demonstrated a significant correlation between proliferating hepatocytes and DEN concentrations, confirming that low and moderate levels of DEN initiate concentration-dependent carcinogenic effects in medaka. Law et al. (1998) used medaka to describe early biochemical events of carcinogenesis, through the identification and quantification of DEN-induced DNA adducts under short-term exposure conditions. The study revealed that ethyl-DNA adducts accumulated in medaka in a sublinear fashion after aqueous DEN-exposure, suggesting saturation of DNA repair enzymes, such as O^6-alkylguanine DNA

alkyltransferase, at higher dose levels. Within this thesis, we utilized *lambda cII* medaka and Big Blue® rats exposed to the genotoxic carcinogen, dimethylnitrosamine (DMN), in a comparative carcinogenesis study using DNA adducts and mutations as molecular dosimeters in an effort to improve inter-species extrapolations in environmental carcinogen risk assessment (Hobbie et al, 2009). We demonstrated that although methyl-DNA adduct concentrations were similar between rats and medaka, *cII* mutant frequencies in DMN-exposed medaka were ~20 times higher than that of Big Blue® rats, suggesting that medaka may be more efficient at converting adducts to mutations (see Chapter 2).

3. Mechanistic Data and Molecular Dosimetry

In their revised *Guidelines for Carcinogen Risk Assessment* (2005), the EPA proposed the use of quantifiable, mechanistic data to more accurately describe the shape of the dose response curve of potential carcinogens at low, environmentally relevant exposures (Anderson et al., 2000). Original cancer guidelines (1983) had utilized a default assumption that chemical carcinogens would exhibit risks at any dose; therefore upper confidence limits on cancer risk are expressed as a linear function of dose in the low dose range (EPA, 1993). However, a growing body of mechanistic evidence suggests that the traditional approach of extrapolating from effects produced at maximally tolerated doses without consideration of the underlying biological processes can provide a misleading picture of the effects of low-dose exposures (Stone, 1995; Golden et al., 1997).

Since carcinogenesis is a multi-step process, consisting of genetic alterations leading to cellular phenotypic changes, quantification of chemically induced lesions at the molecular level could describe responses at doses below those at which tumors can be accurately assessed (Preston, 2002). The EPA has proposed the use of mechanistic data in the form of "mode of action" to describe the shape of the cancer dose-response curve at low exposure levels (Preston, 2002; Vogelstein and Kinzler, 2002). "Mode of action" describes one or more necessary steps in the pathway from a normal cell to a malignant one that, by themselves, are insufficient to complete the process (Swenberg et al., 2008). Genetic endpoints, like DNA adducts and mutations, are indicative of a response at the cell or tissue level to xenobiotic exposure (Law, 2001; La and Swenberg, 1996). *Molecular dosimetry* is the measurement of these genetic endpoints as a dose-estimate for a target tissue; this measurement is considered the molecular dose, *or biological outcome,* for a particular compound.

The molecular dose integrates all the various factors involved in chemical exposure, including absorption, distribution, metabolic activation, detoxication and DNA repair (Swenberg et al., 2008; Law, 2001; La and Swenberg, 1996). An endpoint of this dynamic process, molecular dosimetry compensates for differences in toxicokinetic factors among individuals and species, as well as any non-linearities affecting the quantitative relationships between exposure and molecular dose (Swenberg et al., 2008; La and Swenberg, 1996). Saturation of various processes involved in metabolic activation, detoxication and DNA repair can affect the shape of the dose response. A supra-linear dose response may occur

when metabolic activation is saturated, yielding a lower molecular dose per unit of exposure at high doses. Sub-linear dose responses may occur with saturation of detoxication and/or DNA repair processes, yielding a higher molecular dose per unit of exposure. Changes in these processes also have important implications for mutagenesis and carcinogenesis (Swenberg et al., 2008; La and Swenberg, 1996).

Molecular dosimetry provides a method for integrating individual biological responses to chemical exposure from exposure to effect (Swenberg et al., 2008; La and Swenberg, 1996). Therefore, it provides a basis for conducting high- to low-dose, route-to-route, and interspecies extrapolations. Incorporation of such data into risk assessment may reduce uncertainties and produce more accurate estimates of risk compared to current methods, by extending the observable range of data several orders of magnitude lower than can be achieved with chronic bioassays (Swenberg et al., 2008; La and Swenberg, 1996). Understanding 1) the relationship between administered dose and the amount of each type of DNA adduct present, 2) the efficiency of each DNA adduct to cause mutations, and 3) the extent of cell proliferation present under each dosing scenario would improve understanding of causal factors in carcinogenesis and provide a more accurate prediction of risk (Swenberg et al., 1991).

4. Chemical Carcinogenesis

The carcinogenesis paradigm involves a multistage process of *initation*, irreversible damage to cellular DNA leading to mutations, *promotion*, non-genetic effects such cell

proliferation leading to clonal expansion of initiated cells, and *progression*, a less well characterized stage involving further genetic alterations in a population of initiated cells that have been provided a growth advantage through promotion (Rotchell et al., 2008; Hasegawa et al., 1998). Initiation involves exposure of cells to a sufficient dose of a carcinogenic agent (initiator) to produce a latent, but heritable, alteration in a cell, permitting its subsequent proliferation and development into a neoplasm after exposure to a promoter (Maronpot, 1998). Initiation causes permanent DNA damage (mutations) and, therefore, is rapid and irreversible (Kumar et al., 2005). Initiation is additive and dose dependent; increasing the dose of an initiator increases the yield of neoplasms and shortens the latency to tumor manifestation. Initiation is dependent on the cell cycle in that an initiating event must be "fixed" through a round of cell proliferation (Maronpot, 1998). Promotion is the enhancement of neoplasm formation by agents (promoters) that do not have intrinsic carcinogenic activity by themselves. Typically, promoters allow for the clonal expansion of initiated cells by providing a selective growth advantage (Rotchell et al., 2008). Since the cellular changes resulting from the application of a promoter do not directly modify DNA, they are considered reversible (Kumar et al., 2005). Some promoters can effect neoplastic transformation of cells through modulation of gene expression (*epigenetic* mechanisms) rather than gene structure and, therefore, have carcinogenic activity (Maronpot, 1998; Rotchell et al., 2008). During promotion, cell proliferation is required for clonal expansion of initiated cells, an effect that may contribute to the development of additional mutations and malignant transformation (Kumar et al., 2005). Progression is thought to involve the

accumulation of further genetic alterations in a population of initiated cells that have been provided a growth advantage through promotion (Maronpot, 1998; Rotchell et al., 2008). During this phase, tumors develop cellular heterogeneity, which may provide the tumor with selective advantages, such as increased growth rate, increased invasiveness, and metastases (Maronpot, 1998; Rotchell et al., 2008).

On the basis of differences in carcinogenetic mechanisms, carcinogens may be classified into two broad categories, *genotoxic and epigenetic (or non-genotoxic)* (Williams, 2001; Weisburger and Williams, 1981). In general, genotoxic carcinogens are those that have the capacity to induce structural changes in cellular DNA, whereas epigenetic carcinogens *do not* (Swenberg et al., 1991). Genotoxic carcinogens presumably act via mutational changes in target cells arising from interaction of the carcinogen with DNA (Swenberg et al., 1991). Many genotoxic carcinogens are initiators. They exert their effects by interacting directly, or after conversion to an ultimate carcinogenic form, with DNA. Direct-acting carcinogens have reactive electrophilic groups in their structure that interact with DNA, whereas indirect-acting carcinogens must be bioactivated to electrophilic reactants (Kumar et al., 2005). DNA adducts are the result of covalent interaction of the electrophile with nucleophilic sites on DNA (nucleotides). If the adducted DNA is replicated prior to repair or is repaired incorrectly and the cell undergoes DNA replication, the resultant mutation is made permanent (Rotchell et al., 2008; Williams, 2001). In contrast, epigenetic carcinogens lack DNA reactivity, but may facilitate neoplastic transformation by increasing intracellular reactive oxygen species (ROS), nitric oxide (NO), and lipid peroxidation

products, which have the potential to modify DNA (Williams and Jeffrey, 2000). Epigenetic agents can also *promote* gene expression of mutated or pre-existing latent neoplastic cells via methylation, thereby inducing cancer (Rotchell et al., 2008; Weisburger and Williams, 1981). An antecedent change, such as biotransformation, is usually necessary for an epigenetic carcinogen to exert its effects in a cell (Williams, 2001; Weisburger and Williams, 1981). Many of the known carcinogens have both initiating and promoting properties and are considered "complete carcinogens." Although genotoxic carcinogens are typically thought to be initiators and epigenetic carcinogens promoters, these carcinogenic roles are not always mutually exclusive. Genotoxic carcinogens can be both initiators and promoters, depending upon factors such as dose and time, and the same can be true for epigenetic carcinogens. Thus, both genotoxic and epigenetic (non-genotoxic) agents can be complete carcinogens, although the mechanisms by which they exert their effects are not always completely understood (Hasegawa et al., 1998).

5.1 Dimethylnitrosamine (DMN)

Dimethylnitrosamine (DMN), a member of the nitrosamine family, is an example of genotoxic carcinogen with both initiating and promoting capabilities. Nitrosamines are a large group of carcinogens capable of inducing a variety of tumors in over 40 species of animals (Swenberg et al., 1991; Hasegawa et al., 1998). DMN initiates cells through alkylation of cellular DNA and promotes cellular proliferation, possibly due to the release of mitogenic stimuli from damaged cells (Souliotis et al., 2002). DMN is carcinogenic in a

variety of species, such as the rat, mouse, hamster, and fish, and is often used as a model compound for carcinogenesis studies in these animal species. It is capable of inducing benign and malignant tumors in a variety of tissues, including the liver, kidney, lung, and nasal mucosa. DMN-induced liver tumors predominate and include hepatocellular neoplasms, as well as neoplasms derived from non-parenchymal cells (*biliary epithelial, endothelial, and Kupffer cells*). In addition to its carcinogenic activities, DMN is a potent hepatotoxin and causes liver fibrosis in rats and mice. Many of the biochemical, metabolic and histologic abnormalities associated with DMN-induced liver injury in rodents are similar to that seen with human alcoholic cirrhosis (Fattovich et al., 2004). For this reason, it has been suggested as an animal model for alcoholic cirrhosis and cirrhosis is a risk factor for hepatocellular carcinoma in humans.

Human exposure to DMN is widespread and occurs via the diet (nitrate- and nitrite-treated food and certain beverages), tobacco smoke, automobile exhaust, and endogenous formation in the gastrointestinal tract (Souliotis et al., 2002). Ingestion is the principal route of DMN-exposure to the general human population (Liteplo et al., 2001), although endogenous formation may also represent as a significant source of exposure (Kyrtopoulos, 1998). Epidemiological studies have shown increased risks of gastric, esophageal, laryngeal, oropharyngeal, and lung cancer in humans associated with daily exposures to DMN. Several deaths have been reported due to DMN consumption; two were due to acute exposure to DMN, and the other, chronic exposure over a 2-year period (Liteplo et al., 2001). These fatalities were associated with hepatomegaly, splenomegaly, abdominal distension, ascites,

and hepatic cirrhosis. Low levels of DMN, in the range of 0.1-1.0 ppb, have been reported in human blood and urine, and methylated adducts (mainly O^6-MeG and N^7-MeG) have been recovered from the DNA of humans exposed to tobacco smoke or nitrate-treated foods (Dobo et al., 1998; Kyrtopoulos, 1998; Liteplo et al., 2001). To account for the level of DNA adducts found in human DNA, secondary to DMN-exposure, it is suggested that the exposure level be of the order of hundreds of micrograms of DMN per day (Kyrtopoulos, 1998). A tumorigenic $dose_{05}$ (TD_{05}) of 34 μg/kg body weight per day has been derived for DMN-exposed rats based upon the benchmark dose associated with a 5% increase in hepatic biliary cystadenomas (Liteplo et al., 2001). Considering that comparative studies of the accumulation and repair of methylated adducts in humans and animals treated with methylating cytostatic drugs did not reveal significant species difference and that the metabolism of DMN is qualitatively similar for humans and rats, exposures to DMN likely pose a significant health hazard in humans (Kyrtopoulos, 1998; Liteplo et al, 2001).

5.2 DMN: Drinking Water Disinfection By-Product

The United States Environmental Protection Agency (EPA) has classified DMN as a probable human carcinogen (Choi et al., 2002; Mitch et al., 2003b). Recently, several water agencies in California have observed DMN at levels of concern within disinfected drinking water and wastewater (Mitch et al., 2003b). Evidence suggests that its formation is related to treatments with disinfectants, chlorine and chloramine, classifying them as a potential water disinfection by-product (DBP). Historically, drinking water disinfection by-products became

a concern in the 1970s when the trihalomethane disinfection by-product, chloroform, was associated with cancer in rats (Kundu et al., 2004). Since then, over 600 DBPs have been identified in disinfected drinking water and the EPA regulates them by setting maximum contaminant levels based on potential human health risk (Richardson, 2002; EPA, 1999). Chlorination or chloramination of wastewater effluent can lead to the formation of over 100 ng of DMN/L, while similar treatment of surface waters results in the formation of <10 ng/L (Choi et al., 2003; Mitch et al., 2003a; Mitch et al., 2004).

Risk assessments have identified a theoretical 10^{-6} lifetime risk level of cancer from DMN exposures as 0.7 ng/L (Choi et al., 2002). Currently, no state or federal drinking water maximum contaminant level exists for DMN, although as of 2002, the State of California has set an action level of 10 ng/L for DMN in drinking water (Mitch et al., 2003b). During drinking water disinfection, DMN can form by reaction of monochloramine with either dimethylamine or certain tertiary amines over several days. These reactions form hydrazine intermediates, such as 1,1-dimethylhydrazine for the reaction with dimethylamine, that are rapidly oxidized by chloramines or other oxidants to a number of products, of which DMN is a minor component (Mitch et al., 2002). Recently, it has also been demonstrated, that DMN can form through the reaction dimethylamine with nitrite that is catalyzed or enhanced in rate by the addition of HOCl (Choi et al., 2003). The oxidation of nitrite by HOCl results in the formation of an intermediate, such as dinitrogen tetroxide, N_2O_2, that is a very effective nitrosating agent.

5.3 DMN: Metabolism, Mutagenesis, and Cytotoxicity

On the basis of studies with laboratory animals, DMN is well absorbed, widely distributed, cleared rapidly, with metabolism involving both hepatic and extrahepatic components, and excreted in urine (Liteplo et al., 2001). DMN (CH_3CH_3N-N=O) requires metabolic activation by specific cytochromes before it can react with cellular macromolecules, such as protein and DNA (Frei et al., 2001). In rodents, DMN is metabolized quickly (3 minutes to 1 hour) in the liver the cytochrome P450 2E1 (CYP 2E1)-dependent mixed-function oxidase system via enzymatic denitrosation and/or alpha hydroxylation (Liteplo et al., 2001; Kyrtopolous, 1998; Souliotis et al, 2004). Both pathways proceed through a common intermediate radical $CH_3(CH_2\bullet)$N-N=O generated by Cyp 2E1 (Lee et al., 1996; Liteplo et al., 2001). Enzymatic denitrosation inactivates DMN, resulting in the production of formaldehyde, monomethylamine, and nitric oxide (Streeter et al., 1990). DMN metabolites formed by enzymatic denitrosation may then be eliminated from the body in the urine (Streeter et al., 1990). In alpha hydroxylation, Cyp 2E1 hydroxylates one of the methyl groups yielding the unstable intermediate, hydroxymethyl-methyl-nitrosamine ($HOCH_2CH_3$N-N=O). Hydroxymethyl-methyl-nitrosamine quickly decomposes to formaldehyde and the DNA reactive metabolite, methyldiazonium ion $[CH3\text{-}N{=}N]^+$ (Frei et al., 1999). Methyldiazonium ion then alkylates biological macromolecules such as DNA, RNA, and proteins or reacts with water to form methanol (CH_3OH) and dinitrogen gas (N_2) (Frie et al., 2001; Liteplo et al., 2001).

Methyldiazonium ion's interaction with nucleophilic sites on DNA causes a variety of DNA lesions, including N^7-methylguanine (N^7-MeG), O^6-methylguanine (O^6-MeG), N^3-methyladenine (N^3-MeA), and O^4-methylthymine (O^4-MeT), as well as, a number of minor adducts (Dobo et al., 1998). Approximately 65% of DNA adducts formed are N^7-MeG adducts, while the main secondary adduct is O^6-MeG at ~7%. While N^7-MeG does not possess significant direct premutagenic activity, O^6-MeG is strongly premutagenic and gives rise to GC→AT transitions by direct mispairing of guanine with thymine during DNA replication. Of the other DNA adducts, O^4-MeT is also strongly premutagenic giving rise AT→GC transitions through mispairing of adenine with cytosine (Dobo et al., 1998). Additional DMN-induced mutations include transversions (GC→TA, GC→CG, AT→TA, and AT→CG), frameshifts, deletions, and insertions (Shane et al., 2000). During DNA replication, DMN-modification of DNA presumably leads to mutations when DNA polymerase incorporates an incorrect dNTP opposite the methyl lesion (Spratt et al., 1997). O^6-MeG likely induces GC→AT transition mutations by altering the hydrogen-bonding region of guanine, thereby changing the 1-position of guanine from a hydrogen bond donor to a hydrogen bond acceptor (Spratt et al., 1997). Consequently, specific hydrogen bonding to cytosine is destroyed and the potential exists for a favorable hydrogen-bonding complex with thymine. With methylation of guanine's oxygen, Watson-Crick like base pairing becomes more favorable for thymine than for cytosine, yielding the GC→AT transition during DNA replication (Spratt et al., 1997).

Cellular affects due to DMN exposure are not limited to mutations, but can also include sister chromatid exchanges, chromosome aberrations, recombination, cytotoxicity, and apoptosis (Lin et al., 1999; Margison et al., 2002). Possible mechanisms for DMN-induced cytotoxicity include covalent binding, oxidative stress, glutathione (GSH) depletion, lipid peroxidation, and disruption of calcium homeostasis (Archer et al., 1994; Lin et al., 1998). Evidence suggests that O^6-MeG may also have a role in cytotoxicity and cell death induced by DMN (Margison et al., 2002). GC→AT transition mutations arise at sites of O^6-MeG formation following two cycles of DNA replication. According to Margison et al. (2002), the first round of replication results in an O^6-MeG:T (or possibly O^6-MeG:C) base pair. This base pairing is recognized by mutSα, a complex of mismatch repair proteins MSH2 and MSH6, possibly as part of BASC (BRCA1-associated genome surveillance complex), a super complex of proteins thought to recognize and repair aberrant DNA structures (Wang et al., 2000). Other components of the mismatch repair system (MMR) generate a very long gap (~1 kb) in the newly replicated strand. The mis-paired thymidine is thus excised, only to be replaced, during repair synthesis by another thymidine residue, resulting in a futile repair loop (Margison et al., 2002). During the second round of DNA replication, *it is possible* that some of the MMR single-strand intermediates are replicated and that this results in double-strand breaks, which are highly toxic and elicit cell death (Margison et al., 2002). In addition to the methyldiazonium ion and resultant methyl-DNA adducts, metabolism of DMN by liver microsomal P450 2E1 generates reactive oxygen radicals which can lead to increased levels of 8-OHdG. Lin et al. (2001) demonstrated a

positive correlation between cytotoxicity and levels of 8-OHdG induced by DMN-exposure. They suggested that methylation of DNA and oxidative damage to cellular macromolecules may work additively and/or synergistically to cause cell death and neoplastic transformation.

5.4 DNA Repair of O^6-MeG DNA Adducts

Premutagenic O^6-MeG adducts are repaired by the suicide enzyme O^6-methylguanine-DNA methyltransferase (Mgmt), a protein also referred to as O^6-alkylguanine-DNA alkyltransferase (AGT) (Aoki et al., 1993; Ishikawa et al., 2001; Nakatsuru et al., 1987). The presence of AGT proteins has been demonstrated in various organisms including bacteria, yeast, fish, rodents, monkeys, and man (Aoki et al., 1993; Ishikawa et al., 2001; Nakatsuru et al., 1987). The levels of AGT activity vary greatly among species and also between tissues, the liver having the highest enzyme activity (Aoki et al., 1993; Ishikawa et al., 2001; Nakatsuru et al., 1987). Activity is generally several times higher in humans than in rodents and maintained at appreciable levels throughout the lifetime (Aoki et al., 1993; Ishikawa et al., 2001; Nakatsuru et al., 1987). Carcinogenesis experiments with transgenic mice expressing the Mgmt (AGT) gene indicate that this enzyme plays an important role in protecting animals with low-dose exposure to environmental alkylating carcinogens (Ishikawa et al., 2001).

The current model for the mechanism of AGT is that it binds to methylated-DNA removing the methyl group from the damaged guanine residue by a bimolecular nucleophilic displacement reaction (Souliotis et al., 2004). Specifically, AGT binds to DNA via a helix-

turn-helix motif in the C-terminal domain. The second helix contains an arginine "finger" that flips out the methyl group from the O^6-position of guanine to AGT's active site cysteine residue. A histidine residue within the highly conserved active site PCHRV/I and a glutamic acid residue form a hydrogen bond network with the cysteine residue facilitating the transfer of the methyl group to the repair enzyme (Margison et al., 2002). The stoichiometric reaction results in irreversible inactivation of AGT, thus one AGT molecule is inactivated for each alkyl-lesion repaired. Once AGT is inactivated, the conformation of the DNA-binding domain is altered and the alkylated protein detaches from DNA, targeting it for degradation by ubiquitination. Thus one AGT molecule is inactivated for each methylated lesion repaired. The auto-inactivating mechanism for AGT means that with continued repair of O^6-MeG AGT reserves may be depleted, necessitating *de novo* synthesis of the active protein (Margison et al., 2002; Souliotis et al., 2004). Thus, the ability of a cell to withstand alkylating damage is directly related to the number of AGT molecules it contains and the rate of AGT *de novo* synthesis.

5.5 DMN: Carcinogenesis Models

Peto et al. (1991) examined the carcinogenetic activity of DMN during a major bioassay for the British Industrial Research Association (BIBRA) involving near lifetime exposure of rats to a wide range of DMN concentrations in the drinking water (Souliotis et al., 2002). In this experiment, 4080 inbred male and female Wistar Colworth rats were exposed to 0-16.896 ppm DMN and DEN in their drinking water starting at 6 weeks of age

and continuing throughout life (~ 3 years). The principal aim was to characterize the dose response relationship for the effects of these agents on esophageal cancer (DEN) and various types of liver cancer (DMN and DEN). Predominantly liver tumors were observed, including tumors of the liver cells (hepatocellular carcinomas), bile ducts, blood vessels, and Kupffer cells (Souliotis et al., 2002). DMN's dose-response relationship for hepatocellular neoplasms indicated that, while hepatocarcinogenic efficacy was linearly related to dose at very low doses, it increased sharply at doses above 1 ppm. Considering that the background rate of liver cancer in rats was ~8%, Peto et al. (1991) surmised that at DMN concentrations below 1 ppm [in the water] the excess risk of liver cancer was roughly proportional to the nitrosamine concentration. Therefore, under their experimental conditions, a dose of 1 ppm DMN would cause 25% of rats to develop a liver neoplasm, a dose of 0.1 ppm to cause about a 2.5% to do so, and a dose of 0.01 ppm to cause about 0.25% to do so, etc. With no threshold, the linear dose relationship would hold true at even lower doses, where direct observation was impracticable, for rats and presumably humans (Peto et al., 1991).

Souliotis et al. (1995) reported that the non-linearity of DMN's dose response curve, determined by Peto et al. (1991), had important implications for high-to-low risk extrapolation. They hypothesized that the supralinear increase in hepatocarcinogenic efficiency of DMN observed by Peto et al. was related to depletion of the DNA repair enzyme AGT and abrupt increase in the accumulation of the premutagenic adduct O^6-MeG. Souliotis et al. (1995) treated female Wistar Furth/NCr rats to DMN dissolved in drinking water for up to 28 days at concentrations overlapping those employed for the BIBRA

bioassay. O^6-MeG rapidly accumulated in DNA of liver and blood and was linearly correlated with dose, which was inconsistent with depletion of AGT at higher DMN dose-rates. Since the probability of a DNA adduct giving rise to a mutation depends not only on its concentration in a cell, but also the proliferative state of the cell, they suggested that increased proliferation of adduct-bearing liver cells at higher DMN doses may increase the probability of mutagenesis and lead to the observed non-linear dose response. In a subsequent study, Souliotis et al. (1998) treated λ*lacZ* transgenic mice with intraperitoneal injections of DMN and found a lack of proportionality between mutant induction and the administered dose or the corresponding adduct levels. The time-integrated concentration of O^6-MeG and N^7-MeG were linearly related to DMN dose, whereas the corresponding mutant frequencies demonstrated a superlinear relationship with dose. This suggested that toxicity-induced liver cell proliferation might play an important role in determining DMN mutagenesis in the liver and that extrapolation of DMN mutagenic effects to low dose levels should not be based on the assumption of dose linearity, even if dose is expressed in terms of DNA damage (Souliotis et al., 1998). In a third study, Souliotis et al. (2002) exposed rats to 0.2-2.64 ppm DMN for 180 days in their drinking water to determine if the supralinear (or sublinear) dose-dependence of DMN's hepatocarcinogenic efficacy was related to (a) the induction of DNA replication or (b) the accumulation of N7-MeG and concomitant depletion of AGT. They found that DMN doses higher than 1 ppm induced stronger increases in cell proliferation at an earlier time, compatible with these effects being causatively associated with the abrupt increase in hepatocarcinogenesis above this dose (Souliotis et al., 2002).

This suggested that alterations in hepatocyte DNA replication, in addition to the accumulation of DNA damage during the chronic DMN exposure might have influence the dose-dependence of its carcinogenic efficacy seen in the BIBRA study confirming the importance of underlying mechanisms to the shape of the dose-response curve.

In regards to fish, Khudoley (1984) studied the carcinogenic effects of DMN, DEN, and nitrosomorpholine (NM), as well as the results of varying temperature and exposure-length to these carcinogens, during a short-term (20-21 weeks) experiment in zebrafish (*Danio rerio*) and guppies (*Poecilia reticulata*). 10- to 12-month old, male and female fish were exposed for 2 or 8 weeks to the various nitrosamines, transferred to fresh water (17 °C, 22 °C or 27 °C) for the remainder of the experiment (20-21 weeks), and then held at 22 °C until sacrificed at 52 weeks. DMN doses for zebrafish were 20, 50, and 100 ppm, whereas guppies were exposed to 100 ppm DMN [only]. Within the initial 2-3 weeks of the experiment, Khudoley saw rearrangement of hepatic architecture, focal necrosis, fatty dystrophy of hepatic cells, and nodular accumulations of basophilic hepatocytes; at 5-7 weeks, focal proliferation of bile duct epithelium was noted. All nitroso- compounds induced liver tumors, of which hepatocellular carcinomas predominated. Malignant liver tumors were characterized by pleomorphic hepatocytes with marked polychromism and atypical mitoses, as well as polycentric and invasive growth. Hepatocellular adenomas consisted of basophilic hepatocytes in a trabecular or tubular arrangement. Cystocholangiomas and cholangiocarcinomas were apparent and often accompanied by cholangiofibrosis. Khudoley found that the incidence of tumors in zebrafish increased from

31% to 76% with increasing DMN doses and that the tumor latency and frequency were inversely proportional to the length of exposure. Temperature also influenced tumor latency and frequency; zebrafish kept at 17 °C had a decreased tumor incidence of 38%, whereas fish kept at 27 °C were at 88%. Similar results were noted for DMN-exposed guppies. Khudoley demonstrated that DMN induces hepatocarcinogenesis in fish with progressive stages similar to DMN-exposed rodents *and concluded* that their relatively short tumor latency period and high incidence of neoplasms made them suitable for the short-term screening of environmental pollutants potentially hazardous to human health (Khudoley, 1984).

In comparison to rodents, minimal information exists to describe the underlying mechanisms of DMN's carcinogenic response in fish, nor on the shape of the dose response curve and any dose-dependence. However, as mentioned previously, O^6-methylguanine methyltransferase activity, consistent with the repair of O^6-MeG DNA adducts, has been documented in medaka exposed to DMN (Nakatsuru et al., 1987). In addition, increases in Mgmt (AGT) levels were evident in medaka exposed to methylating agent, methylazoxymethanol (MAM), followed by a decrease and partial recovery of enzyme activity (Aoki et al., 1993); this pattern is similar to AGT depletion and *de novo* synthesis seen in rodents exposed to high doses of methylating agents, such as DMN. More recently, Winn and Norris (2005) demonstrated a 7.1-fold and 16-fold increase in mutant frequencies for λ transgenic medaka exposed to 300 and 600 ppm DMN [respectively] 15 days after a 96-hour exposure. Single base substitutions were the most frequent mutations sequenced from the livers of DMN-treated fish, of which a large percentage were GC→AT transitions. The

GC→AT transition mutations recovered from DNA of DMN-treated medaka were attributed to the mispairing of O^6-MeG with thymine, suggesting a similar mode of action for DMN in fish to that proposed for rodents (Winn and Norris, 2005).

5.6 DMN: Hepatic Cirrhosis Model

DMN-induced liver injury in rats has been reported as a good and reproducible animal model for the study of biochemical and pathophysiological alterations associated with the development of hepatic fibrosis and cirrhosis (George et al., 2004; George and Chandrakasan, 1996). This model demonstrates many of the features of human hepatic fibrosis, such as fibrillar septa formation, focal nodule formation, portal hypertension, ascites, hypoproteinemia, and associated biochemical abnormalities (George et al., 2006; He et al., 2007). The following merits have been attributed to the DMN fibrosis model: 1) fewer rats die during observation period, 2) a shorter time is required for modeling, and 3) the mechanism of DMN-induced liver fibrosis has been shown to be associated with immune function, which is similar to the mechanism of human liver fibrosis (He et al., 2007; Jezequel et al., 1989).

Many protocols exist for the induction of hepatic fibrosis in rats, but all involve multiple intraperitoneal injections (i.p.) of DMN. George et al. (2006) injected rats with DMN every 3 days over a 21-day period, with treated animals sacrificed on days 7, 14, 21 from beginning of exposure. They reported massive hepatic necrosis and collapse of the liver parenchyma with severe centrilobular congestion, central vein and sinusoidal dilatation,

and hemorrhage on day 7. Well-developed fibrosis and early cirrhosis were present on day-14, often accompanied by bridging necrosis, and neutrophil infiltration. On day-21, well-developed cirrhosis with thick collagen fibers, intense neutrophilic infiltration, lobular disarray, and regeneration of hepatocytes was evident (George et al., 2004 and 2006). DMN-induced hepatic fibrosis in rats demonstrated various biochemical abnormalities such as elevated urinary excretion of hydroxyproline, increased lipid peroxidation, decreased cholesterol levels, impaired glucose tolerance with insulin resistance, a reduction in inorganic phosphorous levels, and increased protein and nucleic acid catabolism (George et al., 2000). George et al. (2004) also demonstrated increased staining of hepatic stellate cells (HSC) with α-smooth muscle actin (SMA) and increased levels of serum and hepatic hyaluronic acid (HA), a important component of extracellular matrix, associated with DMN-induction of hepatic fibrosis in rats. They concluded that early elevations of serum HA were presumably due to release from necrotic hepatocytes, whereas later increases were attributed to increased synthesis by activated HSCs and reduced clearance by impaired sinusoidal endothelial cells (George et al., 2004). Increased deposition of collagen has been associated with expression of the cytokine, TGF-β, in hepatic fibrosis (Friedman, 2000). Nakamura et al. (2000) demonstrated that the rat DMN-fibrosis model was TGF-β dependent when injection of an adenovirus expressing a dominant-negative TGF-β type II receptor showed anti-fibrotic effects (de Gouville et al., 2005). Overall, the DMN fibrosis model has important implications for the prevention and treatment of *both* alcoholic cirrhosis and hepatocellular carcinoma (HCC) in humans, since increased risk of HCC is associated with alcoholic

cirrhosis (Fattovich et al., 2004).

6. Hepatic Fibrosis and Transforming Growth Factor (TGF)-β1

Cirrhosis results from excessive deposition of extracellular matrix component (ECM) and a reduction in hepatocyte regenerative capacity (Bissel et al., 2001; Friedman, 2000). ECM is produced by activated hepatic stellate cells (HSC) and consists mainly of type-I collagen. Hepatic stellate cells (also called Ito cells and perisinusoidal cells) are perivascular mesenchymal cells of the liver. Following liver injury, these cells undergo an activation response, which is the transition from quiescent cells to proliferative, fibrogenic, and contractile myofibroblasts. A number of stimuli activate HSC, including reactive oxygen intermediates (ROS) released from injured hepatocytes and Kupffer cells, as well as cellular fibronectin, a multifunctional adhesive protein, from injured sinusoidal endothelial cells. Injured endothelial cells also convert latent transforming growth factor-β1 (TGF- β1) to an active, fibrogenic form through the activation of plasmin, a protein that breaks down fibrin and interferes with its polymerization. TGF- β is a pleiotropic cytokine involved in a variety of biological processes including development, cell growth, differentiation, cell adhesion, migration, ECM deposition, and the immune response and has three isoforms, TGF- β1, TGF- β2, and TGF- β3. In hepatic injury, TGF- β1 is the dominant stimulus to ECM production by stellate cells. TGF- β1 mediates its effects through Smads, its cell signaling proteins. Smads 2 and 3, receptor Smads, complex with Smad 4, a common mediator, prior to their translocation to the nucleus. Smad 3 is responsible for mediating the pro-fibrotic

activity of TGF- β1 (Flanders, 2004). TGF- β1 is increased in experimental (rodent) and human hepatic fibrosis. TGF- β1 also induces growth inhibition and apoptosis of hepatocytes. Inhibition of hepatocyte proliferation is presumably responsible for the loss of regenerative capacity in cirrhotic livers. Tumor suppressor activity is attributed to TGF- β1 due to its ability to inhibit hepatocyte growth and induce hepatocyte apoptosis. Mutations in TGF- β1, TGF- β1 receptors, and/or downstream genes, such as Smad, are sometimes associated with hepatocellular carcinomas (Longerich et al., 2004).

7. The Medaka Lambda *cII* Mutagenesis Assay

The advent of transgenic fish models, such as the lambda *cII* medaka, has enhanced the utilization of fish as indicators of chemical exposure and as non-mammalian models in comparative biology (Winn, 2001). The λ*cII* mutation assay is a positive-selection assay originally developed for transgenic rodents, which uses the 294 basepair *cII* gene target as a logistically simple and cost-effective alternative to the *lacI* mutation assay (Jakubczak et al., 1996; Winn, 2000). Lambda transgenic medaka carry multiple copies of the transgene λLIZ, a 45.5-kb bacteriophage vector which that harbors both *cII* and *lacI* bacterial genes as mutational targets (Kohler et al., 1991; Winn et al., 2000). Transgenic mutation assays, such as the lambda *cII* medaka, provide a means by which mutations can be detected *in vivo* at low frequencies (~1 spontaneous mutation/ 10^5-10^7 loci). The λ*cII* transgene mutation target can be efficiently recovered and screened in large numbers, providing statistically meaningful results and reduction of the number of animals required to manifest a chemically induced

effect. Because the λ*cII* transgene is integrated into the medaka genome, mutations can be examined in virtually any tissue from which DNA can be isolated, facilitating mutational comparisons between different cells, tissues, organs, and species (Winn, 2001). The small size of the λ*cII* gene (±294 bp) facilitates DNA sequence analysis (Jakubczak et al., 1996; Shane et al., 2000). Mutation analyses combined with sequencing of specific mutations (mutation spectra) can aid in disclosing possible mechanisms of mutagen action. In addition, the λ*cII* transgene is genetically neutral, thereby avoiding selective pressures on the mutant frequency in vivo and allowing the accumulation and persistence of mutations (Winn, 2001).

The λ*cII* mutation assay is based on the role that the *cII* protein plays in the commitment of the λ bacteriophage to the lysogenic cycle of the *E. coli* G1250 host strain. The *cII* protein encodes the λ*cI* repressor and λ integrase genes, which are required for lysogeny to occur. The hfl protease gene negatively regulates the level of cII protein present in E. coli. The *E. coli* G1250 host strain carries mutant *hfl*$^-$ genes that increase the stability of the *cII* protein thereby facilitating a lysogenic response. If the level of λ*cII* in *hfl*$^-$ bacteria is high following infection, lysogeny occurs and plaques are not seen on the indicator lawn. If low levels of *cII* protein are present, due to a mutation in λ*cII* gene or altered expression of λ*cI*, lysis occurs and plaques develop (Shane et al., 2000). In addition, λ bacteriophage carries a *cI857* temperature sensitive mutation making the *cI* protein labile at temperatures above 32 ºC. Selection for *cII* mutants is carried out by adsorbing packaged phage to hfl$^-$ G1250 E. coli, plating the bacteria, and monitoring plaque formation after 40 hour incubation at 24 ºC ± 0.5 ºC (Lambert et al., 2005). An estimate of the total amount of packaged phage

particles is determined by incubating the plated samples at 37 ºC, overnight. The mutation frequency (MF) is quantified by dividing the total number of mutant plaques by the estimated amount of total packaged phage for a particular animal. Mutations that are detectable in the *cII* system consist primarily of base-pair substitutions, a few frameshifts, and small insertions and deletions; the assay has limited ability to detect large genetic rearrangements. Due to its small size, however, large deletions cannot be detected in the *cII* gene.

Winn et al. (2000) developed the λ transgenic medaka to "address the dual needs for improved methods to assess potential health risks associated with chemical exposure in aquatic environments and for new models for *in vivo* mutagenesis studies." They demonstrated that the fundamental features of mutation analyses based on λ transgenic rodents were shared by the λ-based transgenic fish mutation assay (Winn et al., 2000). In addition, recovery of λ bacteriophage vector from small amounts of fish genomic DNA, >300,000 plaque forming units (pfu)/ packaging reaction (~60,000-70,000 pfu/μg DNA), greatly exceeded the minimum 100,000 pfu/packaging reaction (10,000-20,000 pfu/ μg DNA) recommended in transgenic rodent assays to obtain adequate statistical power (Piergorsch et al., 1995; Winn et al, 1999). Spontaneous mutant frequencies recovered from the *cII* locus of fish for liver (4.3×10^{-5}), whole fish (2.9×10^{-5}) and testes (1.8×10^{-5}) were similar in range to those of λ transgenic rodents. Treatment of λ*cII* transgenic medaka with direct-acting mutagen, ethylnitrosurea (ENU), resulted in concentration-dependent, tissue-specific, and time-dependent mutation inductions consistent with the mechanism of action for this mutagen (Winn, 2001; Winn et al., 2000). Five days post-ENU exposure, mutants

recovered from the livers of fish increased insignificantly, but at 15, 20, and 30 days post-exposure, mutants increased 3.5-, 5.7-, and 6.7-fold [respectively] above background, illustrating the importance of the mutation manifestation time. The time required for mutations to manifest (*become fixed as mutations through DNA replication*) is affected by multiple variables, including tissue/cell type, mutagen, and mutagen treatment regimen, all of which need to be considered in the design and interpretation of mutation studies (Maronpot, 1998; Winn, 2000). The previously discussed study involving exposure of λ*cII* fish to DMN (Winn and Norris, 2005) exemplifies the need to consider factors, such as cell proliferation, into experimental design; cell proliferation is required for DMN-produced methyl adducts to become fixed as mutations (Mirsalis et al., 1993). Adaptation of a mutagenesis system originally developed for rodents to fish, has increased the utility of the fish model for comparative mutagenesis studies, as well as, provide a means to satisfy the US Congresses mandate to reduce, refine, and replace selected mammals in toxicity testing (Winn, 2001).

8. Medaka Hepatic Morphology

Unlike the multi-lobulated mammalian liver, the medaka liver consists of a single lobe. Despite this structural difference, though, the basic cellular constituents are *essentially* the same. According to Lester et al. (1993), the morphology of the fish liver includes at least ten resident cell types. Hepatocytes are the predominant cell type (~95% of the resident cell number) and occupy 80-85% of the liver volume (Hampton et al., 1989; Hinton et al., 2008). Other epithelial cell types include bile preductular epithelial cells (BPDECs), biliary

epithelial cells of ductules, and biliary epithelial cells of intrahepatic ducts (located near the liver hilus), which together comprise the intrahepatic biliary system (Hinton et al., 2008). The remaining cells are mesodermal in origin and include hepatic stellate cells (HSCs), endothelial cells, blood vessel myocytes, macrophages, and fibroblasts (Hinton et al., 2008).

Like mammals, hepatocytes of fish are responsible for the uptake of xenobiotics and potentially toxic byproducts of metabolism and form water-soluble conjugates that are transported across the plasma membrane into the canaliculi (Hinton et al., 2008). The plasma membranes of hepatocytes form canaliculi, the initial portion of the intrahepatic biliary system. Tight junctions delimit the canalicular lumen, permitting the paracellular exchange of solutes (ion and salts) between blood plasma and canalicular lumens (Arias et al., 1988; Hinton et al., 2008). Bile canaliculi and bile ductules comprise the intrahepatic bile passageways (IHBPs) of fish (Hinton et al., 2008). Bile preductules are transitional passageways formed by junctional complexes between hepatocytes and biliary epithelial cells. Bile preductular epithelial cells (BPDECs) are small, oval cells that form junctional complexes with both hepatocytes and adjacent bile ductular epithelial cells (Hinton et al., 2008). BPDECs share many of the histological and ultrastructural features of mammalian progenitor cells (oval cells). Research suggests that they are the teleost equivalent of the mammalian bipolar hepatic stem cell (Okihiro and Hinton, 2000). Teleost sinusoidal endothelial cells are also fenestrated to facilitate the passage of macromolecules from the sinusoidal lumen to the perisinusoidal space of Disse (Hinton et al., 2008). Perisinusoidal fat-storing cells, consistent with mammalian hepatic stellate cells (HSCs), are present in fish

(Hinton et al., 1984). Numerous desmosomal junctions between HSCs and hepatocytes suggest a mechanical, or supporting, role for these cells (Hinton et al., 2008). Fibroblast-like variants of HSCs that are devoid of lipid droplets have been described in fish (Fujita et al., 1980; Takahashi et al., 1978; Hinton et al., 2008). Kupffer cells (the resident macrophages of mammalian livers) are generally absent in teleost livers (Hinton et al., 2008).

The prevailing 3-dimensional (3-D) model for the medaka liver is a tubular arrangement of hepatocytes, reminiscent of embryonic mammalian liver (Hardman et al., 2007). The tubular concept consists of two rows of hepatocytes (in longitudinal section), the adjacent apical membranes of which form a tubule lumen (bile passageway) into which bile is secreted and the basilar surfaces of hepatocytes that face the sinusoidal *or intertubular space*. Recently, three-dimensional reconstruction of the medaka liver has revealed that the medaka liver is an architectural analogue of the intra-lobular mammalian parenchyma (Hardman et al., 2007). Hardman et al. (2007) suggests that medaka liver and mammalian liver share a common functional/structural unit comprised of (1) a portal tract hilus, a single conduit containing two afferent blood supplies (hepatic portal and arterial vessels) and efferent bile duct(s), (2) a primary efferent vascular conduit, central vein or hepatic vein, and (3) an anastomosing hepatic muralium, perfused via a canalicular network and sinusoidal bed, that bridges the two regions (Hardman et al., 2007).

The mammalian liver can be organized into multiple functional units, *or lobules*. The classic lobule is a hexagonal arrangement of hepatic cords (single cell muralia) connecting the central vein (in the middle) to portal tracts at the lobule periphery. Portal tracts are

variably delineated by perilobular connective tissue containing bile duct(s), portal venule, and hepatic arteriole. Afferent arterial and venous blood enters the lobule at portal tracts and flow towards central veins, whereas bile flows from central veins to efferent bile ducts in the portal areas. Hepatocytes adjacent to portal tracts receive more oxygenated blood than those at the central veins creating functional zones important to the interpretation of toxic insults to the liver (Rotchell et al., 2008). Hardman et al. (2007) suggests that liver hilus of medaka correlates to the portal tract of the mammalian liver and medaka's hepatic vein to the mammalian central vein. With 3-D reconstruction, Hardman et al. (2007) demonstrated that medaka's parenchymal architecture consists of a two-cell thick muralium, which is organized through a polyhedral (hexagonal) structural motif, revealed in the biliary architecture. The intrahepatic biliary system is an interconnected network of canaliculi and bile preductules. The canaliculi-preductular network occupies the majority of the liver corpus, with equal-diameter intrahepatic biliary passageways (1-2 micron) present throughout the liver. Larger bile ductules and ducts were observed predominantly at the hilus. An "arborizing" biliary tree analogous to that of the mammalian liver was absent in the medaka liver. Numerous bile preductular epithelial cells were found throughout the medaka liver. Consideration of the medaka liver as a functional unit similar to the mammalian liver improves interspecies comparisons of hepatopathology.

9. Medaka Hepatic Pathology

The morphologic responses of the medaka to toxic insult are *generally* similar to that seen in the mammalian liver. A common morphologic response of the fish liver to toxicity is loss of hepatic glycogen or lipid (Ferguson, 1989). This can occur as a direct effect of toxicity or secondary to decreased body condition caused by inanition, stress, or concurrent disease (Wolf and Wolfe, 2005). Increased accumulations of fat and glycogen (vacuolation) can also occur secondary to toxic exposure. Hepatocytes can increase in size in response to toxicity due to accumulations of fat/lipid, organelle proliferation (hypertrophy), failure of sublethally injured hepatocytes to mitotically divide (megalocytosis), and vacuolar swelling of the endoplasmic reticulum cisternae (hydropic degeneration) (Hinton et al., 1992; Wolf and Wolfe, 2005). Hypertrophied hepatocytes are often basophilic due to glycogen loss and increased mRNA content. Anisokaryosis and multinucleation of hepatocytes may occur in the repair stages of toxicosis (Ferguson, 1989). Intrahepatic macrophage aggregates (not to be confused with granulomatous inflammation) can increase in size and/or number due to toxin exposure (Wolf and Wolfe, 2005). Granulomatous inflammation tends to be discrete and organized in fish liver. According to Boorman et al. (1997), a finding commonly seen in control and toxin-exposed fish is cystic degeneration of the liver, also referred to as "spongiosis hepatis" or "hepatic cysts." Cystic degeneration occurs as multiple, small, cyst-like structures, often with a retained meshwork of interconnected perisinusoidal cells (Boorman et al., 1997). Hyalinization of hepatocytes can occur as a degenerative change of hepatocytes and can sometimes be seen in liver neoplasms of medaka; it's characterized by

discrete or pancytoplasmic inclusions of refractile, eosinophilic material (Wolf and Wolfe, 2005). Hepatic necrosis is a common and clearly pathologic response of the fish liver to toxins (Wolf and Wolfe, 2005). Necrosis in toxin-exposed fish is typically coagulative, although single-cell necrosis can also occur. Necrotic hepatocytes typically have deeply eosinophilic cytoplasm and pyknotic nuclei (Boorman et al., 2005). Due to differences in hepatic architecture, diagnostic descriptions relating to zonal effects, such as centrilobular or periportal necrosis, do not apply to the medaka liver. Hepatic fibrosis, as a mechanism to repair damaged hepatic parenchyma, is reported to occur less often in fish, than mammals (Ferguson, 1989), although cholangiofibrosis can occur (Wolf and Wolfe, 2005). As in mammals, foci of altered hepatocytes can occur, normally, or as in response to toxin exposure (Wolf and Wolfe, 2005). Foci of altered hepatocytes are classified, in medaka, using rodent nomenclature and consist of eosinophilic, basophilic, clear cell and vacuolated varieties (Wolf and Wolfe, 2005). Foci of altered hepatocytes are considered non-neoplastic hepatocyte proliferations, although basophilic foci may be precursors of primary hepatocellular neoplasms (Hendricks et al., 1984, 1995; Hinton et al., 1988).

Benign and malignant neoplasms can occur in fish secondary to carcinogen-exposure. Carcinogens, such as DEN, an alkylating carcinogen structurally homologous to DMN, have been used extensively in medaka as potent induces of hepatic neoplasms (Okihiro and Hinton, 1999). Neoplasms can be hepatocellular or biliary in origin. Hepatocellular adenomas are usually single, small, discrete lesions with distinct borders (Boorman et al., 1997). They are comprised of a monomorphic population of cells with little or no cellular

pleomorphism and usually lack mitotic figures. Benign neoplastic hepatocytes are usually arranged in normal hepatic cord [tubular] architecture, but are appear more hypercellular and polygonal in shape (Boorman et al., 1997). Hepatocellular carcinomas are usually large, singular lesions that may replace 25% or more of the normal hepatic parenchyma (Boorman et al., 1997). Generally, carcinomas do not have distinct margins and often invade the adjacent normal liver as isolated foci of neoplastic hepatocytes. Moderate to marked pleomorphism, nuclear atypia and mitotic figures are characteristic features of malignant hepatocytes (Boorman et al., 1997). Morphology of hepatocellular carcinomas vary and subtypes include trabecular, solid, small cell, megalocytic and anaplastic (Okihiro and Hinton, 1999). Hepatocytes of trabecular carcinomas are arranged as thick, irregular cords (tubules), whereas solid hepatocellular carcinomas are characterized by complete loss of hepatic architecture and formation of diffuse sheets of neoplastic cells (Okihiro and Hinton, 1999). Small cell carcinomas are composed of monomorphic populations of small, deeply basophilic, glycogen-depleted hepatocytes with scant cytoplasm, high nucleus to cytoplasm ratio, and small hyperchromatic nuclei with prominent nucleoli. Neoplastic "small cells" can be arranged as irregular cords (tubules) or diffuse sheets (Okihiro and Hinton, 1999). Megalocytic hepatocellular carcinomas are characterized by markedly enlarged, pleomorphic hepatocytes with variable karyomegaly (Okihiro and Hinton, 1999). Hepatocytes of anaplastic carcinomas are highly pleomorphic, varying from spindle to stellate to polygonal in shape. Anisokaryosis is often marked and syncytial giant cells may be present (Okihiro and Hinton, 1999). Benign biliary epithelial neoplasms, or cholangiomas, consist of clusters

of well-differentiated bile ducts accompanied by stromal cell proliferation. Cholangiomas are distinguished from bile duct hyperplasia by compression or expansion into the adjacent parenchyma (Boorman et al., 1997). Cholangiocarcinomas consist of densely packed, atypical bile ducts that display invasive growth into the adjacent hepatic parenchyma (Boorman et al., 1997). Malignant bile ducts are typically irregularly shaped, immature, and accompanied by spindle cell stroma. Neoplastic biliary epithelial cells are pleomorphic with numerous mitotic figures. Sometimes neoplastic bile ducts are obscured by spindle cell proliferation. Mixed carcinomas consist of both malignant proliferations of hepatocytes and biliary epithelial cells (Okihiro and Hinton, 1999). Spindle cell neoplasms are large, unencapsulated, irregular tumors comprised of finely tapered spindle cells arranged into densely packed, interweaving fascicles (Okihiro and Hinton, 1999). Spindle cells are typically of unknown origin.

10. Dibromonitromethane: Water Disinfection By-Product

During the early 20th century, the advent of drinking water chlorination dramatically decreased the frequency of water borne disease outbreaks and is considered a landmark of American public health policy (DeAngelo et al., 1991). Chlorine acts as a strong oxidant to kill pathogenic organisms, such as those responsible for typhoid fever, cholera, amoebic dysentery, bacterial gastroenteritis, shigellosis, and Salmonellosis (Kundu, 2001). In addition, chlorination is used to control the taste and odor of drinking water, remove

coloration, prevent algal growth, destroy hydrogen sulfides, and remove iron and manganese (Kundu, 2001).

In the mid-1070s, potentially deleterious by-products were identified in drinking water that formed from the interaction of chlorine with naturally occurring humic acids and organic compounds in surface waters (Dunnick et al., 1993). In 1974, dichloromethane (chloroform) was the first water disinfection by-product to be identified (Bellar et al., 1974; Rook, 1974, Kundu, 2001). Two years later, chloroform was determined to be carcinogenic in rodents by the U.S. National Cancer Institute (NCI, 1976). Over the past quarter century, subsequent drinking water analyses have identified ~600 disinfection by-products (DBPs), which account for <50% of the total organic halide mass in chlorinated drinking water (Kundu et al., 2004; Richardson, 2002; Stevens et al., 1990). In addition, alternative disinfection methods, such as ozone, chlorine dioxide, and chloramine, have also been associated with the formation of DBPs (Kundu, 2001).

DBPs are present in treated water supplies of various countries in the levels of parts per trillion (nag/L) to parts per billion (μg/L) (IARC, 1991). The U.S. Environmental Protection Agency (EPA) is responsible for regulating the total concentration of DBPs in water disinfected for human consumption, by setting maximum contaminant levels. Although some classes of DBPs are well studied, there remain many DBPs with little or no toxicological data available. The US EPA prioritizes these DBPs for research based upon their occurrence in drinking water, the strength of available toxicity data, and the structural similarities to well-studied compounds (Modal et al., 2000).

Epidemiological studies have suggested that there is an association between cancer (bladder, rectal, and colon cancer) in humans and the consumption of chlorination by-products in drinking water (Doyle et al., 1997; Plewa et al., 2004; Dunnick et al., 1993; Kundu et al., 2004). Early-term miscarriage and neural tube defects have also been associated with exposure to DBPs (Waller et al., 1998; Kramer et al., 1992; Gallagher et al., 1998). The halogenated methanes (HMs) constitute a major class of DBPs whose occurrence and toxicology have been studied extensively (Kundu et al., 2004b). Chloroform is a halomethane DBP.

The halonitromethanes (HNMs) are one of the more most recently identified classes of DBPs to be recovered from chlorinated-, chloraminated-, chlorine-ozonated, and chloramine-ozonated drinking water (Plewa et al., 2004; Richardson et al., 1999). Very little information exists on the carcinogenic risk of HNM's and the US EPA has targeted this class as DBPs of increased concern. Structurally, the HNMs are similar to halomethanes, a class of DBPs that have been associated with various cancers. Like halomethanes, HNMs are halogenated (i.e. chlorine and bromine) methanes, but have a nitro-group (NO_2) attached to the central carbon atom instead of hydrogen. Halogens are good "leaving groups" and the nitrogen attached to the central carbon atom has lost one of its valence electrons, making HNMs reactive compounds. The greater electron-withdrawing character of this nitro-group relative to the hydrogen of HMs leads to a greater lability of the departing halogen and a greater reactivity of the formed HNM carbocation (Kundu et al., 2004). This greater reactivity presumably confers a greater cytotoxic and mutagenic potential for HNMs.

In vitro studies, with the *Salmonella typhimurium* (Ames) plate-incorporation mutagenicity assay, have demonstrated the halonitromethanes as a class to be mutagenic and cytotoxic and likely to induce base substitutions at –GC- sites, as well as frameshift mutations (Kundu et al., 2004). Additional studies, using Chinese hamster ovary (CHO) AS52 cells and single cell gel electrophoresis (Comet assay), have demonstrated HNMs to also be genotoxic (Plewa et al., 2004). With Ames and comet assays, brominated nitromethanes were revealed to be more mutagenic, cytotoxic, and genotoxic than their chlorinated analogues, and dibromonitromethane (DBNM) was the most reactive of all HNMs examined. Currently, there is no published data on the reactivity of halonitromethanes *in vivo*.

11. Study Significance and Specific Aim(s)

11.1 Medaka and Rat DMN Molecular Dosimetry Study:

Chronic studies in rats have demonstrated a linear dose response at low dose exposures of DMN that increased sharply at doses higher than 1 ppm (Peto et al., 1991). Therefore, DMN is an example of a probable human carcinogen with a non-linear dose response curve for tumors in rodents (Hobbie et al, 2009). Such non-linearities of the dose-response curve have important implications for high-to-low dose risk extrapolations (Souliotis et al., 1995). Mathematical extrapolations of bioassay tumor data may not be an accurate representation of carcinogenic risk at lower dose, particularly if the dose response for a certain chemical is, in fact, non-linear (Hobbie et al., 2009). Genetic endpoints, such as DNA-adducts and

mutations, are indicative of a response at the cell or tissue level (Hobbie et al., 2009). Molecular dosimetry is the measurement of these genetic endpoints as dose estimates for a target tissue (Bailey et al., 1998). Molecular dosimetry provides a method for integrating biological responses from exposure to effect. Therefore, it provides a basis for conducting high-to-low dose, route-to-route, and interspecies extrapolations. Incorporation of such data into risk assessment may reduce uncertainties and produce more accurate estimates of risk compared to current methods by extending the observable range several orders of magnitude lower than can be achieved with chronic bioassays (La and Swenberg, 1996). Small fish models, such as the Japanese medaka (*Oryzias latipes*), are potentially useful as alternative animal models in chemical toxicity and carcinogen testing (Bailey et al., 1998; Law, 2001; Hawkins et al., 2003). However, little information exists on how to extrapolate such data between rat and fish, much less fish and human (Hobbie et al., 2009).

Specific Aim #1: A molecular equivalent dose can be determined for medaka fish and F344 rats exposed to DMN using DMN-induced DNA adducts and mutations as measurements of dose in the target tissue, liver. The "molecular equivalent dose" is the nominal dose (or concentration) at which the effective dose for a target tissue is the same for two different species exposed to the same chemical. To test this hypothesis, medaka fish and F344 rats will be exposed to the alkylating carcinogen, DMN, in parallel exposures and dose-response curves derived from DMN-induced adduct and mutation data. Via quantitative and qualitative comparisons of rat and medaka dose-response curves, it will be determined

whether the DMN-induced molecular response (biological effect) in these two species is equivalent.

11.2 Medaka and Rat DMN Pathology Study:

DMN-induced hepatic fibrosis in rodents has been reported as a good and reproducible animal model for the study of biochemical and pathophysiological alterations associated with the development of cirrhosis in humans (George et al., 2004; George and Chandrakasan, 1996). This model has important implications for the prevention and treatment of hepatocellular carcinoma (HCC) in humans, since alcoholic cirrhosis is associated with increased risk of HCC (Fattovich et al., 2004). The DMN fibrosis model in rats demonstrates many of the features of human hepatic fibrosis, such as fibrillar septa formation, focal nodule formation, portal hypertension, ascites, hypoproteinemia, and associated biochemical abnormalities (George et al., 2006; He et al., 2007). Increased deposition of collagen has been associated with expression of the cytokine, TGF-β (Friedman, 2000), and the rat DMN-fibrosis model is TGF- β dependent (Nakamura et al., 2000). TGF- β1 is the dominant stimulus to ECM production by hepatic stellate cells (HSCs). TGF- β1 mediates its effects through its cell signaling proteins, Smad 2, 3 and 4. Smad 3 is primarily responsible for mediating the pro-fibrotic activity of TGF- β1 (Flanders, 2004). TGF-β has been isolated and cloned in a number of different fish species (Harms et al., 2000). In the hybrid striped bass and rainbow trout, the gene shows an open reading frame of 1146 bases coding for a 382 amino acid protein similar to that in the rat. A conserved nature for fish TGF-β has been

demonstrated by both biological and antigenic cross-reactivity with bovine TGF-β1. In addition, the Smad genes (2, 3, and 4) have been cloned in the genome of zebrafish (*Danio rerio*) (Dick et al., 2000). DMN is a potent hepatotoxin in fish. A potential exists for DMN as an alternative fibrosis model in medaka; however, the progression of DMN-induced hepatoxicity and associated biochemical mechanisms must first be determined.

Specific Aim #2: a) To determine whether DMN-induced liver injury in medaka will follow a similar progression of lesions to that observed for rats *in the DMN fibrosis model* and b) the underlying biochemical mechanisms associated with these lesions in DMN-exposed medaka will be similar to that which occurs in the rat DMN fibrosis model. To test this hypothesis, medaka and F344 rats will be exposed to DMN and followed for six-months. Possible mechanisms for DMN-induced hepatoxicity in medaka will be evaluated with histochemical and immunohistochemical staining for cellular mediators involved in the pathogenesis of the rat DMN-fibrosis model.

11.3 Lambda Transgenic Medaka Dibromonitromethane Study #3:

The advent of drinking water disinfection with chlorine substantially reduced the frequency of water borne diseases; however, reaction of chlorine with naturally occurring organic matter and humic acids in surface waters has resulted in the formation of many (~600) potentially harmful water disinfection by-products (DBPs) (Richardson, 2002). Within the last decade, epidemiological studies have suggested that there is an association between cancer (bladder, rectal, and colon cancer) in humans and the consumption of

chlorination by-products in drinking water (Doyle et al., 1997; Plewa et al., 2004; Dunnick et al., 1993; Kundu et al., 2004). The halonitromethanes (HNMs), a related class of HNMs, are the most recently identified DBP in chlorinated-, chloraminated-, chlorine-ozonated, and chloramine-ozonated drinking water (Plewa et al., 2004; Richardson et al., 1999). Very little information exists on the carcinogenic risk of HNM's and the US EPA has targeted this class as DBPs of increased concern. *In vitro* studies, with the *Salmonella typhimurium* (Ames) plate-incorporation mutagenicity assay, have demonstrated the halonitromethanes as a class to be mutagenic and cytotoxic (Kundu et al., 2004a,b) and likely to induce base substitutions at –GC-sites in DNA. Studies involving Chinese hamster ovary (CHO) AS52 cells and single cell gel electrophoresis (Comet assay) have demonstrated HNMs to be genotoxic, as well (Plewa et al., 2004). Dibromonitromethane (DBNM) has demonstrated the greatest mutagenic, cytotoxic, and genotoxic potential *in vitro*. However, DBNM's reactivity *in vivo* needs to be characterized before its potential cancer-causing role can be determined. DBNM may have a different effect *in vivo* versus *in vitro* due to metabolic bio-activation or detoxification in the liver. The *lambda* transgenic medaka model has been proven as a valuable animal model to assess health hazards associated with exposure to chemicals in aquatic environments and for alternative non-mammalian animal models in mutagenesis and carcinogenesis studies (Winn et al., 2000).

Specific Aim #3: DBNM will demonstrate equivalent mutagenicity *in vivo* as is evident *in vitro* with the Salmonella mutagenicity assay. In addition, exposure to DBNM will induce base substitution mutations at –GC- sites in DNA. To determine if DBNM is mutagenic *in*

vivo, λ transgenic medaka will be exposed to DBNM in their ambient water. Hepatic DNA with mutated λ bacteriophage will be sequenced and evaluated for base substitution mutations.

REFERENCES

Anderson ME, Meek ME, Boorman GA, Brusick DJ, Cohen SM, Dragan YP, Frederick CB, Goodman JI, Hard GC, O'Flaherty EJ, Robinson DE, 2000. Lessons learned in applying the US EPA Proposed Cancer Guidelines to Specific Compounds. Toxicological Sciences. 53, 159-172.

Aoki K, Nakatsuru Y, Sakurai J, Sato A, Masahito P, Ishikawa T, 1993. Age dependence of O6-methylguanine-DNA methyltransferase activity and its depletion after carcinogen treatment in the teleost medaka (Oryzias latipes). Mutation Research, DNA Repair 293, 225-231.

Arias IM, Jakoby WB, 1988. The Liver: Biology and Pathobiology. Section I. Introduction: Organizational Principles. Raven Press, New York.

Archer MC, Chin W, Lee VM, 1994. Possible mechanisms of N-Nitrosodimethylamine hepatotoxicity. In Leoppky RN (ed.) Nitrosamines and Related N-Nitroso Compounds. ACS Symposium Series 553, American Chemical Society, Washington DC, pp. 279-289.

Bailey GS, Dashwood R, Loveland PM, Pereira C, Hendricks JD, 1998. Molecular dosimetry in fish: quantitative target organ DNA adduction and hepatocarcinogenicity for four aflatoxins by two exposure routes in rainbow trout. Mutation Research 339, 233-244.

Begg CB, 2001. The search for cancer risk factors: when can we stop looking. American Journal of Public Health 91, 360-364.

Bissell DM, Roulot D, George J, 2001. Transforming growth factor β and the liver. Hepatology 34, 859-867.

Boorman GA, Botts S, Bunton TE, Fournie JW, Harshbarger JC, Hawkins WE, Hinton DE, Jokinen MP, Okihiro MS, Wolfe MJ, 1997. Diagnostic criteria for degenerative, inflammatory, proliferative nonneoplastic and neoplastic liver lesions in medaka (*Oryzias latipes*): consensus of a National Toxicology Program pathology-working group. Toxicol Pathol 25, 202-210.

Broussard GW, Norris MB, Schwindt AR, Fournie JW, Winn RN, Kent ML, Ennis DG, 2009. Chronic Mycobacterium marinum infection acts as a tumor promoter in Japanese medaka (*Oryzias latipes*). Comparative Biochemistry and Physiology, Part C 149, 152-160.

Brown-Peterson NJ, Krol RM, Zhu Y, Hawkins WE, 1999. *N*-Nitrosodiethylamine Initiation of Carcinogenesis in Japanese Medaka (*Oryzias latipes*): Hepatocellular Proliferation, Toxicity, and Neoplastic Lesions Resulting from Short Term, Low Level Exposure. Toxicological Sciences 50, 186-194.

Bunton TE, 1996. Experimental chemical carcinogenesis in fish. Toxicologic Pathology 24, 603-618.

Carlson EA, Li Y, Zelikoff JT, 2002. The Japanese medaka (*Oryzias latipes*) model: applicability for investigating the immunosuppressive effects of the aquatic pollutant benzo[a]pyrene (B[a]P). Mar Environ Res 10, 303-315.

Choi J, Valentine RL, 2002. Formation of *N*-nitrosodimethylamine (NDMA) from reaction of monochloramine: a new disinfection by-product. Water Research 36, 817-824.

Choi J and Valentine RL, 2003. *N*-Nitrosodimethylamine Formation by Free-Chlorine-Enhanced Nitrosation of Dimethylamine. Environmental Science and Technology 37, 4871-4878.

Clapp R, 2000. Environment and health: 4. Cancer. Canadian Medical Association Journal. 163, 1009-1012.

DeAngelo AB, Daniel FB, Stober JA Olson GR, 1991. The carcinogenicity of dichloroacetic acid in the male B6C3F1 mouse. Fundam. Appl. Toxicol 16, 337-347.

De Gouville A-C, Boullay V, Krysa G, Pilot J, Brusq J-M, Loriolle F, Gauthier J-M, Papworth SA, Laroze A, Gellibert F, Huet S, 2005. Inhibition of TGF- β signaling by an ALK 5 inhibitor protects rats from dimethylnitrosamine-induced liver fibrosis. British Journal of Pharmacology 145, 166-177.

Dick A, Mayr T, Hermann B, Meier A, Hammerschmidt M, 2000. Cloning and characterization of zebrafish *smad2*, *smad3* and *smad4*. Gene 246, 69-80.

Dobo KL, Eastmond DA, Grosovsky AJ, 1998. Sequence specific mutations induced by N-Nitrosodimethylamine at two marker loci in metabolically competent human lymphoblastoid cells. Carcinogenesis 19, 755-764.

Doll R and Peto R, 1981. The causes of cancer: quantitative estimates of avoidable risks of cancer in the United States today. J Natl Cancer Inst 66: 1191-1308.

Doyle TJ, Zheng W, Cerhan JR, Hong CP, Sellers TA, Kushi LH, Folsom AR, 1997. The association of drinking water source and chlorination by-products with cancer incidence among postmenopausal women in Iowa: a prospective cohort study. Am J Public Health 87, 1168-1176.

Dunnick JK and Melnick RL, 1993. Assessment of the Carcinogenic Potential of Chlorinated Water: Experimental Studies of Chlorine, Chloramine, and Trihalomethanes. Journal of the National Cancer Institute 85, 817-822.

Environmental Protection Agency, 1993. Motor Vehicle-Related Air Toxics Study. Research Triangle Park, N.C.: Technical Support Branch, Emission Planning and Strategies Division, Office of Mobile Sources, Office of Air and Radiation, U.S. Environmental Protection Agency.

Environmental Protection Agency, 1996. Proposed guidelines for carcinogen risk assessment. Fed Reg 61, 17960-18011.

Environmental Protection Agency, 1999. Understanding the Safe Drinking Water Act, U.S. Environmental Protection Agency.

Environmental Protection Agency, 2005. Guidelines for carcinogenic risk assessment, U.S. Environmental Protection Agency, Washington DC.

Fattovich G, Stroffolini T, Zagni I, Donato F, 2004. Hepatocellular Carcinoma in Cirrhosis: Incidence and Risk Factors. Gasteroenterology 127, S35-S50.

Ferguson HW, 1989. Systemic Pathology of Fish: A Text and Atlas of Comparative Tissue Responses in Diseases of Teleosts. Iowa State University Press, Ames, IA, pp. 263.

Flanders KC, 2004. Smad3 as a mediator of the fibrotic response. Int. J. Exp. Path 85, 47-64.

Frei E, Kuchenmeister F, Gliniorz R, Breuer A, Schmezer P, 2001. *N*-nitrosodimethylamine is activated in microsomes from hepatocytes to reactive metabolites, which damage DNA of non-parenchymal cells in rat liver. Toxicology Letters 123, 227-234.

Frei E, Gilberg F, Schröder M, Breuer A, Edler L, Wiessler M, 1999. Analysis of the inhibition of *N*-Nitrosodimethylamine activation in the liver by *N*-Nitro-dimethylamine using a new non-linear statistical method. Carcinogenesis 20, 459-464.

Friedman SL, 2000. Molecular regulation of hepatic fibrosis, an integrated cellular response to injury. The Journal of Biological Chemistry 275, 2247-2250.

Fujita H, Tamaru T, Miyagawa J, 1980. Fine structural characteristics of the hepatic sinusoidal walls of the goldfish (*Carassius auratus*). Arch Histol Jpn 43, 265-273.

Gallagher MD, Nuckols JR, Stallones L, Savitz DA, 1998. Exposure to trihalomethanes and adverse pregnancy outcomes. Epidemiology 9, 484-489.

George J, 2006. Mineral Metabolism in dimethylnitrosamine-induced hepatic fibrosis. Clinical Biochemistry 39, 984-991.

George J, Chandrakasan G, 1996. Glycoprotein metabolism in dimethylnitrosamine induced hepatic fibrosis in rats. Int J Biochem Cell Biol 28, 353-361.

George J and Chandrakasan G, 2000. Biochemical Abnormalities during the Progression of Hepatic Fibrosis Induced by Dimethylnitrosamine. Clinical Biochemistry 33, 563-570.

George J, Tsutsumi M, Takase S, 2004. Expression of hyaluronic acid in *N*-nitrosodimethylamine induced hepatic fibrosis in rats. The International Journal of Biochemistry & Cell Biology 36, 307-319.

Geter DR, Fournie JW, Brouwer MH, DeAngelo AB, Hawkins WE, 2003. *p*-Nitrophenol and glutathione response in medaka (*Oryzias latipes*) exposed to MX, a drinking water carcinogen. Comparative Biochemistry and Physiology, Part C 134, 353-364.

Golden, RJ, Holm, SE, Robinson, DE, Julkumen, PH, Reese, EA, 1997. Chloroform mode of action: implications for cancer risk assessment. Regul. Toxicol. Pharmacol 26, 142-155.

Hampton, JA, Lantz, RC, 1989. Functional units in rainbow trout (*Salmo gairdneri*) liver. III. Morphometric analysis of parenchyma, stroma, and component cell types. Am. J. Anat., 185(1), 58– 73.

Hardman RC, Volz DC, Kullman SW, Hinton DE, 2007. An in vivo look at vertebrate liver architecture: three-dimensional reconstructions from medaka (*Oryzias latipes*). The Anatomical Record 290, 770-782.

Harms CA, Kennedy-Stoskopf S, Horne WA, Fuller FJ, Tompkins WAF, 2000. Cloning and sequencing hybrid striped bass (*Morone saxatilis x M. chrysops*) transforming growth factor-β (TGF- β), and development of a reverse transcription quantitative competitive polymerase chain reaction (RT-qcPCR) assay to measure TGF- β mRNA of teleost fish. Fish & Shellfish Immunology 10, 61-85.

Harvard University (no authors listed), 1996. Harvard report on cancer prevention. Volume 1: Causes of human cancer. Cancer Causes and Control 7 (Suppl) 53-59.

Hasegawa R, Futakuchi M, Mizoguchi Y, Yamaguchi T, Shirai T, Ito N, Lijinsky W, 1998. Studies of initiation and promotion of carcinogenesis by N-nitroso compounds. Cancer Letters 123, 185-191.

Hawkins WE, Walker WW, Fournie JW, Manning CS, Krol RM, 2003. Use of the Japanese medaka (*Oryzias latipes*) and guppy (*Poecilia reticulate*) in carcinogenesis testing under National Toxicology Program protocols. Toxicol. Pathol. 31 (Suppl.), 88-91.

He J-Y, Ge W-H, Chen Y, 2007. Iron deposition and fat accumulation in dimethylnitrosamine-induced liver fibrosis in rat. World J Gastroenterol 13, 2061-2065.

Hendricks JD, Meyers TR, Shelton DW, 1984. Histological progression of hepatic neoplasia in rainbow trout (*Salmo gairdneri*) National Cancer Institute Monograph 65: 321-336.

Hendricks JD, Shelton DW, Loveland PM, Pereira CB, Bailey GS, 1995. Carcinogenicity of dietary dimethylnitrosomorpholine, N-methyl-N'-nitrosoguanidine, and dibromoethane in rainbow trout. Toxicol Pathol 23, 447-457.

Hinton DE, Baumann PC, Gardner GR, Hawkins WE, Hendricks JD, Murchelano RA and Okihiro MS, 1992. Histopathologic markers. In Biomarkers: Biochemical, Physiological and Histological Markers of Anthropogenic Stress. Lewis Publishers, Boca Raton, FL pp. 155-209.

Hinton DE, Couch JA, The SJ, Courtney LA, 1988. Cytological changes during progression of neoplasia in selected fish species. Aquatic Toxicol 11, 77-112.

Hinton D, Segner H, Au DWT, Kullman SW, Hardman RC: Liver Toxicity. In: Toxicology of Fishes, ed. Giulio RT and Hinton DE, 1st ed., 328-379. Taylor & Francis, Boca Raton, FL, 2008.

Hobbie KR, DeAngelo AB, King LC, Winn RN, Law JM, 2009. Toward a molecular equivalent dose: use of the medaka model in comparative risk assessment. Comparative Biochemistry and Physiology, Part C 149, 141-151.

IARC, 1991. Chlorinated drinking water; chlorination by-products; some other halogenated compounds; cobalt and cobalt compounds. International Agency for Research on Cancer (IARC) Working Group, Lyon, 12-19 June 1190, IARC Monogr Eval Carcinog Risks Hum 52, 1-544.

Ishikawa T, Ide F, Qin X, Zhang S, Takahashi Y, Sekiguchi M, Tanaka K, Nakatsuru Y, 2001. Importance of DNA repair in carcinogenesis: evidence for transgenic and gene targeting studies. Mutation Research 477, 41-49.

Jakubczak JL, Merlina G, French JE, Muller WJ, Paul B, Adhya S, Garges S, 1996. Analysis of genetic instability during mammary tumor progression using a novel selection-based assay for in vivo mutation in a bacteriophage I transgene target. Proc Natl Acad Sci USA 93, 9073-9078.

Jezequel AM, Mancini R, Rinaldesi ML, Ballardini G, Fallani M, Bianchi F, Orlandi F, 1989. Dimethylnitrosamine-induced cirrhosis. Evidence for an immunological mechanism. J. Hepatology 8, 42-52

Khudoley VV, 1984. Use of Small Fish Species in Carcinogenicity Testing, National Cancer Institute Monograph 65, NIH Publication No 84-2653. National Cancer Institute, Bethesda, MD.

Kohler SW Provost GS Fieck A Kretz PL Bullock WO Sorge JA Putman DL, Short JM, 1991. Spectra of spontaneous and mutagen-induced mutations in the lacI gene in transgenic mice. Proc Natl Acad Sci USA 88, 316-321.

Kramer MD, Lynch CF, Isacson P, H.J.W., 1992, The association of waterborne chloroform with intrauterine growth retardation. Epidemiology 3, 407-413.

Kisparissis Y, Metcalfe TL, Balch GC, Metcalfe CD, 2003. Effects of the antiandrogens, vinclozolin and cyproterone acetate on gonadal development in the Japanese medaka (*Oryzias latipes*). Aquat Toxicol 29, 391-403.

Kumar V, Abbas AK, Fausto N, eds., 2005. Robbins and Cotran Pathologic Basis of Disease, 7th Edition. Elsevier Saunders, Philadelphia, PA, pp. 319-323.

Kundu B, 2001. Mutagenicity in Salmonella of Nitrohalomethanes, a Recently Recognized Class of Disinfection By-Products: Comparison to Halomethanes. Masters Thesis, Department of Environmental Sciences and Engineering, School of Public Health, University of North Carolina.

Kundu B, Richardson SD, Swartz PD, Matthews PP, Richard AM, DeMarini DM, 2004. Mutagenicity in Salmonella of halonitromethanes: a recently recognized class of disinfection by-products in drinking water. Mutation Research 562, 39-65.

Kyrtopoulos SA, 1998. DNA Adducts in Humans After Exposure to Methylating Agents. Mutat. Res. 405, 135-143.

La DK and Swenberg JA, 1996. DNA adducts: biological markers of exposure and potential applications to risk assessment. Mutat. Res. 365, 129-146.

Lambert IB, Singer T, Boucher SE, Douglas GR, 2005. Draft Detailed Review Paper on Transgenic Rodent Mutation Assays. Organization for Economic Co-operation and Development Environment, Health and Safety Publications, Paris.

Law JM, 2001. Mechanistic considerations in small fish carcinogenicity testing. ILAR Journal 42, 274-284.

Law JM, Bull M, Nakamura J, Swenberg JA, 1998. Molecular dosimetry of DNA adducts in the medaka small fish model. Carcinogenesis 19, 515-518.

Law JM, 2003. Issues related to the use of fish models in Toxicologic pathology: session introduction. Toxicol. Pathol. 31 (suppl.), 49-52.

Lee VM, Keefer LK, Archer MC, 1996. An Evaluation of the Roles of Metabolic Denitrosation and α-hydroxylation in the hepatotoxicity of N-Nitrosodimethylamine. Chem Res Toxicol. 9, 1319-1324.

Lester SM, Braunbeck TA, 1993. Hepatic cellular distribution of cytochrome P-450 IA1 in rainbow trout (Oncorhynchus mykiss), an immunohisto and cytochemical study. Cancer Res., 53(16), 3700– 3706.

Lin H-L and Hollenberg PF, 2001. N-Nitrosodimethylamine-Mediated Formation of Oxidized and Methylated DNA Bases in a Cytochrome P450- 2E1 Expressing Cell Line. Chem Res. Toxicol. 14, 562-566.

Lin H-L, Parsels LA, Maybaum J, Hollenberg PF, 1999. N-Nitrosodimethylamine-mediated cytotoxicity in a cell line expressing P450 2E1: Evidence for Apoptotic Cell death. Toxicology and Applied Pharmacology 157, 117-124.

Lin H-L, Roberts ES, Hollenberg PF, 1998. Heterologous expression of rat P450 2E1 in a mammalian cell line: in situ metabolism and cytotoxicity of N-Nitrosodimethylamine

Liteplo RG, Meek ME, 2001. *N*-nitrosodimethylamine: hazard characterization and exposure-response analysis. Environ. Carcino. And Ecotox. Revs. 19, 281-304.

Longerich T, Breuhahn K, Odenthal M, Petmecky K, Shirmacher P, 2004. Factors of transforming growth factor β signaling are co-regulated in human hepatocellular carcinona. Virchows Arch 445, 589-596.

Margison GP, Santibáñez-Koref MF, Povey AC, 2002b. Mechanisms of carcinogenicity/chemotherapy by O6-methylguanine. Mutagenesis 17, 483-487.

Margison GP, Santibáñez-Koref MF, 2002a. O6-alkylguanine-DNA alkyltransferase: role in carcinogenesis and chemotherapy. BioEssays 24, 255-266.

Maronpot RR: Chemical carcinogenesis. In: Fundamentals of Toxicologic Pathology Eds. Haschek W.M. and Rousseaux C.G., pp. 127-130. Academic Press, San Diego, CA, 1998.

McCarthy JF and Shugart LR, 1990. Biomarkers of Environmental Contamination. Boca Raton: Lewis Publshers.

Meijers JMM, Swaen GMH, Bloemen LJN, 1997. The predictive value of animal data in human risk assessment. Regul Toxicol Pharmacol 25, 94-102.

Mirsalis JC, Provost GS, Matthews CD, Hamner RT, Schindler JE, O'Loughlin KG, MacGregor JT, Short JM, 1993. Induction of hepatic mutations in lacI transgenic mice. Mutagenesis 8, 265-271.

Mitch WA, Gerecke AC, Sedlak DL, 2003. A N-Nitrosodimethylamine (NDMA) precursor analysis for chorination of water and waste water. Water Research 37, 3733-3741.

Mitch WA, Sharp JO, Trussell RR, Valentine RL, Alvarez-Cohen L, Sedlak DL, 2003. N-Nitrosodimethylamine (NDMA) as a Drinking Water Contaminant: A Review. Environmental Engineering Science 20, 389-404

Mitch WA and Sedlak DL, 2004. Characterization and Fate of N-Nitrosodimethylamine Precursors in Municipal Wastewater Treatment Plants. Environ Sci TEchnol 38, 1445-1454.

Mitch WA and Sedlak DL, 2002. Formation of N-Nitrosodimethylamine (NDMA) from Dimethylamine during Chlorination. Environ. Sci. Technol. 36, 588-595.

Moudgal CJ, Lipscomb JC, Bruce RM, 2000. Potential Health Effects of Drinking Water Disinfection By-Products Using Quantitative Structure Toxicity Relationship. Toxicology 147, 109-131.

Nakamura T, Sakata R, Ueno T, Sata M, Ueno H, 2000. Inhibition of transforming growth factor beta prevents progression of liver fibrosis and enhances hepatocyte regeneration in dimethylnitrosamine-treated rats. Hepatology 32, 247-255.

Nakatsuru, Y, Nemoto, N, Nakagawa, K, Masahito, P, Ishikawa, T, 1987. O^6-methylguanine DNA methyltransferase activity in liver from various fish species. Carcinogenesis 8, 1123-1127.

National Cancer Institute (NCI), 1976. Carcinogenesis Bioassay of Chloroform. NCI, Bethseda, MD [National Tech Inform Service No. PB264018/AS].

Okihiro MS, Hinton DE, 1999. Progression of hepatic neoplasia in medaka (*Oryzias latipes*) exposed to diethylnitrosamine. Carcinogenesis 20, 933-940.

Okihiro MS, Hinton DE, 2000. Partial hepatectomy and bile duct ligation in rainbow trout (*Oncorhynchus mykiss*): Histologic, immunohistochemical and enzyme histochemical characterization of hepatic regeneration and biliary hyperplasia. Toxicologic Pathology 28, 342-356.

Patton DE, 1993. The ABCs of Risk Assessment: Some Basic Principles Can Help People Understand Why Controversies Occur. EPA Journal 19, 10-15

Peto R, Gray R, Brantom P, Grasso P, 1991. Effects on 4080 rats of chronic ingestion of *N*-nitrosodiethylamine or *N*-nitrosodimethylamine: a detailed dose-response study. Cancer Res. 51, 6415-6451.

Peto R, Gray R, Brantom P, Grasso P, 1991. Dose and time relationships for tumor induction in the liver and esophagus of 4080 inbred rats by chronic ingestion of *N*-nitrosodiethylamine or *N*-nitrosodimethylamine. Cancer Res. 51, 6452-6459.

Piergorsch WW, Margolin BH, Shelby NM, Johnson A, French JE, Tennant RW, Tindall KR, 1995. Study design and sample sizes for lacI transgenic mouse mutation assay Environ Mol Mutagen 25, 231-245.

Plewa MJ, Wagner ED, Jazwierska P, 2004. Halonitromethane Drinking Water Disinfection Byproducts: Chemical Characterization and Mammalian Cell Cytotoxicity and Genotoxicity. Environ. Sci. Technol. 38, 62-68.

Portier C and Hoel D, 1983. Low-dose-rate extrapolations using the multistage model. Biometrics 39, 987-906.

Preston RJ, 2002. Quantitation of molecular endpoints for the dose-response component of cancer risk assessment. Toxicol. Pathol. 30, 112-116.

Richardson SD, Simmons JE, Rice G, 2002. Disinfection Byproducts: The next generation. Environmental Science and Technology 36, 198A-205A.

Richardson SD, Thruston AD, Caughran TV, Chen PH, Collette TW, Floyd TL, Schenck KM, Lykins BW, Sun G-R, Majetich G, 1999. Identification of New Drinking Water Disinfection Byproducts Formed in the Presence of Bromide. Environmental Science and Technology. 33, 3378-3383.

Rook J, 1974. Formation of haloforms during chlorination of natural waters. Water Treatment Exam. 23, 234-243.

Rotchell JM, Miller MR, Hinton DE, DiGuilio RT, Ostrander GK. Chemical Carcinogenesis. In: Toxicology of Fishes. ed. Giulio RT and Hinton DE, 1st ed., 532–579. Taylor & Francis, Boca Raton, FL, 2008.

Salem H and Katz S, eds., 1998. Advances in Animal Alternatives for Safety and Efficacy Testing. Washington DC: Taylor & Francis.

Shane BS, Smith-Dunn DL, de Boer JG, Glickman BW, Cunningham ML, 2000. Mutant frequencies and mutation spectra of Dimethylnitrosamine (DMN) at the *lacI* and *cII* loci in the livers of Big Blue® transgenic mice. Mutat. Res. 542, 197-210.

Shima A and Mitani H, 2004. Medaka as a research organism: past, present, and future. Mechanisms of Development. 121, 599-604.

Souliotis VL, Henneman JR, Reed CD, Chhabra S, Diwan BA, Anderson LM, Kyrtopoulos SA, 2002. DNA adducts and liver DNA replication in rats during chronic exposure to N-nitrosodimethylamine (NDMA) and their relationships to the dose-dependence of NDMA hepatocarcinogenesis. Mutat. Res. 500, 75-87.

Souliotis VL, Sfikakis PP, Anderson LM, Kyrtopoulos SA, 2004. Intra- and intercellular variations in the repair efficiency of O^6-methylguanine, and their contribution to kinetic complexity. Mutat. Res. 568, 155-170.

Souliotis VL, Chhabra S, Anderson LM, Kyrtopoulos SA, 1995. Dosimetry of O^6-methylguanine in rat DNA after low-dose, chronic exposure to N-nitrosodimethylamine (NDMA). Implications for the mechanism of NDMA hepatocarcinogenesis. Carcinogenesis 16, 2381-2387.

Souliotis VL, van Delft JHM, Steenwinkel MST, Baan RA, Kyrtopoulos SA, 1998. DNA adducts, mutant frequencies and mutation spectra in λlacZ transgenic mice treated with *N*-nitrosodimethylamine. Carcinogenesis 19, 731-739.

Spratt TE and Levy DE, 1997. Structure of the hydrogen bonding complex of O^6-methylguanine with cytosine and thymine during DNA replication. Nucleic Acids Research 25, 3354-3361.

Stevens AA, Moore LA, Slocum CJ, Smith BL, Seeger DR, Ireland JC, 1990. Byproducts of Chlorination at Ten Operating Utilities. In Water Chlorination: Chemistry, Environmental Impact, and Health Effects; Jolley RL, Condie LW, Johnson JD, Katz S, Minear RA, Mattice JS, Jacobs VA, Eds.; Lewis Publishers: Chelsea , MI, 6, p 579.

Stone R, 1995. News & Comment: A Molecular Approach to Cancer Risk. Science 268, 356-357.

Streeter AJ, Nims RW, Sheffels PR, Heur Y-H, Yang CS, Mico BA, Gombar CT, Keefer LK, 1990. Metabolic denitrosation of N-Nitrosodimethylamine in vivo in the Rat. Cancer Research 50, 1144-1150.

Swenberg JA, Fryer-Tita E, Jeong Y-C, Boysen G, Starr T, Walker BE, Albertini RJ, 2008. Biomarkers in toxicology and risk assessment: informing critical dose-response relationships. Chem Res Toxicol 21, 253-265.

Swenberg JA, Hoel DG, Magee PN, 1991. Mechanistic and Statistical Insight into the large Carcinogenesis Bioassays on N-Nitrosodiethylamine and N-Nitrosodimethylamine. Cancer Research 51, 6409-6414.

Takahashi Y, Tsubouchi H, Kobayashi K, 1978. Effects of vitamin A administration upon Ito's fat-storing cells of the liver in the carp. Arch Histol Jpn. 41, 339-349.

Vogelstein B and Kinzler KW (editors), 2002. The genetic basis of human cancer, 2nd edition. New York: McGraw-Hill.

Waller K, Swan SH, DeLorenze G, Hopkins B, 1998. Trihalomethanes in drinking water and spontaneous abortion. Epidemiology 9, 134-140.

Wang Y, Cortez D, Yazdi P, Neff N, Elledge SJ, Qin J, 2009. BASC, a super complex of BRCA1-associated proteins involved in the recognition and repair of aberrant DNA structures. Genes & Development 14, 927-939.

Weisburger JH and Williams, GM, 1981. Carcinogen Testing: Current Problems and New Approaches. Science 214, 401-407.

Williams G, 2001. Mechanisms of chemical carcinogenesis and application to human cancer risk assessment. Toxicology 166, 3-10.

Williams DE, Bailey GS, Reddy A, Hendricks JD, Oganesian A, Orner GA, Pereira CB, Swenberg JA, 2003. The rainbow trout (*Oncorhynchus mykiss*) tumor model: recent applications in low-dose exposures to tumor initiators and promoters. Toxicologic Pathology 31 (Suppl), 58-61.

Williams DE, Orner G, Willard KD, Tilton S, Hendricks JD, Pereira C, Benninghoff AD, Bailey GS, 2009. Rainbow trout (Oncorhynchus mykiss) and ultra-low dose cancer studies. Comparative Biochemistry and Physiology, Part C 149, 175-181.

Winn, RN, 2001. Transgenic fish as models in environmental toxicology. ILAR Journal 42, 322-329.

Winn, RN, Norris, MB: Analysis of mutations in λ transgenic medaka using the cII mutation assay. In:Techniques in Aquatic Toxicology (Volume 2) Ed. Ostrander GK, pp. 705-732. Boca Raton, FL: Taylor and Francis, 2005.

Winn RN, Norris MB, Brayer KJ, Torres C, Muller SL, 2000. Detection of mutations in transgenic fish carrying a bacteriophage λcII transgene target. Proc. Natl. Acad. Sci. USA 97, 12655-12660.

Wittbrodt J, Shima A, Schart M, 2001. Medaka-A Model Organism From the Far East. Nature Reviews, Genetics 3, 53-64.

Wolf JC and Wolfe MJ, 2005. A brief overview of nonneoplastic hepatic toxicity in fish. Toxicologic Pathology 33: 75-85.

CHAPTER 2:

Toward a molecular equivalent dose: use of the medaka model in comparative risk assessment[◊]

Kristen R. Hobbie[a,b], Anthony B. DeAngelo[c], Leon C. King[c], Richard N. Winn[d], J. McHugh Law[a,*]

[a]Comparative Biomedical Sciences Program and Center for Comparative Medicine and Translational Research, College of Veterinary Medicine, North Carolina State University, Raleigh, NC, USA

[b]Integrated Laboratory Systems, Inc., Research Triangle Park, NC, USA

[c]US Environmental Protection Agency, National Health & Environmental Effects Research Laboratory, Research Triangle Park, NC, USA

[d]Aquatic Biotechnology and Environmental Laboratory, Warnell School of Forestry and Natural Resources, University of Georgia, Athens, GA, USA

Published in:

Comparative Biochemistry and Physiology, Part C 149: 141-151, 2009

Abstract

Recent changes in the risk assessment landscape underscore the need to be able to compare the results of toxicity and dose-response testing between a growing list of animal models and, quite possibly, an array of *in vitro* screening assays. How do we compare test results for a given compound between vastly different species? For example, what dose level in the ambient water of a small fish model would be equivalent to 10 ppm of a given compound in the rat's drinking water? Where do we begin? To initially address these questions, and in order to compare dose-response tests in a standard rodent model with a fish model, we used the concept of *molecular dose*. Assays that quantify types of DNA damage that are directly relevant to carcinogenesis integrate the factors such as chemical exposure, uptake, distribution, metabolism, etc. that tend to vary so widely between different phyletic levels. We performed parallel exposures in F344 rats and Japanese medaka (*Oryzias latipes*) to the alkylating hepatocarcinogen, dimethylnitrosamine (DMN). In both models, we measured the DNA adducts 8-hydroxyguanine, N^7-methylguanine and O^6-methylguanine in the liver; mutation frequency using λ *cII* transgenic medaka and Big Blue® rats; and early morphological changes in the livers of both models using histopathology and immunohistochemistry. Pulse dose levels in fish were 0, 10, 25, 50, or 100 ppm DMN in the ambient water for 14 days. Since rats are reported to be especially sensitive to DMN, they received 0, 0.1, 1, 5, 10, or 25 ppm DMN in the drinking water for the same time period. While liver DNA adduct concentrations were similar in magnitude, mutant frequencies in the

DMN-exposed medaka were up to 20 times higher than in the Big Blue rats. Future work with other compounds will generate a more complete picture of comparative dose response between different phyletic levels and will help guide risk assessors using “alternative” models.

1. Introduction

The ways we test chemicals for safety are about to change. Alternative animal models including high throughput fish embryo assays have given us some powerful new tools for risk assessment yet at the same time have underscored the need for ways to compare the results. Under traditional safety testing paradigms, we have been groping in the dark, having essentially little to no clue how to compare dose-response data between various rodent strains, let alone between species as different as fish and man. How do we compare test results for a given compound between vastly different species? For example, what concentration in the ambient water of a small fish model would be equivalent to 10 ppm of a given compound in a rat's drinking water? *Where do we begin?*

Historically, the link between chemical exposure and cancer in humans has been determined with whole animal two-year chronic bioassays using chemical doses that may be several orders of magnitude higher than that encountered by humans in the environment (Law, 2001). Conversion of animal data to estimates of human risk involves extrapolations of high experimental doses to lower, more environmentally relevant doses. The most commonly used dose-response model is the multistage model for quantal data (i.e. data indicating only the number of animals with cancer), which expresses upper confidence limits on cancer risk as a linear function of dose in the low dose range (EPA, 1993). In order to protect public health, this method of risk assessment has to incorporate a high degree of conservatism, particularly when there is a lack of scientific data of sufficient specificity and caliber to better characterize human risk (Golden et al., 1997). It has become increasingly

evident, however, that mathematical extrapolations from bioassay tumor data may not be an accurate representation of carcinogenic risk at lower doses, particularly if the dose response to a certain chemical is, in fact, non-linear. In addition, two-year bioassays are costly in regards to animals and time; evaluation of chemicals at low doses requires more animals to be statistically significant due to the lower incidence of tumors.

In their *Guidelines for Carcinogen Risk Assessment*, the US EPA proposed the use of quantifiable, mechanistic data to more accurately describe the shape of the dose response curve of potential carcinogens at lower exposure levels (EPA, 2005). Since carcinogenesis is a multi-step process, consisting of genetic alterations leading to cellular phenotypic changes, quantification of chemically induced lesions at the molecular level could describe responses at doses below those at which tumors can be accurately assessed (Preston, 2002). Genetic endpoints, such as DNA adducts and DNA mutations, are indicative of a response at the cell or tissue level. *Molecular dosimetry* is the measurement of these genetic endpoints as a dose-estimate for a target tissue (Bailey et al., 1998). The molecular dose integrates all the various factors involved in chemical exposure, including absorption, distribution, metabolic activation, detoxication and DNA repair, as well individual and species-specific differences in toxicokinetic factors, all of which can alter the linearity of the dose-response (Himmelstein et al., 1994; La and Swenberg, 1996; Law et al., 1998). Molecular dosimetry provides a method for integrating individual biological responses to chemical exposure from exposure to effect. Therefore, it provides a basis for conducting high- to low-dose, route-to-route, and interspecies extrapolations. Incorporation of such data into risk assessment may reduce

uncertainties and produce more accurate estimates of risk compared to current methods, by extending the observable range of data several orders of magnitude lower than can be achieved with chronic bioassays (La and Swenberg, 1996).

Small fish models are useful as alternative animal models in chemical toxicity and carcinogenicity testing (Bailey et al., 1996; Law, 2001; Hawkins et al., 2003). Fish can serve as environmental indicators of health as well as surrogates for human health problems, have low husbandry costs and mature quickly, facilitating production of large numbers of fairly uniform animals for a given study. Small fish models such as the well-characterized Japanese medaka (*Oryzias latipes*) are sensitive to a wide variety of chemical carcinogens with a short time to tumorigenesis, but have a low incidence of spontaneous neoplasia (Okihiro and Hinton, 1999; Hawkins et al., 2003).

To initially address the problem of inter-species dose extrapolation, we sought to determine a *molecular equivalent dose* for a known carcinogen. We performed parallel exposures in F344 rats and medaka fish to the alkylating hepatocarcinogen, dimethylnitrosamine (DMN). DMN's electrophilic intermediate, methyldiazonium ion, interacts with DNA to form a number of methyl-DNA adducts, of which N^7-methylguanine (N^7MeG) is the most prevalent and O^6-methylguanine (O^6MeG), the most pre-mutagenic. The O^6MeG adduct causes GC→AT transition mutations in DNA following cell replication and appears to be important in the development of tumors in experimental animals treated with methylating carcinogens (Souliotis et al, 2002). In both medaka and rat models, we measured O^6MeG, N^7MeG, and 8-hydroxyguanine (8-OHdG) adducts in the liver and

compared these data with mutant frequencies recovered from the livers of *λ cII* transgenic medaka (Winn et al., 2000) and *λ cII* transgenic (Big Blue®) rats. The *λ cII* mutagenesis assay is a positive-selection assay that uses the genetically-neutral *cII* gene as a mutational target. (Winn et al., 2001). Chronic studies in rats have demonstrated a linear tumor dose-response at low dose exposures of DMN that increased sharply at doses higher than about 1 ppm (Peto et al., 1991). Therefore, DMN is an example of a *probable* human carcinogen with a non-linear dose-response curve for tumors in rodents.

2. **Materials and Methods**

2.1 Chemicals

Dimethylnitrosamine (DMN, $C_2H_6N_2O$; 99.9%, CAS 62-75-9, MW 74.08 g/mol) was purchased from Sigma-Aldrich, St. Louis, MO, and was stored in a brown bottle sealed within a metal container at 4 ºC. All other chemicals and reagents used during the λ*cII* mutagenesis assay and DNA adduct isolation were of the highest purity available from commercial resources.

2.2 Animals: Rats and Medaka

Three month-old Japanese medaka (*Oryzias latipes*) and one-month old Big Blue® Fischer 344 rats, both transgenic for the *lambda* LIZ bacteriophage vector, were used in the *λ cII* mutagenesis assay. Male and female, *λ* transgenic medaka were obtained from in-house populations at the Aquatic Biotechnology and Environmental Laboratory (ABEL), University

of Georgia, Athens, GA. Male, heterozygous, F344 Big Blue® rats were obtained from Stratagene, La Jolla, CA. Wild type, 3-month old medaka and one-month old rats were used for the isolation of DNA adducts. Male and female, orange-red medaka (outbred, laboratory strain) were obtained from ABEL and from lab stocks at Duke University (kind gift from Dr. David Hinton). Male F344 rats (non-transgenic) were obtained from Charles River (Wilmington, MA). Medaka were acclimated for 2 weeks in reconstituted (1 g/L Instant Ocean® salts) reverse osmosis-purified (RO) water within a re-circulating, freshwater culture system under an artificial light photoperiod (16 hours light: 8 hours dark) at a temperature of 26 ± 0.5ºC. Rats were cage housed randomly in rooms maintained on a 12-hour light: 12-hour dark artificial light photoperiod, and acclimated for 7 days prior to treatment. Animal care and use were in conformity with protocols approved by the Institutional Animal Care and Use Committee in accordance with the National Academy of Sciences Guide for the Care and Use of Laboratory Animals.

2.3 DMN Exposures

Medaka were dosed identically for the DMN *cII* mutagenesis and DNA adduct experiments. One hundred and twenty-one fish were randomly and evenly divided into eleven 4-liter glass beakers containing 3 liters of reconstituted RO water at a 1 g/L salt concentration. Treatment beakers were placed within a re-circulating, heated water bath to maintain temperature at 26 +/- 0.5 ºC throughout the exposures. Ninety-nine fish were treated twice weekly for two weeks with 10, 25, 50, or 100 µL/L (ppm) DMN. The

compound was replaced every 3-4 days to accommodate for photo-degradation of the compound (Mizgireuv et al., 2004; personal communication with S. Revskoy, 2005). The high-dose group contained 11 extra fish, due to increased post-exposure deaths, to bring the total number of animals used in each experiment to 121 medaka. DMN dilutions were made from 1.5 liters of a 1000 ppm DMN stock solution prepared new prior to each treatment. Twenty-two untreated fish served as control animals. Water quality was maintained with 50% water changes prior to each DMN treatment. Fish were fed once daily with Aquatox® Flake fish food (Zeigler Brothers, Gardners, PA, USA). Animals were observed twice daily for physiological and behavioral responses and signs of overt toxicity. Following the two-week DMN exposure, medaka used for DNA adduct isolation were euthanized, immediately, whereas medaka used for the *cII* assay were rinsed in clean water, replaced into the re-circulating, freshwater culture system and euthanized 30 days post-exposure. All fish were euthanized with an over-dose of tricaine methanesulfonate (MS-222, Argent Laboratories, Redmond, WA, USA). Livers were removed from each medaka, flash-frozen in liquid nitrogen, and stored at -80 ºC until processed for DNA isolation. However, subsamples from each treatment group were fixed, whole, in 10% neutral buffered formalin, de-mineralized in 10% formic acid, and routinely processed for histopathology.

For the *cII* assay, 25 male F344 Big Blue® rats (5/ group) were randomized and exposed for 2 weeks to DMN in their drinking water. Dose groups included 0.1, 1.0, 5.0, 10, and 25 ppm DMN. Five untreated Big Blue® rats served as control animals. Two deaths, one in the control group and the other in the high-dose group, brought the total number of

rats (treated and untreated) to twenty-eight. For the isolation of DNA adducts, exposure methods were similar to that of the *cII* experiment, except that 20 rats were exposed to DMN with four untreated control rats. The animals were maintained at 20-22 °C and 40-60% humidity on a 12-hour light-dark cycle. They were housed 2-3 per cage, and provided Purina Rodent Laboratory Chow (St. Louis, MO, USA) and water *ad libitum*. DMN dilutions were made from 1000 ppm stock solutions; drinking water bottles containing the control and dosing solutions were changed twice weekly. DMN solutions were administered in brown glass water bottles fitted with Teflon® stoppers and stainless steel, double-balled sipper tubes. Animals were observed daily for physiological and behavioral responses and signs of overt toxicity. Mortality and morbidity checks were made twice daily. Body weights and water consumption were measured twice weekly. Following the two week DMN exposure, rats used for DNA adduct isolation were immediately euthanized, whereas rats used for the *cII* assay were given food and water [alone] for 30 days, and euthanized on day 30. All rats were euthanized in a carbon dioxide chamber. Their livers were removed, flash-frozen in liquid nitrogen, and stored at -80 °C until processed for DNA isolation.

2.4 λcII Mutagenesis Assay: DNA Isolation

Fish genomic DNA was obtained for the λ *cII* mutagenesis assay using procedures to optimize isolation of high molecular weight DNA for *in vitro* packaging (Winn et al, 2000). For each fish, the entire liver (~10 mg) was digested with 1x SSC/20% SDS/20 mg/ml proteinase K at 37 ºC for 5-10 minutes. Samples were extracted 1-2 times with equal

volumes phenol/chloroform by using wide-bore pipette tips to minimize DNA shearing. 8 *M* potassium acetate (KAc) was added to a final concentration of 1 *M* followed by final extraction with an equal volume of chloroform. DNA was precipitated with ethanol, removed with a flame-sealed glass pipette, and re-suspended in 15-30 µL of tris-ethylenediamine tetra-acetic acid (Tris·EDTA, pH 7.5). Re-suspended DNA (~10-20 µg) was stored at 4 ºC until packaging.

Rat genomic DNA was obtained for the λ *cII* mutagenesis assay using the RecoverEase® DNA isolation kit (Stratagene, La Jolla, CA, USA), which isolates high molecular weight DNA without organic solvent or ethanol precipitation (Shane et al., 2000). With rodent tissues, RecoverEase® DNA isolation kit provides higher packaging efficiencies than the traditional phenol: chloroform DNA extraction method (Gollapudi et al., 1998). Approximately, 80 mg of liver was homogenized in ice-cold buffer (1.75 g Na_2HPO_4, 8.0g NaCl, 0.2g KH_2PO_4, 20 mL 0.5M EDTA, pH 8.0) with a loose pestle to disaggregate the cells and then with a tight pestle to rupture the cells and release the nuclei. The homogenate was filtered through a nylon mesh filter and centrifuged at 1200-x *g* for 10 minutes at 4 ºC. The supernatant was decanted, and the pellet incubated at 50 ºC for 45 minutes in the presence of digestion buffer containing RNAaceIt® (20µL/mL buffer) (Stratagene, La Jolla, CA, USA) and proteinase K. The contents of the tube were dialyzed for 24 hours, by placing the DNA extract on the wetted surface of a membrane floating on 10mM Tris/1 mM EDTA buffer, ph 7.4. The viscous DNA was harvested and stored at 4 ºC until packaging.

2.5 Lambda cII Mutagenesis Assay: Packaging and Plating of DNA

For medaka and rats, recovery of the bacteriophage vector was accomplished by incubating liver genomic DNA with *in vitro* packaging extracts (30 ºC, for 3 hours), which excised and packaged the vector as viable phage particles (Winn et al., 2000). To select *cII* mutants, 100 µL of undiluted packaged phage were mixed with 200 µL of *E. coli* G1250 cells and 2.5 mL of TB1 top agar and plated on ten TB1 plates at 24 ºC (±0.5 ºC) for 40 hours. Lambda phage containing wild-type *cII* underwent lysogenization and was indistinguishable in the bacterial lawn, whereas λ phage with mutated *cII* gene multiplied through the lytic cycle, forming plaques. To determine the total number of packaged phage, a 20 µL aliquot of a 1:100 dilution of packaged phage was mixed with *E. coli* G1250 cells, plated on three TB1 plates, and incubated at 37 ºC overnight. Mutant frequencies were calculated by dividing the total number of *cII* mutant plaque-forming units (PFUs) on selective screening plates (10 plates/sample) by the estimated total λ+ and *cII* phage on the titer plates (3 plates/sample). Mutant frequencies (MF) are presented as a mean MF ± standard error of the mean for a treatment group. Comparisons of mutation frequencies were tested for significance by using the generalized Cochran-Armitage test (Carr et al., 1995), using the COCHARM analytical program (Proctor and Gamble, Cincinnati, OH, USA).

2.6 Lambda cII Mutagenesis Assay: CII Sequence Analysis

To verify mutant λ *cII* phenotypes, a portion of mutant plaques were randomly cored (1 plaque per plate), incubated in SM buffer at 4 ºC overnight, purified individually on G1250

E. coli cells, and re-plated at low density under selective conditions. Each plate represents an individual mutation, and multiple plaques on each plate are copies of the same individual mutation. A 446-bp λ DNA fragment, including the entire 294-bp *cII* gene, was amplified from a phage lysate (1 plaque per 25 μL DNA grade water) by PCR using primers: 5′-CCACACCTATGGTGTATG-3′ and 5′-CCTCTGCCGAAGTTGAGTAT-3′ (Integrated DNA Technologies, Inc., Coralville, IA, USA). PCR products were electrophoresed on 1.5% agarose gel, purified with QIAquick PCR Purification Kit (Qiagen, Valencia, CA, USA), quantified, and sent to MC Lab, San Francisco, CA (USA), for sequencing. *CII* mutants were verified using a BLAST *cII* sequence as reference.

2.7 DNA Adducts: DNA Isolation

Genomic DNA was isolated from medaka and rat livers using the Puregene® DNA Isolation Kit (Gentra Systems, Inc., Minneapolis, MN, USA). The method was modified from the manufacturer's protocol to include the use of the antioxidant 2,2,6,6-tetramethyl-1-piperidinyloxy (TEMPO) (Sigma Chemical Co., St. Louis, MO, USA). Protocol modifications were also made to accommodate smaller sample sizes (livers) in the medaka experiment. Approximately, 200-400 mg of liver per rat was used for DNA isolation, so that there were four animals representing four data points per DMN treatment group. The small size of the medaka liver (1 liver weighing ~10 mg) necessitated pooling liver samples to obtain 100-120 mg of tissue per treatment group, so that ~12 animals represented one data point with three data points per DMN treatment group. For rat DNA isolation, 6 mL of Cell

Lysis Solution and TEMPO was added to frozen liver tissue and homogenized for 30 seconds with a polytron homogenizer. One hundred-five micro-liters of Proteinase K Solution (20 mg/mL) was added to the lysate, mixed, and incubated at 37 ºC for 3 hours. After cooling to room temperature, 105 µL of RNase A solution added (4 mg/mL or 80 units/ml), the sample mixed, and incubated at 37 ºC for 1 hour. The sample was cooled for 2 hours, 2mL of Protein Precipitation Solution added, the solution vortexed, and kept at 4 ºC overnight. Then, the sample was centrifuged at 2,000-x *g* for 10 minutes, precipitated proteins forming a tight pellet. The supernatant (containing the DNA) was added to 6 mL of cold 100% isopropanol, mixed, and centrifuged at 2,000-x *g* for 3 minutes. DNA was visible as a small white pellet. The supernatant was discarded, 6 mL of cold 70% ethanol added to the DNA pellet, and mixed. The solution was centrifuged at 2,000 x *g* for 1 minute and the ethanol poured off, without losing the DNA pellet. The DNA pellet was allowed to air dry for 10-15 minutes, and then 500 µL of DNA hydration solution was added to re-hydrate the DNA. The sample was vortexed for 30 seconds and incubated at 37 ºC for 1 hour. The DNA sample was transferred to a 1.5 mL microcentrifuge tube, analyzed by spectrophotometer for concentration and purity, and stored at -80 ºC. To isolate DNA from medaka livers, the same protocol was used with the following modifications: 100-120 mg of liver, 3 mL of Cell Lysis Solution, 15 µL of Proteinase K Solution, 15 µL of RNase A, 1 mL of Protein Precipitation Solution, 3 mL of 100% isopropanol, and 3 mL of ethanol.

2.8 DNA Adducts: Enzymatic Digestion and HPLC/ECD Analysis

For rats and medaka, 100 µg of DNA/sample were placed into 1.5 mL microcentrifuge tubes, 150 µL of HPLC water added, and the sample solution, vortexed. Fifteen micro-liters of 200 mM Sodium Acetate, pH 5.0, and 15 µL of Nuclease P1 were added to the mixed DNA solution, and the sample placed in an incubator for 1 hour at 37 ºC. Upon completion of the first incubation, 15 µL of 1 M Tris-HCl buffer, pH 7.4, and 7 µL of alkaline phosphatase were added to the solution, and the sample placed into the incubator for an additional hour at 37 ºC. Filters were inserted into Microcon Centrifugal Filter Devices, the DNA enzymatic samples pipetted into the filters, and the attached caps sealed. The vials with filters and DNA samples were then centrifuged for 15 minutes at 14000 rpms. The filters were discarded and the samples were centrifuged for an additional 3 minutes at 14000 rpms.

Prior to HPLC/ECD analysis, 4 liters of HPLC grade methanol and 4 liters 20 mM Sodium Citrate/50 mM Sodium Acetate buffer, pH 3.01 buffer were filtered separately through Sep-pack C-18 columns (Waters Corporation, Milford, MA, USA) to remove residual organics, using 45 µm nitrocellulose filter and filtration system (Millipore, Bedford, MA, USA). DNA bases were separated using an ACE Analytical 3µm C18 column (4.6 x 150 mm) with a guard column (Advanced Chromatography Technologies, Aberdeen, Scotland, UK). Digested DNA samples were removed from the microcentrifuge following filtration and the 100 µL samples placed into auto-sampler vials for HPLC analysis. The adducted nucleosides were eluted from the HPLC column with 20 mM Sodium Citrate/ 50

mM Sodium Acetate buffer, pH 3.01 (96%)/4% methanol at a flow-rate of 0.9mL/min through isocratic mobile phase pump equipped with an electrochemical detector (ESA CoulArray ECD, ESA, Inc., Chelsford, MA, USA) containing a glassy carbon working electrode and an Ag/AgCl reference electrode. The column temperature was set at 30 ºC, the eight coulometric cells of the ECD detector set to the following potentials: 250, 300, 400, 500, 600, 700, 800, 1000 mV, and the sensitivity set at 10 nA. The HPLC-ECD system was calibrated using a standard curve for N^7-methylguanosine, O^6-methylguanosine, 8-OHdG DNA adduct and 2-deoxyguanosine. A standard mixture that consisted of 100 pmoles of N^7-methylguanosine, 20 pmoles of O^6-methylguanosine, 270 fmoles of 8-OHdG DNA adduct, 50 fmoles of M1dG, and 1 nmoles of 2-deoxyguanosine were analyzed every six samples in the analysis of the unknown samples. Peaks were quantified by measuring peak heights after peak identity had been confirmed by "spiking" with an authentic standard and also by analyses using an HP1100 Diode Array Detector.

2.9 Statistical Analyses of Adduct and Mutant Frequency Data

Comparisons of mutation frequencies were tested for significance using the generalized Cochran-Armitage test (Carr et al., 1995) in COCHARM. Comparison of DMN dose response curves for O^6MeG adducts and mutant frequencies in rats versus medaka were tested for significance by performing non-linear regression of normalized data and an analysis of variance (ANOVA F test) for the EC_{50} using GraphPad Prism version 4.00 (San Diego, CA).

3. Results

3.1 DNA Adducts

The means for each dose group and DNA adduct species are shown in tables 1-2, as well as figures 1-6, for rats and medaka. Liver samples from control rats contained guanine adducts in the range of 1 to 2,680,000 fmol per 10 million normal guanine bases, whereas control medaka livers had guanine adducts in the range of 0.00007 to 2.23 fmol per 10 million normal guanine bases.

For rats, the mean concentration of O^6MeG in hepatic DNA for the 0.1 ppm and 1 ppm DMN dose groups varied little from that of untreated control rats (~1.0 fold) (Fig. 1). For the 5, 10, and 25 ppm dose groups, O^6MeG concentrations were increased by 1.43 to 1.67 fold over the control O^6MeG concentrations. In medaka, no difference was apparent in the average O^6MeG concentration for the control group and 10 ppm DMN dose group (~1.0 fold) (Fig. 2) whereas O^6MeG concentrations were 1.96 fold higher in the 25 ppm dose group and 2.66 fold higher for the 50 ppm dose group. For the 100 ppm dose group, the mean O^6MeG concentration in medaka dropped to 1.52 fold over the control average. O^6MeG adduct dose responses in DMN-exposed rats and medaka were graphed using non-linear regression. When O^6MeG adduct curves were compared via analysis of variance for medaka versus rats exposed to DMN, the curves were *not* found to be statistically different at $p = 0.0613$ (Fig. 7). A p value < 0.05 was considered to be significant.

The mean concentration of N^7MeG in rats for the 0.1, 1.0, and 10.0 ppm DMN dose groups varied little from that of the control average (~1.3 fold) compared to a 1.53 fold increase for the 5.0 ppm group and a 2 fold increase for the 25 ppm dose group above concurrent controls (Fig. 3). For the medaka, no difference was evident for the average concentration of N^7MeG in the control and 10 ppm dose groups (1.04 fold). However, N^7MeG concentrations were increased by ~3 fold in the 25 ppm and 50 ppm dose groups and 5.57 fold in the 100 ppm dose group (Fig. 4).

Mean 8-OHdG adduct concentrations were variable among all rat dose groups. In the 0.1 ppm DMN dose group, the average 8-OHdG concentrations was only slightly higher (1.3 fold) than that of control rats (Fig. 5). In the 1.0 ppm and 5.0 ppm dose groups, the averages dropped below that of the controls by 1.3 fold. 8-OHdG concentrations increased above the control average 1.44 fold for the 10 ppm dose group and 1.53 fold for the 25 ppm dose group. In medaka, 8-OHdG concentrations were increased 2.36 fold for the 10 ppm dose group, 3.71 fold for the 25 ppm dose group, 22.6 fold for the 50 ppm dose group, and 48.6 fold for the 100 ppm dose group over the mean 8-OHdG concentration in control fish (Fig. 6).

3.2 CII Mutant Frequencies (MF)

The mean MF of 5.37×10^{-5} observed in livers of untreated control rats corresponded closely with historical *spontaneous* MF values reported in Big Blue® rats and mice (Gollapudi et al., 1998; Shane et al., 2000) (Table 3). The mean MF in rats treated with 0.1

ppm DMN (6.58×10^{-5}; $p = 0.1094$) and 1 ppm DMN (8.01×10^{-5}; $p = 0.0504$) were not significantly elevated above the mean MF of control rats, in this study. A p value < 0.05 was considered significant. The mean MF for rats in the 5 ppm (19.86×10^{-5}; $p = 0.0032$), 10 ppm (21.29×10^{-5}; $p = 0.0084$), and 25 ppm (19.52×10^{-5}; $p = 0.0032$) DMN dose groups were all statistically significant in comparison to controls with the MF leveling off at 5 ppm DMN. The mean MF of 3.09×10^{-5} observed in livers of untreated control medaka corresponded with that reported for *spontaneous* MF values in λ transgenic medaka (Winn et al., 2000). By comparison, the mean MF in all DMN-exposed medaka was significantly increased above that of control fish (Table 4). The MF increased in each DMN exposure concentration beginning with the 10 ppm DMN treatment, which exhibited a 30-fold mutant induction compared to controls (91.81×10^{-5}; $p = 0.0025$). The MF of medaka exposed to 25 ppm DMN and 50 ppm DMN were induced 95 fold (294.18×10^{-5}; $p = 0.0005$) and 130 fold (403.72×10^{-5}; $p = 0.0019$), respectively, compared to control fish; whereas, the mean MF in fish exposed to 100 ppm DMN was elevated 100 fold above controls (308.01×10^{-5}; $p = 0.0252$). Mutant frequency dose response for DMN-exposed rats and medaka were graphed using non-linear regression. When MF curves were compared using analysis of variance for medaka versus rats exposed to DMN, the curves were found to be statistically different at $p<0.0001$ [figure 8]. A p value < 0.05 was considered significant.

3.3 Spectra of cII Mutations

To characterize and verify the spectra of *cII* mutations recovered from rats exposed to DMN, a portion of the total λ *cII* was sequenced from rats within the control and 25 ppm exposure groups. Ten mutant plaques were randomly selected (5 plaques/treatment group; 1 plaque/ clonal plate) from untreated rats and rats exposed to 25 ppm DMN for sequencing analysis [Table 5]. In the control group, one mutation was found outside the *cII* protein-coding region and was excluded. Of the four remaining mutations, two were single-base substitutions, specifically transition mutations (TA→CG and GC→AT), at positions 152 and 159, respectively. The other two were frameshift mutations comprised of one insertion (added G) at position 178 and one deletion (deleted G) at position 179. In the 25 ppm DMN exposure group, five mutations were present within the *cII* protein coding region. Four of the five mutations were frameshift mutations comprised of insertions (added G) at *cII* gene position 178. The remaining mutation present within plaques evaluated from the 25 ppm treatment group was a single base substitution or transversion (AT→TA) at position 107.

To characterize and verify the spectra of *cII* mutations recovered from DMN-exposed medaka, a portion of total λ *cII* was sequenced from fish in the control, 10 ppm DMN, and 50 ppm DMN treatment groups [Table 3]. Sixteen mutant plaques (1 plaque/ clonal plate) were randomly chosen for analysis from control (5 plaques), 10 ppm DMN (5 plaques), and 50 ppm DMN (6 plaques) treatment groups. In the control group, one mutation found outside the *cII* protein-coding region was excluded. Of the four remaining mutations, two were single-base substitutions comprised of transitions at positions 115 (CG→TA) and 103

(GC→AT); whereas, the other two were frameshifts comprised of insertions (added G) at position 178. In the 10 ppm DMN exposure group, all mutations analyzed consisted of single base substitutions, specifically GC→AT transitions, at positions, 129, 220, 94, 94, and 220. In the 50 ppm DMN treatment group, all six mutations analyzed were single base substitutions. Five of the six single base substitutions were transitions, of which three (GC→AT) were at positions 180, 180, and 122, while the other two (CG→TA) were at positions 52 and 155. The remaining single base substitution was a transversion mutation (GC→TA) at position 169.

4. Discussion

A growing list of new animal models, including fish models that may soon afford high throughput mechanistically based testing, presents special challenges in inter-species dose-response extrapolation. Computation of dose extrapolation factors for various chemical classes and between animal models using the common denominator of molecular dose will give us a framework with which to make more defensible study comparisons. The current study was an *initial* attempt at determining a *molecular equivalent dose* for aqueous nitrosamine exposure between two commonly used laboratory animals, the F344 rat and the medaka fish. Even though DNA adducts and mutant frequencies are merely surrogates for internal dose at a given time after exposure, these measurements give us much more insight into a chemical's mechanism and ultimate fate than nominal or tissue doses. By using fold differences in apparent compound potency at the common molecular level, we can

approximate dose comparisons between the two species (Fig. 7, 8). To address the question posed at the beginning concerning a 10 ppm aqueous exposure: using the ratio of MF to DNA adducts (Fig. 9), we see that medaka are at least 4 times more efficient at converting a given dose of DMN to mutations in the liver. Thus, can we venture that a 10 ppm ambient exposure in the medaka fish approximates a 40 ppm drinking water exposure in the rat? Certainly there are more steps involved in multi-stage carcinogenesis, and the ultimate comparison lies in actual liver tumor incidence, but these comparisons earlier in the neoplastic process may prove useful, as further comparisons are needed across divergent phyletic levels.

Small fish models, as bioindicators of environmental health, can provide valuable scientific insight into potential environmental hazards to human health. Their advantage in numbers, sensitivity to a variety of known carcinogens, and low spontaneous tumor rate make them an ideal alternative to traditional rodent carcinogenicity assays, particularly with regard to low dose chemical exposures. Transgenic models may enhance the utility of fish models in reducing, refining, and replacing select mammals in toxicity testing (Winn, 2001). Comparative, mechanistically based dosimetry models that can quantitatively describe, at the molecular level, how an individual interacts with a chemical from *exposure to response* may be the means by which to apply data across species, as well as across phyletic levels (Csänady et al., 1991). Currently, there are little available data concerning comparative, mechanistically based, dosimetry models for rodents versus humans, much less for fish and humans.

The experimental design in our study was based on typically used protocols for the F344 rat and medaka small fish model. Our goal was to derive an approximate molecular dose equivalency between these two models as they are often used in carcinogenicity testing. Thus we used 1-month-old rats versus 3-month-old medaka and performed the exposures at different ambient temperatures. The dose ranges of DMN used were chosen for rats and medaka based on the data available in the literature (Khudoley et al., 1984; Anderson et al., 1986; Winn et al., 2005) and in consultation with experts in the field. Due to an increased sensitivity to the toxic effects of DMN at concentrations at or above 25 ppm in rodents, the maximum dose for rats was 4 times less than the highest exposure in medaka (personal communication with L. Anderson; Liteplo et al., 2001). This made dose-response comparisons more difficult and, in hindsight, we probably could have used the higher dose ranges for DMN in rats as well. Designing parallel carcinogenesis studies between two different species was challenging; however, measurement of the molecular dose (effect of DMN exposure on macromolecules, such as DNA) integrates differences in drug uptake, tissue dose, and metabolism between the two species. In addition, the use of the genetically neutral transgene (*cII*) for the measurement of mutant frequencies in DMN-exposed rats and medaka facilitates comparisons between these two species. Both animals have the same mutational target, despite species-specific chromosomal differences.

In rats, DMN is metabolized in the liver by cytochrome P450 2E1 (CYP 2E1) to the DNA-reactive metabolite, methyldiazonium ion. The methyldiazonium ion methylates DNA and forms a variety of DNA adducts, of which N^7-methylguanine (N^7MeG) is the most

predominant and O^6-methylguanine (O^6MeG) is the most premutagenic. In both rats and medaka, the predominant DMN-induced mutations are GC→AT transitions, which are attributed to the mispairing of O^6MeG with thymine (Souliotis et al., 1998; Winn et al., 2005). GC→AT mutations have been found to occur frequently in cancer-related genes (i.e. K-*ras*) of DMN-induced animal tumors, suggesting an important role for O^6MeG in carcinogenesis (Mirsalis et al., 1993; Souliotis et al, 1998). N^7MeG adducts are not directly mutagenic, but can undergo enzymatic or spontaneous depurination to form mutagenic apurinic sites (Souliotis et al., 1998). Other DNA adducts induced by DMN include N^3MeA, O^4MeT, and other minor adducts. The contribution of these adducts to the molecular mechanism of DMN hepatocarcinogenesis is unknown (Swenberg et al., 1991).

This is the first report of DMN-induced methylated adducts in fish. A sublinear dose-response curve was apparent in medaka for N^7MeG with adduct levels reaching 7.46E+00 fmols per 10^6dG for the 100 ppm dose group, approximately 5 times higher than that measured in un-exposed fish and 10 ppm DMN-exposed fish (Table 2, Figure 4). The dose-response curve for O^6MeG in fish was also sublinear with adduct values for the 50 ppm group reaching 2.63E+00 fmols per 10^6dG, almost 3 times higher than that observed for un-exposed fish and 10 ppm DMN-exposed fish (Table 2, Figure 2). However, O^6MeG dropped to 1.49E+00 fmols per 10^6dG in medaka exposed to 100 ppm DMN. These results are consistent with previous medaka work using diethylnitrosamine (DEN), in which DEN-induced adducts accumulated much faster at 100 ppm than 10 or 0 ppm DEN (Law et al., 1998). The sublinear dose response curves noted for DMN-induced methylated adducts in

medaka may be due to depletion of suicide repair enzyme, methyl-guanine methyltransferase, as DMN dose increased. The drop in O^6MeG concentration in fish for the 100 ppm dose group is less likely due to DNA repair and more likely reflective of increased cell death due to toxicity noted for that dose group (unpublished data) and/or individual fish variability. N^7MeG adducts are much more prevalent than O^6MeG adducts, which may explain why a similar drop was not noted at 100 ppm for that adduct. 8-OHdG adducts, reflective of oxidative damage, increased sublinearly in fish for the 100 ppm dose group with the concentration of 8-OHdG being ~48 times higher at 0.00680 fmols per 10^6dG than that observed in un-exposed fish.

DMN induced dose-related increases in mutant frequency in the *cII* target genes of both medaka and rats exposed for two weeks to DMN (Tables 3 & 4). For rats, MF's in the 5, 10, and 25 ppm dose groups were all significant ($p < 0.05$) and increased ~4 fold above the MF in untreated rats. MF's in rats exposed to DMN via their drinking water in our study were within the range of MF's recorded in rats exposed to 0.2, 0.6, 2.0, and 6.0 mg/kg/day of DMN via gavage for 12 days (Gollapudi et al., 1998). At the highest dose, Gollapudi and colleagues reported a 4.5 fold increase in MF above untreated animals. Both the MF for rats in the current study and the Gollapudi study were similar to MF's in mice exposed to 4 mg/kg DMN via intraperitoneal injection for five days (Shane et al., 2000). The intraperitoneal injections in that study induced a 3-fold increase in MF in DMN-treated mice above untreated animals.

The fold increases in MF recorded in medaka fish for all DMN doses in this study were unprecedented. Winn et al. (2005) reported 8- and 18-fold respective increases in MF for medaka exposed to 300 ppm and 600 ppm DMN in ambient water for 96 hours compared to MF's recorded for untreated control fish. In our current study, MF's for medaka exposed 10, 25, 50, and 100 ppm DMN were, respectively, 30-fold, 95-fold, 134-fold, and 103-fold higher than that recorded for corresponding untreated control medaka. MF's for medaka exposed to DMN, in this study, are the highest recorded for *lambda* transgenic medaka (personal communication with R. Winn).

The specific mutation spectrum associated with DMN exposure is well documented in rodents and medaka (Gollapudi et al., 1998; Shane et al., 2000; Winn et al., 2005). In the current study, a subset of mutants was sequenced to verify that the mutations within the *cII* gene were consistent with DMN exposure. Mutants from untreated and 25 ppm DMN-exposed rats were chosen, as well as mutants from untreated, 10 ppm-exposed, and 50 ppm DMN-exposed medaka. The mutational spectrum in untreated rats and rats exposed to 25 ppm DMN corresponded closely with the historical spectra of spontaneous mutations observed in Big Blue® mice (Harbach et al., 1999). The transition mutation, GC→AT, typically associated with O^6MeG adducts, was not identified within the five *cII* mutants sequenced for Big Blue® rats exposed to 25 ppm DMN. The frameshift mutations identified within control and 25 ppm DMN treated rats fall within the homonucleotide run of six guanines (nucleotides 179-184, sense strand), a known mutation hotspot in the *cII* gene (Watson et al., 1998; Harbach et al., 1999; Winn et al., 2001). Mutations within this region

of the gene are likely due to replication errors via the slippage model and are considered spontaneous (Shane et al., 2000). In untreated medaka, spontaneous mutations occurred within the homonucleotide run of six guanines, as well as at position 103, a 5'-CpG-3' sequence (103). CpG sites in the *cII* gene are also hotspots for spontaneous mutations. Cytosines at CpG sites are often 5'-methylated and known to undergo spontaneous deamination to form thymine, resulting in GC→AT transitions (Harbach et al., 1999). All mutations sequenced from medaka fish exposed to 10 ppm DMN, GC→AT transitions, occurred at unique sites in the *cII* gene and were consistent with mutations due to DMN's premutagenic adduct O^6MeG. Three GC→AT transition mutations occurred in fish exposed to 50 ppm; however, only one occurred at a unique site in the *cII* gene (position 122). The other two occurred within the homonucleotide run of guanosines at position 180, the mutational hotspot. Two transition mutations, CG→TA, occurred at unique sites, positions 52 and 155. Mirsalis et al. (1993) reported CG→TA transition mutations to be associated with DMN exposure in *lac*I mice. The last mutation within the 50 ppm fish exposure group, a GC→TA transversion, also occurred at a unique site within the *cII* gene, position 169. It is not specific for O^6MeG; however, its occurrence is increased in the *cII* gene of mice exposed to DMN (Shane et al., 2000). It is unclear why GC→AT transition mutations were not apparent in the subset of sequenced mutants from DMN-exposed rats while they were present in mutants from DMN-exposed medaka. However, considering that the reportedly observed range of spontaneous mutant frequencies in λ transgenic fish is slightly lower than, but comparable to, the ranges reported for λ transgenic rodents (Winn et al., 2001), it is possible

that the number of mutants sequenced (our sample size) was not sufficiently large enough to detect DMN-inducible mutations, such as GC→AT transitions, in the rats.

In review of the mutant frequency data from Big Blue® rats and *lambda* transgenic medaka exposed to the carcinogen, DMN, medaka appear to be much more sensitive to the mutagenic effects of DMN. For the two common dose groups, 10 ppm and 25 ppm DMN, it is apparent that the mutant frequencies for DMN-exposed medaka are up to 20X higher than that of the rats (Fig. 9). Mutant frequencies for medaka were ~4X higher than rats at 10 ppm DMN and ~15 fold higher at 25 ppm DMN. The ratio of mutant frequency to adduct concentration (Fig. 9) suggests a more efficient conversion of adducts to mutations by the *λcII* medaka. Out of the various adducts associated with DMN-exposure, we chose the most pre-mutagenic adduct, O^6MeG, to determine our adduct→mutation conversion efficiency. Although O^6MeG is *not* the most prevalent methylated adduct associated with DMN-exposure, it is presumably the most relevant adduct to DMN-inducible carcinogenesis. Usage of N^7MeG levels to measure conversion efficiency could dramatically change the data comparison of rats to medaka; however, N^7MeG is not directly mutagenic, despite its high prevalence. In the medaka, mean O^6MeG adduct levels (9.85E-01 fmoles/10^A6dG) for the 10 ppm dose group varied little from that measured for the untreated control fish (9.83E-01 fmoles/10^A6dG). Conversely, the mean MF in medaka for the 10 ppm dose group (91.81 x 10^{-5}) was ~30 times higher than that of untreated medaka (3.09 x 10^{-5}). This might suggest that other adducts could be contributing to mutagenesis in medaka exposed to 10 ppm DMN. Other adducts do occur with DMN-exposure, although they occur at an even lower frequency

than O^6MeG adducts (Souliotis et al., 2002). In addition, all mutants sequenced from medaka in the 10 ppm DMN dose group were all GC→AT transitions, mutations attributed to mispairing of O^6MeG with thymine.

A number of different factors could have been responsible for the drastically different mutation response in medaka versus rats exposed to DMN such as the range of exposure concentrations and/or exposure period. Historically, rodents are sensitive to the toxic effects of DMN at concentrations of 25 ppm and higher (personal communication with L. Anderson), whereas fish appeared to be much more tolerant of DMN exposure, according to the literature (Khudoley et al., 1984; Winn et al., 2005). Considering that we saw no evidence of hepatotoxicity and/or tumor induction in rats at 6 months post-exposure (unpublished pathology data), it is possible that we could have safely exposed the rats to 50 ppm DMN for two weeks and seen a greater elevation in the mutation frequency; that seems unlikely, however, since the MF response in rats leveled off at 5 ppm DMN (Fig. 8). For medaka, delayed DMN-induced hepatotoxicity was apparent in the 100 ppm DMN exposure group with a ~50% mortality rate at two-weeks post-exposure. Fish from the 100 ppm group that survived the mutation manifestation period (30 days post-exposure) had small, pale, and friable livers; the decrease in mutant frequency noted for this dose group (Fig. 8) was presumably due to poor quality DNA. Due to the delayed toxicity at 100 ppm DMN in medaka, a lower dose range for fish would probably been more appropriate for this study; however, a dose range in fish more comparable to that in the rat would not likely have produced comparable mutation frequencies, considering the fold differences at 10 and 25

ppm DMN. A four-week exposure period might have increased the mutagenesis response in the DMN-exposed rats, but the additional two weeks exposed to DMN might also have caused a toxic response in the 25 ppm rat group. In addition, medaka in the high dose exposure group would not have tolerated exposure to 100 ppm DMN for four weeks (unpublished data).

Species-specific variability in DMN metabolism or repair of DMN-induced DNA adducts may have contributed to the much greater mutant frequencies noted for medaka versus rats exposed to DMN. In mammals, the mechanism by which DMN exerts its biological effects is well documented. DMN is metabolized in the liver by the phase I microsomal enzyme, cytochrome (CYP) P450 2E1, to a reactive intermediate, methyldiazonium ion, which methylates cellular macromolecules, such as DNA (Souliotis et al., 1998). The basic metabolic machinery is also present in small fish species in regards to Phase I and Phase II metabolism, however the role of CYP 2E1 in medaka is less certain. In studying the metabolism of the groundwater contaminant, trichloroethylene, Lipscomb et al (1998) found the CYP1A was readily detectable in medaka liver by immunohistochemistry, whereas CYP2E1 was present at very low levels. Geter et al (2003) examined the role of P450 2E1 in metabolism of 3-chloro-4-(dichloromethyl)-5-hydroxy-2[*5H]*-furanone (MX) in medaka liver by measuring MX-induced CYP2E1 activity using CYP2E1 specific substrate *p*-nitrophenol (PNP). Both medaka liver microsomes and S-9 fractions catalyzed the hydroxylation of PNP, suggesting CYP2E1-like activity in the medaka, although the cytochrome responsible for this activity and its genetic relationship to those in other species

was not confirmed. In the current study, identification of DNA adducts, N^7MeG and O^6MeG, both indicative of DMN exposure, support CYP2E1-like activity in DMN-exposed medaka.

A difference between medaka and rats in their ability to repair DMN-induced methyl adducts prior to "fixation" as mutations may be responsible for the marked variation between medaka and rat mutant frequencies. The methylguanine-DNA methyltransferase (MGMT) enzyme, O^6-methylguanine-DNA methyltransferase, is responsible for repairing O^6MeG adducts. O^6-methylguanine-DNA methyltransferase (O^6-MT) is a suicide enzyme that is inactivated when it transfers the methyl group from the O^6-position of guanine to its active site cysteine (Ishikawa et al., 2001; Souliotis et al., 2002). One MGMT molecule is inactivated for each lesion repaired. Thus, the ability of a cell to withstand damage is directly related to the number of MGMT molecules it contains and to the rate of *de novo* synthesis of MGMT (Esteller, 1999). The presence of MGMT proteins has been demonstrated in a number of organisms, including bacteria, yeast, fish, rodents, monkeys, and man (Ishikawa et al., 2001). The levels of MGMT activity may vary greatly among species and also between tissues, with liver having the highest enzyme activity. Nakatsuru et al. (1987) measured the O^6-MT activities in livers of eight species of fish, of which medaka had the highest level of the enzyme, similar to that of the mouse. In medaka exposed to methylazoxymethanol (MAM), Aoki et al. (1993) found dose-dependent suppression of O^6-MT activity suggesting fish became unable to repair O^6MeG in DNA for prolonged periods, probably due to rapid exhaustion and very slow re-synthesis of O^6-MT after exposure to

alkylating agents. This may explain why fish are highly susceptible to the effects of carcinogens. However, rodents given high doses of methylating agents also have a rapid repair phase that depletes O^6-MT levels, followed by a slower repair phase dependent on *de novo* synthesis of O^6-MT (Souliotis et al., 2004). It is possible that the high, prolonged exposures of medaka to DMN exhausted their ability to repair methylated adducts, permitting more to be fixed as mutations. Considering that medaka and mice have similar levels of O^6-MT, ineffective methyltransferase removal of O^6MeG seems to be a more likely culprit for the dramatic increase in medaka mutant frequencies than a lower basal level of O^6-MT molecules in comparison to rats.

A final factor that may have been responsible for the dramatic fold-difference in DMN-induced mutant frequencies for medaka versus rats was DMN-induced cellular proliferation. DMN is a potent inducer of hepatic cell proliferation (Mirsalis et al., 1993). In a major bioassay involving near life-time exposures of rats to DMN in drinking water, Peto et al. (1991) observed a sub-linear tumor response in which hepatocarcinogenic efficacy at low doses was linearly related, but increased sharply at doses higher than 1ppm. Souliotis et al. (1995) found that for rats exposed for 28 days to DMN in their drinking water at concentrations overlapping Peto's study, O^6MeG adduct accumulation was linear and could not by itself account for the dose-dependence of the hepatocarcinogenic efficacy of DMN in rats. In their subsequent paper, Souliotis et al. (2002) determined that alterations in hepatocyte DNA replication, in addition to the accumulation of DNA damage, likely influenced DMN's carcinogenic efficacy. The probability of a DNA adduct giving rise to a

mutation and the eventual development of neoplasia depends not only on its concentration in the cell, but also on the proliferative state of the cell (La and Swenberg, 1996). In the current study, hepatotoxicity and hepatocellular proliferation was apparent in medaka exposed to DMN, particularly at the higher dose levels (unpublished pathology data). Within the six-month grow-out period, most medaka had evidence of hepatocellular regeneration and/or tumor induction. This is compared to the rats, who at six-months, had no evidence of DMN-induce toxicity, much less DMN tumor induction. The evidence, microscopically, of increased cell turn-over in medaka exposed to DMN, suggests that hepatocellular proliferation, in addition to accumulation of DNA damage, likely enhanced the mutagenic effect of DMN in medaka compared to rats.

5. Summary

The goal of this study was to determine a molecular equivalent dose for Japanese medaka and F344 rats exposed to the known carcinogen, DMN, by measuring DMN-induced DNA adducts and DNA mutations as biological markers of DMN exposure and effect. Molecular dosimeters, such as adducts and mutations, integrate various individual pharmacokinetic factors that may affect the biological outcome of chemical exposure, permitting species-to-species, dose-to-dose, and route-to-route extrapolations. Although DNA adduct concentration was similar for medaka and rats exposed to DMN, associated mutant frequencies were up to 20X higher for medaka than that measured in rats at comparable DMN concentrations. Small fish models, particularly transgenic fish models,

have the potential to provide mechanistic data valuable to the risk determinations for humans exposed to potential environmental carcinogens.

Acknowledgements

The authors thank Michelle Norris (UGA), Michael George (EPA), Leon King (EPA), Stephen Kilburn (EPA) and Dr. Fred Fuller (NCSU) for excellent technical assistance. NCSU College of Veterinary Medicine state appropriated funds and the NCSU/EPA Cooperative Training Program in Environmental Health Sciences Research Training Agreement CT826512010 supported this work.

REFERENCES

Anderson L.M., Harrington, G.W., Pylypiw, Jr., H.M., Hagiwara, A., Magee, P.N., 1986. Tissue levels and biological effects of *N*-Nitrosodimethylamine in mice during chronic low or high dose exposure with or without ethanol. Drug Metab. Dispos. 14, 733-739.

Aoki, K., Nakatsuru, Y., Sakurai, J., Ayumi, S., Masahito, P., Ishikawa, T., 1993. Age dependence of O^6-methylguanine-DNA methyltransferase activity and its depletion after carcinogen treatment in the teleost medaka (*Oryzias latipes*). Mutat. Res. DNA Repair 293, 225-231.

Bailey, G.S., Dashwood, R., Loveland, P.M., Pereira, C., Hendricks, J.D., 1998. Molecular dosimetry in fish: quantitative target organ DNA adduction and hepatocarcinogenicity or four aflatoxins by two exposure routes in rainbow trout. Mutat. Res 339, 233-244.

Carr, G.J. and Gorelick, N.J., 1995. Statistical design and analysis of mutation studies in transgenic mice. Environ. Mol. Mutagen. 25, 246-255.

Csänady G.A., Bond, J.A., 1991. Species differences in the biotransformation of 1,3-butadiene to DNA-reactive epoxides: role in cancer risk assessment. C.I.I.T. 11, 8. Environmental Protection Agency, 1993. Motor Vehicle-Related Air Toxics Study. Research Triangle Park, N.C.: Technical Support Branch, Emission Planning and Strategies Division, Office of Mobile Sources, Office of Air and Radiation, U.S. Environmental Protection Agency.

Environmental Protection Agency, 2005. Guidelines for Carcinogenic Risk Assessment. Washington D.C.: Risk Assessment Forum, U.S. Environmental Protection Agency.

Esteller M., Hamilton, S.R., Burger, P.C., Baylin, S.B., Herman, J.G., 1999. Inactivation of the DNA repair gene O^6-methylguanine-DNA methyltransferase by promoter hypermethylation is a common event in primary human neoplasia. Cancer Res. 59, 793-797.

Geter, D.R., Fournie, J.W., Brouwer, M.H., DeAngelo, A.B., Hawkins, W.E., 2003. p-Nitrophenol and glutathione response in medaka (*Oryzias latipes*) exposed to MX, a drinking water carcinogen. Comp. Biochem. Physiol. 134, 353-364.

Golden, R.J., Holm, S.E., Robinson, D.E., Julkumen, P.H., Reese, E.A., 1997. Chloroform mode of action: implications for cancer risk assessment. Regul. Toxicol. Pharmacol 26, 142-155.

Gollapudi, B.B., Jackson, K.M., Stott, W.T., 1998. Hepatic lacI and cII mutation in transgenic (λ LIZ) rats treated with dimethylnitrosamine. Mutat. Res. 419, 131-135.

Harbach, P.R., Zimmer, D.M., Filipunas, A.L., Mattes, W.B., Aaron, C.S., 1999. Spontaneous mutation spectrum at the lambda cII locus in liver, lung, and spleen tissue of Big Blue® transgenic mice. Environ. Mol. Mutagen. 33, 132-143.

Hawkins, W.E., Walker, W.W., Fournie, J.W., Manning, C.S., Krol, R.M., 2003. Use of the Japanese medaka (*Oryzias latipes*) and guppy (*Poecilia reticulate*) in carcinogenesis testing under National Toxicology Program protocols. Toxicol. Pathol. 31 (Suppl.), 88-91.

Himmelstein M.W., Turner M.J., Asgharian B., Bond J.A., 1999. Comparison of blood concentrations of 1,3-butadiene and butadiene epoxides in mice and rats exposed to 1,3-butadiene by inhalation. *Carcinogenesis* 15: 1479-1486.

Ishikawa, T., Ide, F., Qin, X., Zhang, S., Takahashi, Y., Sekiguchi, M., Tanaka, K., Nakatsuru, Y., 2001. Importance of DNA repair in carcinogenesis: evidence from transgenic and gene targeting studies. Mutat. Res. 477, 41-49.

Khudoley, V.V., 1984. Use of Small Fish Species in Carcinogenicity Testing, National Cancer Institute Monograph 65, NIH Publication No 84-2653. National Cancer Institute, Bethesda, MD.

La, D.K., Swenberg, J.A., 1996. DNA adducts: biological markers of exposure and potential applications to risk assessment. Mutat. Res. 365, 129-146.

Law, J.M., Bull M., Nakamura J., Swenberg J.A., 1998. Molecular dosimetry of DNA adducts in the medaka small fish model. Carcinogenesis 19, 515-518.

Law, J.M., 2001. Mechanistic considerations in small fish carcinogenicity testing. ILAR Journal 42, 274-284.

Law, J.M., Lopez, L., DeAngelo, A.B., 1998. Hepatoxicity of the drinking water disinfection byproduct, dichloroacetic acid, in the medaka small fish model. Toxicol. Lett. 94, 19-27.

Lipscomb, J.C., Confer, P.D., Miller, M.R., Stamm, S.C., Snawder, J.E., Bandiera, M., 1998. Metabolism of trichloroethylene and chloral hydrate by the Japanese medaka (*Oryzias latipes*) in vitro. Environ. Toxicol. Chem. 17, 325-332.

Liteplo, R.G., Meek, M.E., 2001. *N*-nitrosodimethylamine: hazard characterization and exposure-response analysis. Environ. Carcino. And Ecotox. Revs. 19, 281-304.

Mirsalis, J.C., Provost, G.S., Matthews, C.D., Hamner, R.T., Schindler, J.E., O'Loughlin, K.G., MacGregor, J.T., Short, J.M., 1993. Induction of hepatic mutations in lacI transgenic mice. Mutagenesis 8, 265-271.

Mizgireuv, I.V., Majorova, I.G., Gorodinskaya, V.M., Khudoley, V.V., Revskoy, S.Y., 2004. Carcinogenic effect of N-nitrosodimethylamine on diploid and triploid zebrafish (*Danio rerio*). Toxicol Pathol. 32, 514-518.

Nakatsuru, Y., Nemoto, N., Nakagawa, K., Masahito, P., Ishikawa, T., 1987. O6-methylguanine DNA methyltransferase activity in liver from various fish species. Carcinogenesis 8, 1123-1127.

Okihiro, M.S., Hinton, D.E., 1999. Progression of hepatic neoplasia in medaka (*Oryzias latipes*) exposed to diethylnitrosamine. Carcinogenesis 20, 933-940.

Peto, R., Gray, R., Brantom, P., Grasso, P., 1991. Effects on 4080 rats of chronic ingestion of *N*-nitrosodiethylamine or *N*-nitrosodimethylamine: a detailed dose-response study. Cancer Res. 51, 6415-6451.

Peto, R., Gray, R., Brantom, P., Grasso, P., 1991. Dose and time relationships for tumor induction in the liver and esophagus of 4080 inbred rats by chronic ingestion of *N*-nitrosodiethylamine or *N*-nitrosodimethylamine. Cancer Res. 51, 6452-6459.

Preston, R.J., 2002. Quantitation of molecular endpoints for the dose-response component of cancer risk assessment. Toxicol. Pathol. 30, 112-116.

Shane, B.S., Smith-Dunn, D.L., de Boer, J.G., Glickman, B.W., Cunningham, M.L., 2000. Mutant frequencies and mutation spectra of Dimethylnitrosamine (DMN) at the *lacI* and *cII* loci in the livers of Big Blue® transgenic mice. Mutat. Res. 542,197-210.

Souliotis V.L., Chhabra, S., Anderson, L.M., Kyrtopoulos, S.A., 1995. Dosimetry of O^6-methylguanine in rat DNA after low-dose, chronic exposure to N-nitrosodimethylamine (NDMA). Implications for the mechanism of NDMA hepatocarcinogenesis. Carcinogenesis 16, 2381-2387.

Souliotis, V.L., Henneman, J.R., Reed, C.D., Chhabra, S., Diwan, B.A., Anderson, L.M., Kyrtopoulos, S.A., 2002. DNA adducts and liver DNA replication in rats during chronic exposure to N-nitrosodimethylamine (NDMA) and their relationships to the dose-dependence of NDMA hepatocarcinogenesis. Mutat. Res. 500, 75-87.

Souliotis, V.L., Sfikakis, P.P., Anderson, L.M., Kyrtopoulos, S.A., 2004. Intra- and intercellular variations in the repair efficiency of O^6-methylguanine, and their contribution to kinetic complexity. Mutat. Res. 568, 155-170.

Souliotis, V.L., van Delft, J.H.M., Steenwinkel, M.S.T., Baan, R.A., Kyrtopoulos, S.A.,1998. DNA adducts, mutant frequencies and mutation spectra in λlacZ transgenic mice treated with *N*-nitrosodimethylamine. Carcinogenesis 19, 731-739.

Swenberg, J.A., Hoel, D.G., Magee, P.N., 1991. Mechanisms and statistical insight into the large carcinogenesis bioassays on *N*-nitrosodiethylamine and *N*-nitrosodimethylamine. Cancer Res. 51, 6409-6414.

Watson, D.E., Cunningham, M.L., Tindall, K.R., 1998. Spontaneous and ENU-induced mutation spectra at the cII locus in Big Blue® Rat2 embryonic fibroblasts. Mutagenesis 13, 487-497.

Winn, R.N., 2001. Transgenic fish as models in environmental toxicology. ILAR Journal 42, 322-329.

Winn, R.N., Norris, M.B., 2005. (In) Techniques in Aquatic Toxicology (Volume 2). Boca Raton, FL: Taylor and Francis.

Winn, R.N., Norris, M.B., Brayer, K.J., Torres, C., Muller, S.L., 2000. Detection of mutations in transgenic fish carrying a bacteriophage λcII transgene target. Proc. Natl. Acad. Sci. USA 97, 12655-12660.

Winn, R.N., Norris, M.B., Muller, S., Torres, C., Brayer, K., 2001. Bacteriophage λ and Plasmic pUR288 Transgenic Fish Models for Detecting In Vivo Mutations. Mar. Biotechnol. 3, S185-S195.

Winn, R.N., Kling H., Norris, M.B., 2005. Antimutagenicity of green tea polyphenols in the liver of transgenic medaka. Environ. Mol. Mutagen. 46, 88-95.

Table 1
Methyl and Oxidative DNA Adducts in DMN Exposed F344 Rats

DMN ppm	fmoles N^7MeG/ 10A6dG	fmoles O^6MeG/ 10A6dG	fmoles *8*-OHdG/ 10A6dG
0	1.87E+01	1.02E+00	1.57E+06
0	1.03E+01	1.71E+00	1.85E+06
0	1.84E+01	7.31E-01	1.86E+06
0	1.77E+01	8.59E-01	2.85E+06
0.1	1.86E+01	1.01E-01	4.60E+06
0.1	1.48E+01	9.41E-01	2.68E+06
0.1	3.10E+01	1.44E+00	1.72E+06
0.1	2.35E+01	1.39E+00	1.64E+06
1.0	1.03E+01	6.81E-01	1.26E+06
1.0	1.54E+01	1.22E+00	2.00E+06
1.0	1.88E+01	1.26E+00	1.26E+06
1.0	1.30E+01	9.37E-01	1.64E+06
5.0	1.54E+01	1.15E+00	8.50E+05
5.0	5.05E+01	2.78E+00	3.33E+06
5.0	8.92E+00	6.94E-01	5.92E+05
10.0	4.07E+01	1.99E+00	3.21E+06
10.0	1.70E+01	8.26E-01	3.35E+06
10.0	1.80E+01	1.43E+00	3.28E+06
10.0	9.54E+00	1.19E+00	1.89E+06
25.0	1.95E+01	1.53E+00	4.58E+06
25.0	8.06E+01	3.02E+00	6.53E+06
25.0	1.95E+01	1.40E+00	4.68E+05
25.0	1.01E+01	1.24E+00	8.41E+05

GROUP STATISTICS

DMN ppm	Mean	SD	Mean	SD	Mean	SD
0	1.63E+01	4.01E+00	1.08E+00	4.37E-01	2.03E+06	5.60E+05
0.1	2.20E+01	6.98E+00	9.67E-01	6.19E-01	2.66E+06	1.38E+06
1.0	1.44E+01	3.61E+00	1.02E+00	2.69E-01	1.54E+06	3.54E+05
5.0	2.49E+01	2.24E+01	1.54E+00	1.10E+00	1.59E+06	1.51E+06
10.0	2.14E+01	1.34E+01	1.36E+00	4.88E-01	2.93E+06	6.94E+05
25.0	3.24E+01	3.25E+01	1.80E+00	8.25E-01	3.11E+06	2.94E+06

Table 2
Methyl and Oxidative DNA Adducts in DMN Exposed Medaka.

DMN ppm	fmoles N^7MeG/ 10^A6dG	fmoles O^6MeG/ 10^A6dG	fmoles *8*-OHdG/ 10^A6dG
0	2.23E+00	1.68E+00	0.00023
0	1.39E+00	9.00E-01	0.00012
0	4.17E-01	3.73E-01	0.00007
10	1.16E+00	8.47E-01	0.00024
10	1.01E+00	9.74E-01	0.00021
10	2.00E+00	1.13E+00	0.00052
25	2.83E+00	1.53E+00	0.00039
25	2.35E+00	1.28E+00	0.00050
25	6.46E+00	2.96E+00	0.00068
50	3.24E+00	1.72E+00	0.00243
50	6.24E+00	4.16E+00	0.00382
50	3.27E+00	2.00E+00	0.00322
100	1.04E+01	1.92E+00	0.00911
100	6.04E+00	1.16E+00	0.00398
100	5.95E+00	1.40E+00	0.00732

GROUP STATISTICS

DMN ppm	Mean	SD	Mean	SD	Mean	SD
0	1.34E+00	9.06E-01	9.83E-01	6.56E-01	0.00014	0.00008
10	1.39E+00	5.37E-01	9.85E-01	1.44E-01	0.00033	0.00017
25	3.88E+00	2.25E+00	1.93E+00	9.07E-01	0.00052	0.00015
50	4.25E+00	1.73E+00	2.63E+00	1.34E+00	0.00316	0.0007
100	7.46E+00	2.53E+00	1.49E+00	3.89E-01	0.0068	0.00261

Table 3
Frequencies of *cII* mutant recovered from livers of untreated and DMN-treated Big Blue® Rats.

DMN ppm	Animal ID	Number of Mutants	Total plaques screened	MF (x 10^{-5})
Zero	A1	8	130,000	6.15
Zero	A2	14	236,500	5.92
Zero	A4	5	151,667	3.30
Zero	A6	9	151,667	5.93
0.1	A7	5	100,000	5.00
0.1	A8	14	170,000	8.24
0.1	A9	8	158,500	5.05
0.1	A10	15	210.000	7.14
1	A13	29	345,000	8.41
1	A15	41	410,000	10.00
1	A16	7	176,000	3.98
1	A17	12	180,000	6.67
5	A19	27	135,000	20
5	A20	16	83,500	19.16
5	A21	26	125,000	20.80
5	A23	30	155,000	19.35
10	A25	48	135,000	35.56
10	A26	32	225,000	14.22
10	A27	22	143,500	15.33
10	A29	51	215,000	23.72
25	A31	21	86500	24.28
25	A32	25	165,000	15.15
25	A34	27	140,000	19.29
25	A35	20	85,000	23.53

GROUP STATISTICS

Dose (ppm)	MF (x 10^{-5})	SD	1 Tail P (p <0.05 is significant)
0	5.37	1.09	--------
0.1	6.58	1.32	0.1094
1	8.01	2.01	0.0504
5	19.86	0.62	0.0032
10	21.29	2.39	0.0084
25	19.52	3.77	0.0032

Table 4
Frequencies of *cII* mutants recovered from the livers of untreated and DMN-treated λ transgenic medaka.

DMN ppm	Animal ID	Number of Mutants	Total plaques screened	MF (x 10^{-5})
0	A1	53	1,795,000	2.95
0	A11	28	1,580,000	1.77
0	A13	69	2,115,000	3.26
0	A2	30	1,160,000	2.59
0	A3	41	783,333	5.23
0	A6	38	940,000	4.04
10	B1	858	1,114,500	74.93
10	B2	728	1,120,000	65
10	B4	562	348,333	161.34
10	B5	845	1,460,000	57.88
10	B6	2442	1,925,000	126.86
10	B7	770	760,000	101.32
25	C1	2300	720,000	319.44
25	C2	2988	1,040,000	287.31
25	C4	2228	546,667	407.56
25	C5	2858	720,000	396.94
25	C7	3758	1,605,000	234.14
25	C9	1744	765,000	227.97
50	D1	2112	550,000	384.00
50	D2	3780	850,000	444.71
50	D3	1167	208,333	560.16
50	D4	2228	546,667	407.56
50	D7	2904	650,000	446.77
50	D8	1152	500,000	230.40
100	E9	2160	580,000	372.41
100	E10	362	155,000	233.55
100	E11	160	75,000	213.33
100	E12	293	130,000	225.38
100	E17	769	290,000	265.17
100	E18	368	105,000	350.48

GROUP STATISTICS

Dose (ppm)	MF (x 10^{-5})	SD	1 Tail P (p <0.05 is significant)
0	3.09	0.85	--------
10	91.81	34.23	0.0025
25	294.18	66.63	0.0005
50	403.72	76.63	0.0019
100	308.01	79.31	0.0252

Table 5
***CII* mutants recovered from livers of untreated and DMN-treated *λ* transgenic medaka and Big Blue® rats.**

Sample ID	DMN ppm	Mutation	Mutation Type	Position	Sequence
Rat θ-1	0	TA→CG	Transition	152	TCC
Rat θ-2	0	GC→AT	Transition	159	TGC
Rat θ-3	0	Deleted G	Deletion	179	GGG[2]
Rat θ-4	0	*None*[1]	*N/A*	*N/A*	*N/A*
Rat θ-5	0	Added G	Insertion	178	TGG[2]
Rat 25-1	25	Added G	Insertion	178	TGG[2]
Rat 25-2	25	Added G	Insertion	178	TGG[2]
Rat 25-3	25	Added G	Insertion	178	TGG[2]
Rat 25-5	25	AT-TA	Transversion	107	GAT
Rat 25-6	25	Added G	Insertion	178	TGG[2]
Medaka θ-1	0	*None*[1]	*N/A*	*N/A*	*N/A*
Medaka θ-2	0	CG→TA	Transition	115	GCA
Medaka θ-3	0	Added G	Insertion	178	TGG[2]
Medaka θ-4	0	Added G	Insertion	178	TGG[2]
Medaka θ-6	0	GC→AT	Transition	103	CGT[3]
Medaka 10-2	10	GC→AT	Transition	129	GGA
Medaka 10-3	10	GC→AT	Transition	220	AGT
Medaka 10-4	10	GC→AT	Transition	94	AGC
Medaka 10-5	10	GC→AT	Transition	94	AGC
Medaka 10-6	10	GC→AT	Transition	220	AGT
Medaka 50-2	50	CG→TA	Transition	52	GCT
Medaka 50-5	50	CG→TA	Transition	155	TCA
Medaka 50-6	50	GC→AT	Transition	180	GGG[2]
Medaka 50-8	50	GC→AT	Transition	180	GGG[2]
Medaka 50-11	50	GC→TA	Transversion	169	TGT
Medaka 50-12	50	GC→AT	Transition	122	AGC

[1]Mutation occurred outside of *cII* gene
[2]Homonucleotide run of six guanines; mutation hotspot
[3]5'-CpG-3' sequence; mutation hotspo

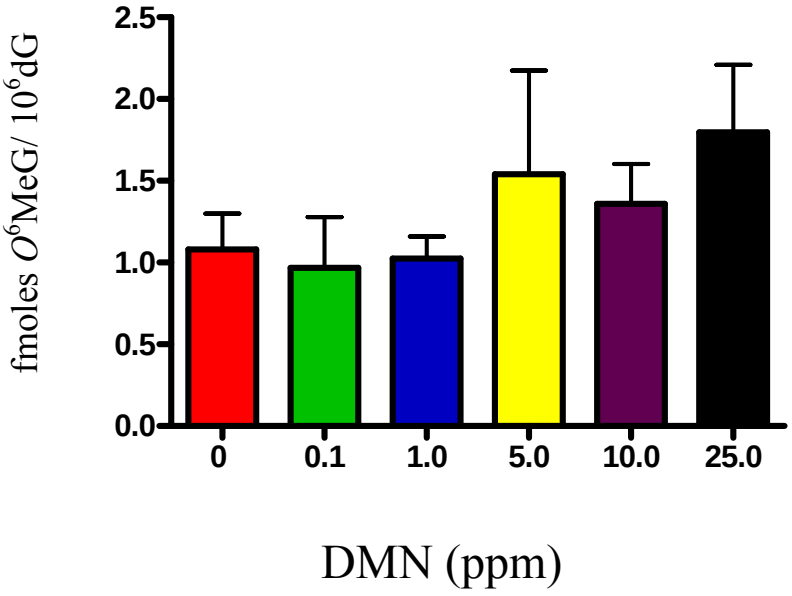

Figure 1. Fmoles of O^6-methylguanine (O^6MeG) adducts/ 10^6deoxyguanine (10^6dG) in F344 rats exposed to 0, 0.1, 1.0, 5.0, 10.0 and 25.0 ppm DMN.

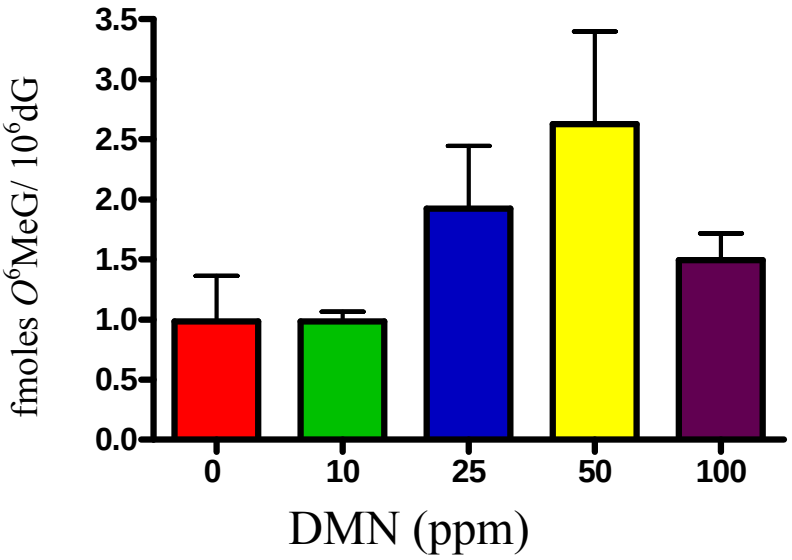

Figure 2. Fmoles of O^6-methylguanine (O^6MeG) adducts/ 10^6deoxyguanine (10^6dG) in medaka fish exposed to 0, 10, 25, 50, and 100 ppm DMN.

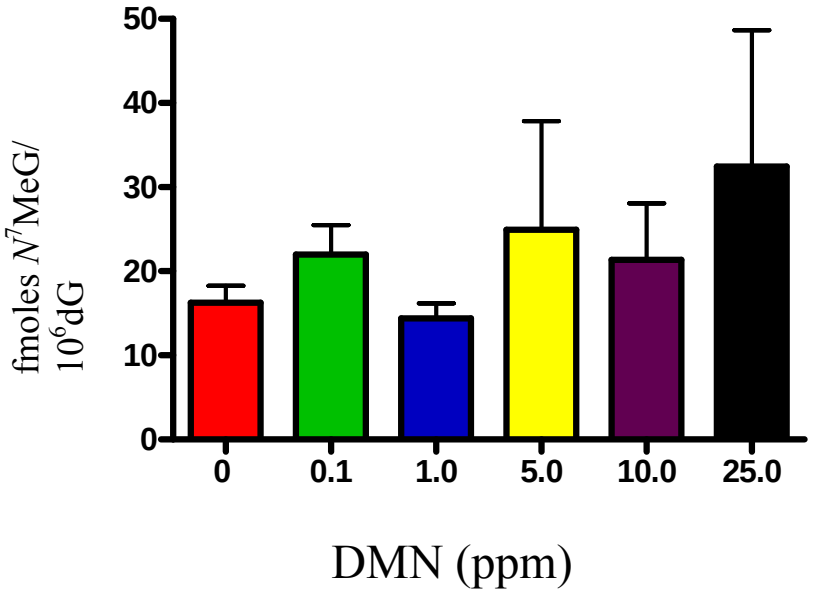

Figure 3. Fmoles of N^7-methylguanine (N^7MeG) adducts/ 10^6deoxyguanine (10^6dG) in F344 rats exposed to 0, 0.1, 1.0, 5.0, 10.0 and 25.0 ppm DMN.

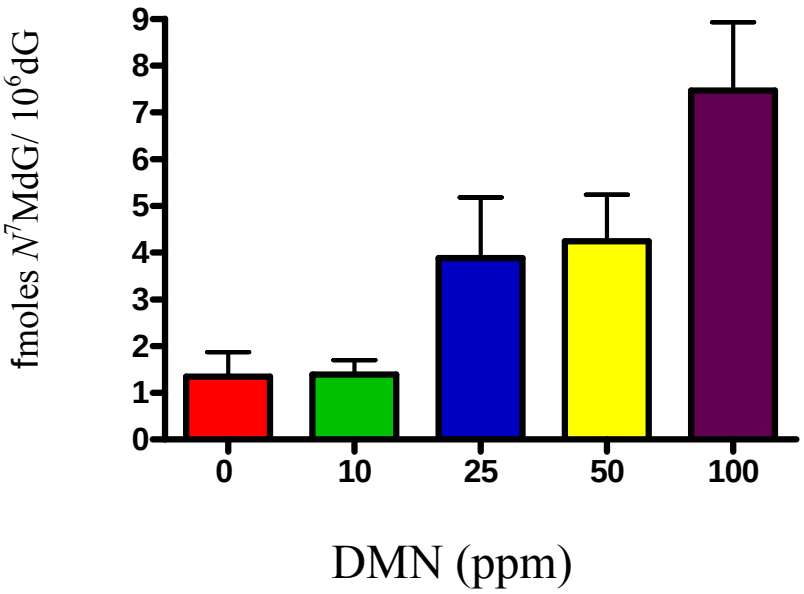

Figure 4. Fmoles of N^7-methylguanine (N^7MeG) adducts/ 10^6deoxyguanine (10^6dG) in medaka fish exposed to 0, 10, 25, 50, and 100 ppm DMN.

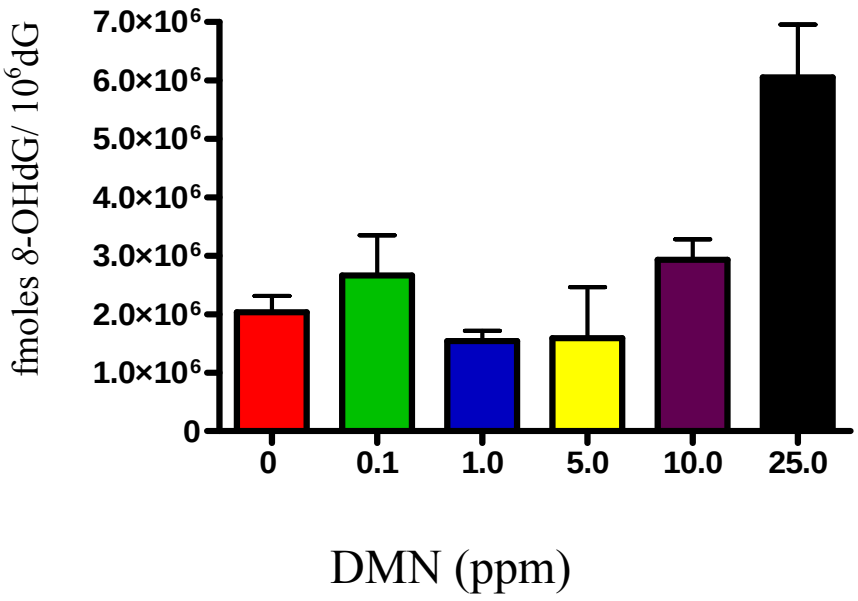

Figure 5. Fmoles of *8*-hydroxyguanine (*8*-OHdG) adducts/ 10^6deoxyguanine (10^6dG) in F344 rats exposed to 0, 0.1, 1.0, 5.0, 10.0 and 25.0 ppm DMN.

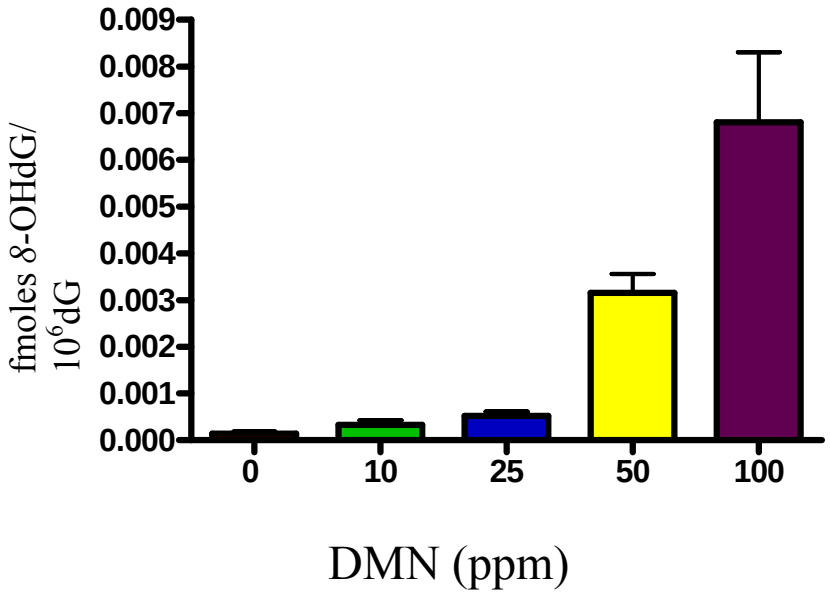

Figure 6. Fmoles of *8*-hydroxyguanine (*8*-OHdG) adducts / 10^6deoxyguanine (10^6dG) in medaka fish exposed to 0, 10, 25, 50, and 100 ppm DMN.

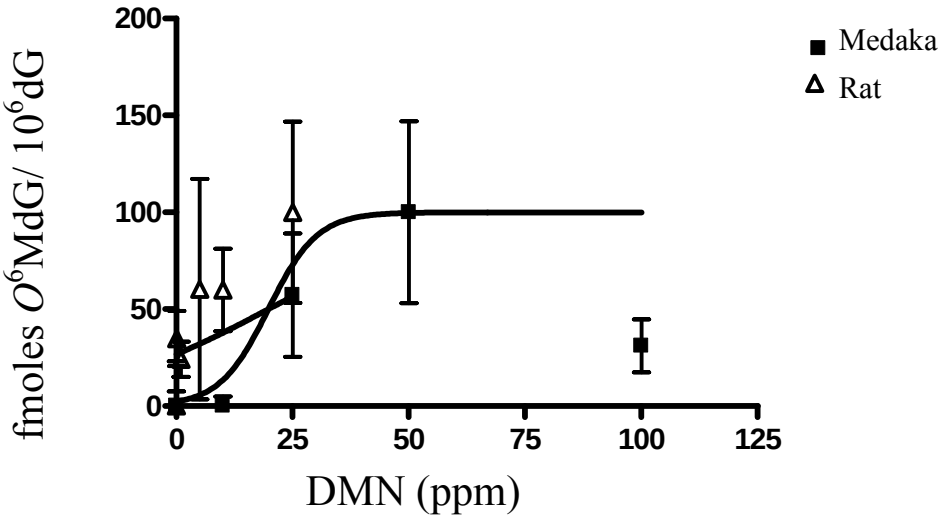

Figure 7. Dose-response comparison of normalized O^6-methylguanine (O^6MeG) adduct-data in medaka fish versus F344 rats exposed to DMN graphed by non-linear regression. An analysis of variance determined the curves to not be statistically different at p=0.0613 ($p < 0.05$ considered significant).

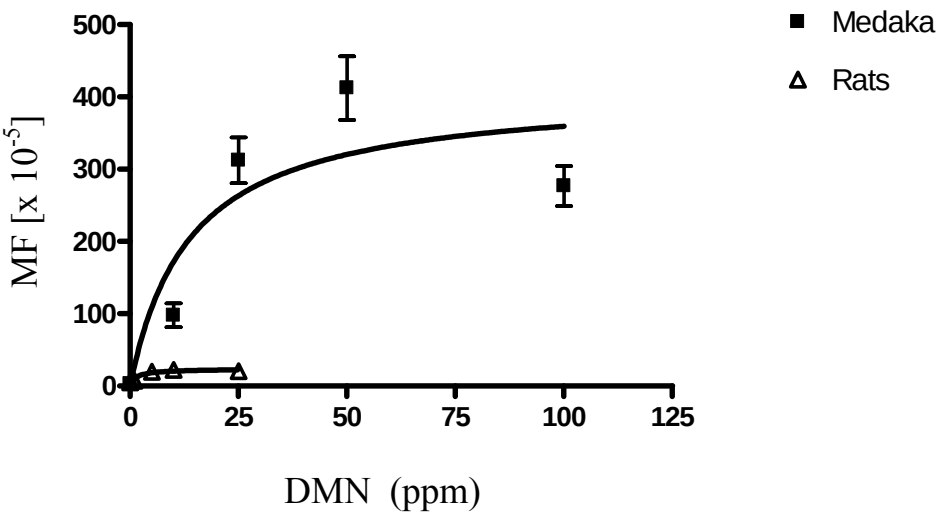

Figure 8. Dose-response comparison of mutant frequencies in λ transgenic medaka and Big Blue® rats exposed to DMN using non-linear regression. An analysis of variance determined the curves to be statistically different at $p<0.0001$ ($p<0.05$ considered significant).

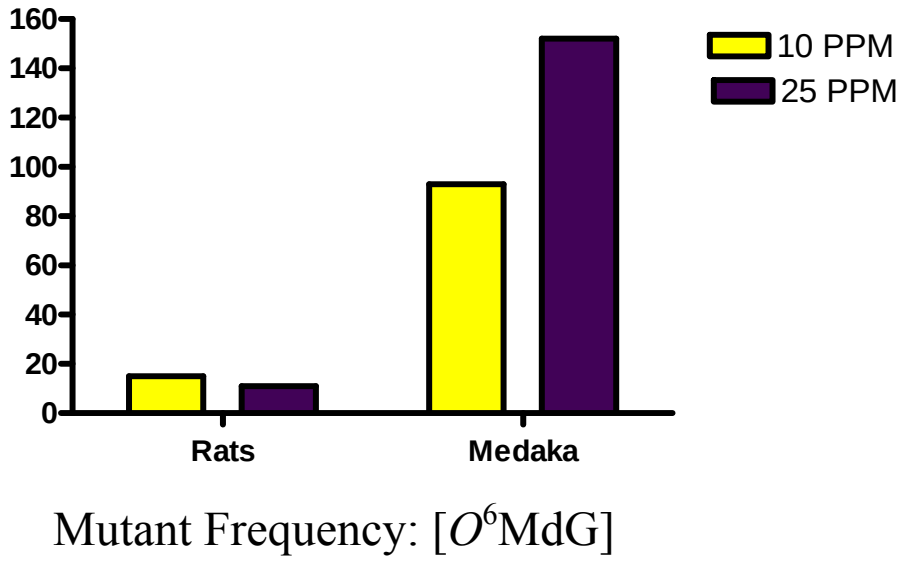

Figure 9. Comparison of the mutant frequency to O^6MeG-adduct ratio for F344 rats and medaka fish exposed to 10 ppm DMN and 25 ppm DMN. Ratio comparisons suggest a more efficient conversion of adducts to mutations by the λ transgenic medaka.

CHAPTER 3:

Hepatocarcinogenesis in Japanese Medaka (Oryzias latipes) Exposed to Dimethylnitrosamine

Kristen R. Hobbie[a,b], Anthony B. DeAngelo[c], J. McHugh Law[a,*]

[a]Comparative Biomedical Sciences Program and Center for Comparative Medicine and Translational Research, College of Veterinary Medicine, North Carolina State University, Raleigh, NC, USA

[b]Integrated Laboratory Systems, Inc., Research Triangle Park, NC, USA

[c]US Environmental Protection Agency, National Health & Environmental Effects Research Laboratory, Research Triangle Park, NC, USA

Abstract

Research has demonstrated the usefulness of small fish as alternative animal models in the testing of chemical toxicity and carcinogenicity. However, the practical application of data acquired from non-mammalian models to humans still remains a concern in the realm of risk assessment. Demonstration of common tissue morphological changes associated with specific biochemical alterations may be one means by which data can be compared across divergent phyletic levels for a given chemical. Dimethylnitrosamine (DMN), an alkylating carcinogen, is used to model human alcoholic cirrhosis and hepatic neoplasia in the rat liver. Progression of DMN-induced hepatic neoplasia is well characterized in the rat, and the pathogenesis by which DMN-induced fibrosis occurs is similar for humans and rodents. TGF-β1 has been associated with hepatic fibrosis and neoplasia in both humans and rodents, and TGF- β1 expression is increased in DMN-exposed rats. TGF-β1 has tumor suppressor activity through growth-inhibition and apoptosis of hepatocytes, and mutations involving the TGF-β1 pathway have been associated with hepatic neoplasia. TGF-β1's role as a profibrotic cytokine and tumor suppressor protein has been documented in humans and rodents, and DMN-induced lesions in rodents are TGF-β1 dependent. DMN is also a potent hepatotoxin and carcinogen in fish, although the progression of morphological changes associated with DMN-exposure is less well characterized than other carcinogens such as diethylnitrosamine (DEN). Mutagenesis studies in DMN-exposed medaka have demonstrated DNA lesions similar to those seen in rodents; however, biochemical alterations associated with progression

of DMN-induced hepatopathology are yet to be described for the medaka fish. We performed parallel exposures in F344 rats and Japanese medaka (*Oryzias latipes*) to the alkylating hepatocarcinogen, dimethylnitrosamine (DMN). In both models, animals were intermittently sacrificed for histopathology, histochemistry, and immunohistochemistry (IHC). No gross or microscopic lesions were noted within the DMN-exposed rats. Lesions in the fish were confined to the liver. Results in the fish included: hepatocellular necrosis, apoptosis, regeneration, and dysplasia; HSC and spindle cell proliferation; hepatocellular and biliary carcinomas; and TGF-β1 expression by dysplastic hepatocytes on IHC. TGF-β1 expression associated with specific morphological changes in livers of DMN-exposed medaka *suggests* a similar cytokine-dependence to that in rodents. Mechanistic comparisons between animal models at different phyletic levels, such as between DMN-exposed medaka and rats, will help facilitate interspecies extrapolations so vital in toxicological risk assessment.

1. Introduction

Exposure to an archetypal carcinogen does not guarantee archetypal histopathology results, especially when comparing animal models as different as fish and rats. Nitrosamines have been some of the most commonly used experimental liver carcinogens, perhaps due to their reliability, potency, and water solubility. Dimethylnitrosamine (DMN) is an alkylating agent well known as both a carcinogen and as an inducer of an alcoholic cirrhosis-like condition in the rat liver.[12,13,35,43] However, while many fish studies have used diethylnitrosamine (DEN), only a few have been reported that used its close cousin, DMN. Recently, we showed some striking differences in the mutagenicity of DMN in fish vs. rats.[21] Thus, in the present study, we sought to determine the step-wise differences in hepatic histomorphology between Japanese medaka (*Oryzias latipes*) and Fischer 344 rats after exposure to DMN.

Small fish models are becoming commonplace in the laboratory, and have been used for decades in chemical toxicity and carcinogenicity testing.[1,18,27,28] Fish may serve as environmental indicators as well as surrogates for human health problems. They have low husbandry costs and mature quickly, facilitating production of large numbers of similarly aged animals for a given study. Small fish species such as the well characterized Japanese medaka are sensitive to a wide variety of chemical carcinogens, have a short time to tumorigenesis, and a low incidence of spontaneous neoplasia.[18,33,27,28] Use of small fish models has increased as pressures to find alternatives to current *in vivo* rodent models have grown. But how do we apply risk assessment data across such divergent phyletic levels as

fish and rats, much less fish and humans? Demonstration of common disease mechanisms, such as chemically-induced biochemical alterations, may facilitate such inter-species extrapolations.

In a previous study, we sought to determine a "molecular equivalent dose" for aqueous dimethylnitrosamine (DMN) exposure between the F344 rat and the medaka model, using DNA adducts and mutant frequencies as surrogates for internal dose.[21] Although DNA adduct levels were comparable between medaka and rats, mutation induction in medaka was many fold higher than that in the rat, suggesting a greater capacity for fish to convert DMN-induced DNA adducts to mutations. Presumably, differences at the molecular level such as mutation induction would manifest as downstream, phenotypic effects in histomorphology.

Nitrosamines may be considered archetypal carcinogens, and DMN is a well established model carcinogen in rodents.[35,43] Tumors associated with DMN-exposure involve the liver, lungs, kidneys and nasal cavity.[43] Liver tumors are the most commonly observed neoplasms, with hepatocellular carcinomas (HCC) the predominant type.[35] DMN is also used in a rodent model of human alcoholic cirrhosis.[12,13] Patterns of DMN-induced liver injury and subsequent repair in the rat liver are similar to those described in humans with alcohol-induced liver disease.[12,19] In the few fish studies that used DMN, liver tumors also predominated. Rainbow trout, zebrafish and guppies had >75% hepatocellular carcinomas, with individual tumor phenotypes of the liver similar to those occurring in rodent studies.[14,24] Behavioral changes in zebrafish and guppies exposed to DMN have been associated with

DMN-induced hepatic injury; however, information regarding biochemical alterations associated with DMN-induced hepatic injury in fish is not known.

Transforming growth factor (TGF)-β1 is the predominant pro-fibrogenic stimulus in DMN-induced fibrosis in the rat and alcoholic cirrhosis in human[7]. Mediation of the fibrogenic response occurs via TGF- β1's cell-signaling protein, Smad-3. Hepatocellular injury induces transdifferentiation of hepatic stellate cells (HSCs) to type-I collagen-producing myofibroblasts-like cells (activated HSCs). TGF-β1 stimulates extracellular matrix (type-1 collagen) production by the activated HSCs. These biochemical events either lead to hepatic repair and lesion resolution or perpetuation of collagenous matrix deposition and cirrhosis.[2,11] In addition to its pro-fibrogenic activity, TGF-β1 affects DMN-induced injury via proliferative and growth-inhibition activities. TGF- β1 has the potential to function both as a tumor suppressor and as a tumor promoter.[9] In humans, cirrhosis often progresses to HCC and these neoplasms frequently display higher levels of TGF- β1 mRNA and protein than found in normal liver.[38] Both TGF-β1 and Smad-3 have been cloned from fish tissues.[8,16] However, the roles that TGF-β1 and Smad-3 play in DMN-induced injury, repair, and carcinogenesis are unknown in these valuable animal models. Thus, in the present study, we sought to characterize DMN-induced hepatic injury and carcinogenesis in medaka fish and determine if the lesions have similar biochemical alterations as those reported for DMN-exposed rats.

2. Materials and Methods

2.1 Chemicals

Dimethylnitrosamine (DMN, $C_2H_6N_2O$; 99.9%, CAS 62-75-9, MW 74.08 g/mol) was purchased from Sigma-Aldrich, St. Louis, MO and stored in a brown bottle sealed within a metal container at 4 ºC. All other chemicals and reagents used throughout the DMN pathology experiment(s) were of the highest purity available from commercial resources.

2.2 Animals

Three-month-old Japanese medaka (*Oryzias latipes*) and one-month-old F344 rats (*Rattus norvegicus*) were used. Male and female, orange-red medaka (outbred, laboratory strain) were obtained from laboratory stocks at Duke University (kind gift from Dr. David Hinton) and Aquatic Research Organisms (Hampton, NH). Male and female, λ transgenic medaka were obtained from in-house populations at the Aquatic Biotechnology and Environmental Laboratory (ABEL), University of Georgia, Athens, GA (USA). Male Fischer 344 rats were obtained from Charles River (Wilmington, MA). Medaka were acclimated for 2 weeks in reconstituted (1 g/L Instant Ocean® salts) reverse osmosis-purified (RO) water within a re-circulating, freshwater culture system under an artificial light photoperiod (16 hours light: 8 hours dark) at a temperature of 26 ± 0.5ºC. Rats were cage housed randomly in rooms maintained on a 12 h light: 12 h dark artificial light photoperiod, and acclimated for 7 days prior to treatment. Animal care and use were in conformity with

protocols approved by the Institutional Animal Care and Use Committee in accordance with the National Academies of Science Guide for the Care and Use of Laboratory Animals.

2.3 DMN Exposures: Medaka

Three groups of medaka were exposed to DMN in the ambient water. The first group consisted of 100 orange-red medaka and 50 λ transgenic medaka, the second of 110 orange-red medaka, and the third, 60 orange-red medaka. All fish were exposed in 4-L glass beakers containing 3 L of reconstituted RO water at 1 g/L salt concentration. For all exposures, medaka were randomly distributed among 4-L glass beakers, 10-12 fish/beaker. Transgenic and non-transgenic medaka were exposed to DMN, separately, during the first exposure. Treatment beakers were placed within a re-circulating, heated water bath to maintain temperature at 26 +/- 0.5 ºC throughout the exposures. The first group of medaka was exposed to 0, 10, 50, 100, or 200 μL/L (ppm) DMN twice weekly for four weeks (Table 1). Due to increased mortality in the 200 ppm DMN group, the second and third exposure groups were exposed to 0, 10, 25, 50 or 100 ppm DMN twice weekly for two weeks. DMN was replaced every 3-4 days to allow for photo-degradation of the compound (S. Revskoy, personal communication).[31] DMN dilutions were made from 1.5 L of a 1000 ppm DMN stock solution prepared new prior to each treatment. Water quality was maintained with 50% water changes prior to each DMN treatment (ammonia levels remained below ~0.02 mg/L). Fish were fed once daily with Aquatox® Flake fish food (Zeigler Brothers, Gardners, PA). Animals were observed twice daily for physiological and behavioral responses and signs of

overt toxicity. Following the 4 week and 2 week exposures, fish from 1st and 2nd exposures were removed from the treatment beakers, gently rinsed in clean water, and replaced into the re-circulating, freshwater culture system for up to 6 months. For the 3rd exposure group, fish designated for DNA adduct isolation were euthanized immediately post-exposure, whereas, fish designated for pathology were grown-out for 1 month in freshwater.

2.4 DMN Exposures: Rats

Thirty male F344 rats (5/ group) were randomized and exposed for 2 weeks to 0, 0.1, 1, 5, 10 or 25 ppm DMN in their drinking water. Rats were maintained at 20-22 °C and 40-60% humidity on a 12-hour light-dark cycle. They were housed 2-3 per cage, and provided Purina Rodent Laboratory Chow (St. Louis, MO) and water ad libitum. DMN dilutions were made from 1000 ppm stock solutions; drinking water bottles containing the control and dosing solutions were changed twice weekly. DMN solutions were administered in brown glass water bottles fitted with Teflon stoppers and stainless steel, double-balled sipper tubes. Animals were observed daily for physiological and behavioral responses and signs of overt toxicity. Mortality and morbidity checks were made twice daily. Body weights and water consumption were measured twice weekly. Following the two week exposure, rats received food and water [alone] for 6 months, maintained under the same housing conditions as previously described.

2.5 Sampling Methodology

Every two months within the six-month grow-out period, a subset of medaka were removed from the experiment, placed into water-filled glass beakers, and euthanized with an over-dose of [dissolved] tricaine methanesulfonate (MS-222, Argent Laboratories, Redmond, WA, USA), except for the third exposure group in which all fish were euthanized 1 month post-exposure (Table 1). The body cavity of each fish was opened along the ventral midline to enhance fixation and embedding. Fish were processed one fish per cassette. Specimens were fixed in 10% neutral buffered formalin for 48 hours, de-mineralized in 10% formic acid for 24 hours, and transferred to 70% ethanol. At study completion, all rats were euthanized in a carbon dioxide chamber and a complete necropsy was performed on each animal. Liver, lung, heart, spleen, kidney, esophagus, trachea, stomach, small intestine, colon, cecum, and urinary bladder were removed from each rat, trimmed and fixed in 10% buffered formalin for a 48-hour period, and transferred to 70% ethanol. Post-fixation, sections of rat tissue (2 mm thick) were placed into cassettes.

2.6 Tissue Processing and Histopathology

All tissues were processed using standard histological techniques. Fish were embedded left side down in paraffin, sectioned at 5 μm, and stained with hematoxylin and eosin (HE). Rat tissues were also embedded in paraffin, sectioned at 5 μm, and stained with HE. Medaka were examined microscopically in multiple para-median and mid-sagittal

sections, with particular emphasis placed on the liver. Multiple sections of liver, lung, kidney and spleen were examined from the rats.

2.7 Histochemistry/ Immunohistochemistry

Additional paraffin tissue sections from fish (3/treatment group) and rats (3/control, 10 ppm and 25 ppm DMN dose groups) were examined via histochemistry and immunohistochemistry. Four-micron sections of the fish were stained with the histochemical stains, Sirius red, Masson's trichrome, and reticulin. Fish tissue stained poorly with Masson's trichrome, so rat tissue was stained with Sirius red and reticulin [only]. Primary antibodies used for immunohistochemistry in fish included cytokeratin (AE1/AE3), α-smooth muscle actin (α-SMA), muscle-specific actin (MSA), glial fibrillary acid protein (GFAP), factor VIII, transforming growth factor (TGF)-β1, and Smad-3 (TGF-β1 signaling protein). Rat tissues were stained for cytokeratin, MSA, GFAP, TGF-β1, and Smad-3 [only]. Cytokeratin, α-SMA, MSA, GFAP, and factor VIII stains were purchased from Ventana Medical Systems (Tucson, AZ, USA) and prepared with the Ventana automated stainer (Ventana Medical Systems, Tucson, AZ, USA), whereas immunohistochemistry for rabbit polyclonal antibodies, TGF-β1 (Santa Cruz Biotechnology Inc, Santa Cruz, CA, USA) and Smad-3 (Abcam, Cambridge, MA, USA) was done manually. Biotinylated goat anti-rabbit and/or biotinylated goat anti-mouse IgG (Biogenex Laboratories Inc., San Ramon, CA, USA) was used as the secondary antibody for TGF-β1 and Smad-3. De-paraffinized tissue sections were treated with 3% hydrogen peroxide for 10 minutes to block endogenous peroxidases

and goat serum for 20 minutes to prevent non-specific binding of the secondary antibody. Tissues were incubated with TGF-β1 (1:500) at 4 °C overnight and Smad-3 (1:100) at room temperature for 30 minutes. Tissues were then rinsed in phosphate-buffered saline (PBS) (0.1M, pH 7.4) and subsequently incubated with the secondary antibody (1:40) for 20 minutes. Tissues were treated for 20 minutes with streptavidin peroxidase. Visualization was achieved by treatment of tissues with liquid 3,3-diaminobenzidine (DAB) chromagen for 30-120 seconds, which in the presence of peroxidase produces a brown precipitate insoluble in alcohol. Slides were rinsed in water and counter-stained with Mayer's hematoxylin for 20-40 seconds. Tissue sections were then dehydrated with alcohol and rinsed in xylene. Slides were cover-slipped with Permount™ Mounting Media (Fischer Scientific, Hanover, IL, USA).

3. Results

3.1 Histomorphologic Findings

In total, 220 fish from the three exposures were examined microscopically for treatment-related lesions (Table 1). Because of unscheduled mortalities in the high dose (200 ppm) fish groups during the first exposure, concentrations ("doses") were adjusted *down* for subsequent exposures to include 100, 50, 25, 10, and 0 ppm DMN. Exclusion of the 200 ppm DMN exposure group and re-adjustment of the exposure period to two weeks decreased the total number of exposure-related deaths to 5% in the second exposure and 0% in the third exposure. Microscopically, 100% of orange-red medaka exposed to 100 ppm DMN 30 days

post-exposure had diffusely necrotic livers. This finding was consistent with Hobbie et al. (2009) in which small, pale, and friable livers were seen grossly in λ transgenic medaka exposed to 100 ppm DMN for two weeks. No difference was noted in the number of exposure-related deaths or DMN-induced pathology for transgenic versus non-transgenic medaka.

No remarkable microscopic abnormalities were seen in tissues other than the liver in medaka. The normal medaka liver is depicted in Figs. 1 & 2. Liver lesions of DMN-exposed medaka were identified and described based on criteria reported by the National Toxicology Program.[3] Degenerative and proliferative changes of the liver were the most prevalent lesions (Figs. 3-11), with neoplasms occurring less often (Figs. 12-17). Degenerative changes in the liver included glycogen loss, hyalinization of hepatocyte cytoplasm, vacuolation of hepatocyte cytoplasm, hepatocellular apoptosis and necrosis, cystic degeneration (*spongiosis hepatis*), and hepatic cysts. Proliferative changes of the liver included hyperplasia of bile ducts, bile pre-ductular epithelial cells (BPDECs), and hepatic stellate cells (HSC); spindle cell hyperplasia with collagen matrix deposition; and foci of altered hepatocytes. DMN-induced neoplasms were predominantly malignant and included hepatocellular carcinoma, cholangiocellular carcinoma, mixed hepatocellular and biliary carcinomas, and spindle cell tumors.

Liver lesions had similar morphology among the three exposure groups (Table 2). The overall incidence and severity of many lesions increased with higher DMN exposure levels for all three exposures. Livers from fish exposed to 10 ppm DMN for four weeks (exposure

1) were histologically normal until the third sacrifice (6-months post-exposure), when degenerative changes became apparent. Some degree of cellular degeneration was apparent at all dose levels and time periods in fish exposed to DMN for two weeks (exposures 2 & 3), although the severity increased with higher DMN doses. More DMN-induced neoplasms were noted in the second exposure group (13/68 fish) compared to the first exposure group (6/105 fish); no neoplasms were present in the third exposure group (Table 3). In the F344 rats, no degenerative, proliferative, or neoplastic lesions of the liver or other examined organs were noted at 6 months post-exposure in animals exposed to 0.1, 1, 5, 10, or 25 ppm DMN in the drinking water for two weeks.

Degenerative changes of the liver in DMN-exposed medaka were characterized by generalized glycogen and/or lipid depletion of hepatocytes (Fig. 3), individual and/or clusters of swollen hepatocytes with vacuolated or glassy, hypereosinophilic (hyalinized) cytoplasm (Figs. 4, 5), and cellular drop-out. With lesion progression, swelling and hyalinization of hepatocytes became more diffuse with loss of the normal hepatic cords and collapse of sinusoids (Fig. 6). Degenerate hepatocytes were often distended by variably sized, hypereosinophilic, intra-cytoplasmic globules. Degenerative changes were variably accompanied by chronic inflammatory infiltrates, predominantly lymphocytes and macrophages. Multifocal regions of necrotic liver were replaced by multiloculated cyst-like structures (cystic degeneration) often comprised of a meshwork of interconnected perisinusoidal cells (HSCs) and/or flocculent eosinophilic material (Fig. 7). Hepatic cysts,

characterized by clear cavities lined by hepatocytes, were less common. Inflammation was occasionally associated with cystic degeneration of the liver and/or hepatic cysts.

With progressive loss of the hepatic parenchyma, BPDECs (purported liver stem cells) and intermediate cells (immature bile duct epithelial cell and/or hepatocytes) proliferated along hepatic plates (Fig. 8), often forming small basophilic tubules (bile ducts and/or regenerative hepatocytes). Proliferating HSCs and/or BPDECs surrounded and "individualized" hepatocytes (satellitosis), giving affected portions of the liver a fenestrated appearance (Fig. 9). As hepatic degeneration became more chronic, multifocal spindle cells (possible myofibroblasts or biliary origin) dissected the hepatic parenchyma, accompanied by bundles of pale, eosinophilic fibrillar matrix (presumed collagen). Often, only this matrix was apparent as fine, pale, eosinophilic fibrillar tendrils multifocally infiltrating between and around hepatocytes (Fig. 6). In addition, proliferation of fibrous connective tissue was accompanied by localized hyperplasia of bile ducts. In some medaka, hepatocytes became dysplastic, increasing dramatically in size with bizarre euchromatic nuclei and large magenta nucleoli (Figs. 5, 9). Dysplastic hepatocytes were sometimes multinucleated with multiple, variably sized nucleoli. As described in Okihiro et al.,[33] "nodular proliferations" of hepatocytes, characterized by distinct borders, loss of the normal hepatic architecture, and megalocytosis and pleomorphism of affected hepatocytes, were present. With progressive hepatotoxicity, cirrhotic-like nodules characterized by nodular accumulations of degenerate hepatocytes surrounded by spindle cells and collagenous connective tissue became more apparent (Fig. 10). Eventually, the hepatic architecture changed remarkably from the normal

single lobe to multinodular, as significant portions of liver were lost and replaced (Fig. 11). Regeneration of the liver was evident, in some fish, as nodular to diffuse replacement of the hepatic parenchyma by plump, densely basophilic and/or amphophilic (regenerative) hepatocytes.

Foci of altered hepatocytes were apparent in DMN-exposed medaka within 90 days post-exposure (Table 3). Eosinophilic foci were more prevalent than basophilic or clear cell foci (9/12 foci). All foci were small, discrete areas of normal hepatocytes, save for the distinct tinctorial change in their cytoplasm. Hepatocytes of clear cell foci had finely vacuolated, clear cytoplasm and centrally placed nuclei. Aside from their tinctorial demarcation, foci otherwise appeared to blend imperceptibly with the surrounding hepatic parenchyma.

Neoplasms included hepatocellular carcinomas (solid, megalocytic, trabecular, and anaplastic variants), mixed carcinomas, and a cholangioma. Neoplasms seen in DMN-exposed fish were predominantly malignant and similar to those described for medaka exposed to diethylnitrosamine (DEN).[33] Hepatocellular carcinomas (HCCs) were the most common neoplasm (12/19) diagnosed in DMN-exposed medaka with solid variants occurring much more often than megalocytic, trabecular, or anaplastic HCCs (Table 3). Mixed (hepatocellular and biliary) carcinomas were the second most prevalent hepatic tumors (6/19). One cholangioma was present. The cholangioma was a small, well-circumscribed, non-encapsulated, expansile mass that compressed the adjacent hepatic parenchyma. It was

comprised of well differentiated bile duct epithelial cells that formed, closely packed, tortuous ducts in a collagenous stroma.

The solid variant of HCC was characterized by replacement of the normal hepatic architecture by diffuse, poorly demarcated sheets of neoplastic hepatocytes (Fig. 8 &12). Neoplastic hepatocytes of solid HCCs were variable in size and shape with abundant amounts of pale, glassy, eosinophilic cytoplasm, and indistinct cell borders. Nuclei were centrally located with lacy chromatin and 1-2 magenta nucleoli. Quite often, neoplastic hepatocytes contained round, euchromatic nuclei with one, large, centrally located nucleolus. Multinucleated neoplastic hepatocytes were fairly common with mitoses variably present. Megalocytic HCC differed from the solid variant in that neoplastic hepatocytes were markedly enlarged and pleomorphic and had larger nuclei (Fig. 13). Trabecular HCCs were characterized by mildly pleomorphic, amphophilic hepatocytes arranged as thick, irregular cords (>2 cells thick) that maintained the general hepatic architecture (Fig. 14). Anaplastic HCC contained highly pleomorphic hepatocytes, varying from spindle to stellate or polygonal in shape (Fig. 15). Anaplastic hepatocytes had indistinct cell borders and were densely but haphazardly arranged. Phenotypic features of neoplastic hepatocytes quite often overlapped among the different variants of HCC; HCC variant was diagnosed based upon the predominant neoplastic feature. Biliary (cholangiocellular) carcinomas were characterized by moderately pleomorphic, small to large cuboidal epithelial cells arranged as irregular ducts or highly pleomorphic, bizarre, angular epithelial cells that formed, poorly defined, tortuous, and infiltrative tubules (Fig. 16). Mixed carcinomas or *hepatocholanicarcinomas*

were comprised of both neoplastic hepatocytes and neoplastic biliary epithelial cells (Fig. 17). These tumors were poorly defined, often large, multinodular masses that replaced most or all of the liver. Neoplastic hepatocytes varied from well differentiated, amphophilic hepatocytes, similar to those of trabecular HCC, to pleomorphic hepatocytes akin to anaplastic HCC with spindle, stellate or polygonal features. Groups of neoplastic hepatocytes would occasionally contain multiple, hypereosinophilic globules within their cytoplasm, similar to that described for degenerative hepatocytes (Fig. 12). The malignant biliary component of mixed carcinomas was similar to that described for cholangiocellular carcinomas (Fig. 16). Neoplastic bile ducts were separated by variable amounts of supporting fibrous stroma. In anaplastic mixed carcinomas, spindyloid hepatocytes and biliary epithelial cells were often difficult to distinguish from each other, blending imperceptibly. One mixed carcinoma was comprised predominantly of finely tapered spindle cells (presumed biliary origin) arranged as densely packed, interweaving fascicles that entrapped multifocal, irregular islands of neoplastic hepatocytes (Fig. 17). In some neoplasms (HCC and/or mixed), small cells with scant eosinophilic cytoplasm and small, hyperchromatic nuclei, consistent with BPDECs, were arranged "single file" in and around neoplastic cells (Fig. 8). Occasionally, these cells would form small acini and thin, irregular ductules within the neoplasm. Usually, degenerative changes similar to those previously described were present in the hepatic parenchyma adjacent to HCCs and/or mixed carcinomas.

3.2 Histochemical and Immunohistochemical Findings

Histochemical and immunohistochemical methods were used to further characterize DMN-induced degenerative, proliferative and neoplastic changes in the Japanese medaka liver and to determine potential mechanisms of action for these changes based on similar changes documented for DMN-exposed rodents. Histochemical and immunohistochemical stains used for these purposes included transforming growth factor (TGF)-β1, Smad-3, cytokeratin, Sirius red, reticulin, α-smooth muscle actin (α-SMA), muscle-specific actin (MSA), factor VIII (Von Willebrands Factor), and glial fibrillary acid protein (GFAP). Function and cellular activity for these stains in the liver of medaka are present in Tables 4. Medaka tissue sections were chosen for special staining based on dose and lesion type. Specific lesions of interest included hepatocellular necrosis/apoptosis, alteration of the hepatic architecture, BPDEC proliferation, HSC hyperplasia, hepatocellular regeneration, spindle cell proliferation, fibrosis, cellular dysplasia, and hepatic neoplasms. Staining of medaka tissue with Factor VIII and α-SMA proved unsuccessful. Although no lesions were grossly or microscopically apparent in the DMN-exposed rats, liver sections from rats in the control, 10 ppm DMN, and 25 ppm DMN groups were also stained for TGF-β1, Smad-3, cytokeratin, Sirius red, reticulin, MSA, and GFAP. Results of histochemical and immunohistochemical staining in livers of medaka are summarized in Tables 5.

Staining of liver tissue for TGF-β1, Smad 3, cytokeratin, Sirius red, reticulin, and MSA in control fish is illustrated in Figs. 18-23. In control fish, faint (1+), positive staining with TGF-β1 was limited to the cytoplasm of multifocal BPDECs positioned at the interface of

hepatocytes and intrahepatic biliary passageways (IHBP; also bile canaliculi) (Fig. 18). Faint (1+) staining with Smad 3 was evident in cytoplasm of hepatocytes directly adjacent to IHBPs (Fig. 19). The cytoplasm of bile ducts and BPDECs stained positively (1+) with cytokeratin (Fig. 20). The collagen in blood vessel walls of control medaka stained positively (2+) with the Sirius red stain (Fig. 21). Myofibroblasts along the perimeter of occasional bile ductules stained positively (1+) with the MSA stain; otherwise, MSA staining was not detected in medaka livers (Fig. 22). The basement membranes of multifocal, large blood vessels and small arterioles stained intensely with the reticulin stain (Fig. 23). The livers of control medaka did not stain with GFAP; however, positive GFAP staining was apparent in the brain and spinal cord of the control fish. In control and DMN-treated rats, faint (1+), positive staining for TGF-β1 was present in the cytoplasm of centrilobular hepatocytes. Faint (1+) staining of Smad 3 was evident in the cytoplasm of hepatocytes throughout the livers of control and DMN-exposed rats, although staining was slightly more intense in centrilobular hepatocytes. Positive Smad 3 staining was predominantly localized to the basolateral surface of rat hepatocytes. As in the fish, blood vessels of rats stained positively for Sirius red (collagen walls) and reticulin (vessel basement membranes). Rat livers stained negatively for cytokeratin, MSA, and GFAP.

Staining for TGF-β1, Smad 3, cytokeratin, Sirius red, reticulin, and MSA in livers of DMN-treated fish is illustrated in Figs. 24-32. Increased staining with TGF-β1 (1 - 4+) was evident in all DMN-treated medaka (Table 5). Positive TGF-β1 staining increased with increasing DMN exposure, although subjectively there was little staining variation between

medaka in the 50, 100, and 200 ppm DMN groups. As in control medaka, BPDECs of treated fish stained for TGF-β1, although the number of BPDECs affected was often markedly increased (Fig. 24). In addition, many intermediate cells, immature hepatocytes and fewer mature hepatocytes stained for TGF-β1, particularly in DMN-treated medaka with degenerative lesions. Cells with similar morphologic features present within hepatic neoplasms also stained for TGF- β1 (Fig. 25). Dysplastic hepatocytes tended to stain consistently for TGF-β1; whereas TGF-β1 staining of neoplastic cells was occasionally decreased. Negative staining of neoplastic cells for TGF-β1 often correlated with negative staining of the same types of cells for Smad 3 (TGF-β1's cell-signaling protein). Sometimes, neoplastic cells stained for TGF- β1, but stained negatively for Smad 3, whereas other neoplasms stained for both TGF- β1 and Smad 3 (Fig. 25, 26). Overall, positive staining with Smad 3 was less distinct and characterized by patchy, cell-specific increases in the amount and intensity of cytoplasmic staining for Smad 3. Occasionally, individual cells demonstrated nuclear staining for Smad 3. Regions of increased Smad 3 staining in DMN-treated fish usually correlated with the general distribution of increased TGF-β1 staining. Increased Smad 3 staining occurred in all DMN treatment groups, except for fish exposed to 10 ppm DMN. Like TGF-β1, staining for cytokeratin was apparent in all treated medaka, although intensity and amount of staining was greater in the 50, 100, and 200 ppm DMN exposure groups. Increased cytokeratin staining usually correlated with increased numbers of BPDECs and intermediate cells present within the affected liver sections (Fig. 27). BPDECs and intermediate cells that stained for cytokeratin often stained for TGF-β1 as well

(Fig. 24). The pale, eosinophilic fibrillar material (presumptive collagen) seen on H&E stain in livers of treated medaka stained positively with the Sirius red histochemical stain (Fig. 28). Pericellular material surrounding degenerative hepatocytes often stained positively for Sirius red (Fig. 29). Staining of the fibrillar material with Sirius red was generally fainter than the staining of blood vessel walls by the same stain. Sometimes this correlated with positive staining with cytokeratin (Fig. 30). Staining for Sirius red was increased only in medaka treated with 50, 100, or 200 ppm DMN. Reticulin staining was increased in livers of medaka evaluated from the 25, 50, 100, and 200 ppm DMN groups. Increased reticular staining was often associated with marked structural changes in the liver, the reticulin stain highlighting a complex network of branching basement membranes (Fig. 31). Rare perisinusoidal cells (presumed HSC) and bile ductule myofibroblasts stained faintly positive (1-2+) with MSA in fish exposed to 50, 100, and 200 ppm DMN (Fig. 32). Occasionally, MSA staining of perisinusoidal cells was accompanied by focal deposition of fibrillar matrix material within the hepatic parenchyma. Positive staining of HSCs with GFAP was not present in any of the livers examined from DMN-treated medaka.

4. Discussion

Pathology is more than what is observed at the tissue level. Thus, determining common mechanisms for specific lesions can help to determine whether a particular animal model is suitable for representing human disease. Small fish models, as bioindicators of environmental health, can provide valuable scientific insight into potential environmental

hazards to human health. Their advantages in numbers, sensitivity to a variety of known carcinogens, and low spontaneous tumor rate make them an ideal alternative to traditional rodent carcinogenicity assays, particularly with regard to low dose chemical exposures.[18,27,28,33] However, more comparative data across phyletic levels is necessary to validate the use of fish as models for specific human diseases.

In a previous study, we sought to determine the "molecular equivalent dose" for aqueous nitrosamine exposure between two commonly used laboratory animals, the F344 rat and the Japanese medaka.[21] Using DMN-induced DNA adducts and mutant frequencies as surrogates for hepatic molecular dose, we made dose comparisons between the two species by using fold differences in apparent compound potency at the common molecular level. The purpose of our current study was to compare DMN-induced hepatopathology between medaka fish and F344 rats and to determine common biochemical mechanisms in order to improve toxicological comparisons between different animal models.

DMN-induced liver injury in rats is considered a good and reproducible model for studying biochemical and pathophysiological alterations associated with the development of hepatic fibrosis/cirrhosis and neoplasia in human beings.[12,13] The tissue pathological changes of DMN-induced fibrosis in rats are reported to include massive centrilobular hepatocellular necrosis, collapse of the liver parenchyma, congestion and hemorrhage, fibrillar (*collagenous*) septa formation, cirrhotic nodules, hepatocellular regeneration, and specific biochemical abnormalities.[12,19] However, more detailed data on DMN-induced hepatic injury in fish has not been reported.

To compare the progression of DMN-induced liver injury and carcinogenesis in medaka to that reported for DMN-exposed rats and to determine common DMN-induced biochemical and pathophysiological alterations between the two species, medaka fish were exposed to various DMN concentrations in their ambient water for two or four weeks and intermittently sacrificed over a period of six months. Since juvenile F344 rats had also been exposed to DMN in a parallel experiment to measure DNA adducts and mutations[21], we examined liver sections from these animals as well. However, probably because the dose levels we chose for the rats in that experiment were very conservative, no treatment-associated morphological changes were apparent at six months post-exposure. Depending upon the desired endpoint, DMN exposure protocols for rats include intra-peritoneal injections of DMN for 3 days to induce hepatic fibrosis and lengthy drinking water exposures (1-1.5 years) to induce carcinogenesis. A species-specific difference in the effective DMN dose and time to effect was a challenge in directly comparing DMN-induced lesions of medaka and rats. Nonetheless, we can still compare the well-established, published reports of DMN-induced liver pathology in rats to the DMN-associated liver lesions described in the medaka from our current study.

Neoplasms occurred much less frequently in DMN-exposed medaka than degenerative lesions. However, the specific types of tumors (hepatocellular and/or biliary origin) were consistent with those reported for rats exposed at length to DMN in their drinking water (Table 3). Similar to Peto et al., the predominant hepatic neoplasms in DMN-exposed medaka were hepatocellular carcinomas.[35] However, unlike the rat, neoplasms involving

other tissues, such as kidney, were not found in medaka exposed to DMN. More neoplasms were noted in medaka exposed to DMN for two weeks versus medaka exposed to DMN for four weeks. Cutroneo et al.[6] noted that excessive fibrosis and formation of benign tumors was associated with persistent expression of TGF-β1. TGF-β1 expression may have been prolonged in livers of medaka exposed to DMN for four weeks, thereby favoring promotion of fibrosis and inhibition of neoplasia (proliferation of phenotypically altered hepatocytes) in these animals. The four-week DMN exposure protocol may also have selected for more tumor-resistant fish or fish that would have developed tumors died prior to tumor formation (higher mortalities were experienced with this protocol).

Changes in the liver similar to those in rats given 3-day DMN intra-peritoneal injections were apparent in medaka exposed to DMN for two and four weeks. These lesions included progressive hepatic necrosis, collapse of the hepatic architecture, inflammation, BPDEC (stem cell) hyperplasia, hepatic stellate cell hyperplasia, perisinusoidal collagen deposition, biliary duct hyperplasia and fibrosis, hepatocellular regeneration, and multi-nodular re-structuring of the liver (Table 2) (Figs. 3-11). Lesion patterns, such as centrilobular necrosis and bridging (septal) fibrosis were absent in the medaka due to differences in the structure of the medaka liver versus rat (mammalian) liver. Medaka livers have the same cellular constituents and same basic structural/functional unit (portal tract, afferent blood flow and efferent bile flow, central/ hepatic vein, and hepatic muralia) as rats. However, mammalian livers are comprised of many lobules with multiple "functional units," whereas the medaka liver is a single lobule with one "functional unit."[15] In mammals, the

enzyme responsible for the biotransformation of DMN (P450 2E1) is more concentrated in the centrilobular hepatocytes, increasing their susceptibility to DMN's hepatotoxic effects. DMN-induced centrilobular necrosis is an example of metabolic zonation in the mammalian liver.[20] Fish have a relatively homogeneous distribution of cytochrome P450s in their livers and, therefore, no metabolic zonation.[46] The diffuse distribution of biotransforming enzymes in medaka livers is presumably responsible for the random distribution of DMN-induced hepatocellular necrosis. Cirrhotic-like nodules similar to those which occur in DMN-exposed rats were present in some DMN-exposed medaka (Fig. 10), although predictably no consistent pattern of fibrosis was present given that the medaka liver is one functional unit (lobule).[15] Initial collagen deposition was similar between medaka and rats.[22] In medaka, collagen was deposited early as a fine, fibrillar matrix along the reticular framework of the denuded hepatic parenchyma. Matrix deposition was often accompanied by arrangement of spindle-shaped cells along residual reticular fibers. These same cells surrounded individual and/or clusters of degenerate hepatocytes (satellitosis) (Fig. 9). A similar pattern of spindle cell proliferation has been reported in livers of Sprague-Dawley rats and Wistar rats exposed to DMN.[17,22] According to Jin et al., spindyloid hepatic stellate cells (activated HSCs) migrate along the residual reticular framework of the necrotic liver.[22] Early evidence of fibrosis was associated with diffuse distribution of the activated HSCs along the hepatic sinusoids in livers of DMN-exposed Wistar rats. Hepatic stellate cells are present in the medaka liver.[46] Laurén et al. noted that the stellate processes of quiescent HSCs form the framework in which hepatocytes reside in the medaka liver.[25] However, it is unclear on

H&E whether the "spindle-shaped" cells present in livers of DMN-exposed medaka represent activated HSCs, proliferating BPDECs, or a mixture of both (Fig. 9). In acutely necrotic livers of DMN-exposed medaka, hepatocellular loss was associated with maintenance of a "honey-comb" reticular framework, which may represent the stellate processes of HSCs that surround hepatocytes in these animals.

The biochemical alterations associated with DMN-induced hepatic injury and fibrosis in rats are well characterized and similar to what occurs in alcoholic cirrhosis in humans.[11,12,14] Transforming growth factor (TGF)-β1 is the predominant pro-fibrogenic stimulus. Reactive oxygen intermediates (ROI) released from macrophages and injured hepatocytes stimulate transdifferentiation of quiescent hepatic stellate cells (HSCs) to contractile myofibroblasts. Injured endothelial cells convert latent TGF-β1 to the active, fibrogenic form through the activation of plasmin. TGF-β1 stimulates extracellular matrix (type-1 collagen) production by activated hepatic stellate cells. Smad 3, a cell-signaling protein of TGF-β1, is the mediator of TGF-β1's fibrogenic response, combining with other Smad proteins and translocating to the nucleus to affect gene transcription.[10,37] Activation of HSCs involves a phenotypic change and up-regulation of α-smooth muscle actin (SMA), an indication of their ECM-producing capabilities.[23] HSCs lay down collagen to facilitate healing of the hepatic parenchyma. The liver parenchyma either regenerates and/or chronic injury leads to excessive matrix deposition and cirrhosis.[2,11] TGF-β1 also has an anti-proliferative effect.[10] Hepatic progenitor cells are more sensitive to TGF-β1 expression than oval cells (stem cells) in rats. Presumably, the injured hepatic parenchyma is replaced via

oval cell lineage and not hepatic progenitor cells due to their suppression by TGF-β1.[32] TGF-β1 and Smad 3 are also potent inhibitors of cell progression at the G1 phase.[30] Altered regulation of TGF-β1 is thought to be important in some cases of HCC.[2] In the present study, histochemical and immunohistochemical stains were used to determine if similar biochemical alterations were present in the livers of DMN-exposed medaka to those processes known to occur in rats exposed to DMN and human alcoholic cirrhosis. Although positive staining is not definitive evidence of genetic expression, it does suggest up-regulation of cellular markers that may be indicative of a DMN-induced response in fish tissue. Medaka and rat tissue were stained for TGF-β1, Smad 3, Cytokeratin (AE1/AE3), Sirius red, reticulin, muscle specific actin (MSA), and glial fibrillary acidic protein (GFAP). Initial attempts at staining medaka tissue with α-SMA and Factor VIII were unsuccessful and were not included in the final staining regimen. Control and DMN-treated rats stained negatively for all histochemical and immunohistochemical stains, which was consistent with the lack of DMN-induced lesions seen on HE. Presumably, the DMN doses and/or exposure periods were not sufficient to induce hepatic injury and/or subsequent hepatic neoplasia in our DMN-exposed F344 rats.

Livers of DMN-exposed medaka stained positively with the TGF-β1 antibody. Positive staining was evident in the cytoplasm of bile preductular epithelial cells (BPDECs), intermediate cells, immature hepatocytes, and mature hepatocytes. This is in comparison to control fish, in which only scattered BPDECs stained positively for TGF-β1. The staining of hepatocytes for TGF-β1 associated with DMN-induced injury in medaka livers is similar to

that which occurs in rats and humans and suggests a role for this cytokine in hepatic repair mechanisms in fish.[5,42] In control rats, only Kupffer cells and sinusoidal endothelial cells stain positively in the normal liver. It is unclear why BPDECs stain positively for TGF-β1 in the livers of control medaka. It has been reported that cholangiocytes are a source of the pro-fibrogenic cytokine, TGF-β2, an isoform of TGF-β1.[36] The TGF-β1 antibody used on medaka livers, although labeled as TGF-β1-specific, has cross-reactivity with TGF-β2. It is possible that the TGF-β1 antibody was linking with TGF-β2 on the cell surfaces of BPDECs in the control fish. However, staining of BPDECs for TGF-β1 in DMN-exposed medaka was increased in comparison to control fish. In rats, bile duct ligation induces proliferation of biliary epithelial cells that stain strongly positive for TGF-β1; these cells promote fibrogenesis via transdifferentiation of peribiliary fibroblasts and HSCs.[44] It is possible that the positive staining of BPDECs with TGF-β1 indicates TGF-β1 expression by these cells, *not* cross-reactivity with TGF-β2, and potentially a fibrogenic role for BPDECs in DMN-exposed medaka. In addition, many BPDECs and intermediate cells stained positively for TGF- β1 and Smad 3 within neoplastic foci of DMN-exposed medaka (Figs. 25, 26). In the 'Solt-Farber' and choline deficiency carcinogenic protocols, designed to study the development and relationship of foci and nodules as precursor lesions to HCC, bipolar ductal progenitor cells and small periductal cells appear to be the HCC cells of origin.[40] Positive staining of BPDECs and intermediate cells in hepatic neoplastic nodules of some DMN-exposed medaka may indicate a stem cell origin for hepatic neoplasms in these animals. This is in contrast to HCCs arising from phenotypically altered and dysplastic hepatocytes.[45]

Positive staining with Smad 3 was less definitive in DMN-exposed medaka; however, general patterns of increased hepatocellular cytoplasmic and nuclear staining corresponded with regions of increased hepatocellular and/or biliary staining with TGF-β1. This is consistent with that reported for TGF-β1 and Smad 3 expression in hepatocytes of human patients with chronic liver disease.[5] Nuclear staining, indicating translocation of Smad 3 to the hepatocyte nucleus, was rare but present in some liver sections of DMN-exposed medaka. Some fish demonstrated decreased staining of neoplastic cells associated with increased staining of TGF- β1 suggesting disruption of the TGF- β1 pathway and loss of responsiveness to TGF- β1's antiproliferative effects. It is thought that altered regulation of TGF-β1 (decreased inhibition to growth inhibitory signals) and not decreased expression is responsible for formation of some HCCs in humans.[2,38] In one fish, however, TGF-β1 and Smad 3 staining was decreased in neoplastic hepatocytes (HCC), suggesting decreased expression of TGF- β1 in the neoplasm of this fish.

Proliferating BPDECs and intermediate cells stained intensely with cytokeratin antibody (Figs. 27, 30). In some liver sections, these cells were numerous and their staining was quite extensive. Cytokeratin-positive BPDECs and intermediate cells densely infiltrated the hepatic parenchyma along hepatic plates and the denuded reticular framework, supporting the hypothesis that they play a vital role in regeneration of the hepatic parenchyma.[34] Often a fine, fibrillar network of collagen, evident with the Sirius red stain, accompanied the parenchymal infiltration of BPDECs and intermediate cells (Fig. 29). It is possible that TGF-β1 expression by these cells induced a fibrogenic response by local, transdifferentiated HSCs

and/or peribiliary fibroblasts. Thicker bands of collagen were also evident with the Sirius red stain (Fig. 28), occasionally accompanied by spindle cell proliferation (presumed biliary origin). Increased staining of type III collagen (reticular) fibers by the reticulin silver stain often correlated with Sirius red staining, consistent with increased collagen matrix deposition and restructuring of the hepatic architecture in response to DMN-induced hepatic injury (Fig. 31). Perisinusoidal staining with MSA in DMN-treated medaka was marginally successful (Fig. 32). This was consistent with that reported by Bunton for medaka exposed to diethylnitrosamine (DEN) and methylazoxymethanol acetate (MAM-Ac).[4] Periductal staining of fibroblasts with MSA was often more apparent than positive perisinusoidal staining, suggestive of activated HSCs, although positive staining of activated HSC with MSA only occurred in DMN-treated fish and not in controls. Jin et al. noted that positive staining of activated HSCs with α-SMA in DMN-exposed Wistar rats was time-dependent.[22] Activated HSCs migrating into the necrotic hepatic parenchyma stained for α-SMA at day 5 post-DMN injection; however, activated HSCs were negative at 14 days post-injection when the necrotic parenchyma was replaced by regenerating hepatocytes and fibrosis. It is possible that MSA-expression by activated HSCs in DMN-exposed medaka is also time-dependent and that positive staining of HSCs with MSA would have been more significant at an early time point. In mammals, quiescent HSCs stain positively for glial fibrillary acidic protein (GFAP). Medaka HSCs did not stain with GFAP stain in either control or DMN-injured livers; however, GFAP successfully stained neural tissue in treated and control medaka. Negative staining of HSCs with GFAP may indicate structural and/or functional differences

between medaka (or fish) HSCs and mammalian HSCs. Quiescent HSCs in codfish have been reported to stain positively for cytokeratin.[41] Intense pericellular staining occurred with the cytokeratin antibody in DMN-exposed medaka (Fig. 30); however, it is unlikely that this represents positive staining of transdifferentiated HSCs (myofibroblast phenotype) for cytokeratin, since quiescent (epithelial phenotype) HSCs did not stain for cytokeratin in control medaka.

5. Summary

Our goal from this study was to determine (descriptively and mechanistically) if DMN-induced hepatic injury and carcinogenesis in medaka were comparable to DMN-induced hepatic cirrhosis and carcinogenesis in rats. Despite differences in the hepatic architecture of medaka and rats, we found that DMN-induced pathology was similar in both species, particularly when evaluated at the cellular level. Although transcriptional evidence (such as obtained by RT-PCR) is necessary for more definitive conclusions of comparable biochemical alterations (i.e. alterations in TGF-β1 expression) for DMN-exposed medaka and rats, the histochemical and immunohistochemical data suggest a similar mechanism for repair of DMN-induced hepatic injury. Correlation of hepatic neoplasia in DMN-treated medaka with previously reported mutant frequencies for similarly exposed fish (Hobbie et al., 2009) suggests a common pathogenesis for hepatic neoplasia to that historically reported for the rat. In addition, the remarkable hepatic necrosis apparent in DMN-exposed medaka suggests that cell proliferation with clonal expansion of mutated cells was likely responsible

for the significant increase in MF seen with DMN-exposed λ transgenic medaka (Hobbie et al., 2009). Pathology comparisons accompanied by mechanistic data, such as mutation spectra, will help inter-species comparisons across divergent phylogenies.

Acknowledgements

The authors thank Monica Mattmuller (NCSU) and Michael George (EPA) for their excellent technical assistance. This work was supported by NCSU College of Veterinary Medicine state appropriated funds and the NCSU/EPA Cooperative Training Program in Environmental Health Sciences, Research Training Agreement CT826512010.

REFERENCES

1. Bailey GS, Williams DE, Hendricks, JD: Fish models for environmental carcinogenesis: the rainbow trout. Environmental Health Perspectives 104 (Suppl 1): 5-21, 1996.

2. Bissell DM, Roulot D, George J: Transforming growth factor β and the liver. Hepatology 34: 859-867, 2001.

3. Boorman GA, Botts S, Bunton TE, Fournie JW, Harshbarger JC, Hawkins WE, Hinton DE, Jokinen MP, Okihiro MS, Wolfe MJ: Diagnostic criteria for degenerative, inflammatory, proliferative nonneoplastic and neoplastic liver lesions in medaka (*Oryzias latipes*): consensus of a National Toxicology Program pathology working group. Toxicol Pathol 25: 202-210, 1997.

4. Bunton TE: Expression of actin and desmin in experimentally induced hepatic lesions and neoplasms from medaka (Oryzias latipes). Carcinogenesis 16:1059-1063, 1995.

5. Calabrese F, Valente M, Giacometti C, Pettenazzo E, Benvegnu L, Alberti A, Gatta A, Pontisso P: Parenchymal transforming growth factor beta-1: Its type II receptor and Smad signaling pathway correlate with inflammation and fibrosis in chronic liver disease of viral etiology. J of Gastroenterology and Hepatology 18: 1302-1308, 2003.

6. Cutroneo KR, White SL, Chiu J-F, Ehrlich HP: Tissue fibrosis and carcinogenesis: divergent or successive pathways dictate multiple molecular therapeutic targets for oligo decoy therapies. Journal of Cellular Biochemistry 97: 1161-1174, 2006.

7. De Gouville A-C, Boullay V, Krysa G, Pilot J, Brusq J-M, Loriolle F, Gauthier J-M, Papworth SA, Laroze A, Gellibert F, Huet S: Inhibition of TGF- β signaling by an ALK 5 inhibitor protects rats from dimethylnitrosamine-induced liver fibrosis. British Journal of Pharmacology 145: 166-177, 2005.

8. Dick A, Mayr T, Hermann B, Meier A, Hammerschmidt M: Cloning and characterization of zebrafish *smad2*, *smad3* and *smad4*. Gene 246: 69-80, 2000.

9. Elliot EL, Blobe GC: Role of transforming growth factor beta in human cancer. Journal of Clinical Oncology 23:2078-2093, 2005.

10. Flanders KC: Smad3 as a mediator of the fibrotic response. Int J Exp Path 85: 47-64, 2004.

11. Friedman SL: Molecular regulation of hepatic fibrosis, an integrated cellular response to injury. The Journal of Biological Chemistry 275: 2247-2250, 2000.

12. George J: Mineral metabolism in dimethylnitrosamine-induced hepatic fibrosis. Clinical Biochemistry 39: 984-991, 2006.

13. George J, Tsutsumi M, Takase S: Expression of hyaluronic acid in *N*-nitrosodimethylamine induced hepatic fibrosis in rats. The International Journal of Biochemistry & Cell Biology 36: 307-319, 2004.

14. Grieco MP, Hendricks JD, Scanian RA, Sinnhuber RO, Pierce DA: Carcinogenicity and acute toxicity of dimethylnitrosamine in Rainbow Trout (*Salmo gairdneri*). J Natl Cancer Inst 60: 1127-1131, 1978.

15. Hardman RC, Volz DC, Kullman SW, Hinton DE: An in vivo look at vertebrate liver architecture: three-dimensional reconstructions from medaka (Oryzias latipes). The Anatomical Record 290:770-782, 2007.

16. Harms CA, Kennedy-Stoskopf S, Horne WA, Fuller FJ, Tompkins WAF: Cloning and sequencing hybrid striped bass (Morone saxatilis x M. chrysops) transforming growth factor-β (TGF- β), and development of a reverse transcription quantitative competitive polymerase chain reaction (RT-qcPCR) assay to measure TGF- β mRNA of teleost fish. Fish & Shellfish Immunology 10: 61-85, 2000.

17. Hata J, Ikeda E, Uno H, Asano S: Expression of hepatocyte growth factor mRNA in rat liver cirrhosis induced by N-nitrosodimethylamine as evidenced by in situ RT-PCR. The Journal of Histochemistry & Cytochemistry 50: 1461-1468, 2002.

18. Hawkins WE, Walker WW, Fournie JW, Manning CS, Krol RM: Use of the Japanese medaka (*Oryzias latipes*) and Guppy (*Poecilia reticulata*) in carcinogenesis testing under National Toxicology Program protocols. Toxicologic Pathology 31(Suppl 1): 88-91, 2003.

19. He J-Y, Ge W-H, Chen Y: Iron deposition and fat accumulation in dimethylnitrosamine-induced liver fibrosis in rat. World J Gastroenterol 13: 2061-2065, 2007.

20. Hinton DE, Segner H, Braunbeck T: Toxic responses of the liver. In: Target Organ Toxicity in Marine and Freshwater Teleosts, ed. Schlenk D and Benson WH, 1st ed., pp. 224-261. Taylor & Francis, New York, NY, 2001.

21. Hobbie KR, DeAngelo AB, King LC, Winn RN, Law JM: Toward a molecular equivalent dose: use of the medaka model in comparative risk assessment. Comparative Biochemistry and Physiology, Part C 149: 141-151, 2009.

22. Jin Y-L, Enzan H, Kuroda N, Hayashi Y, Nakayama H, Zhang Y-H, Toi M, Miyazaki E, Hiroi M, Guo L-M, Saibara T: Tissue remodeling following submassive hemorrhagic necrosis in rat livers induced by an intraperitoneal injection of dimethylnitrosamine. Virchows Arch 442:39-47, 2003.

23. Kang JS, Morimura K, Salim EI, Wanibuchi H, Yamaguchi S, Fukushima S: Persistence of liver cirrhosis in association with proliferation of nonparenchymal cells and altered location of α-smooth muscle actin-positive cells. Toxicologic Pathology 33:329-335, 2005.

24. Khudoley VV: Use of Aquarium Fish, Danio rerio and Poecilia reticulata, as Test Species for Evaluation of Nitrosamine Carcinogenicity. National Cancer Institute Monograph 65:65-70, 1984.

25. Laurén DJ, The SJ, Hinton DE: Cytotoxicity phase of diethylnitrosamine-induced hepatic neoplasia in medaka. Cancer Research 50:5504-5514, 1990.

26. Law, JM: Mechanistic considerations in small fish carcinogenicity testing. ILAR Journal 42:274-284, 2001.

27. Law, JM: Issues related to the use of fish models in toxicologic pathology: session introduction. Toxicologic Pathology 31 (Suppl):49-52, 2003.

28. Lim Y-S, Kim K-A, Jung J-O, Yoon J-H, Suh K-S, Kim CY, Lee H-S: Modulation of cytokeratin expression during in vitro cultivation of human hepatic stellate cells: evidence of transdifferentiation from epithelial to mesenchymal phenotype. Histochem Cell Biol 118:127-136, 2002.

29. Lowes KN, Croager EJ, Olynyk JK, Abraham LJ, Yeoh GCT: Oval cell-mediated liver regeneration: Role of cytokines and growth factors. Journal of Gasteroenterology and Hepatology 18:4-12, 2003.

30. Matsuura I, Denissova NG, Wang G, He D, Long J, Liu F: Cyclin-dependent kinases regulate the antiproliferative function of Smads. Letters to Nature 430: 226-231, 2004.

31. Mizgireuv IV, Majorova IG, Gorodinskaya VM, Khudoley VV, Revskoy SY: Carcinogenic effect of N-nitrosodimethylamine on diploid and triploid zebrafish (Danio rerio). Toxicologic Pathology 32:514-518, 2004.

32. Nguyen LN, Furuya MH, Wolfraim LA, Nguyen AP, Holdren MS, Campbell JS, Knight B, Yeoh GCT, Fausto N, Parks, WT: Transforming growth factor-beta differentially regulates oval cell and hepatocyte proliferation. Hepatology 45:31-41, 2007.

33. Okhiro MS, Hinton DE: Progression of hepatic neoplasia in medaka (Oryzias latipes) exposed to diethylnitrosamine. Carcinogenesis 20:933-940, 1999.

34. Okhiro MS, Hinton DE: Partial hepatectomy and bile duct ligation in rainbow trout (Oncorhynchus mykiss): Histologic, immunohistochemical and enzyme histochemical characterization of hepatic regeneration and biliary hyperplasia. Toxicologic Pathology 28:342-356, 2000.

35. Peto R, Gray R, Brantom P, Grasso P: Effects on 4080 rats of chronic ingestion of N-nitrosodiethylamine or N-nitrosodimethylamine: A detailed dose-response study. Cancer Research 51:6415-6451, 1991.

36. Popov Y, Patsenker E, Fickert P, Trauner M, Schuppan D: Mdr2 (Abcb4)-/- mice spontaneously develop severe biliary fibrosis via massive dysregulation of pro- and antifibrogenic genes. Journal of Hepatology 43:1045-1054, 2005.

37. Roberts AB, Tian F, DaCosta Byfield S, Stuelten C, Ooshima A, Saika S, Flanders KC: Smad3 is key to TGF-β-mediated epithelial-to-mesenchymal transition, fibrosis, tumor suppression and metastasis. Cytokine & Growth Factor Review 17:19-27, 2006.

38. Rossmanith W, Schulte-Hermann R: Biology of transforming growth factor β in hepatocarcinogenesis. Microscopy Research and Technique 52:430-436, 2001.

39. Sato Y, Harada K, Ozaki S, Furubo S, Kizawa K, Sanzen T, Yasoshima M, Ikeda H, Sasaki M, Nakanuma Y: Cholangiocytes with mesenchymal features contribute to progressive hepatic fibrosis of the polycystic kidney rat. The American Journal of Pathology 171: 1859-1871, 2007.

40. Sell S: Cellular origin of hepatocellular carcinomas. Cell & Developmental Biology 13:419-424, 2002.

41. Senda T, Nomura R: The expression of cytokeratin in hepatic stellate cells of the cod. Arch Histol Cytol 66:437-444, 2003.

42. Song S-L, Gong Z-J, Zhang Q-R, Huang T-X: Effects of Chinese traditional compound, JinSanE, on expression of TGF- β1 and TGF- β1 type II receptor mRNA, Smad3 and Smad7 on experimental hepatic fibrosis *in vivo*. World J Gasterenterol 11:2269-2276, 2005.

43. Souliotis VL, Chhabra S, Anderson LM, Kyrtopoulos SA: Dosimetry of O^6-methylguanine in rat DNA after low-dose, chronic exposure to N-nitrosodimethylamine (NDMA). Implications for the mechanism of NDMA hepatocarcinogenesis. Carcinogenesis 16:2381-2387, 1995.

44. Tao L-H, Enzan H, Hayashi Y, Miyasaki E, Saibara T, Hiroi M, Toi M, Kuroda N, Naruse K, Jin Y-L, Guo L-M: Appearance of denuded hepatic stellate cells and their subsequent myofibroblasts-like transformation during the early stage of biliary fibrosis in the rat. Med Electron Microsc 33:217-230, 2000.

45. Thorgeirsson SS, Grisham JW: Molecular pathogenesis of human hepatocellular carcinoma. Nature Genetics 31:339-346, 2002.

46. Wolf JC, Wolfe MJ: A brief overview of nonneoplastic hepatic toxicity in fish. Toxicologic Pathology 33: 75-85, 2005.

Table 1. DMN Pathology Exposures in Medaka Fish and Rats

Medaka Exposure	**Medaka Strain**	**Number of Fish**	**DMN Doses (ppm)**	**Exposure Length**	**Grow-out Period**	**Sacrifice(s)**
1	*cII* Transgenic	50	0, 10, 50, 100, 200	4 weeks	6 months	3
1	Orange-Red	100	0, 10, 50, 100, 200	4 weeks	6 months	3
2	Orange-Red	110	0, 10, 25, 50, 100	2 weeks	6 months	3
3	Orange-Red	60	0, 10, 25, 50, 100	2 weeks	1 month	1
Rat Exposure	**Rat Strain**	**Number of Rats**	**DMN Doses (ppm)**	**Exposure Length**	**Grow-out Period**	**Sacrifice(s)**
1	F344	30	0, 0.1, 1, 5, 10, 25	2 weeks	6 months	1

Table 2. Degenerative and proliferative hepatic lesions in medaka per DMN exposure and sacrifice.

Group/Dose/ Days PE[1]	Cellular Deg.[2]	Necrosis/ Apoptosis	Architectural Change	BPDEC Prolif.[3]	Stellate Cells⇧	Bile Duct Hyperplasia	Fibrosis/ Spindle Cell⇧	Cellular Dysplasia	Liver Regener.[4]
I/200/30d	3/6	6/6	6/6	4/6	4/6	4/6	2/6	1/6	0/6
I/100/30d	6/10	6/10	6/10	7/10	6/10	5/10	2/10	2/10	0/10
I/50/30d	3/8	0/8	1/8	1/8	1/8	3/8	1/8	1/8	0/8
I/10/30d	0/8	0/8	0/8	0/8	0/8	0/8	0/8	0/8	0/8
I/0/30d	0/9	0/9	0/9	0/9	0/9	0/9	0/9	0/9	0/9
I/200/90d	0/0	0/0	0/0	0/0	0/0	0/0	0/0	0/0	0/0
I/100/90d	4/6	5/6	3/6	2/6	1/6	4/6	3/6	2/6	0/6
I/50/90d	5/9	5/9	3/9	1/9	1/9	2/9	3/9	2/9	1/9
I/10/90d	0/8	0/8	0/8	0/8	0/8	0/8	0/8	0/8	0/8
I/0/90d	0/9	0/9	0/9	0/9	0/9	0/9	0/9	0/9	0/9
I/200/150d	0/0	0/0	0/0	0/0	0/0	0/0	0/0	0/0	0/0
I/100/150d	3/3	2/3	3/3	0/3	0/3	0/3	1/3	1/3	3/3
I/50/150d	7/10	5/10	3/10	2/10	1/10	3/10	1/10	3/10	2/10
1/10/150d	3/9	0/9	0/9	0/9	0/9	3/9	0/9	0/9	1/9
I/0/150d	1/10	0/10	0/10	0/10	0/10	2/10	0/10	0/10	0/10
II/100/60d	4/4	3/4	3/4	3/4	2/4	2/4	2/4	2/4	2/4
II/50/60d	3/4	2/4	1/4	0/4	0/4	1/4	1/4	0/4	0/4
II/25/60d	3/6	2/6	1/6	0/6	0/6	0/6	0/6	1/6	0/6
II/10/60d	2/6	1/6	0/6	0/6	0/6	0/6	0/6	0/6	0/6
II/0/60d	1/5	0/5	0/5	0/5	0/5	0/5	0/5	0/5	0/5
II/100/120d	2/2	1/2	2/2	1/2	1/2	1/2	2/2	2/2	0/2
II/50/120d	4/4	2/4	2/4	0/4	0/4	1/4	1/4	1/4	0/4
II/25/120d	2/5	0/5	1/5	0/5	0/5	0/5	0/5	0/5	0/5
II/10/120d	0/4	0/4	0/4	0/4	0/4	0/4	0/4	0/4	0/4
II/0/120d	1/5	0/5	0/5	0/5	0/5	0/5	0/5	0/5	0/5
II/100/180d	4/4	3/4	2/4	2/4	1/4	3/4	2/4	0/4	0/4
II/50/180d	3/4	2/4	3/4	2/4	1/4	1/4	2/4	1/4	0/4
II/25/180d	4/5	3/5	1/5	1/5	0/5	2/5	1/5	1/5	0/5
II/10/180d	2/4	0/4	0/4	0/4	0/4	1/4	0/4	0/4	0/4
II/0/180d	0/6	0/6	0/6	0/6	0/6	0/6	0/6	0/6	0/6
III/100/30d	4/5	5/5	5/5	5/5	5/5	4/5	3/5	5/5	1/5
III/50/30d	8/10	4/10	10/10	10/10	8/10	6/10	9/10	8/10	3/10
III/25/30d	5/12	1/12	2/12	3/12	2/12	3/12	1/12	0/12	0/12
III/10/30d	6/12	0/12	0/12	1/12	0/12	1/12	0/12	0/12	0/12
III/0/30d	1/8	0/8	0/8	0/8	0/8	0/8	0/8	0/8	0/8

[1]Group (*exposure groups I, II, III*)/ Dose (*ppm DMN*)/ Days PE (*post-exposure*)
[2]Cellular Degeneration
[3]Bile Pre-ductular Epithelial Cell Proliferation
[4]Liver Regeneration

Table 3. Hepatic foci of cellular alteration and neoplasms in medaka at each DMN exposure and sacrifice.

Group/Dose Days PE[1]	Foci of Cellular Alteration	Solid HCC	Megalocytic HCC	Trabecular HCC	Anaplastic HCC	Mixed Carcinoma	Cholangioma
I/200/30d	–[2]	–	–	–	–	–	–
I/100/30d	–	–	–	–	–	–	–
I/50/30d	–	–	–	–	–	–	–
I/10/30d	–	–	–	–	–	–	–
I/0/30d	–	–	–	–	–	–	–
I/200/90d	–	–	–	–	–	–	–
I/100/90d	1/6	–	–	–	–	–	–
I/50/90d	1/9	2/9	–	–	–	–	–
I/10/90d	–	–	–	–	–	–	–
I/0/90d	–	–	–	–	–	–	–
I/200/150d	–	–	–	–	–	–	–
I/100/150d	1/3	–	–	1/3	–	–	–
I/50/150d	1/10	2/10	–	–	–	1/10	–
1/10/150d	–	–	–	–	–	–	–
I/0/150d	–	–	–	–	–	–	–
II/100/60d	–	–	–	–	–	–	–
II/50/60d	–	–	–	–	–	1/4	–
II/25/60d	–	–	–	–	–	–	–
II/10/60d	–	–	–	–	–	–	–
II/0/60d	–	–	–	–	–	–	–
II/100/120d	–	–	1/2	–	–	1/2	1/2
II/50/120d	2/4	2/4	–	–	–	–	–
II/25/120d	1/5	–	–	–	–	–	–
II/10/120d	–	–	–	–	–	–	–
II/0/120d	–	–	–	–	–	–	–
II/100/180d	–	1/4	–	–	–	1/4	–
II/50/180d	1/4	1/4	–	1/4	1/4	1/4	–
II/25/180d	3/5	–	1/5	–	–	1/5	–
II/10/180d	1/4	–	–	–	–	–	–
II/0/180d	–	–	–	–	–	–	–
III/100/30d	–	–	–	–	–	–	–
III/50/30d	–	–	–	–	–	–	–
III/25/30d	–	–	–	–	–	–	–
III/10/30d	–	–	–	–	–	–	–
III/0/30d	–	–	–	–	–	–	–

[1]Group (*exposure groups I, II, III*)/ Dose (*ppm DMN*)/ Days PE (*post-exposure*)
[2][–] indicates that lesion is not present

Table 4. Function and cellular activity (normal and treatment-related) of select histochemical and immunohistochemical stains in the livers of fish.

Stain	Function	Normal Activity	Treatment-Related Activity
TGF-β1[1]	Reacts with 25 kD TGF-β1 protein	BPDECs[2]	BPDECs, intermediate cells, immature hepatocytes, hepatocytes
Smad 3[3]	Reacts with 50 kD Smad 3 protein	Hepatocyte cytoplasm	Hepatocyte cytoplasm and nuclei [increased staining]
Cytokeratin AE1/AE3[4]	Recognizes high & low molecular weight cytokeratins	Bile duct epithelium	BPDECs and intermediate cells; HSCs (?)
Sirius Red	Reacts with collagen	Blood vessel walls	Pericellular fibrillar material [*presumed* collagen]
Reticulin	Reacts with reticular fibers [type III collagen]	Blood vessel wall basement membrane	Pericellular staining increased, new basement membranes
MSA[5]	Reacts with 42kD protein specific for actins in skeletal, cardiac, and smooth muscle	Periductal myofibroblasts	Pericellular staining [presumed activated HSCs]; also periductal myofibroblasts
GFAP[6]	Reacts with class II intermediate filament protein	Astrocytes/astroglia	None

[1]Transforming Growth Factor- β1

[2]Bile Pre-Ductular Epithelial Cells

[3]Mammalian homologs of the Drosophila Mothers against dpp (Mad) and *C.elegans* (Sma)

[4]AE1 recognizes 10,14, 15, 16, &19; AE3 recognizes 1, 2, 3, 4, 5, 6, & 8

[5]Muscle specific actin

[6]Glial fibrillary acidic protein

Table 5. Results of histochemical and immunohistochemical staining in livers of medaka exposed to DMN

DMN [ppm]	TGF-β1	SMAD3	Cytokeratin	Sirius Red	Reticulin	α-SMA[a]	MSA[b]	Factor VIII	GFAP[c]
200	3/3 [2-3+][d]	3/3 [2-3+]	3/3 [3-4+]	3/3 [2-3+]	3/3 [2-3+]	–[e]	3/3 [1+]	–	0/3
100	2/3 [1-4+]	3/3 [3-4+]	3/3 [2-4+]	3/3 [1-3+]	3/3 [1-3+]	–	3/3 [1-2+]	–	0/3
50	3/3 [2-4+]	2/3 [2+]	2/3 [2-4+]	3/3 [1-3+]	3/3 [2-4+]	–	2/3 [1-2+]	–	0/3
25	3/3 [1+]	1/3 [1+]	1/3 [1+]	0/3	2/3 {1+]	–	0/3	–	0/3
10	3/3 [1+]	0/3	2/3 [1+]	0/3	0/3	–	0/3	–	0/3
0	0/3	0/3	0/3	0/3	0/3	–	0/3	–	0/3

[a] α-smooth muscle actin
[b] muscle-specific actin
[c] glial fibrillary acidic protein
[d] 1+ (minimal), 2+ (mild), 3+(moderate), and 4+(marked) increase in staining
[e] [–] indicates that the stain did not work on medaka tissue

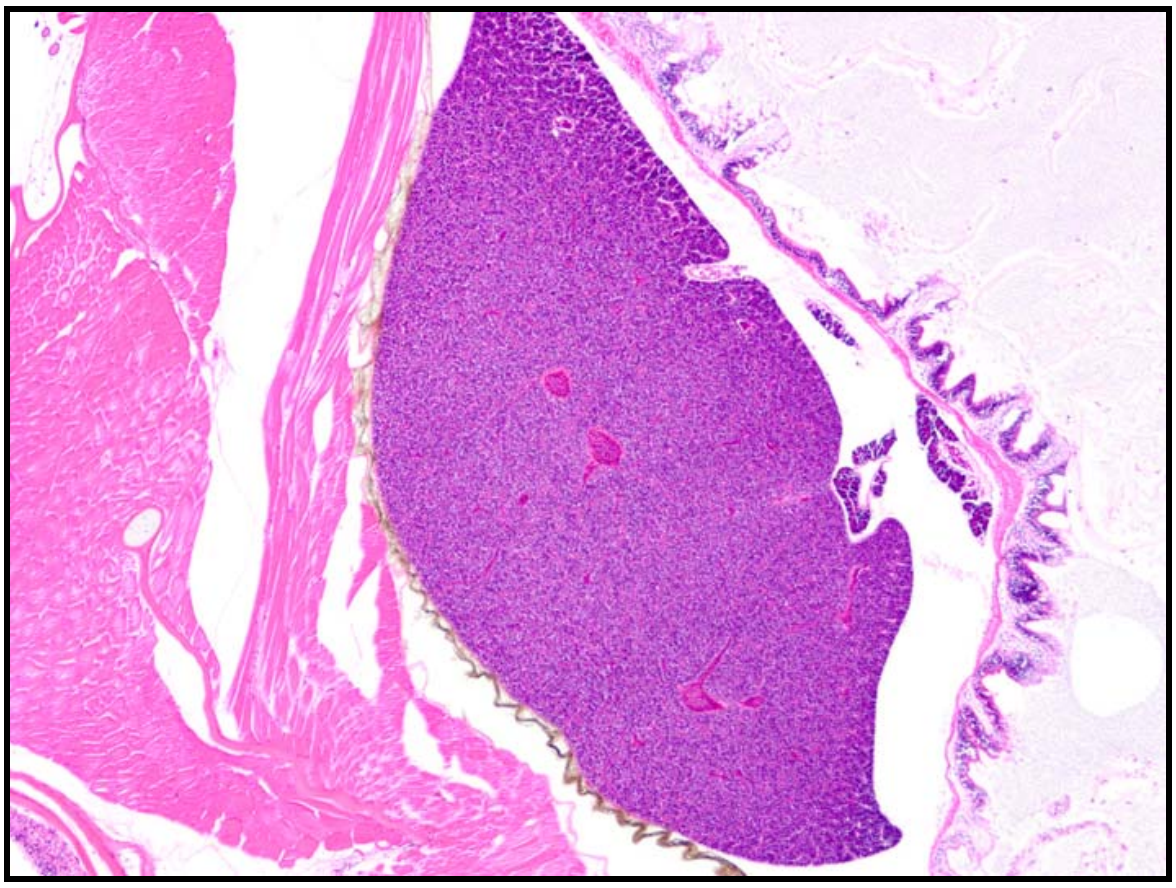

Fig 1. Normal liver, control medaka (0 ppm DMN) at 2 months post-exposure (PE) (20X).

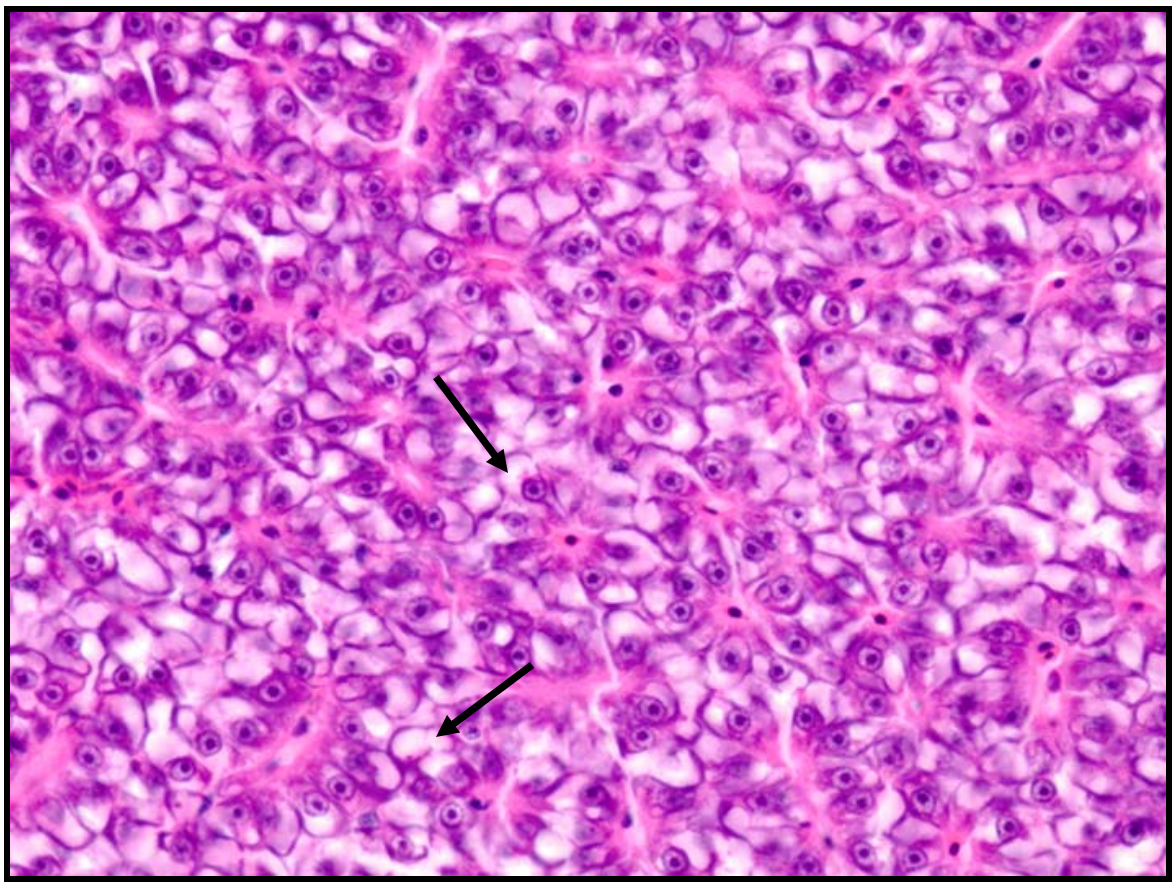

Fig 2. Control medaka liver, 2 months PE (400X). Higher magnification of normal hepatic parenchyma. Note clear intracytoplasmic vacuoles (arrows) within hepatocytes (presumed glycogen and/or lipid).

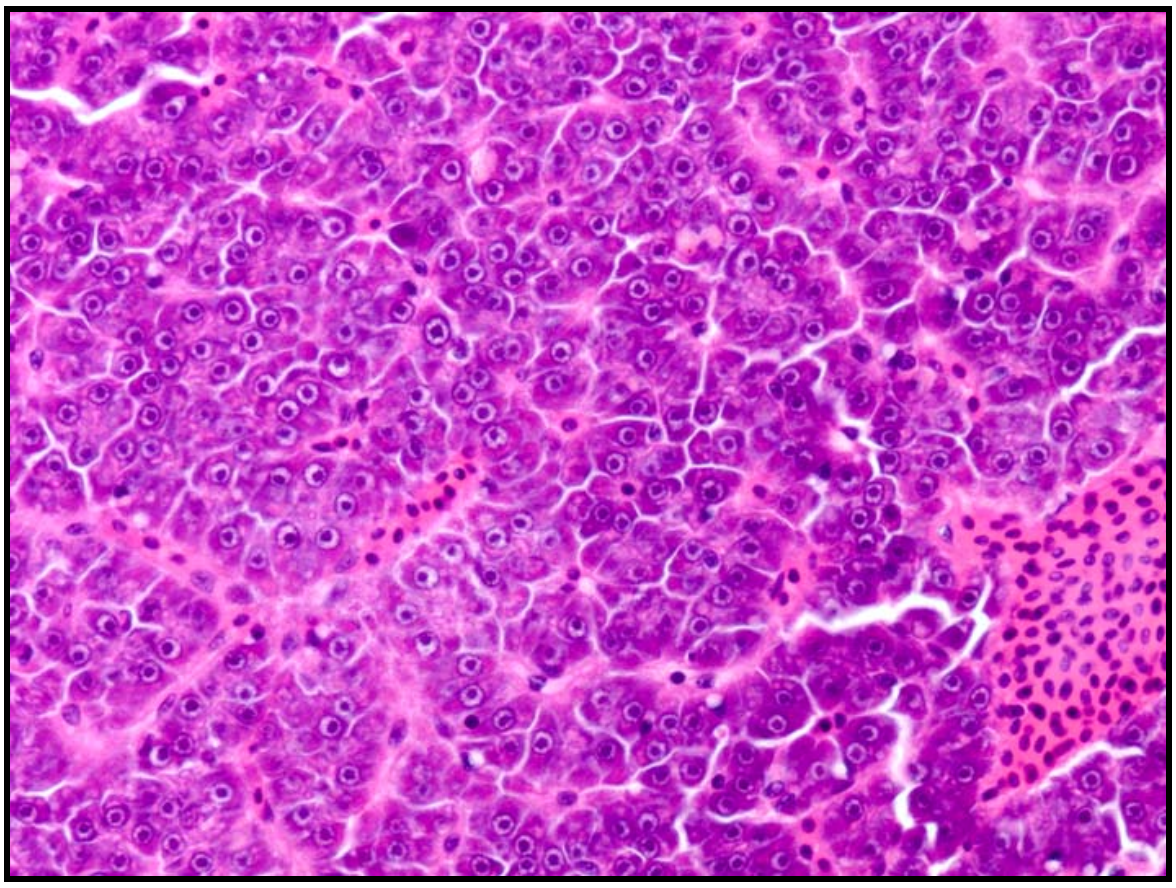

Fig 3. Medaka liver, 10 ppm DMN at 6 months PE (400X). Note depeletion of normal glycogen and/or lipid stores.

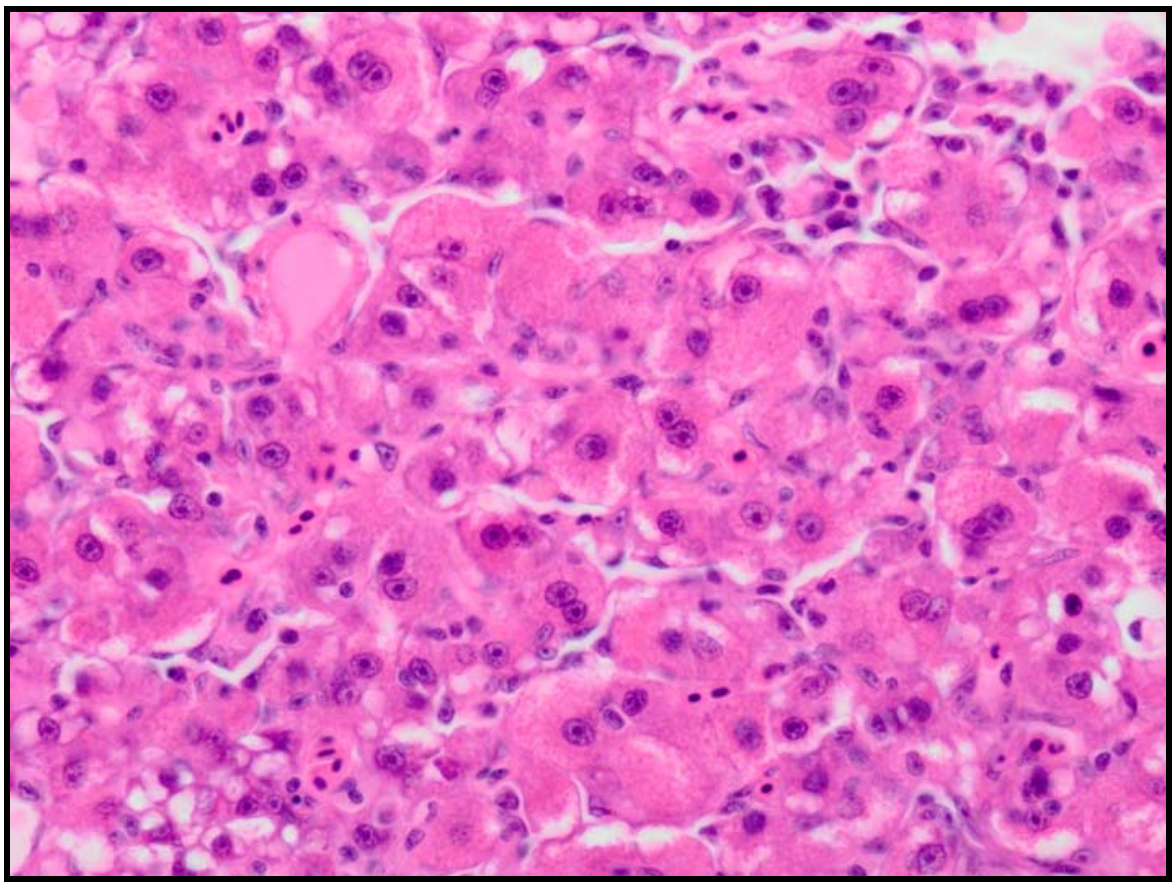

Fig 4. Medaka liver, 50 ppm DMN at 6 months PE (600X). Note cell swelling and hyalinization of hepatocyte cytoplasm.

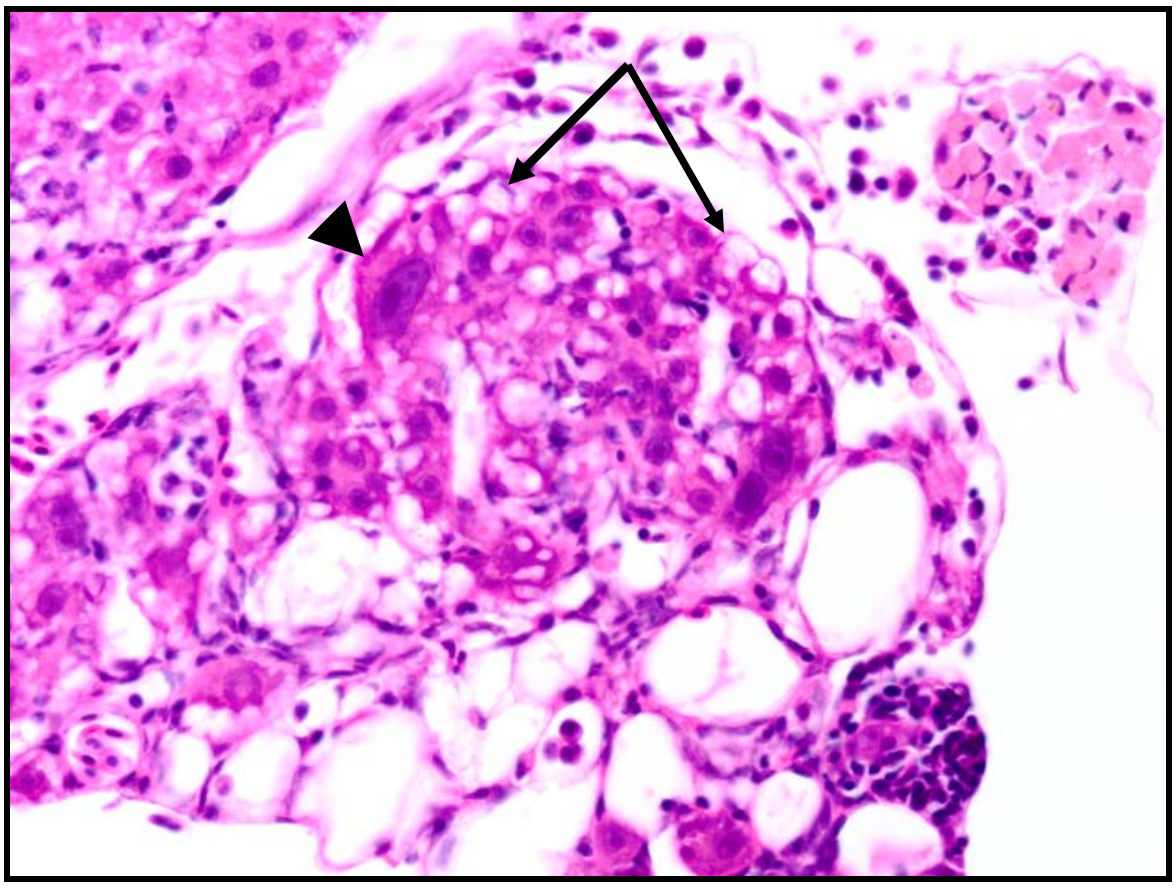

Fig 5. Medaka liver, 100 ppm DMN at 4 months PE (600X). Note hepatocyte swelling, cytoplasmic vacuolization (arrows), and cytomegaly (arrowhead). The reticular framework is retained as individual hepatocytes are lost (600X).

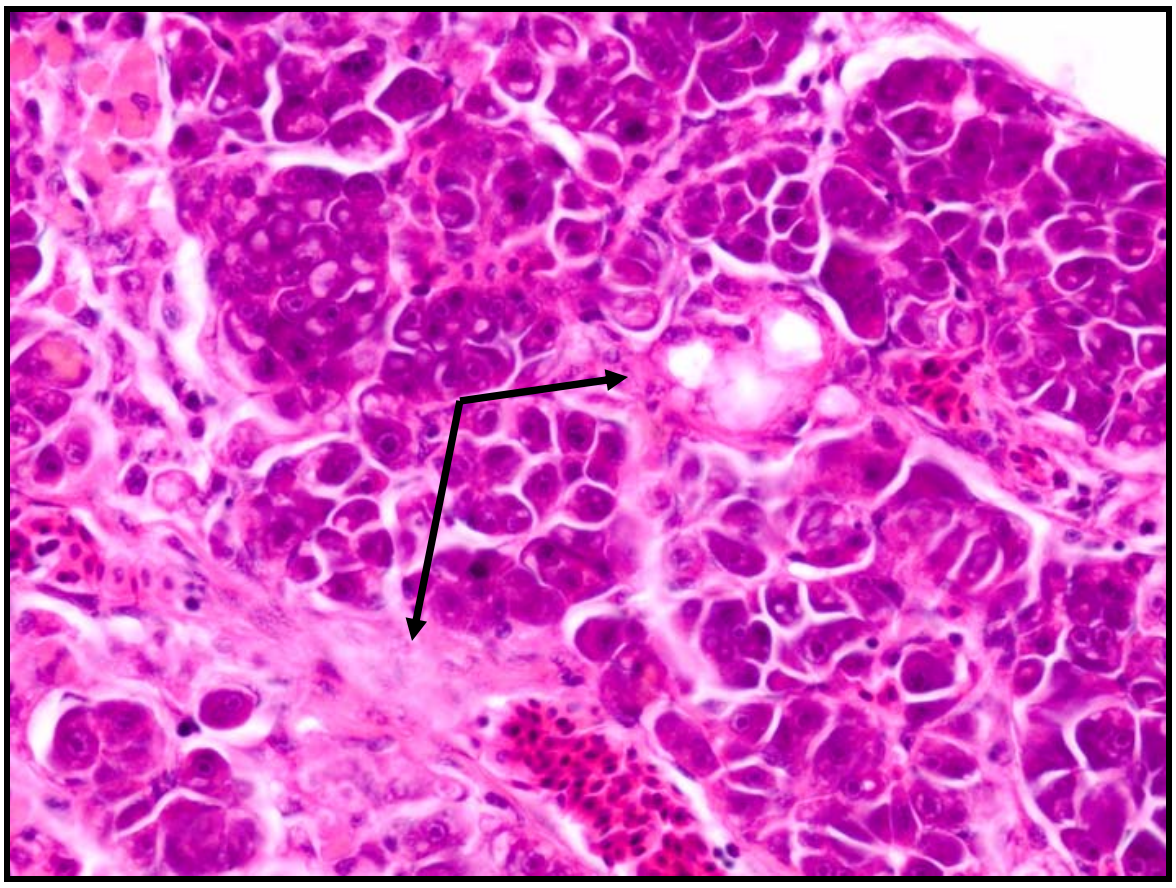

Fig 6. Medaka liver, 50 ppm DMN at 4 months PE (400X). Note increased pericellular extracellular matrix (collagen) deposition (arrows).

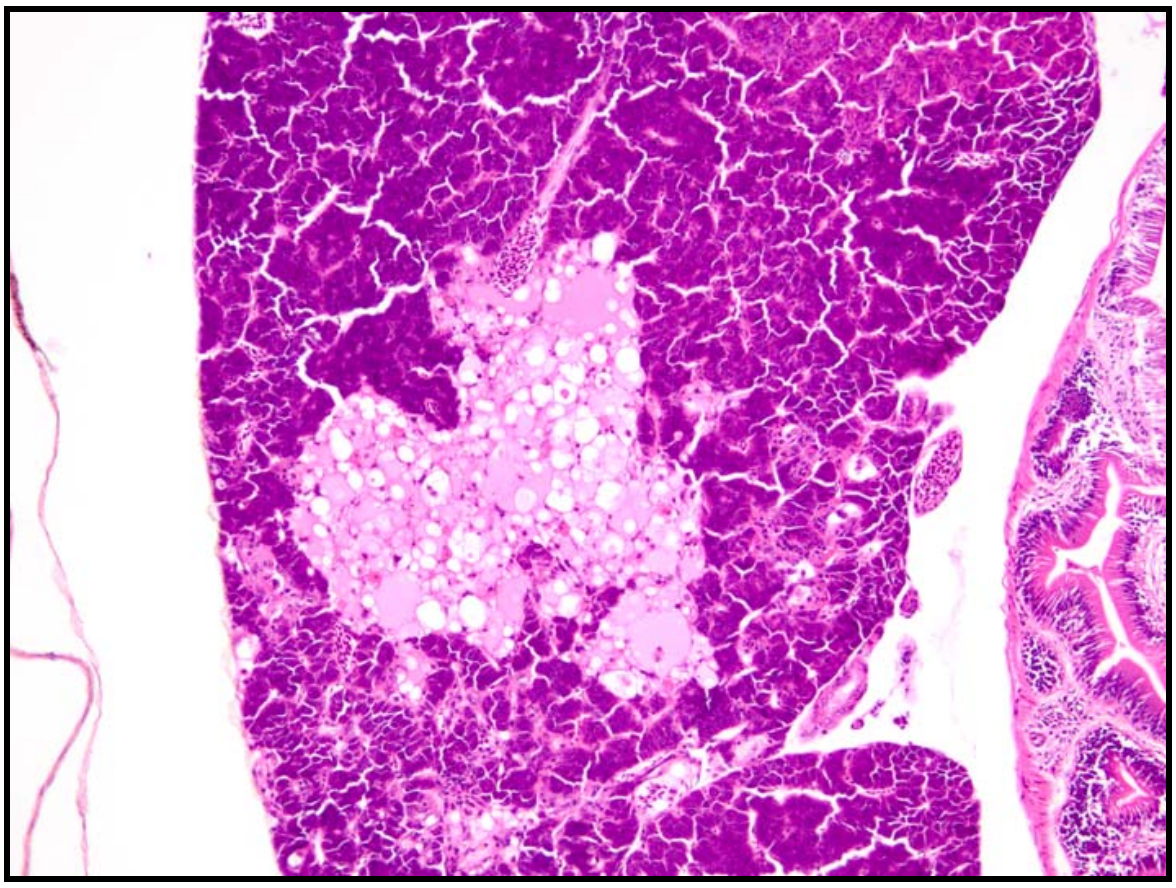

Fig 7. Medaka liver, 100 ppm DMN at 6 months PE (200X). Note cystic degeneration of liver comprised of a multilocular meshwork of interconnected perisinusoidal cells (HSCs) and/or flocculent eosinophilic material.

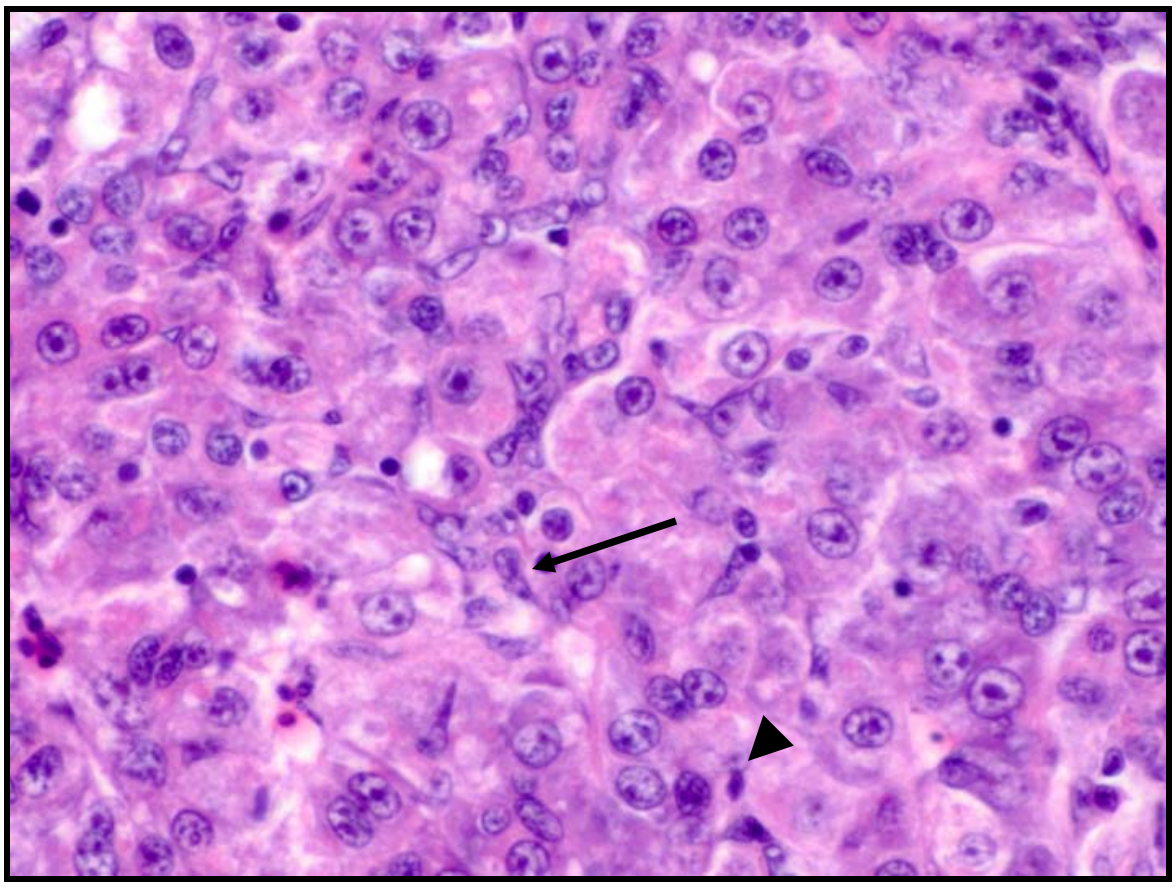

Fig 8. Medaka liver, 100 ppm DMN at 2 months PE (600X). Note peri-hepatocellular proliferation of small cells with scant cytoplasm and round to oval hyperchromatic nuclei consistent with bile preductular epithelial cells (BPDEC) (arrowhead). Slightly larger cells with oval euchromatic nuclei are presumably intermediate cells (arrow).

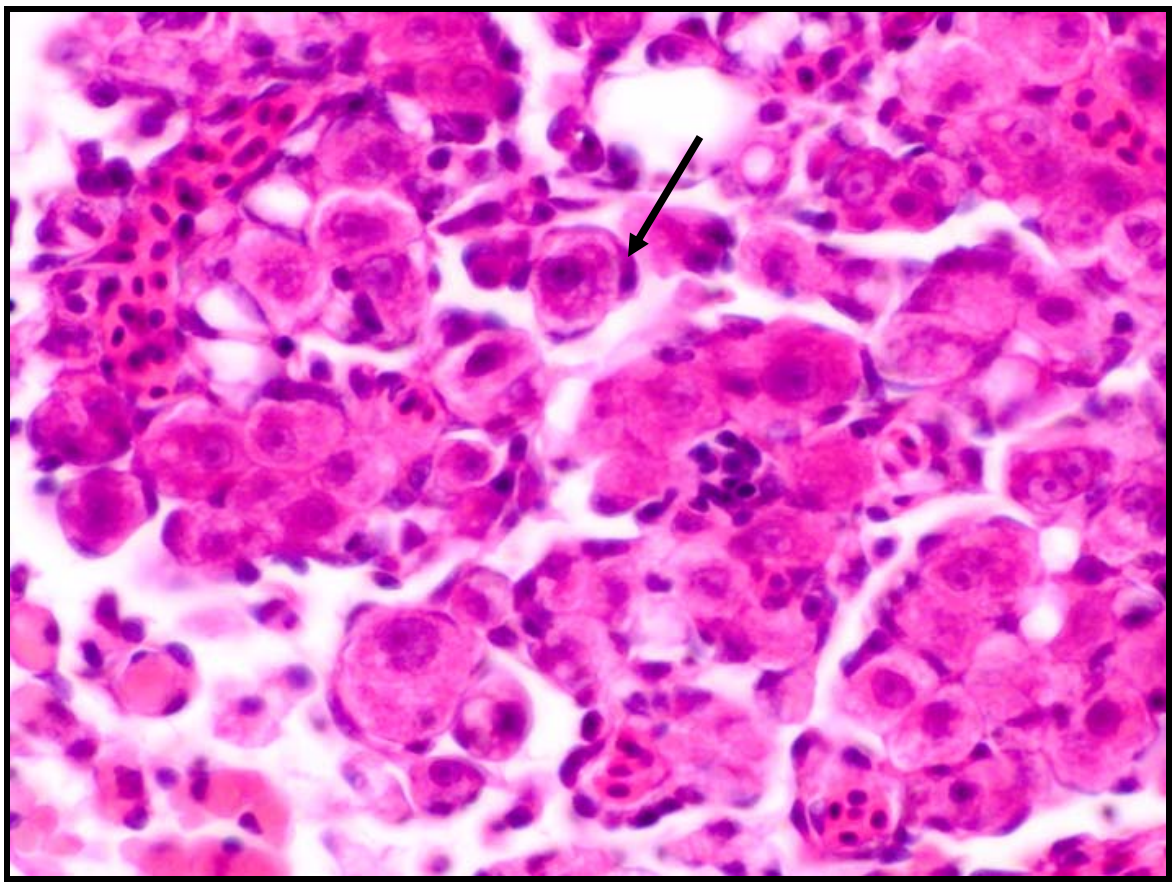

Fig 9. Medaka liver, 100 ppm DMN at 2 months PE (600X). Note hepatic stellate cell (HSC) and/or BPDEC proliferation and how the cells wrap around individual hepatocytes (arrow) giving a fenestrated appearance to the tissue.

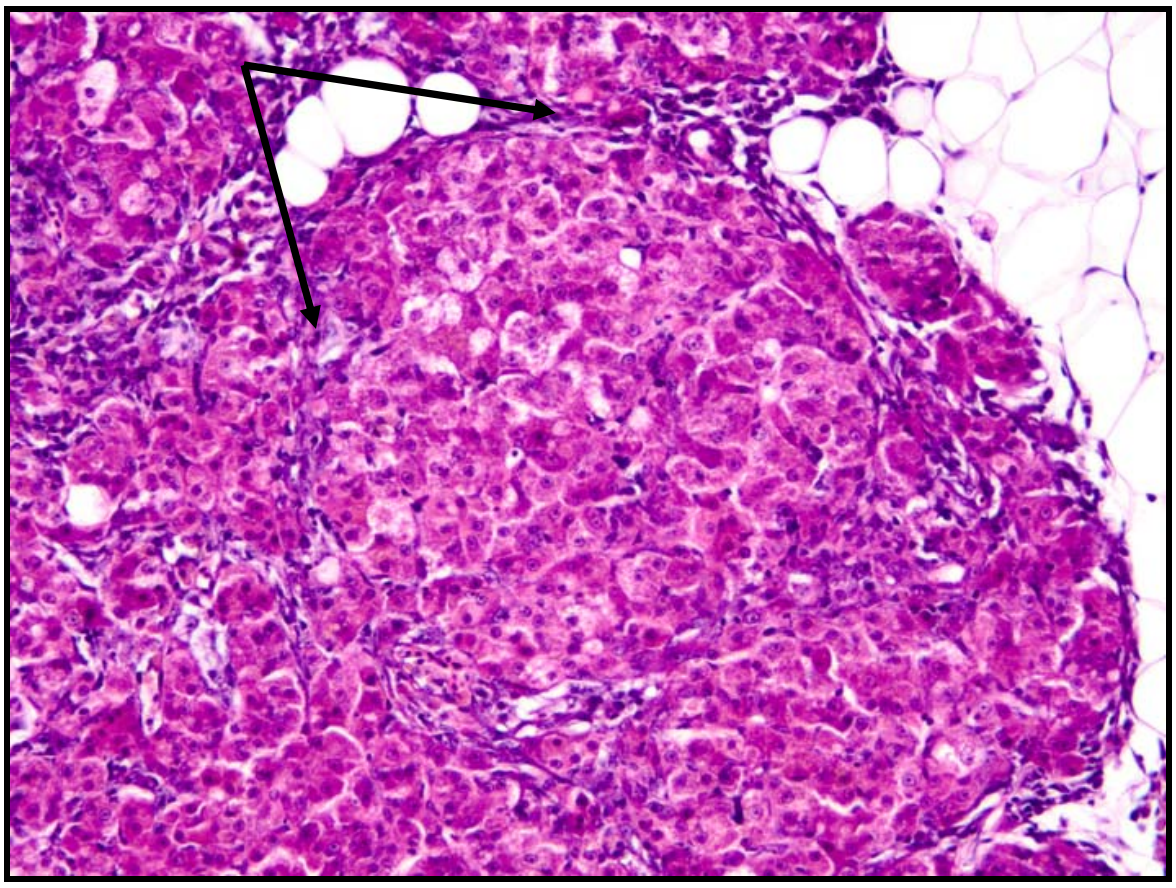

Fig 10. Medaka liver, 100 ppm DMN at 1 month PE (200X). Note cirrhotic-like nodule of regenerative hepatocytes bordered by fibrils of connective tissue (arrows).

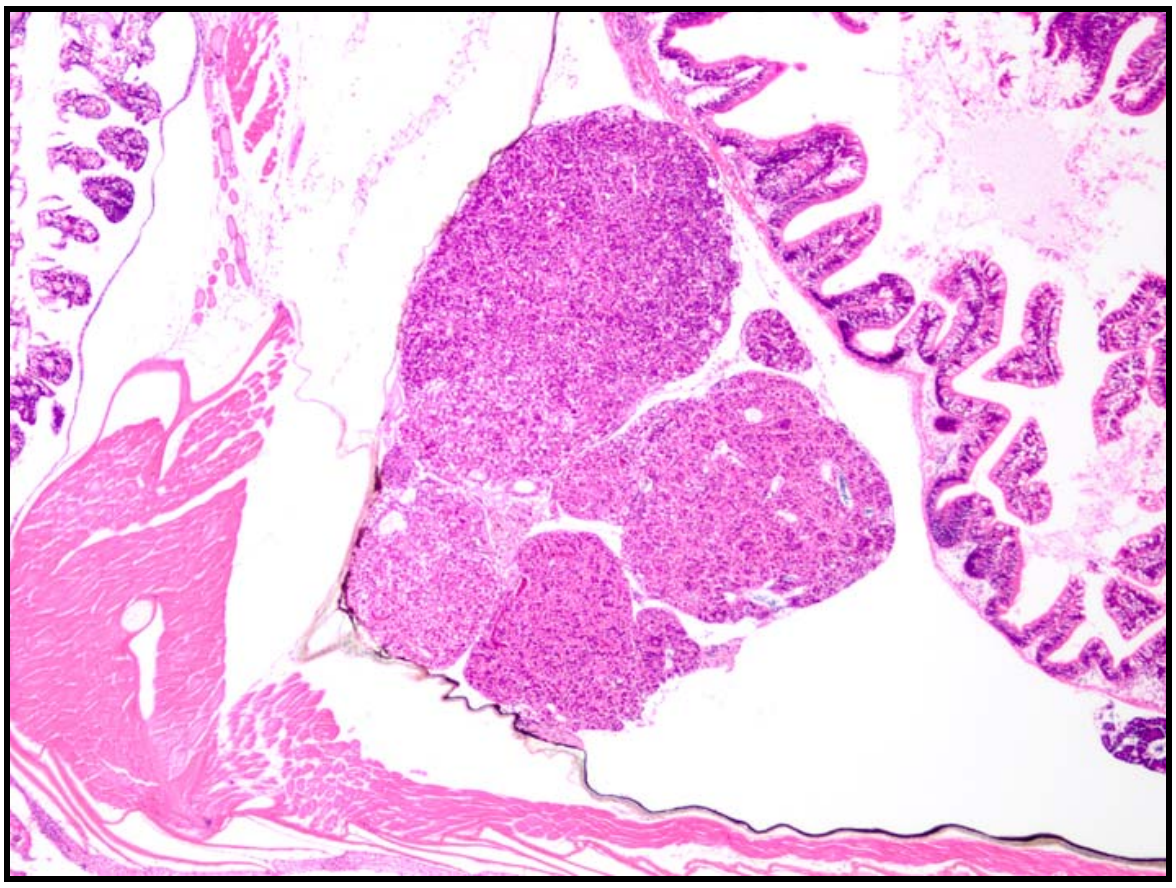

Fig 11. Medaka liver, 100 ppm DMN at 4 months PE (40X). Chronic hepatotoxicity with loss, collapse, and regeneration of the hepatic parenchyma resulting in a multinodular (or multilobulated) liver.

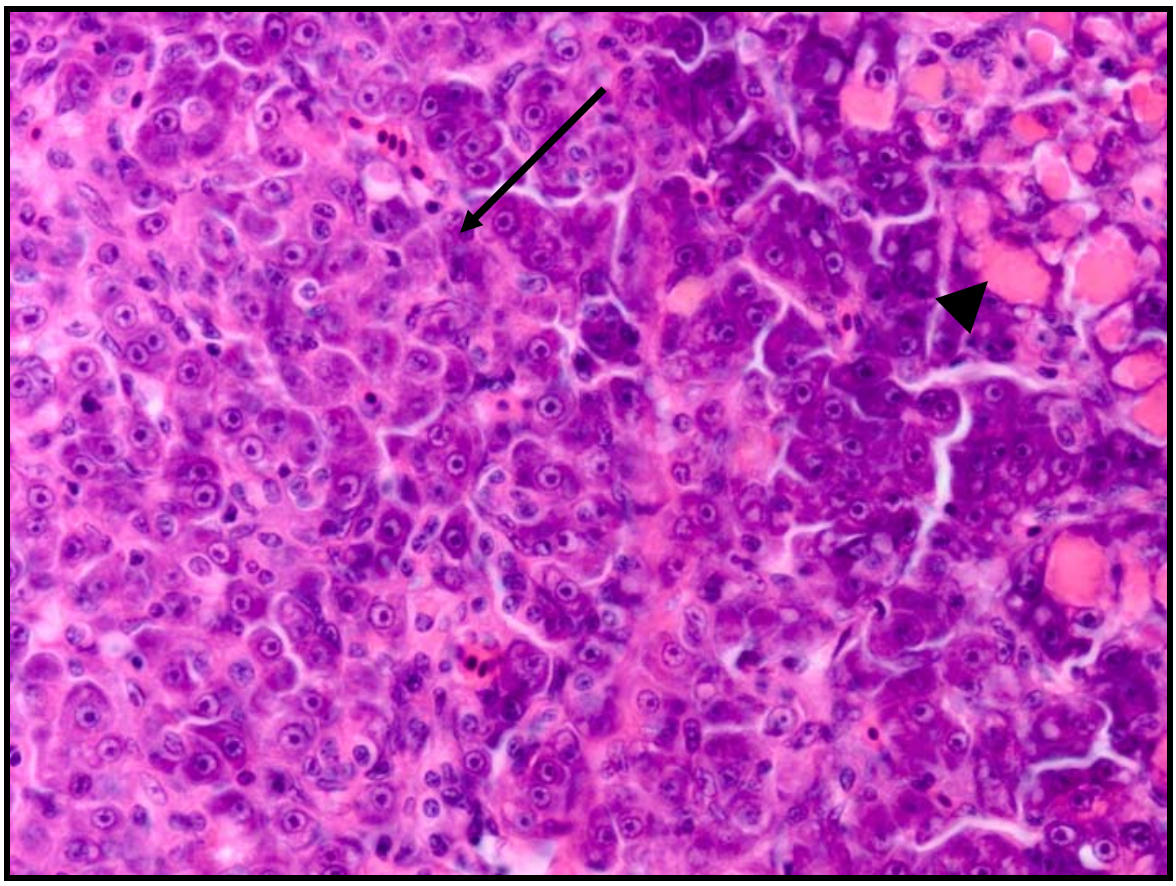

Fig 12. Medaka liver, 25 ppm DMN at 6 months PE (400X). Solid version of hepatocellular carcinoma (arrow). Note degenerate hepatocytes with hypereosinophilic cytoplasm (arrowhead).

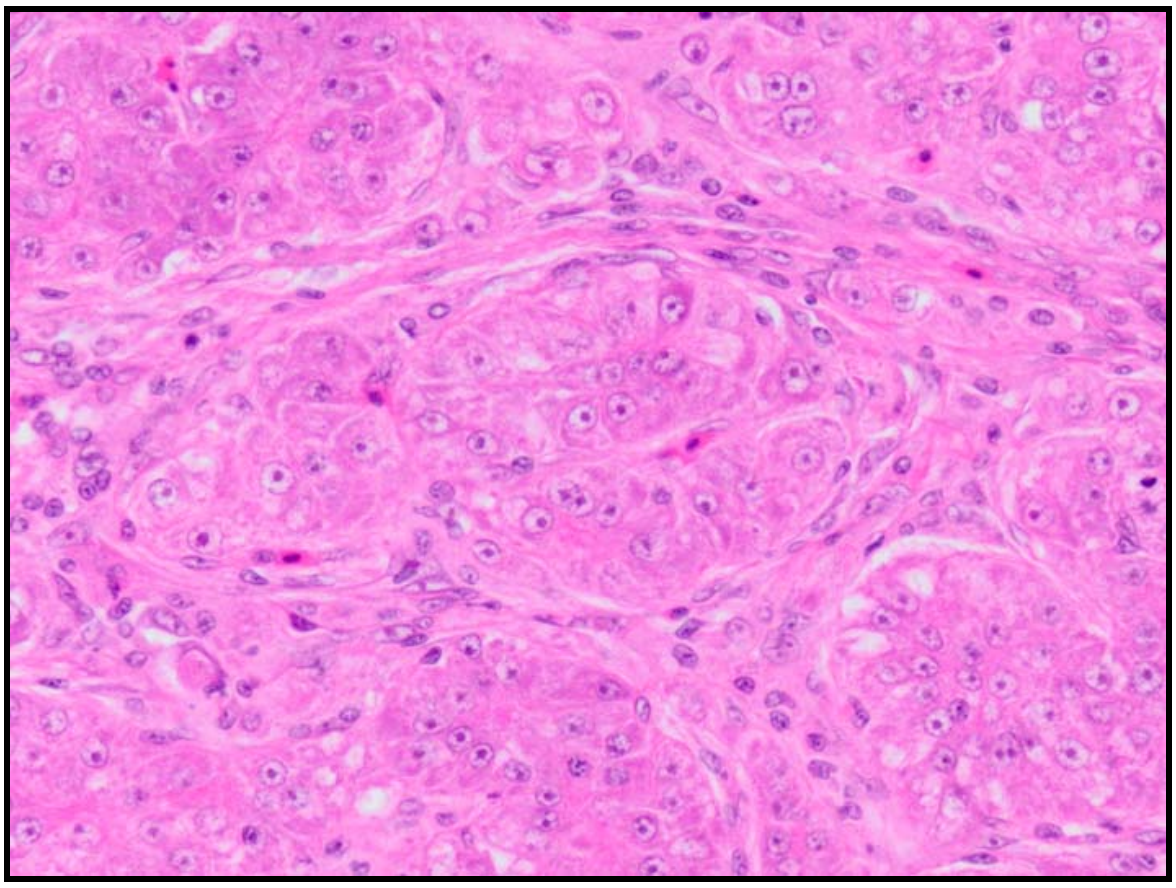

Fig 13. Medaka liver, 100 ppm DMN at 4 months PE (400X). Megalocytic hepatocellular carcinoma characterized by cytomegalic neoplastic hepatocytes.

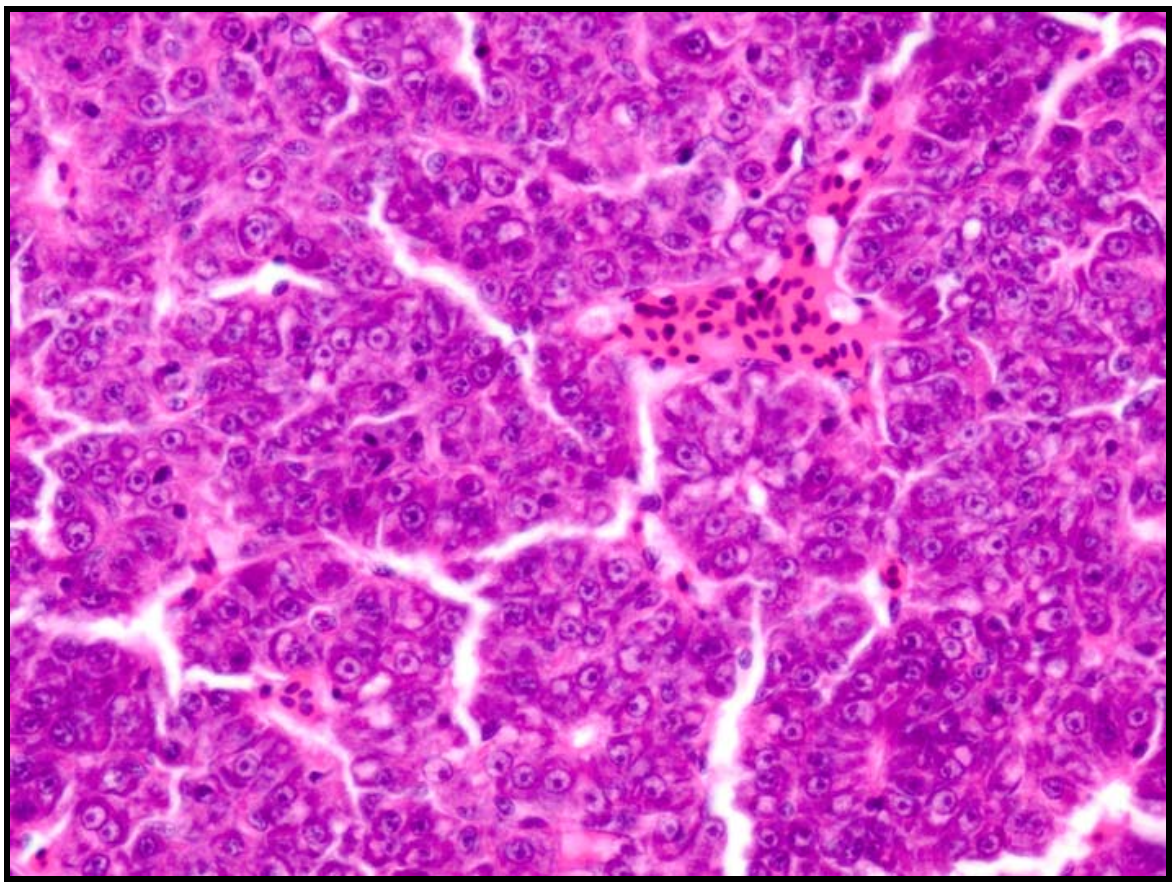

Fig 14. Medaka liver, 100 ppm DMN at 6 months PE (400X). Trabecular hepatocellular carcinoma characterized by cords of well-differentiated neoplastic hepatocytes 3-6 cells thick.

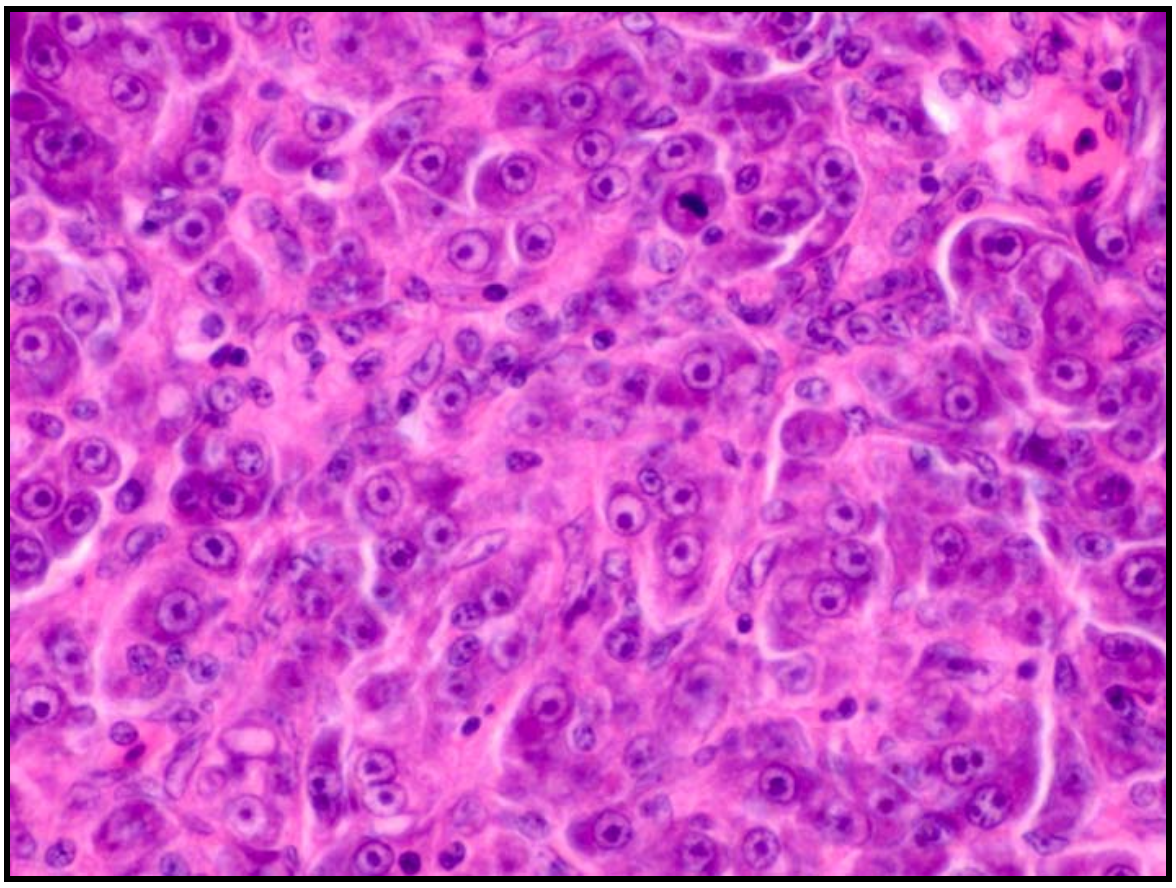

Fig 15. Medaka liver, 25 ppm DMN at 6 months PE (600X). Anaplastic hepatocellular carcinoma characterized by haphazardly arranged, poorly differentiated, pleomorphic neoplastic hepatocytes.

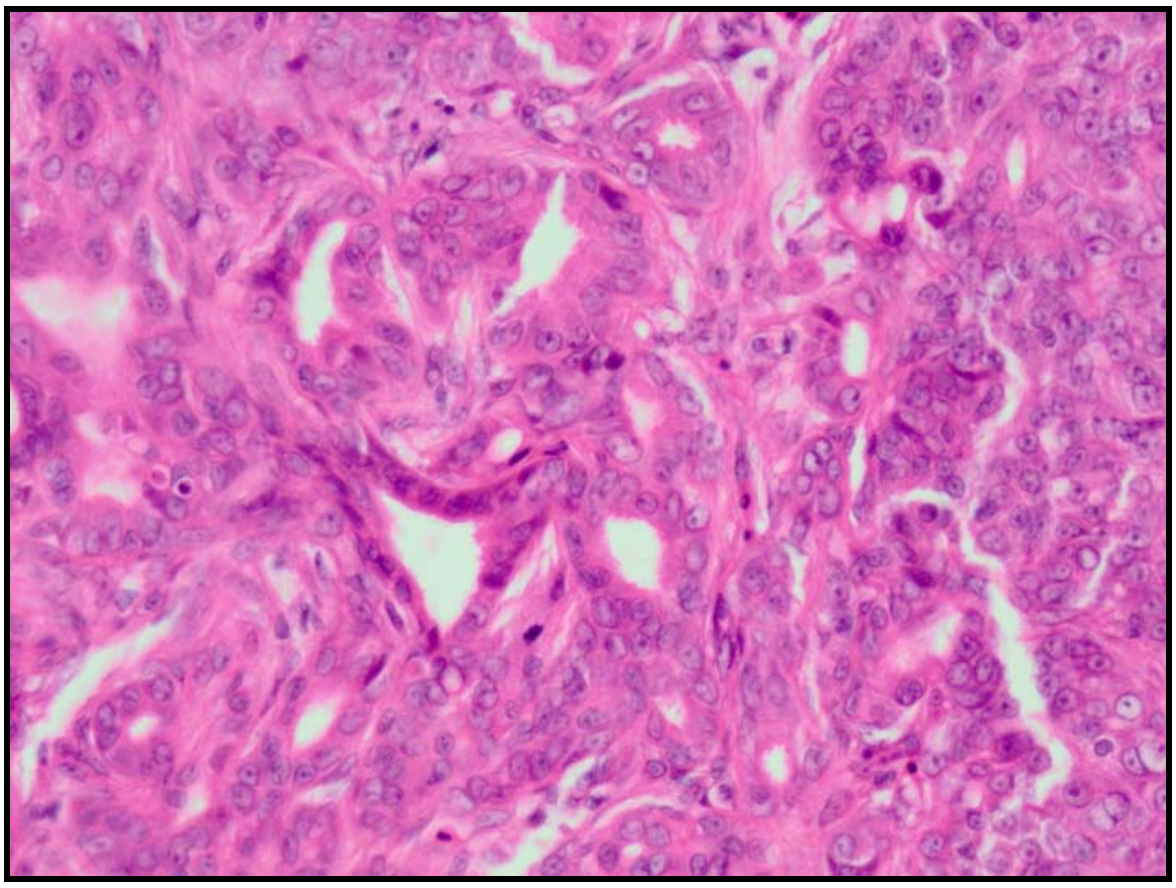

Fig 16. Medaka liver, 100 ppm DMN at 2 months PE (400X). Biliary carcinoma consisting of haphazardly arranged neoplastic biliary epithelial cells forming variably shaped ducts.

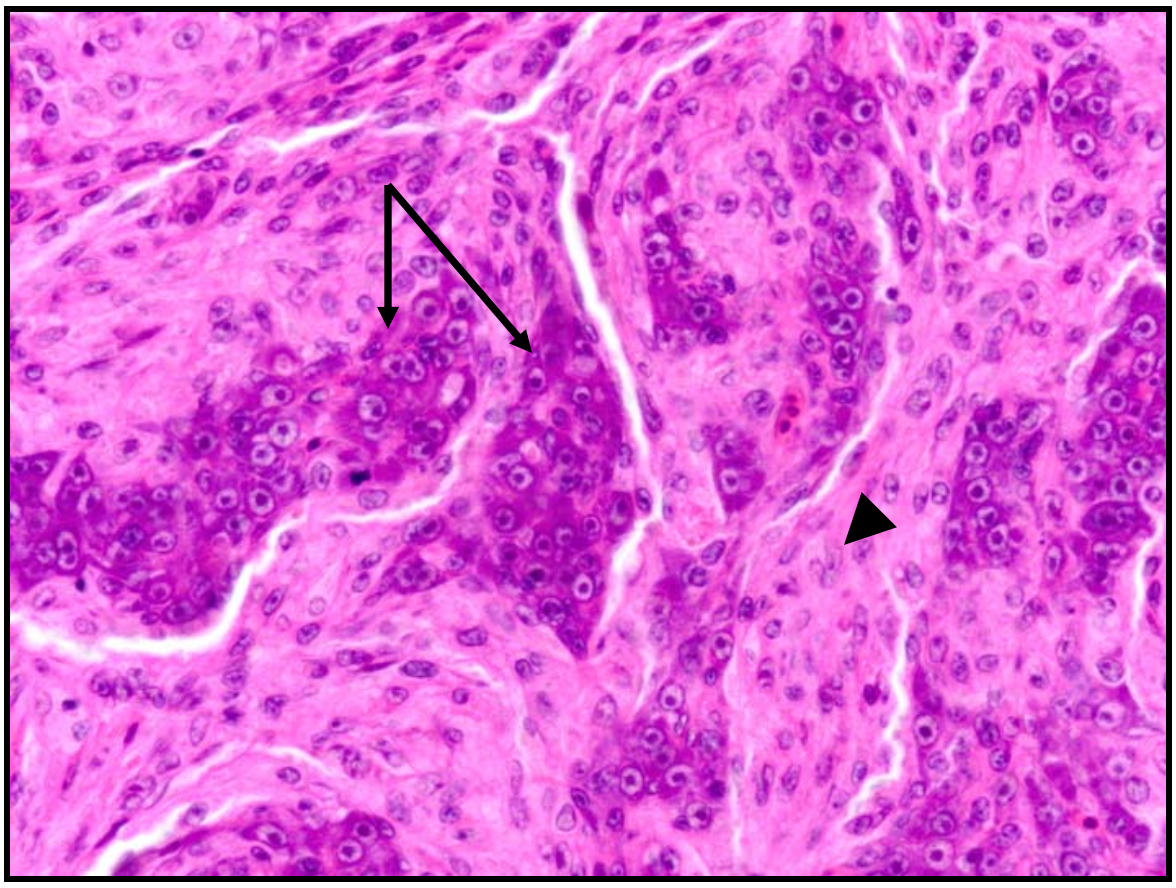

Fig 17. Medaka liver, 50 ppm DMN at 6 months PE (400X). Mixed (hepato-cholangiocellular) carcinoma characterized by mixture of neoplastic hepatocytes (arrows) and biliary epithelial cells (arrowhead).

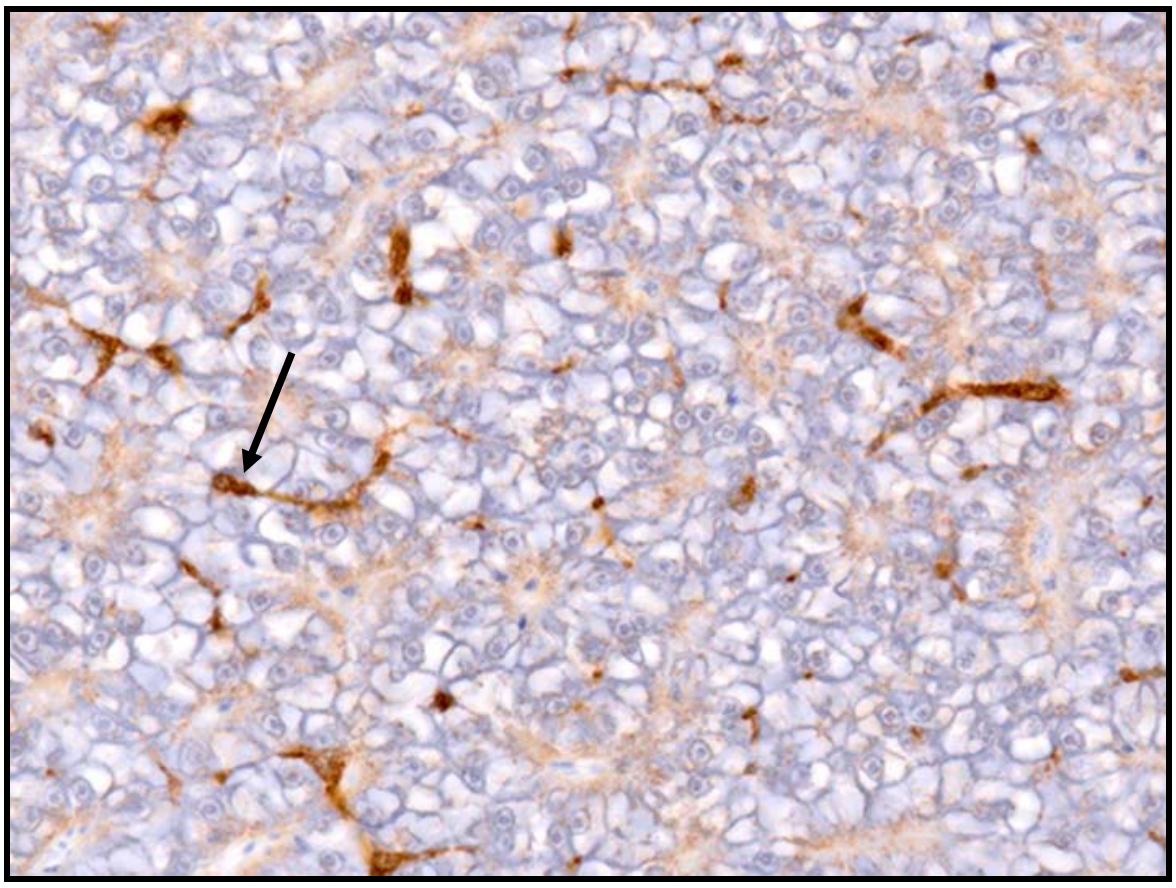

Fig 18. Medaka liver, control at 2 months PE (400X). Immunohistochemical (IHC) staining for Transforming Growth Factor (TGF)-β1. Note positive (brown) staining of BPDECs (arrow).

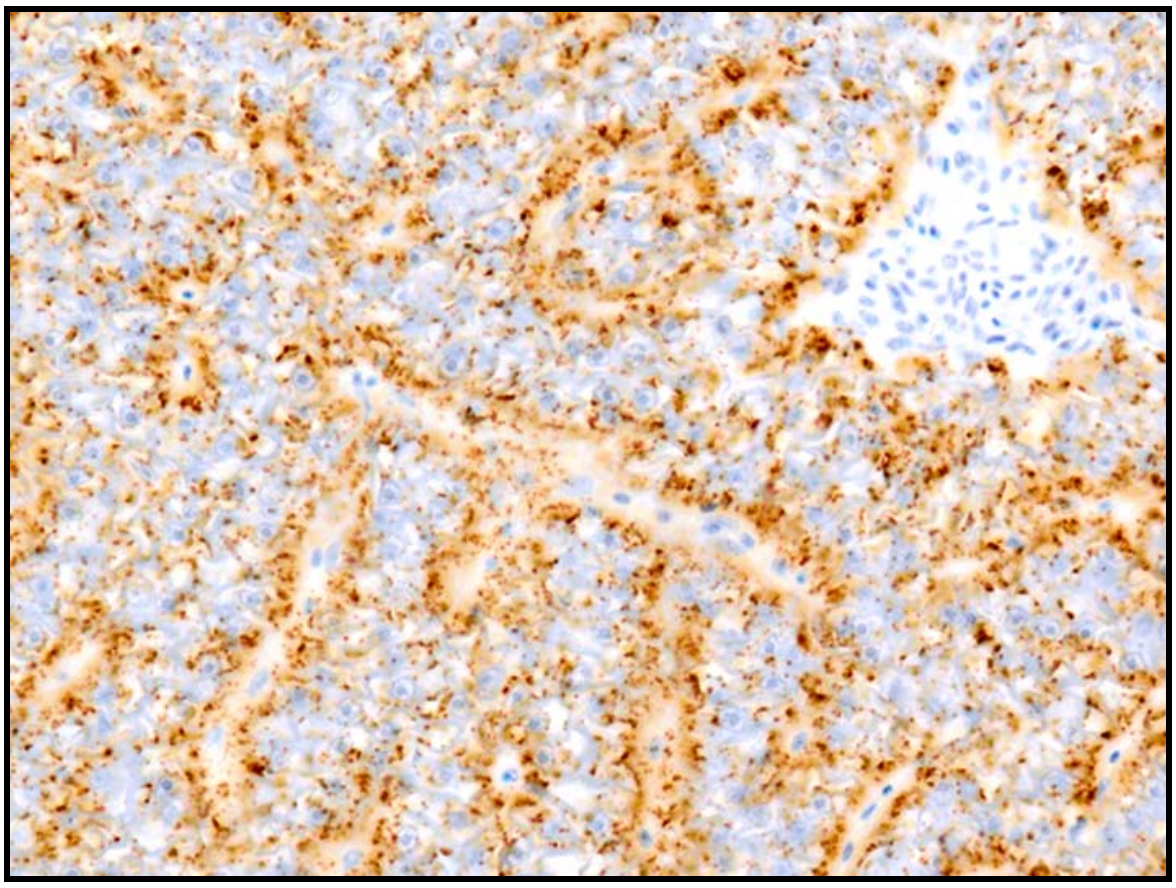

Fig 19. Medaka liver, control at 2 months PE (400X). IHC staining for Smad 3. Note positive staining of hepatocyte cytoplasm adjacent to sinusoids.

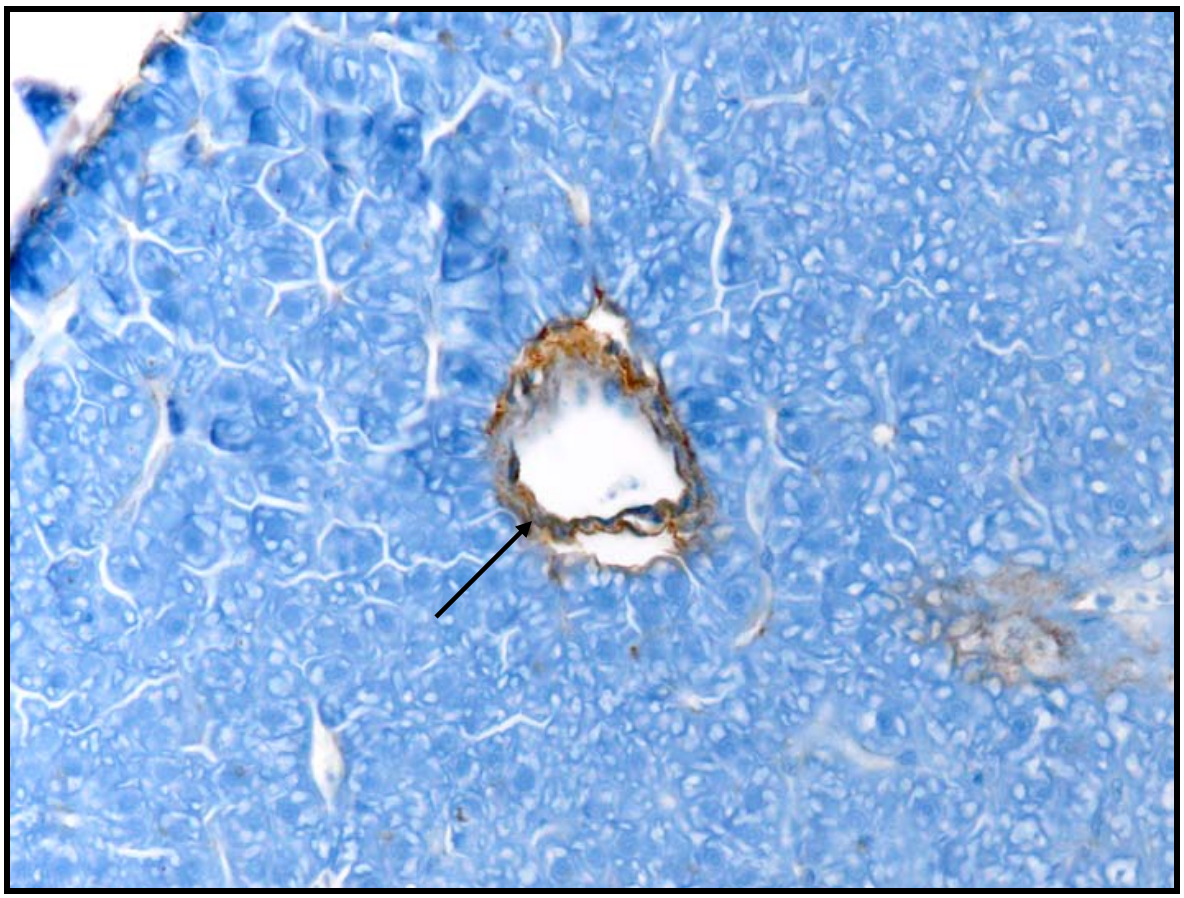

Fig 20. Medaka liver, control at 2 months PE (400X). IHC staining for AE1/AE3 cytokeratin. Note positive staining of bile duct epithelium.

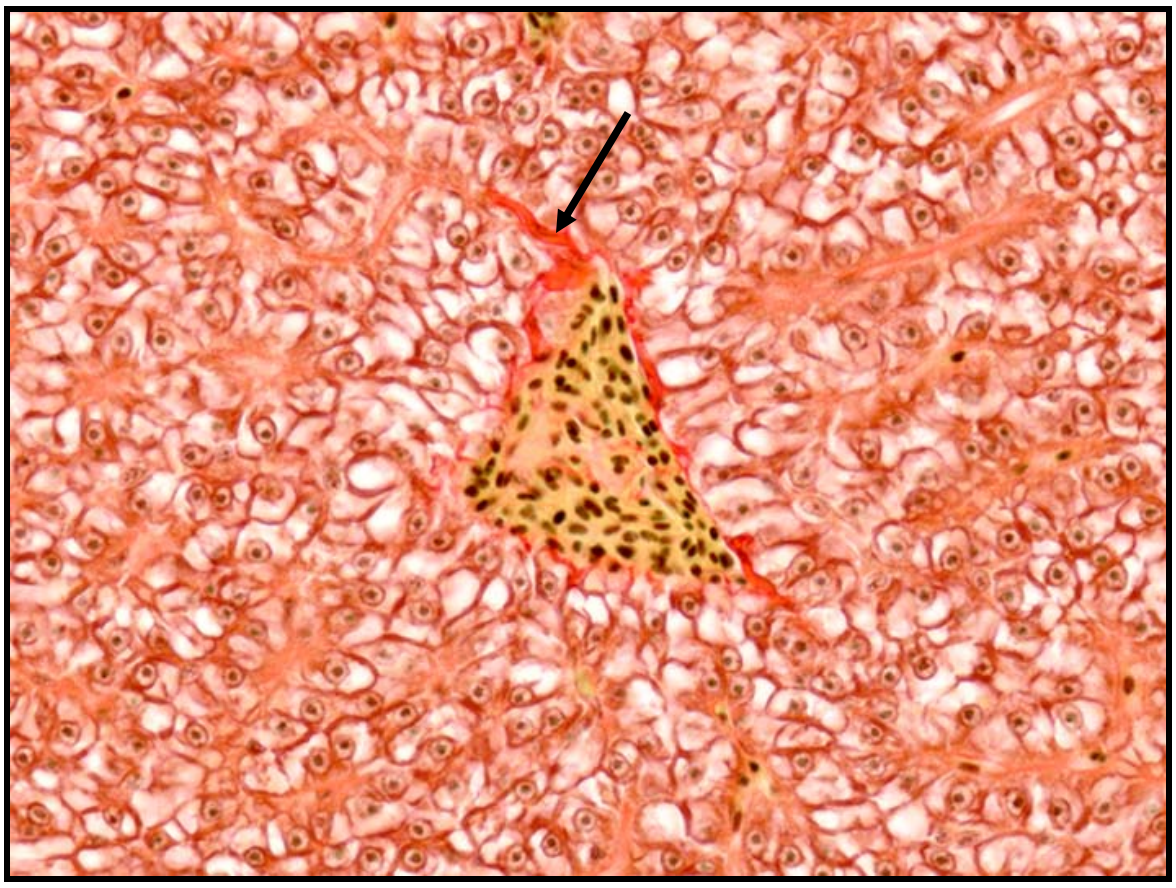

Fig 21. Medaka liver, control at 2 months PE (400X). Histochemical (HC) staining for Sirius red. Note positive (dark red) staining of collagenous blood vessel wall (arrow).

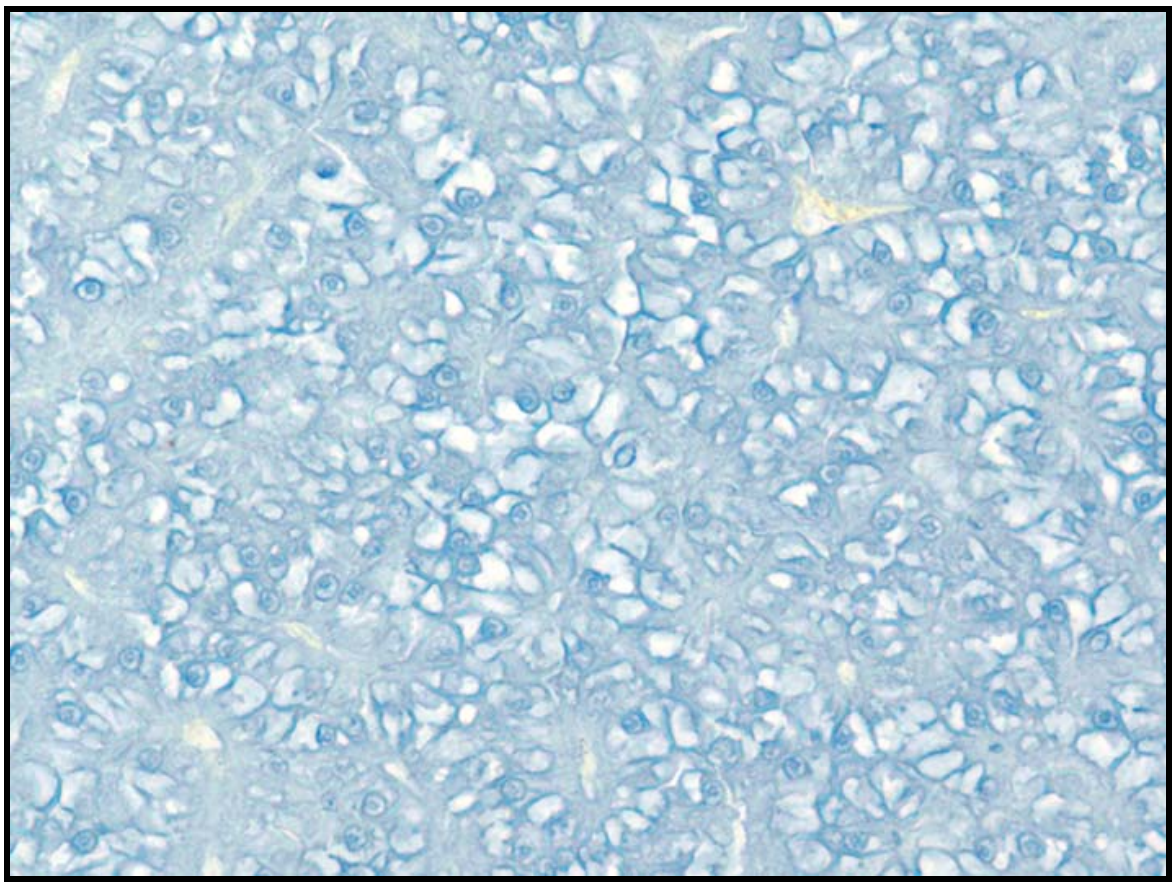

Fig 22. Medaka liver, control at 2 months PE (400X). IHC staining for muscle-specific actin (MSA). Note negative staining of hepatic parenchyma.

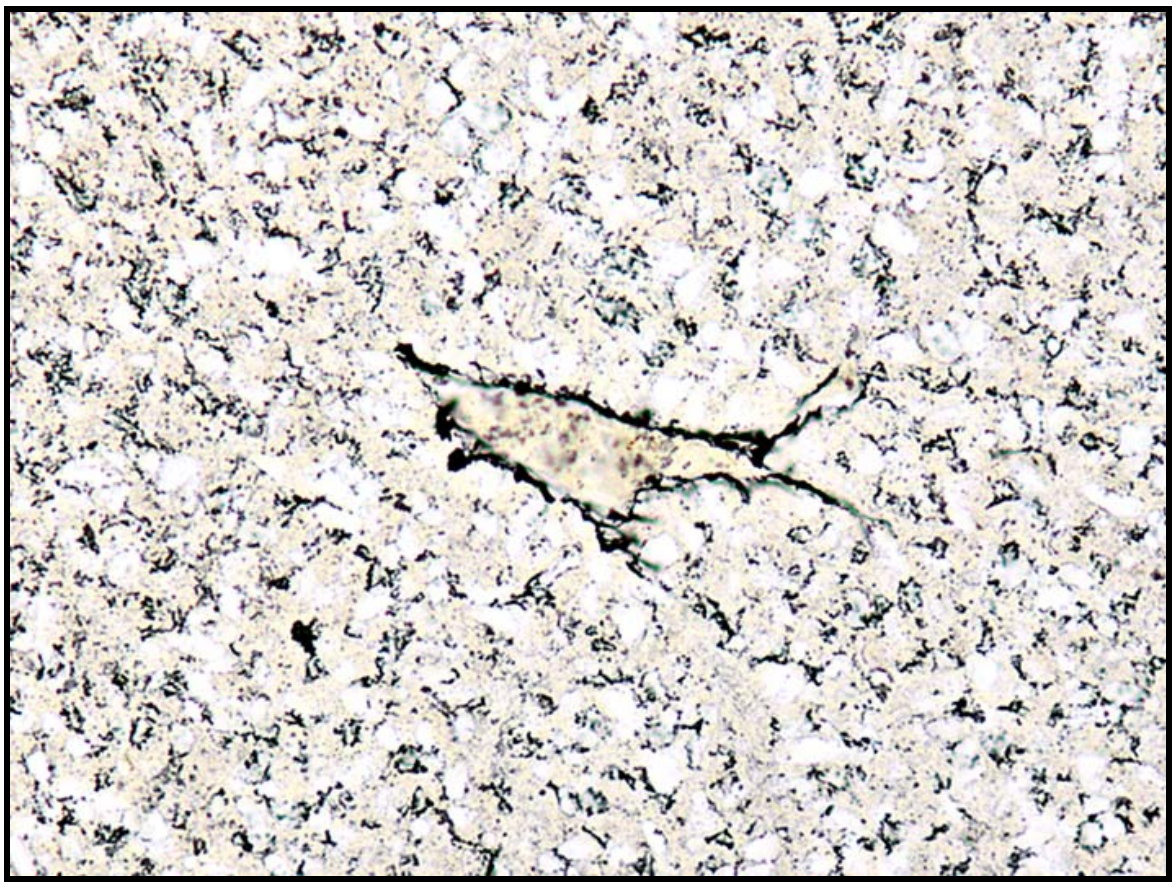

Fig 23. Medaka liver, control at 2 months PE (400X). HC staining with reticulin silver stain. Note positive (black) staining of blood vessel wall (basement membrane).

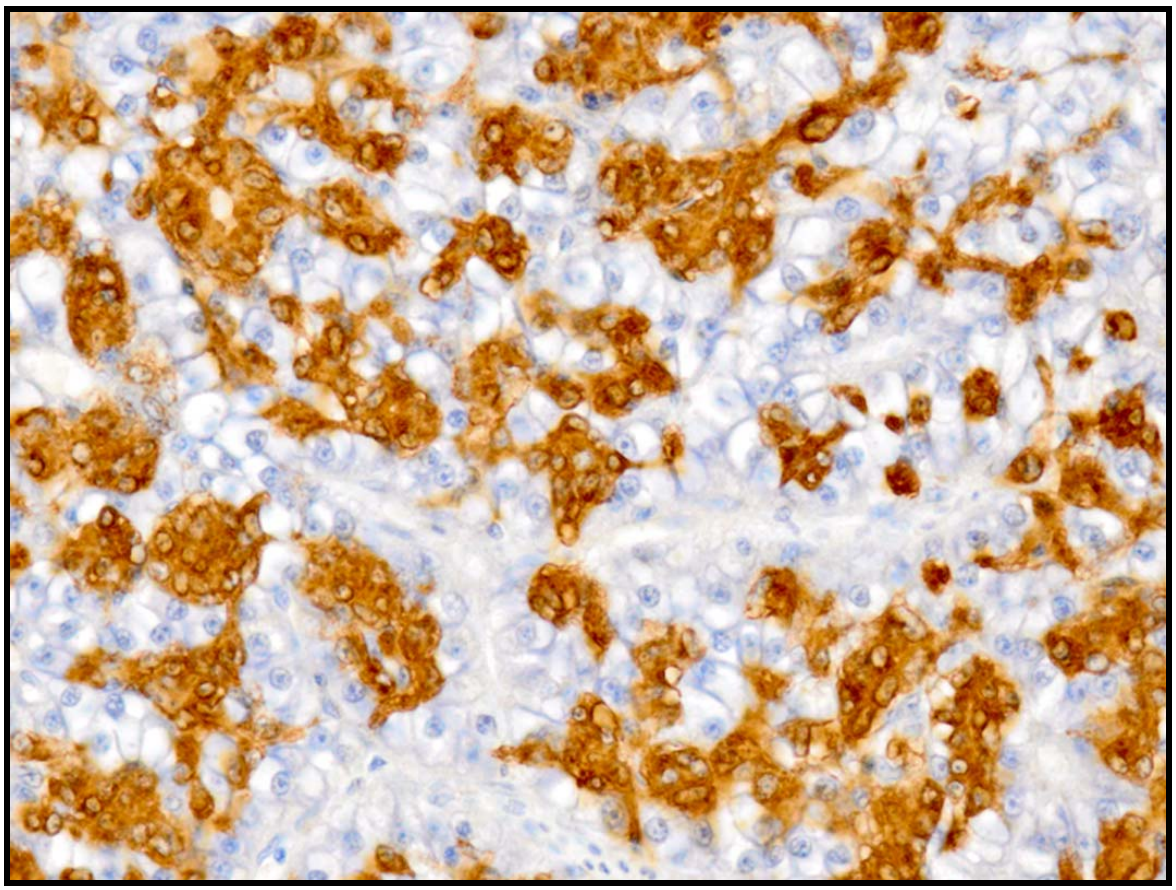

Fig 24. Medaka liver, 50 ppm DMN at 6 months PE (400X). Positive cytoplasmic staining of BPDECs and intermediate cells for TGF-β1.

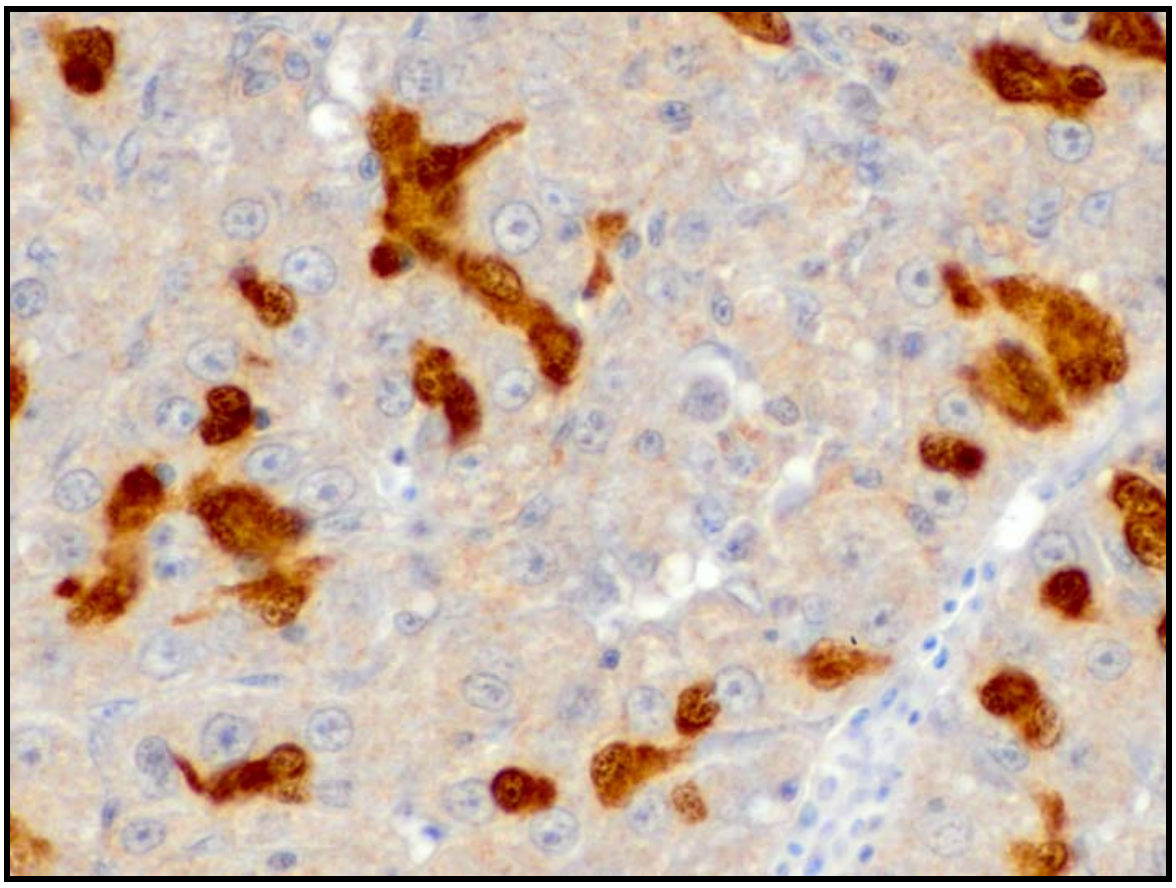

Fig 25. Medaka liver, 100 ppm DMN at 2 months PE (400X). Positive cytoplasmic staining of immature hepatocytes and intermediate cells for TGF-β1.

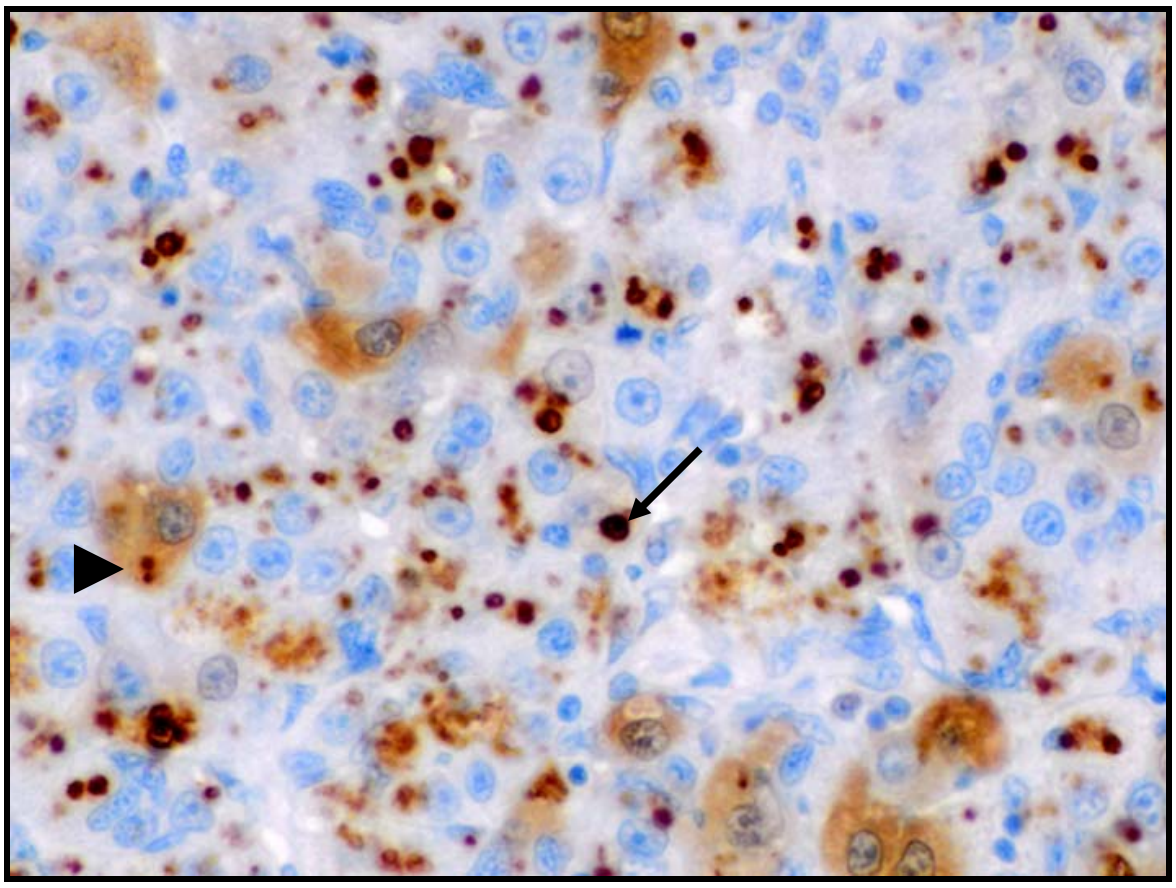

Fig 26. Medaka liver, 100 ppm DMN at 2 months PE (400X). Positive staining of BPDECs, intermediate cells and/or hepatocytes for Smad 3. Note cytoplasmic (arrowhead) and nuclear staining (arrow).

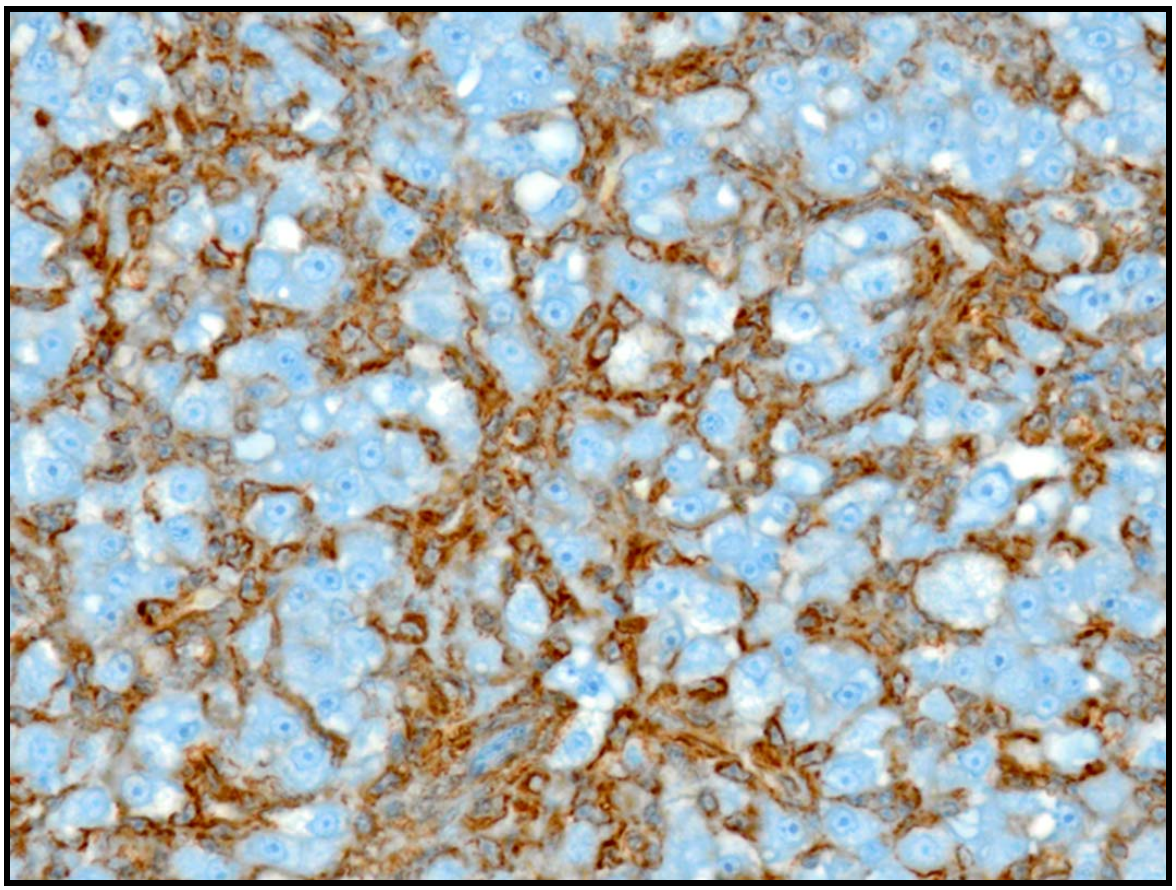

Fig 27. Medaka liver, 50 ppm DMN at 6 months PE (400X). Positive cytoplasmic staining of BPDECs and intermediate cells for AE1/AE3 cytokeratin.

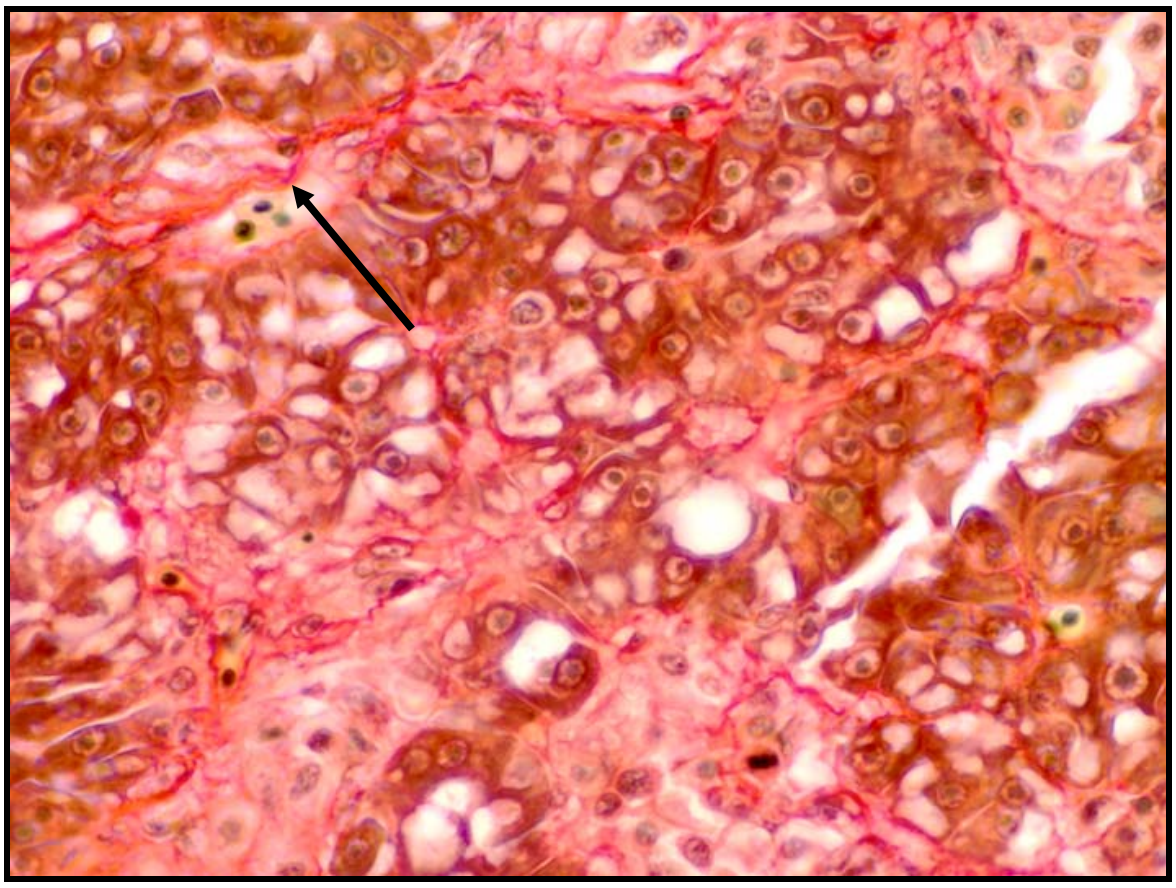

Fig 28. Medaka liver, 50 ppm DMN at 4 months PE (400X). Note increased staining (dark red) of pericellular fibrillar material for Sirius red (arrow).

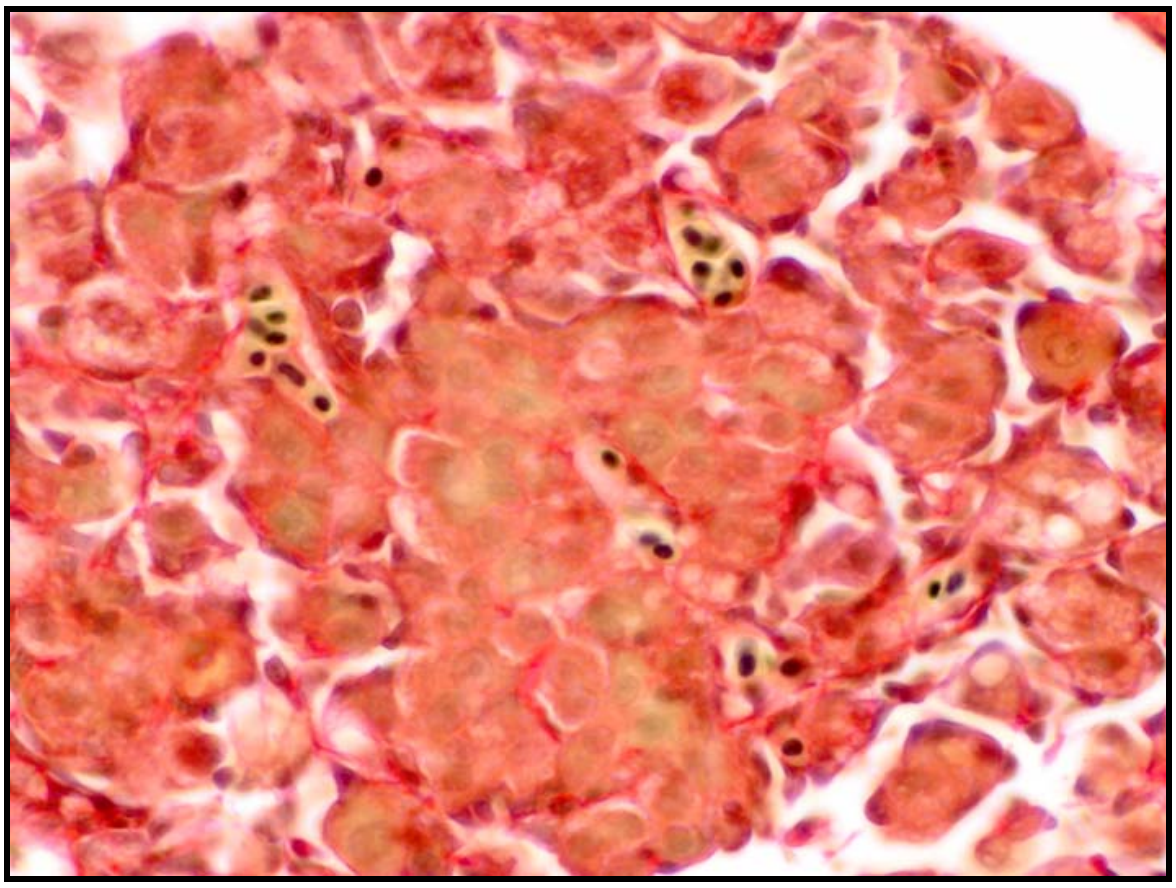

Fig 29. Medaka liver, 100 ppm DMN at 2 months PE (400X). Increased pericellular staining (dark red) with Sirius red and close association with HSCs.

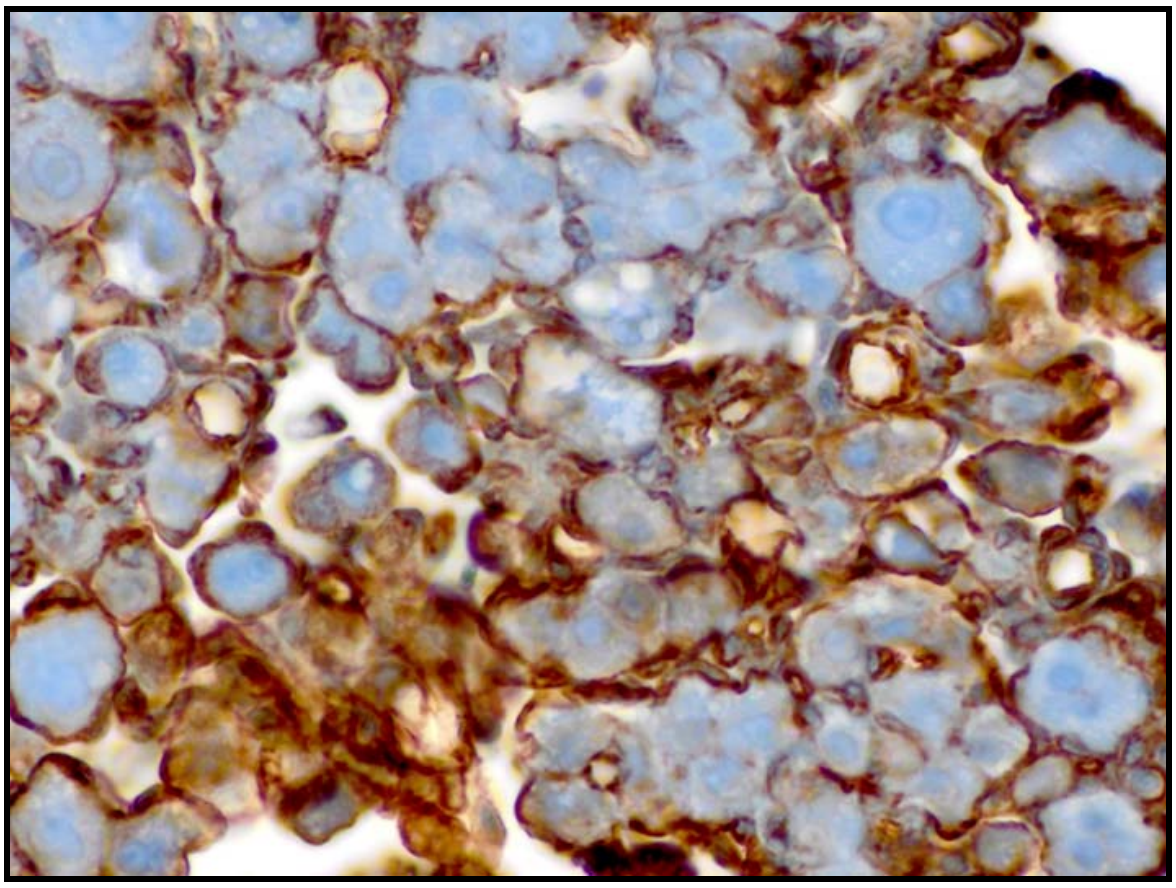

Fig 30. Medaka liver, 100 ppm DMN at 2 months PE (400X). Increased pericellular staining with AE1/AE3 cytokeratin. Positively stained cells may be HSCs or BPDECs.

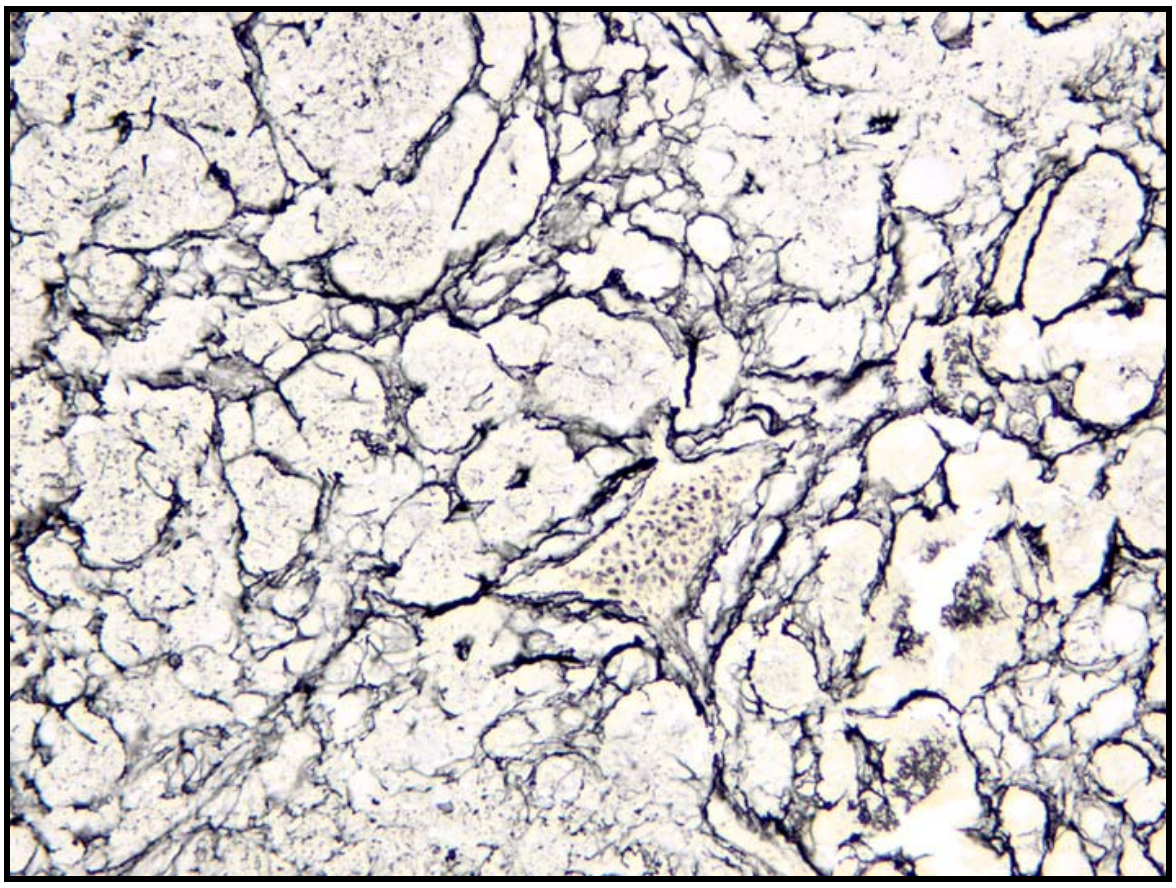

Fig 31. Medaka liver, 50 ppm DMN at 4 months PE (400X). Increased staining with reticulin silver stain. Note marked increase in new basement membrane deposition in comparison to control (Fig.ure 23).

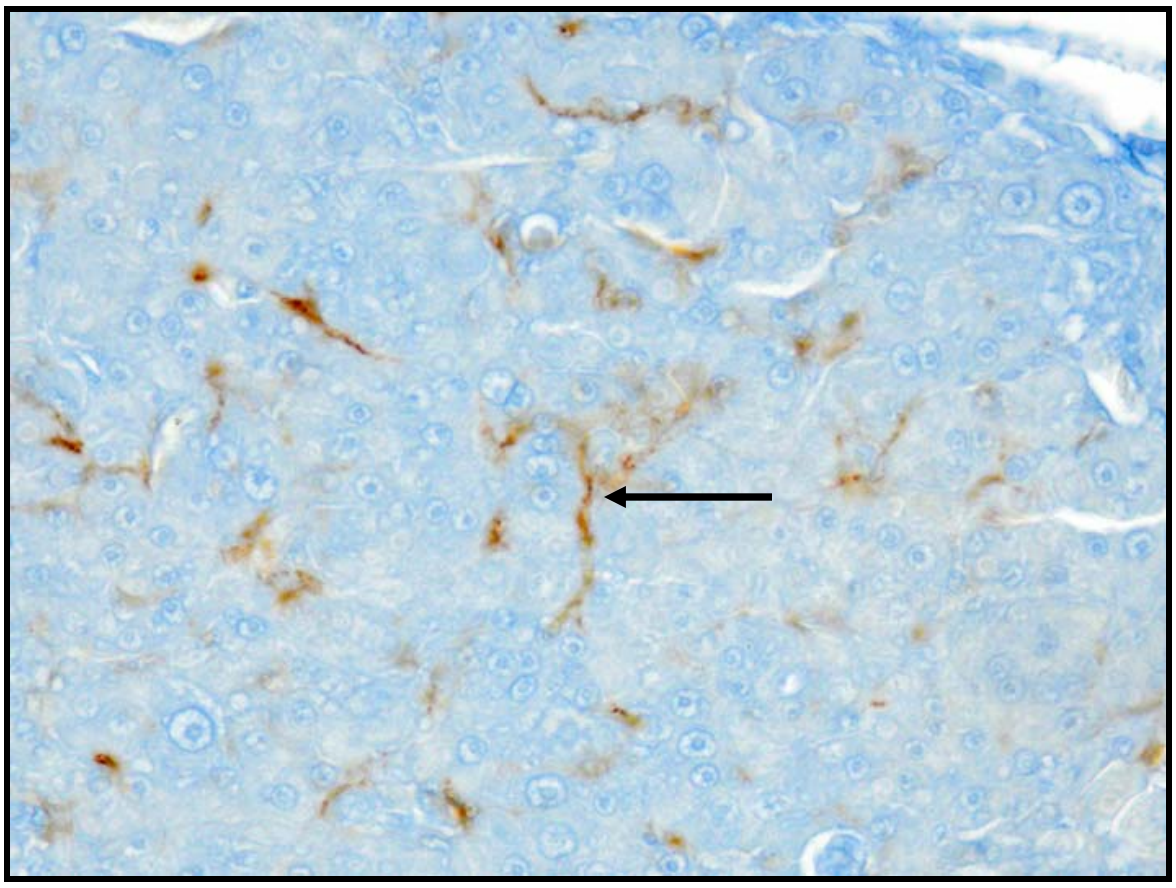

Fig 32. Medaka liver, 50 ppm DMN at 4 months PE (400X). Increased pericellular staining for MSA (arrow). Cells staining positively for MSA are presumably transdifferentiated HSCs.

CHAPTER 4:

Dibromonitromethane, a Drinking Water Disinfection By-Product, Does Not Induce Mutations in λ*cII* Transgenic Medaka

Kristen R. Hobbie[a,b], Anthony B. DeAngelo[c], Leon C. King[c], Richard N. Winn[d], J. McHugh Law[a,*]

[a]Comparative Biomedical Sciences Program and Center for Comparative Medicine and Translational Research, College of Veterinary Medicine, North Carolina State University, Raleigh, NC, USA

[b]Integrated Laboratory Systems, Inc., Research Triangle Park, NC, USA

[c]US Environmental Protection Agency, National Health & Environmental Effects Research Laboratory, Research Triangle Park, NC, USA

[d]Aquatic Biotechnology and Environmental Laboratory, Warnell School of Forestry and Natural Resources, University of Georgia, Athens, GA, USA

Abstract

In vitro mutagenicity studies with Salmonella have demonstrated the halonitromethane (HNM) class of water disinfection byproducts to be mutagenic and cytotoxic and likely to induce base substitutions at –GC- sites, as well as frameshift mutations (Kundu et al., 2004a,b). Additional studies, using Chinese hamster ovary (CHO) AS52 cells and single cell gel electrophoresis (Comet assay), have demonstrated HNMs to be genotoxic. With Ames and comet assays, brominated nitromethanes were revealed to be more mutagenic, cytotoxic, and genotoxic than their chlorinated analogues, and dibromonitromethane (DBNM) was the most reactive of all HNMs examined. Currently, there is no *published* data on the reactivity of halonitromethanes *in vivo*. Unpublished data with rats and DBNM has shown direct interaction with DNA and the formation of DBNM-guanine and -adenine adducts. Currently, the ability of DBNM to induce mutations was investigated in the liver of *cII* transgenic medaka (Oryzias latipes), a small fish model that utilizes the λLIZ bacteriophage vector as an *in vivo* mutational target. In addition, ^{32}P-postlabeling methods were used to identify DBNM adducts in medaka hepatic DNA. The known medaka mutagen, benzo[a]pyrene (B[a]P), was used as a positive control. Medaka were exposed to DBNM at 0, 10, 100, and 500 ppb DBNM for 96 hours. Following exposure, medaka designated for adduct isolation were euthanized immediately, whereas those used for the *cII* mutagenicity assay and histopathological evaluation were returned to regular culture conditions for 30 days. Mutations were not induced in medaka exposed to DBNM for 96 hours, and neither DBNM

nor B[a]P adducts were recovered from medaka livers. DNA extraction procedures may have been responsible for the lack of adducts recovered from medaka DNA. In conclusion, *cII* results in λ transgenic medaka suggest that DBNM is not mutagenic in livers of medaka. However, considering the direct-acting mechanism of action for DBNM, mutant induction at sites of initial contact, such as gills and skin, cannot be ruled-out.

1. Introduction

During the early 20th century, the advent of drinking water chlorination dramatically decreased the frequency of water borne disease outbreaks and is considered a landmark of American public health policy (DeAngelo et al., 1991). However, in the mid-1970s, potentially deleterious by-products were identified in drinking water that formed when chlorine interacted with naturally occurring humic acids and organic compounds in surface waters (Dunnick et al., 1993). Over the past quarter century, drinking water analyses have identified approximately 600 disinfection by-products (DBPs), which account for <50% of the total organic halide mass in chlorinated drinking water (Kundu et al., 2004; Richardson et al., 2002; Stevens et al., 1990). The halogenated methanes (HMs) constitute a major class of DBPs whose occurrence and toxicology have been studied extensively (Kundu et al., 2004). The U.S. Environmental Protection Agency (EPA) is responsible for regulating the total concentration of trihalomethanes in water disinfected for human consumption.

The halonitromethanes (HNMs), a class of DBPs related to HMs, are one of the more recently identified DBPs in chlorinated-, chloraminated-, chlorine-ozonated, and chloramine-ozonated drinking water (Plewa et al., 2004; Richardson et al., 1999). Very little information exists on the carcinogenic risk of HNM's and the U.S. EPA has targeted this class as DBPs of increased concern. Structurally, the HNMs are similar to halomethanes, a class of DBPs that have been associated with various cancers. Like halomethanes, HNMs are halogenated (i.e. chlorine and bromine) methanes, but have a nitro group (NO_2) attached to the central carbon atom instead of hydrogen. The greater electron-withdrawing character of this nitro

group relative to the hydrogen of HMs leads to a greater lability of the departing halogen and a greater reactivity of the formed HNM carbocation (Kundu et al., 2004). This greater reactivity presumably confers a greater cytotoxic and mutagenic potential for HNMs.

In vitro studies, with the *Salmonella typhimurium* (Ames) plate-incorporation mutagenicity assay, have demonstrated the halonitromethanes as a class to be mutagenic and cytotoxic and likely to induce base substitutions at –GC- sites, as well as frameshift mutations (Kundu et al., 2004). Additional studies, using Chinese hamster ovary (CHO) AS52 cells and single cell gel electrophoresis (Comet assay), have demonstrated HNMs to be genotoxic (Plewa et al., 2004). With Ames and comet assays, brominated nitromethanes were revealed to be more mutagenic, cytotoxic, and genotoxic than their chlorinated analogues, and dibromonitromethane (DBNM) was the most reactive of all HNMs examined. Currently, there is no published data on the reactivity of halonitromethanes *in vivo*.

A concern exists that HMN exposure may be associated with an increased risk of cancer, specifically colon and bladder cancer (Dunnick et al., 1993). Results with the Salmonella mutagenicity assay would suggest that HNMs are mutagenic *in vivo*; however, biological factors such as absorption, distribution, metabolic activation, detoxication, and DNA repair can affect the ultimate outcome of chemical exposure *in vivo*. Historically, the link between chemical exposure and cancer in humans has been determined with whole animal two-year chronic bioassays using chemical doses that may be several orders of magnitude higher than that encountered by humans in the environment (Law, 2001). Conversion of animal data to estimates of human risk involves extrapolations of high

experimental doses to lower, more environmentally relevant exposures (Hobbie et al., 2009). Two-year bioassays are costly in regards to animals and time. In addition, evaluation of chemicals at lower doses requires more animals to provide statistically significant data due to lower tumor frequencies. Measurements of genetic endpoints, such as DNA adducts and mutations, integrate biological factors involved in chemical exposure and provide mechanistic data for potential carcinogens at lower doses than that required for tumor induction in a shorter time period. In addition, alternative animal models, such as small fish models, are available that can provide mechanistic data for potential carcinogens more economically than traditional rodent models.

The usefulness of the small fish model, *Oryzias latipes* (medaka), for testing environmental carcinogens is well documented (Bunton, 1996; Hawkins et al., 1988; Hinton et al., 1985; Hoover, 1984; Law et al., 1998). Medaka are easy to breed and maintain in large numbers under laboratory conditions; are sensitive to a large number of known carcinogens with a short time to tumorigenesis; and have an extremely low spontaneous tumor rate. In addition, recent advances in the production of transgenic fish have enhanced the utility of these animals in providing new animal models (Geter et al., 2004; MacLean, 1998). Transgenic models, such as the *cII* transgenic medaka, facilitate the acquisition of mechanistic data invaluable to carcinogen risk assessment. *CII* transgenic medaka carry copies of the lambda LIZ bacteriophage vector which harbors the *cII* gene as a genetically neutral mutational target. The *cII* medaka is useful for the detection of mutations *in vivo*. This is the same mutational target available in Big Blue® rats and mice.

The purpose of this study was to determine if the halonitromethane, DBNM, was mutagenic *in vivo* for cII transgenic medaka exposed to DBNM for 96 hours in their tank water. This is the first report of DBNM exposure in fish. To verify an effect of DBNM *in vivo*, DNA adducts were identified and verified against *in vitro* DBNM adduct standards, DNA were isolated to look for significant mutant induction, and individual fish examined for early morphological and histochemical changes secondary to DBNM exposure. Considering the positive mutagenicity results for DBNM in Salmonella, we hypothesized that DBNM would be mutagenic in the livers of DBNM-exposed medaka and that DNA adduct isolation could be correlated to mutant induction.

2. Materials and Methods

2.1 Chemicals

Dibromonitromethane (DBNM) (>90% pure) was purchased from Cansyn Chemical Corp (New Westminster, BC). Benzo[a]pyrene (B[a]P; >97% pure, HPLC grade) was purchased from Sigma (St. Louis, MO). All other reagents used were of the highest grade commercially available.

2.2 Animals

Lambda *(λ)* transgenic Japanese medaka (*Oryzias latipes*) were obtained from laboratory reared populations at the Aquatic Biotechnology and Environmental Laboratory (ABEL), University of Georgia, Athens, GA. The *λ* transgene consists of a 45.5-kb LIZ

bacteriophage vector that contains both *cII* and *lacI* mutation target genes flanked by cos sites to allow for excision and packaging (Geter et al., 2004; Kohler et al., 1991). Medaka were acclimated for 2 weeks in reconstituted (1 g/L Instant Ocean® salts) reverse osmosis-purified (RO) water within a re-circulating, freshwater culture system under an artificial light photoperiod (16 hours light: 8 hours dark) at a temperature of 26 ± 0.5ºC. Animal care and use were in conformity with protocols approved by the Institutional Animal Care and Use Committee in accordance with the National Academy of Sciences Guide for the Care and Use of Laboratory Animals.

2.3 DBNM and B[a]P Exposures

Three-to-four month-old medaka were exposed to DBNM at 0, 10, 100 or 500 μg/L (ppb) or to B[a]P at 50 ppb in the ambient water for 96 hours. Exposures were conducted with fasted medaka to ensure good water quality (Geter et al., 2004). One hundred and twenty-five fish were randomly divided into 500 mL glass beakers, 5 fish per beaker. Treatment beakers were placed into a re-circulating, heated water bath at 26 ºC. DBNM and B[a]P concentrations were renewed every 24 hours. DBNM dilutions were prepared from 100 mL of a 100 mg/L (ppm) stock solution. B[a]P was prepared by dissolving 12.5 mg of B[a]P into 50 mL of acetone (HPLC-grade; Fischer Scientific, Phillipsburg, NJ) and 100 μL added directly to the water to obtain a nominal exposure concentration of 50 μg/L (ppb) (Winn et al, 2005). Following exposure, medaka intended for adduct isolation were immediately euthanized, whereas, medaka designated for the *cII* assay and histopathology

were rinsed, transferred to clean water, and held until euthanized at 30 days post-exposure. Medaka were euthanized with an over-dose of tricaine methanesulfonate (MS-222, Argent Laboratories, Redmond, WA, USA). For adduct isolation and the *cII* assay, livers were dissected from the test fish, flash frozen in liquid nitrogen, and stored at -80 °C until processed for DNA extraction. Coeloms of remaining fish were opened along the ventral midline and their tails trimmed at an angle to the posterior body cavity prior to placement into individually labeled histologic cassette (1 fish/cassette). Fish were fixed, whole, in 10% neutral buffered formalin for 48 hours, de-mineralized in 10% formic acid for 24 hours, and transferred to 70% ethanol.

2.4 DBNM Adduct Standards

A reaction mixture containing CT DNA (10 mg), DBNM (26 mM) in 10 mL of 0.1 M potassium phosphate buffer (pH 7.4) was incubated for 18 hours at 37 ºC. The reaction was quenched by the addition of 10 mL ethyl acetate, and DBNM-modified CT DNA adducts were isolated as previously described (Amin et al., 1989). The isolated DBNM-modified DNA sample was resuspended in 1.0 mL HPLC-grade water and stored in a -80 ºC freezer until time of adduct analysis. Reaction mixtures (10 mg each) containing the nucleotides 3'-dGMP or 3'-dAMP, DBNM (26 mM) in 10 mL of 0.1 M potassium phosphate buffer (pH 7.4) were incubated for 18 hours at 37 ºC. The reactions were quenched with an equal volume of ethyl acetate and diethyl ether (1:1), extracted three times with a 1:1 concentration of ethyl acetate: diethyl ether, and centrifuged at 1500 rpm for 15 minutes. Removal of the

unreacted nucleotides from the aqueous phase was achieved by loading the reaction mixtures on primed (10 mL HPLC grade water and 10 mL of methanol) Sep-Pak classic cartridges (Water, Millipore Corporation, Milford, MA) and washing with 10 mL HPLC grade water and 10 mL of methanol to elute the modified nucleotides. The methanol was removed *in vacuo* and the samples resuspended in 1.0 mL of HPLC water and stored at -80 ºC until time of adduct analysis.

2.5 ^{32}P-Postlabeling of DBNM adducts

Genomic DNA was isolated from medaka livers using the Puregene® DNA Isolation Kit (Gentra Systems, Inc., Minneapolis, MN) as described in Hobbie et al. (2008). Medaka livers were "pooled" to obtain ~50 µg of DNA per treatment group (control, 500 ppb DBNM, and 50 ppb B[a]P). Liver samples were homogenized in cell lysis solution and TEMPO and digested with proteinase K at 37 ºC for 3 hours. Proteins were precipitated with a protein precipitation solution and discarded. Cold 100% isopropanol was added to the supernatant and the solution centrifuged at 2,000-x *g* for 3 minutes. Samples were kept at 4 °C for 48 hours and centrifuged at 2,000-x *g* to facilitate DNA precipitation. The supernatants were discarded and cold 70% ethanol added to the DNA pellets. The solutions were centrifuged at 2,000 x *g* for 1 minute and the ethanol discarded. After drying for 10-15 minutes, the DNA was re-hydrated with DNA hydration solution, the samples vortexed and incubated at 37 ºC for 1 hour. Genomic DNA and DBNM-modified CT DNA were then digested to mononucleotides at 37 ºC for 3.5 hours with micrococcal endonuclease and calf spleen

phosphodiesterase as previously described (King et al., 1994). DNA adducts were enriched by butanol extraction and evaporated to dryness *in vacuo*. The samples including DBNM-modified 3'-dGMP and 3'-dAMP nucleotides were incubated with 50 μCi of [γ^{32}P]ATP (Amersham, 3000 Ci/mmol) and 3.5 units of T_4 polynucleotide kinase (3' phosphatase free) for 30 minutes at 37 ºC. The total incubates were spotted on 10 x 10-cm polyethyleneimine (PEI)-cellulose thin layer chromatography (TLC) plates and separated using a TLC system (D1 direction only) (King et al., 1994). The radioactive areas of adducts were located by autoradiography (exposure to Kodak XARS X-ray film for 16 hours at -80 ºC). The excised adduct spots were counted using 5 mL 95% ethanol as scintillant. The radioactive spots for the high performance liquid chromatography (HPLC) analysis were eluted from the PEI plates with 4.0 M pyridinium formate (pH 4.0) for 18 hours and analyzed according to the method previously described (King et al., 1994). The adduct levels were calculated from the amount of radioactivity (cpm) for each adduct spot on the chromatogram, quantity of DNA, and the specific activity of [γ^{32}P]ATP used for labeling (George et al., 1998).

2.6 Lambda cII Mutagenesis Assay

The lambda *cII* mutagenesis assay was performed as described by Winn et al. (2000). Fish genomic DNA was obtained for the λ *cII* mutagenesis assay using procedures to optimize isolation of high molecular weight DNA for *in vitro* packaging. For each fish, the entire liver (~10 mg) was digested with proteinase K at 37 ºC for 5-10 minutes. Samples were extracted 1-2 times with equal volumes of phenol and chloroform by using wide-bore

pipette tips to minimize DNA shearing. Potassium acetate (KAc) was added to a final concentration of 1 *M* followed by final extraction with an equal volume of chloroform. DNA was precipitated with ethanol, removed with a flame-sealed glass pipette, and re-suspended in Tris-ethylenediamine tetra-acetic acid (Tris·EDTA, pH 7.5). Recovery of the bacteriophage vector was accomplished by incubating liver genomic DNA with *in vitro* packaging extracts, which excised and packaged the vector as viable phage particles (Winn et al., 2000). To select *cII* mutants, individually packaged phage were mixed with *E. coli* G1250 cells and TB1 top agar and plated on ten TB1 plates at 24 ºC (±0.5 ºC) for 40 hours. Lambda phage containing wild-type *cII* underwent lysogenization and was indistinguishable in the bacterial lawn, whereas λ phage with a mutated *cII* gene multiplied through the lytic cycle, forming plaques. To determine the total number of packaged phage, a subsample of the packaged phage was mixed with *E. coli* G1250 cells, plated on three TB1 plates, and incubated at 37 ºC overnight. Mutant frequencies were calculated by dividing the total number of *cII* mutant plaque-forming units (PFUs) on selective screening plates by the estimated total λ+ and *cII* phage on the titer plates. Mutant frequencies (MF) are presented as a mean MF ± standard error of the mean for a treatment group. Comparisons of mutation frequencies were tested for significance by using the generalized Cochran-Armitage test (Carr et al., 1995), using the COCHARM analytical program (Proctor and Gamble, Cincinnati, OH). Unlike the *cII* mutant data reported by Hobbie et al. (2009) for medaka exposed to dimethylnitrosamine (DMN), mutant *λcII* phenotypes were not verified by

polymerase chain reaction (PCR)-amplification and sequencing of the *cII* gene for medaka exposed to DBNM for 96 hours.

2.7 Tissue Processing and Histopathologic Analyses

Fixed fish tissues were processed using standard histological techniques. Fish were embedded, left side down, in paraffin and sectioned at 5 μm. Sagittal and para-sagittal sections of fish were mounted on glass slides and stained with hematoxylin and eosin (HE). Most internal organs and tissues of medaka were examined microscopically, with particular emphasis placed on the liver. HE liver sections from medaka and rats were evaluated for any DBNM-associated degenerative, proliferative, and/or neoplastic lesions.

3. Results

3.1 Medaka DBNM Exposure

In each treatment group, 10 fish were intended for the cII assay, 6 for DNA adduct isolation, 3 for histopathology, and 6 for uptake. During the 96 hour DBNM exposure, seven medaka in the 500 ppb group and one medaka in the 10 ppb group died. At the end of the 96 hours, 6 fish per treatment group (total = 30) were removed for adduct isolation. During the 30 day grow-out period, 10 fish died in the 500 ppb DBNM group, 6 fish died in the 100 ppb DBNM group, 7 fish died in the 10 ppb DBNM group, 6 fish died in the control group (0 ppb DBNM) and 6 fish died in the 50 ppb B[a]P group. Three fish per treatment group were

removed for histopathology and the remaining fish used for the cII assay. Insufficient numbers of fish remained for compound uptake measurements.

3.2 ^{32}P-postlabeling and HPLC Analyses

To determine whether DBNM adducted with liver DNA *in vivo*, ^{32}P-postlabeled digests of hepatic DNA from medaka exposed to 0 ppb or 500 ppb DBNM were separated by thin layer chromatography, quantified with high performance liquid chromatography, and compared to the retention times of *in vitro* DBNM adduct standards. Adduct standards were created via incubation of DBNM with calf thymus DNA, guanine monophosphates, and adenine monophosphates. Chromatograms of *in vitro* ^{32}P-postlabeling data confirmed that DBNM formed adducts when combined with calf thymus DNA, as well as with adenine and guanine monophosphates (Figure 1). Peaks indicative of guanine adducts were present at retention times of 0.68, 0.83, 1.00, and 1.09 minutes, whereas peaks for adenine adducts were present at 0.83 and 1.00 minutes. Guanine adducts represented ~80% of total measured adducts, and adenine adducts the remaining 20% for DBNM in calf thymus DNA (information provided by Dr. Leon King). Representative HPLC analyses of ^{32}P-postlabeled digests from control medaka (0 ppb DBNM) and medaka exposed to 500 ppb DBNM (Figure 2) revealed neither guanine nor adenine adducts when compared to the DBNM + calf thymus DNA or DBNM + adenine- or guanine-monophosphate adduct standards (Figure 1). In addition, no peak at 0.92 minutes consistent with the major B[a]P-DNA adduct, *anti*-BP-7,8-diol-9,10-epoxide (Figure 1), was evident in fish exposed to 50 ppb B[a]P (Figure 2).

3.3 Lambda cII Mutagenesis Assay

To test whether DBNM was mutagenic *in vivo*, the mutation frequencies in livers of lambda (λ) transgenic medaka were determined after a thirty day mutation manifestation period (Table 1). COCHARM statistical analysis revealed that the mutant frequencies in livers of treated fish did not increase significantly above background spontaneous mutant frequencies after DBNM exposure. One-tailed t-test "p values" derived for DBNM treatment groups were all greater than 0.05 ($p < 0.05$ being significant) with corresponding mutation frequencies similar to that of the control fish ($2.09 \pm 1.57 \times 10^{-5}$). Fish exposed to 10 ppb, 100 ppb, or 500 ppb DBNM had mean mutant frequencies of $3.20 \pm 1.27 \times 10^{-5}$ ($p = 0.1256$), $3.13 \pm 1.39 \times 10^{-5}$ ($p = 0.1530$), and $2.86 \pm 0.81 \times 10^{-5}$ ($p = 0.1752$), respectively (Figure 3). The mean mutant frequency of 2.09×10^{-5} observed in livers of [untreated] control medaka corresponded moderately well with that reported for spontaneous mutant frequency values in λ transgenic medaka (Winn et al., 2000; Winn et al., 2005). Although the average mutant frequency of fish exposed to B[a]P in the current study was statistically significant at $p = 0.0286$ (Table 1), the mean mutant frequency of $8.26 \pm 4.45 \times 10^{-5}$ was lower than that reported by Winn et al. (2005) for medaka exposed to 50 ppb B[a]P for 96 hours ($14.1 \pm 2.1 \times 10^{-5}$) and held for a 15-day mutation manifestation period.

3.4 Histopathology

To determine if DBNM-associated lesions were present in medaka exposed to 0, 10, 100, and 500 ppb DBNM, multiple HE-stained sections of fish (whole mounted) were examined via histopathology. After complete examination of all tissues and organ systems, no remarkable macroscopic or microscopic lesions were apparent in control (0 ppm DBNM)- or DBNM-treated medaka. In addition, no macroscopic or microscopic lesions were evident in fish exposed to 50 ppb B[a]P.

4. Discussion

From the work presented here, we propose that DBNM is not a mutagenic compound in the medaka liver after aqueous exposure. The identification of guanine and adenine adducts via ^{32}P-postlabeling after *in vitro* incubation of DBNM with calf thymus DNA, guanine monophosphate, and adenine monophosphate confirms that DBNM directly interacts with DNA. These results are consistent with that previously reported by Kundu et al. (2004) for DBNM with the *Salmonella* plate incorporation assay (Ames Assay). Kundu et al. found that DBNM was weakly mutagenic or mutagenic in the presence and absence of aroclor-induced rat liver S9 microsomal fractions for multiple Salmonella strains indicating that, at least qualitatively, metabolic biotransformation had only a minor influence on the mutagenicity of DBNM in Salmonella. The current *in vitro* data in the face of that reported by Kundu et al. (2004) suggest that metabolic activation may not be necessary for DBNM to exert an effect on genomic DNA. Unpublished *in vivo* adduct data (provided by Drs.

Anthony B. DeAngelo and Leon King of the U.S. Environmental Protection Agency) for Fischer 344 rats exposed to DBNM in their drinking water isolated guanine and adenine adducts from hepatic DNA via ^{32}P-postlabeling and HPLC analysis. One-month-old male and female rats were exposed to 0 or 200 ppb DBNM in their drinking water for thirty days. HPLC analysis of ^{32}P-postlabeled adducts from rat hepatic DNA demonstrated four peaks indicative of guanine and adenine adducts at the same retention times of the DBNM adduct standards for rats exposed to 200 ppb DBNM (data presented with permission of Drs. DeAngelo and King in Figure 4).

For comparison purposes, hepatic DNA from medaka fish exposed to 0 ppb or 500 ppb DBNM via aqueous exposure for 96 hours was labeled with γ^{32}P and analyzed by HPLC. Unlike rats exposed to DBNM in their drinking water, no guanine or adenine adducts were evident at retention times, 0.68, 0.83, 1.00, and 1.09 minutes, for medaka exposed to 500 ppb DBNM (Figure 2). ^{32}P-postlabeling results from hepatic DNA for medaka exposed to 500 ppb were no different than those for unexposed control fish (Figure 2). These results may suggest that the liver is not a target organ for DBNM in medaka. DBNM *in vitro* adduct results and mutagenicity results from the Ames assay (Kundu et al., 2004) would suggest a direct-acting mechanism for DBNM on DNA. The liver is often a target organ for indirect-acting xenobiotic compounds such as B[a]P that require metabolic activation to reactive metabolites in order to interact with DNA. If DBNM has a direct-acting mechanism in medaka, then tissues of initial contact such as skin and gills may be target organs, and not liver. The presence of DNA adducts in livers of DBNM-exposed rats may be a species-

specific difference in compound uptake/distribution and/or metabolism. In addition, no hepatic *anti*-BPDE guanine adducts consistent with metabolic bioactivation were evident in medaka exposed to B[a]P (Figure 2). It may be that medaka liver simply lacks the metabolic machinery to convert DBNM to the toxic metabolite(s). More work will need to be done on metabolism of HNMs in various test animals in order to sort this out. The lack of DBNM guanine and adenine adducts as well as anti-BPDE guanine adducts in medaka also raises the possibility that the integrity of the DNA was compromised during the ^{32}P-postlabeling procedure. The butanol extraction procedure may have been too harsh and degraded the medaka DNA prior to ^{32}P-postlabeling.

Although DNA adduct isolation from medaka hepatic DNA was unsuccessful, bacteriophage lambda was effectively recovered from livers of transgenic medaka exposed to 0, 10, 100 or 500 ppb DBNM, or to 50 ppb B[a]P. Mutant frequencies calculated for all exposed fish were not statistically different from those calculated for unexposed controls. The lack of significant induction of mutants above the background mutant frequency for DBNM-treated medaka suggests that DBNM is not mutagenic in livers of transgenic medaka. These results are contrary to that observed by Kundu et al. (2004) for DBNM with the Salmonella mutagenicity assay. Kundu et al. reported DBNM to be mutagenic in TA98, TA100, and RSJ100 Salmonella strains suggesting that DBNM was capable of inducing both base substitutions at GC/CC sites and frameshift mutations. A similar situation occurred for the drinking water disinfection by-product, MX [3-chloro-4(dichloromethyl)-5-hydroxy-2[5H]-furanone]. Mutagenicity assays with Salmonella demonstrated that MX was a

mutagen; however, mutation induction was not observed in the livers of *cII* transgenic medaka exposed to MX for 96 hours (Geter et al., 2004). Considering the gill DNA-damaging potential of MX in shellfish (Sasaki et al., 1997), Geter et al. could not rule out that MX expressed its DNA damaging effects only the tissues of initial contact and suggested gills and skin be examined for mutant induction. DBNM also has the potential to damage DNA. Plewa et al. (2004) reported DBNM to be the most potent mammalian cell cytotoxin and genotoxin in Chinese hamster ovary cells using the microplate cytotoxicity and single cell gel electrophoresis assays. During preliminary experiments with DBNM (unpublished data), medaka demonstrated acute respiratory distress and death associated with exposure to high concentrations of DBNM (>1000 ppb DBNM). Gill capillary aneurysms were evident on histopathology presumably due to the DBNM exposure. Despite determination of an approximate LC_{50} for DBNM in medaka, deaths occurred during and after DBNM exposure, particularly in the 500 ppb DBNM dose group. As with MX and medaka, it is possible that DBNM expresses its damaging effects only on the tissues of initial contact (i.e. gills and skin). DBNM's ability to interact with DNA without the need to be activated to a reactive metabolite supports a direct mechanism of action for DBNM in fish. Although DBNM was not mutagenic in the livers of exposed medaka, mutant induction in tissues of initial contact such as gills and skin cannot be ruled out for DBNM in fish.

5. Summary

The DNA adduct and *cII* mutagenicity assay data demonstrate that DBNM has a different effect in medaka than in F344 rats. They also suggest that a potential exists for the DBNM rat liver data to be in agreement with the positive mutagenicity results reported by Kundu et al. (2004) for DBNM in Salmonella, whereas the negative DBNM mutagenicity data in the livers of fish is contradictory. However, without adduct data for DBNM-exposed medaka and *cII* mutagenicity data for similarly exposed rats, further species-to-species and *in vivo*-to-*in vitro* comparisons cannot be discerned. In addition, although Kundu et al. reported DBNM to be the most mutagenic HNM in Salmonella, the overall number of revertants (<1000 rev/μmol) for HNMs [in general] classified them as only weak mutagens in Salmonella. It is possible that the reactive DBNM carbocation adducts to DNA in both rats and fish, but at sufficiently low levels as to be repaired prior to DNA replication and mutation fixation. The lack of significant mutant induction for medaka fish exposed to DBNM in the face of positive mutagenicity results in Salmonella stresses the importance of considering the effects of potential carcinogens *in vivo* in addition to *in vitro* when determining the risks of a chemical to human health.

Acknowledgements

The authors thank Michael George (EPA) and Steven Kilburn (EPA) for their excellent technical assistance. This work was supported by NCSU College of Veterinary Medicine state appropriated funds and the NCSU/EPA Cooperative Training Program in Environmental Health Sciences, Research Training Agreement CT826512010.

REFERENCES

Bunton TE, 1996. Experimental Chemical Carcinogenesis in Fish. Toxicologic Pathology 24: 603-618.

Carr GJ, Gorelick NJ, 1995. Statistical Design and analysis of mutation studies in transgenic mice. Environ Mol Mutagen 25, 246-255.

DeAngelo AB, Daniel FB, Stober JA Olson GR, 1991. The carcinogenicity of dichloroacetic acid in the male B6C3F1 mouse. Fundam. Appl. Toxicol 16, 337-347.

Dunnick JK and Melnick RL, 1993. Assessment of the Carcinogenic Potential of Chlorinated Water: Experimental Studies of Chlorine, Chloramine, and Trihalomethanes. Journal of the National Cancer Institute 85, 817-822.

George SE, Allison JC, Brooks LR, Eischen BT, Kohan MJ, Warren SH, King LC, 1998. Modulation of 2,6-Dinitrotoluene Genotoxicity by Alachlor Treatment of Fischer 344 Rats. Environmental and Molecular Mutagenesis 31, 274-281.

Geter DR, Winn RN, Fournie JW, Norris MB, DeAngelo AB, Hawkins WE, 2004. MX [3-Chloro-4-(Dichloromethyl)-5-Hydroxy-2[5]-Furanone], a Drinking Water Carcinogen, Does Not Induce Mutations in the Liver of cII Transgenic Medaka (Oryzias latipes). Journal of Toxicology and Environmental Health, Part A 67, 373-383.

Hawkins WE, Overstreet RM, and Walker WW, 1988. Small fish models for identifying carcinogens in the aqueous environment. Water Resources Bulletin 24, 941-949.

Hinton DE, Hampton JA, and McCuskey PA, 1985. Japanese medaka liver tumor model: review of literature and new findings. In Jolley R, Bull R, Davis W, Katz S, Roberts M, and Jacobs V, eds., Water Chlorination: Chemistry, Environmental Impact, and Health Effects, vol. 5, Lewis Publishers, Chelsea, MI, pp.439-450.

Hobbie KR, DeAngelo AB, King LC, Winn RN, Law JM, 2009. Toward a molecular equivalent dose: use of the medaka model in comparative risk assessment. Comparative Biochemistry and Physiology, Part C 149, 141-151.

Hoover KL, ed., 1984. Use of small fish species in carcinogenicity testing. Bethesda: National Cancer Institute.

King LC, George M, Gallagher JE, Lewtas J, 1994. Separation of 32P-postlabeled DNA adducts of polycyclic aromatic hydrocarbons and nitrated polycyclic aromatic hydrocarbons by HPLC. Chem Res Toxicol 7, 503-510.

Kohler SW Provost GS Fieck A Kretz PL Bullock WO Sorge JA Putman DL, Short JM, 1991. Spectra of spontaneous and mutagen-induced mutations in the lacI gene in transgenic mice. Proc Natl Acad Sci USA 88, 316-321.

Kundu B, Richardson SD, Swartz PD, Matthews PP, Richard AM, DeMarini DM, 2004. Mutagenicity in Salmonella of halonitromethanes: a recently recognized class of disinfection by-products in drinking water. Mutation Research 562, 39-65.

Law, JM, 2001. Mechanistic considerations in small fish carcinogenicity testing. ILAR Journal 42, 274-284.

Law, JM, Bull M, Nakamura J, Swenberg JA, 1998. Molecular dosimetry of DNA adducts in the medaka small fish model. Carcinogenesis 19, 515-518.

MacLean N, 1998. Regulation and exploitation of transgenes in fish. Mutation Research 399, 255-266.

Plewa MJ, Wagner ED, Jazwierska P, 2004. Halonitromethane Drinking Water Disinfection Byproducts: Chemical Characterization and Mammalian Cell Cytotoxicity and Genotoxicity. Environ. Sci. Technol. 38, 62-68.

Richardson SD, Simmons JE, Rice G, 2002. Disinfection Byproducts: The next generation. Environmental Science and Technology 36, 198A-205A.

Richardson SD, Thruston AD, Caughran TV, Chen PH, Collette TW, Floyd TL, Schenck KM, Lykins BW, Sun G-R, Majetich G, 1999. Identification of New Drinking Water Disinfection Byproducts Formed in the Presence of Bromide. Environmental Science and Technology. 33, 3378-3383.

Sasaki YF, Izumiyama F, Nishidate F, Ishibashi S, Tsuda S, Matsusaka N, Asano N, Saotome K, Sofuni T, Hayashi M, 1997. Detection of genotoxicity of polluted sea water using shellfish and the alkaline single-cell gel electrophoresis (SCE) assay: A preliminary study. Mutation Research 393, 133-139.

Stevens AA Moore LA Slocum CJ Smith BL Seeger DR Ireland JC, 1990. Byproducts of Chlorination at Ten Operating Utilities. In Water Chlorination: Chemistry, Environmental Impact, and Health Effects; Jolley RL, Condie LW, Johnson JD, Katz S, Minear RA, Mattice JS, Jacobs VA, Eds.; Lewis Publishers: Chelsea , MI, 6, p 579.

Winn RN, Norris MB, Brayer KJ, Torres C, Muller SL, 2000. Detection of mutations in transgenic fish carrying a bacteriophage λcII transgene target. Proc. Natl. Acad. Sci. USA 97, 12655-12660.

Winn RN, Norris MB 2005. Analysis of mutations in lambda transgenic medaka using the cII mutation assay. Chapter 38. In: Techniques in Aquatic Toxicology, 2nd Ed. G.K. Ostrander (Ed.) pp. 705-734

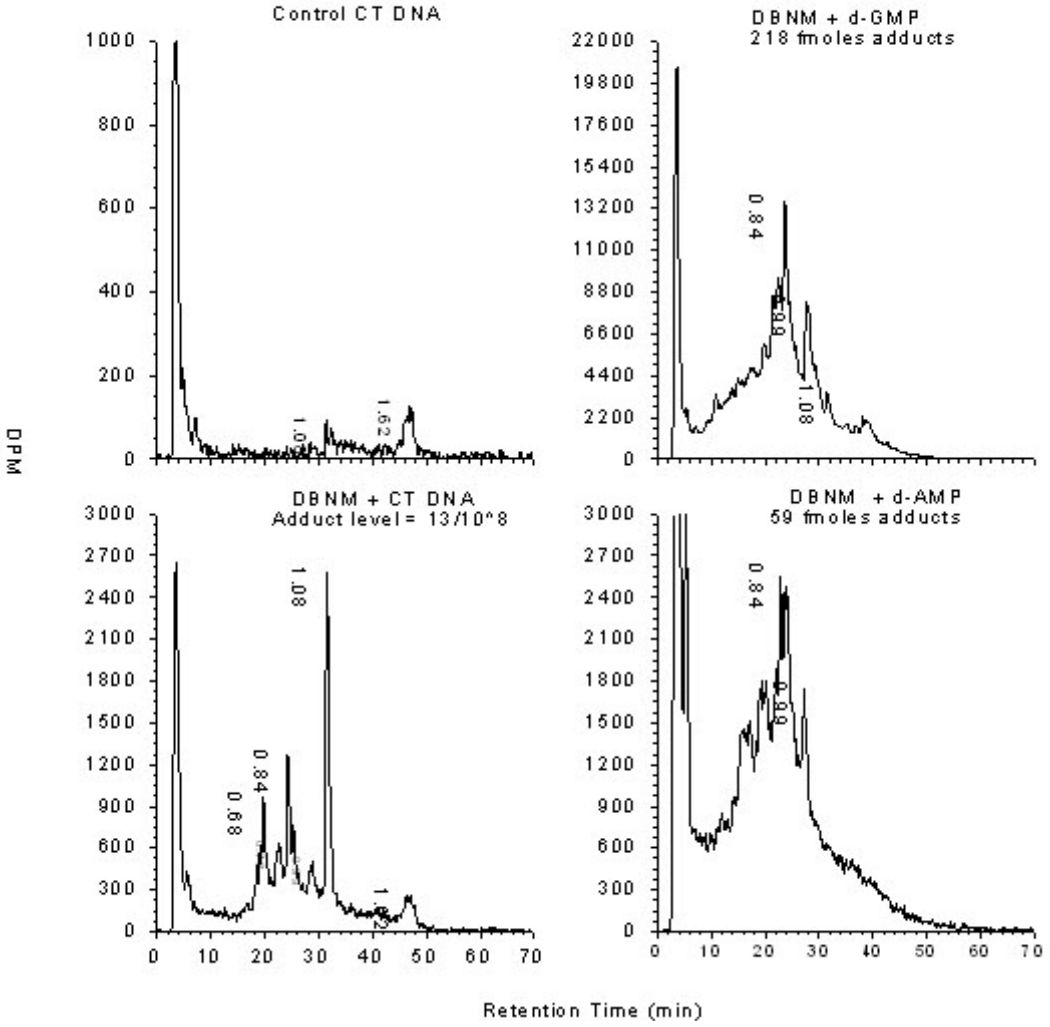

Figure 1. ^{32}P-postlabeling results for control calf-thymus DNA *and* DBNM adducted calf-thymus DNA, guanine monophospate (dGMP) and adenine monophosphate (dAMP). Peaks indicative of guanine adducts were present at retention times of 0.68, 0.83, 1.00, and 1.09 minutes, whereas peaks for adenine adducts were present at 0.83 and 1.00 minutes. Guanine adducts represented ~80% of total measured adducts, and adenine adducts the remaining 20% for DBNM in calf thymus DNA

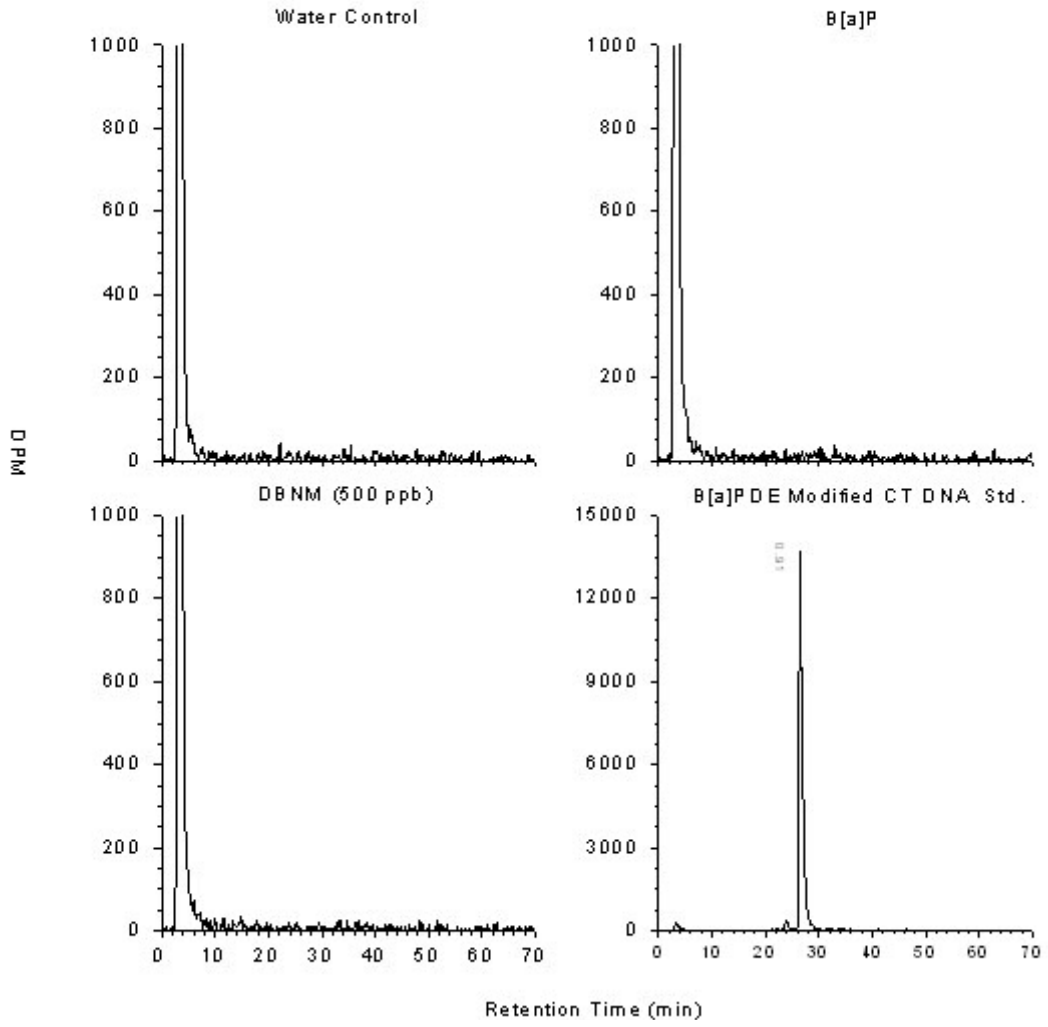

Figure 2. ^{32}P-postlabeled digests from control medaka (0 ppb DBNM) and medaka exposed to 500 ppb DBNM revealed neither guanine nor adenine adducts when compared to the DBNM + calf thymus DNA or DBNM + adenine- or guanine-monophosphate adduct standards (Figure 1). In addition, no peak at 0.92 minutes consistent with the major B[a]P-DNA adduct, *anti*-BP-7,8-diol-9,10-epoxide, was evident in fish exposed to 50 ppb B[a]P.

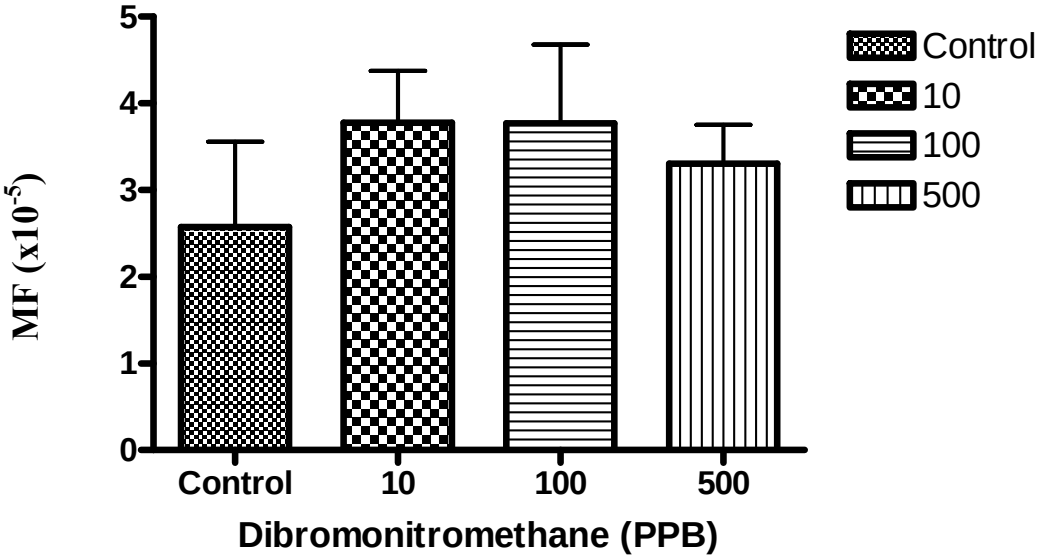

Figure 3. Mean mutant frequencies for livers of lambda (λ) transgenic medaka exposed to 10 ppb, 100 ppb, or 500 ppb DBNM were $3.20 \pm 1.27 \times 10^{-5}$ ($p = 0.1256$), $3.13 \pm 1.39 \times 10^{-5}$ ($p = 0.1530$), and $2.86 \pm 0.81 \times 10^{-5}$ ($p = 0.1752$), respectively. One-tailed t-test "p values" derived for DBNM treatment groups were all greater than 0.05 ($p < 0.05$ being significant) with corresponding mutant frequencies similar to that of the control fish ($2.09 \pm 1.57 \times 10^{-5}$).

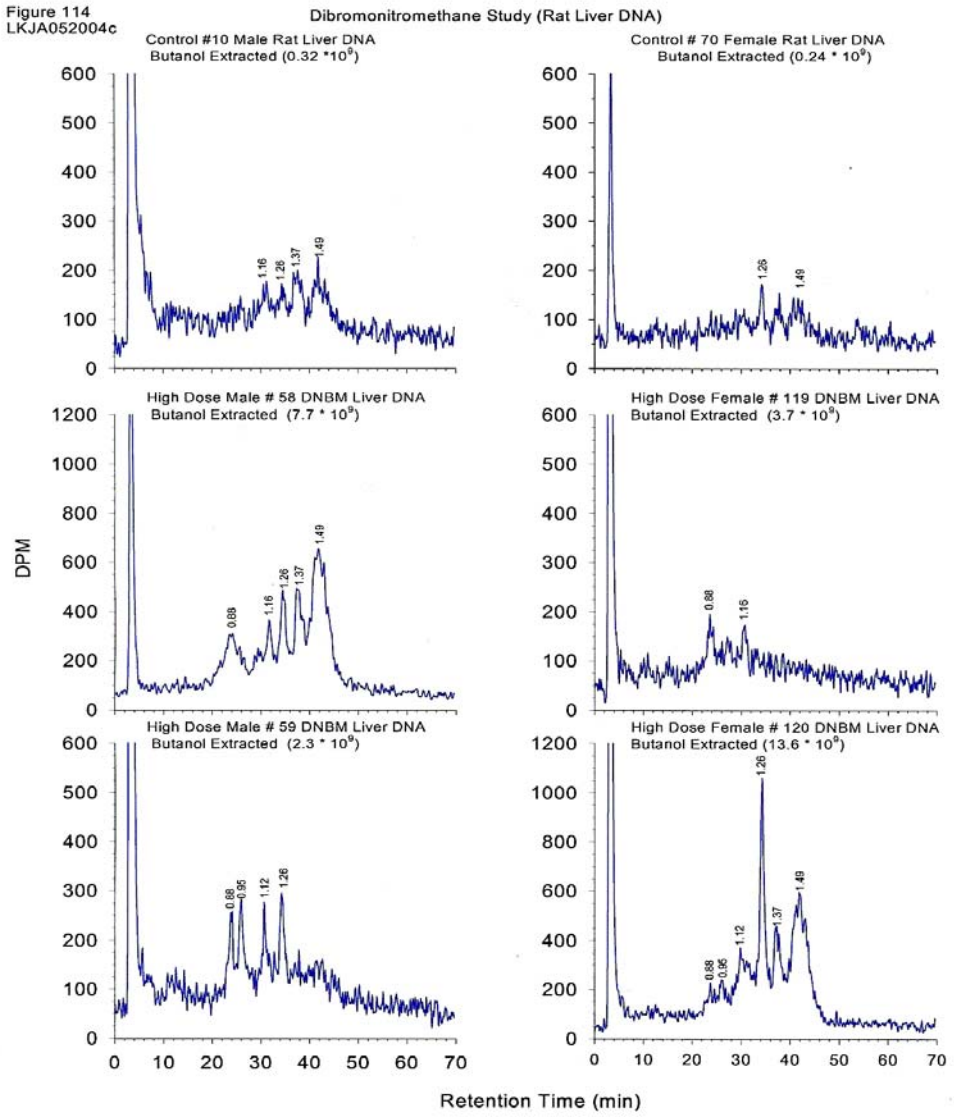

A

Figure 4. HPLC analysis of ^{32}P-postlabeled adducts from rat hepatic DNA demonstrated four peaks indicative of guanine and adenine adducts at the same retention times of the DBNM adduct standards for rats exposed to 200 ppb DBNM (data presented with permission of Drs. DeAngelo and King). DBNM-guanine or adenine adducts were evident at retention times, 0.68, 0.83, 1.00, and 1.09 minutes

Table 1
Frequencies of *cII* mutants recovered from the livers of untreated and DBNM-treated λ transgenic medaka.

DBNM ppb	Animal ID	Number of Mutants	Total plaques screened	MF (x 10^{-5})
0	CL1	10	1,185,000	0.84
0	CL2	8	665,000	1.20
0	CL3	23	2,135,000	1.08
0	CL4	60	1,520,000	3.95
0	CL5	22	380,000	5.79
10	10DB-1	19	490,000	3.88
10	10DB-2	33	2,235,000	1.48
10	10DB-3	92	2,730,000	3.37
10	10DB-4	66	1,740,000	3.79
10	10DB-5	31	515,000	6.02
10	10DB-6	26	630,000	4.13
100	100DB-1	133	3,375,000	3.94
100	100DB-2	38	1,075,000	3.53
100	100DB-3	78	1,810,000	4.31
100	100DB-4	40	2,200,000	1.82
100	100DB-5	29	380,000	7.63
100	100DB-6	33	2,380,000	1.39
500	500DB-1	22	625,000	3.52
500	500DB-2	26	610,000	4.26
500	500DB-3	40	1,840,000	2.17
500	500DB-4	39	1,640,000	2.38
500	500DB-5	24	570,000	4.21
50 ppb B[a]P	B[a]P-1	245	4,045,000	6.06
50 ppb B[a]P	B[a]P-2	111	2,155,000	5.15
50 ppb B[a]P	B[a]P-3	261	1,270,000	20.55

GROUP STATISTICS

Compound	Dose (ppb)	MF (x 10^{-5})	SD	1 Tail P (p <0.05 is significant)
DBNM	0	2.09	0.70	--------
	10	3.20	1.27	0.1256
	100	3.13	1.39	0.1530
	500	2.86	0.81	0.1752
B[a]P	50	8.26	4.45	0.0286

CHAPTER 5: Overall Discussion

Cancer is the second leading cause of death in humans, second only to heart disease. Historically, approximately 80% of human cancers have been associated with exposure to environmental contaminants (Doll and Peto, 1981; Law, 2001). This percentage has been modified overtime; however, human exposure to environmental carcinogens still remains a concern (Begg CB, 2001; Clapp R, 2000; Harvard, 1996). Prompt identification and regulation of environmental toxicants and carcinogens is critical to safeguarding human health. The standard for determining carcinogenic risk is the 2-year rodent bioassay, which evaluates chemicals at doses that may be several orders of magnitude higher than occurs in the environment. Chronic bioassays are based on the assumption that effect (tumors) is linearly related to carcinogenic dose, "a no threshold-effect." However, it has become increasingly apparent, that the dose-response relationships for many carcinogens are in fact, *not linear*. Therefore, high-dose to low-dose extrapolations of bioassay tumor data may not accurately represent risk at lower, more environmentally relevant exposures. The incorporation of mechanistic data into carcinogenic risk assessment has provided valuable insight into the shapes of the dose-response relationships (Preston, 2002). Chemical uptake, metabolism, and mode of action (*genotoxic versus epigenetic effects*), as well as an individual organism's response to chemical exposure (detoxification, bioactivation, DNA repair, cell proliferation, and programmed cell death, etc.) can all contribute to non-linearities in the dose-response.

Despite these advances, carcinogenic risk assessment is still costly, with regard to funds and time (Weisburger and Williams, 1981), prompting the investigation of alternative, non-mammalian models in the study of chemically induced mutagenesis and carcinogenesis (Law, 2001; Winn, 2000). Small fish models, such as the medaka, are a cost-effective alternative to more costly rodent bioassays, and with the advent of transgenic species, provide mechanistic data comparable to rodent transgenic models. Non-mammalian animal models provide a powerful new tool for risk assessment. However, more information is needed on how to compare inter-species data, particularly two species as vastly different as fish and human (Hobbie et al., 2009). Demonstration of common, *or equivalent*, molecular and biochemical responses to chemical exposure may be the means to facilitate species-species comparisons, reduce default assumptions used in the assessment of risk, and strengthen non-mammalian models of human disease (Himmelstein et al., 1994; Hinton et al., 2005).

A number of toxicokinetic factors modulate the final dose of a carcinogen achieved at the target site *in vivo*, therefore it can be misleading when tumor incidence data are expressed in terms of the chemical's exposure concentration (Bailey et al., 1998). Molecular dosimetry is the measurement of genetic endpoints, such as DNA adducts and/or mutations, as the *effective* dose for a target tissue. The effective, or *molecular,* dose compensates for individual and species-specific differences in toxicokinetic parameters, as well as the effects of these parameters have on the linearity of the dose-response curve. In addition, DNA

adducts and mutations reflect the mechanism or mod*e* of action (MOA) for a particular compound, and understanding this MOA is the basis for species-to-species comparisons. Thus, molecular dosimetry provides a mechanistic basis for high- to low-dose, route-to-route, and interspecies extrapolations, and risk assessments that correlate dosimetry data with tumor data should provide more reliable estimates of risk (Law, 1998).

Concerning species-to-species extrapolations, the data provided in this work address the "molecular equivalent dose" concept in carcinogenic risk assessment. The "molecular equivalent dose" is the nominal dose (or concentration) at which the effective dose for a target tissue is the same for two different species exposed to the same chemical. Regardless of the chemical exposure concentration(s) or route(s), the molecular equivalent dose represents an equivalent, quantifiable biological outcome for both species. Providing a common mode of action, as well as comparable mechanisms of DNA repair and metabolism, the molecular equivalent dose (in theory) could be used to determine a dose extrapolation factor for species of different phylogenies exposed to the same chemical. This extrapolation factor could then be used to determine exposure regimens for unknown chemicals of similar classes.

In Chapter 2, to address how molecular dosimetry can be used to compare test results for a given compound between vastly different species, medaka and F344 rats were exposed to the known alkylating hepatocarcinogen, dimethylnitrosamine (DMN) (Hobbie et al., 2009). For both models, DNA adducts (O^6-MeG, N^7-MeG, 8-OHdG) and mutant frequencies (MF) were measured in liver, and early morphological changes were described using

histopathology and immunohistochemistry. Pulse dose levels in fish were 0, 10, 25, 50, or 100 ppm DMN in ambient water, and rats were exposed to 0, 0.1, 1, 5, 10, and 25 ppm DMN in their drinking water for 14 days. Adduct concentrations were determined to be similar in magnitude, whereas MFs for DMN-exposed fish were up to 20x higher than that observed for DMN-exposed rats.

For comparable nominal DMN concentrations, the adduct data *would suggest* that the biological response (DNA adducts) was equivalent for DMN-exposed medaka and rats, and that the extrapolation factor would be "one-to-one." However, the MF data for fish was remarkably higher than that of similarly exposed rats, suggesting that something *not* integrated into the molecular dose influenced the *effective* (MF) dose response in DMN-exposed medaka. DMN is a known, potent inducer of cell proliferation (Mirsalis et al., 1993; Souliotis et al., 2002) and cell proliferation is a requisite for DMN-produced methyl adducts to become fixed as mutations (Winn and Norris, 2005). In considering molecular dosimetry, La and Swenberg (1996) stated that cell proliferation is *not* factored into the molecular dose. Although we did not measure it directly in these studies, increased cell proliferation apparently occurred in DMN-exposed medaka, manifested as chronic hepatotoxicity and hepatic neoplasia, whereas no microscopic lesions were apparent in livers of DMN-exposed rats. DMN-induced hepatopathology in medaka correlates well with the significant increase in MF for DMN-treated λ transgenic medaka (Chapter 1). The adduct- and MF dosimetry data combined with the histopathology in DMN-exposed medaka and rats reflects the importance of cell proliferation in the carcinogenic dose-response. Additional sequencing of

hepatic DNA from DMN-treated λ transgenic medaka would help to further elucidate the role of cell proliferation and clonal expansion in the MF and hepatopathology response.

It would appear from the MF dosimetry data that the effects of DMN exposure are markedly different for rats and fish, and that an extrapolation coefficient derived from adduct- data would not provide an accurate estimate of DMN's mutagenic potential between these two species. Differences such as these in carcinogenic response are not specific to species of divergent phylogenies. In a butadiene dosimetry model designed by CIIT, mice had higher concentrations of mutagenic butadiene metabolites than rats, which correlated with an enhanced susceptibility of mice to the genotoxic and carcinogenic effects of butadiene (Csanády and Bond, 1991; Himmelstein et al., 1994; Recio et al., 1997). When butadiene metabolism in human tissue was compared to that of mice and rats, the response in human tissue was closer to that of rats than of mice, suggesting that extrapolations based on the assumption that humans are as sensitive as the most sensitive model would likely be inaccurate for butadiene. When investigating the molecular pathogenesis of hepatocellular carcinoma in mice, rats, and humans, Grisham (1996) stated that, although the features of hepatocarcinogenesis were similar among the three species, the cellular lesions that precede hepatocellular carcinoma differ among rodents and humans. Therefore, he concluded that tests of chemical carcinogenesis in rodents were likely to include a significant number of both false-positive and false-negative risks for humans. However, according to Rall et al. (1987), experimental evidence indicates that there are more physiological, biochemical, and metabolic similarities between laboratory animals and humans than there are differences and

that these similarities increase the probability that results observed in laboratory settings will predict similar results for humans (Maronpot et al., 2004).

To investigate the high incidence of O^6-MeG adducts in the blood of humans, Kyrtopoulos (1998) demonstrated that there was no qualitative or quantitative difference in the accumulation of O^6-MeG adducts for humans and mice exposed to methylating chemotherapeutic drugs, procarbazine and dacarbazine. Considering the O^6-MeG adduct-response for DMN-exposed mice, he surmised that an analogous similarity might exist for humans and mice exposed to environmental methylating agents like DMN, and that of methylating chemotherapeutics. *If* the accumulation of O^6-MeG in humans due to DMN exposure is analogous to that of mice, and DMN-induced O^6-MeG concentrations in mice are comparable to that of rats and medaka, but medaka have a greater mutagenic potential than rats and mice, which model is the most appropriate for carcinogenic risk in humans? The adduct- and MF dosimetry data provided here, for medaka and rats exposed to DMN, do not answer this question. This was not the purpose or within the scope of this study. The data do demonstrate, however, how such information can provide valuable insight into the shapes of dose-response relationships for different species exposed to the same chemical. Although a precise equivalent dose is difficult to determine for MFs in DMN-exposed medaka and rats, the adduct and MF dosimetry data do exemplify the heterogeneity of multistage chemical carcinogenesis and how important it is to consider both individual and species-specific biological responses to carcinogen exposure when determining risk in humans.

Correlation of tumor data with molecular dosimetry data, as well as the identification of specific biochemical alterations associated with chemically induced morphologic changes in a target organ, will both provide more reliable estimates of risk than mathematical extrapolations (Law, 1998). As previously mentioned, a correlation was noted between the incidences of DMN-induced hepatoxicity and neoplasia in medaka and the dramatic DMN-induced mutant frequencies in medaka, particularly when compared to corresponding DMN rat data. The objective of the DMN pathology study (Chapter 3) was to describe the progression of morphological changes in the livers of DMN-exposed medaka and use histochemistry (HC) and immunohistochemistry (IHC) to elucidate possible biochemical alterations associated with DMN-induced injury. Regarding the investigation of diethylnitrosamine (DEN) in medaka, Okihiro and Hinton (1999) stated that despite physiological and anatomical differences between fish and rodents, liver carcinogenesis occurs via a multistage process in both species. They put forward that, "if it can be shown that fish and rodents respond in similar fashion to the same classes of carcinogens, then the continued use of fish can be justified and perhaps even used to augment conventional rodent bioassays currently in use (Okihiro and Hinton, 1999)."

Dimethylnitrosamine (DMN) is a structural homologue to the alkylating carcinogen, DEN. Extensive work as been accomplished with DEN in medaka (Okihiro and Hinton, 1999; Boorman et al., 1997; Brown-Peterson et al., 1999; Laurén et al, 1990; Bunton, 1990, 1995). However, medaka's hepatopathology associated with exposure to DMN is less well characterized. As previously mentioned, DMN is a known animal carcinogen (Khudoley,

1984; Souliotis et al., 1995) and it is used in a rodent model of alcoholic cirrhosis in humans (George et al., 2001). The cytokine, transforming growth factor (TGF)-β1, is the predominant pro-fibrogenic stimulus in DMN-induced fibrosis in the rat and alcoholic cirrhosis in humans (Bissel et al., 2001; de Gouville et al., 2005; Friedman, 2000). TGF-β1 has both proliferative and growth-inhibitory activities and mutations involving the TGF-β1 pathway have been associated with hepatic neoplasia (Elliot et al., 2005; Rossmanith et al., 2001). TGF-β and its cell signaling proteins, Smad 2, Smad 3, and Smad 4, have been cloned from fish DNA and TGF-β's role in immune regulation and embryogenesis of fish has been established (Choi et al., 2007; Dick et al., 2000; Harms, 2000; Harms et al., 2000; Johnson et al., 2006). However, TGF-β 's involvement in DMN-induced hepatic fibrosis and neoplasia in fish is not known.

Considering that DMN's mode of action appears to be conserved in medaka (Hobbie et al., 2009; Winn and Norris, 2005) and rodents (Gollapudi et al., 1998; Souliotis et al., 1995; Souliotis et al., 2002), it was hypothesized that DMN-induced hepatic neoplasia and chronic hepatotoxicity in medaka progress along similar phenotypic/morphological pathways, and via similar TGF-β1-dependent mechanisms, as those of DMN-exposed rats. Specifically, the goals were to determine if DMN exposure has a similar extent of fibrosis, or phenotype, in the medaka as the rat, and identify possible mechanisms of DMN-induced hepatocarcinogenesis in medaka. To address these questions, a similar DMN exposure regimen as that used for the molecular dosimetry study was conducted in medaka and rats. After DMN exposure, medaka and rats were grown out for six months. Medaka were

intermittently sacrificed every two months, whereas rats were sacrificed at the end of the 6 month period. Medaka and rat tissue sections were examined via routine histopathological methods, as well as by immunohistochemistry (IHC) and histochemistry (HC). IHC and HC stains included TGF-β1 and its fibrogenic mediator, Smad3; α-smooth muscle actin (SMA) and muscle specific actin (MSA) as markers of transdifferentiated hepatic stellate cells (HSCs); cytokeratin (AE1/AE3) epithelial antibody; Factor VIII endothelial cell marker; glial fibrillary acid protein (GFAP) as an HSC marker; trichrome and Sirius red for collagen; and reticulin for basement membranes.

In DMN-exposed medaka, lesions indicative of chronic hepatotoxicity predominated, whereas the incidence of DMN-induced hepatic neoplasia was lower. Descriptively, lesions were characterized according to criteria set by a National Toxicology Program (NTP) pathology working group for degenerative, inflammatory, and proliferative nonneoplastic and neoplastic lesions associated with DEN exposure in medaka (Boorman et al., 1997). Hepatocellular carcinomas were the most prevalent DMN-induced tumors present with fewer numbers of cholangiocarcinomas, mixed biliary and hepatocellular carcinomas, and spindle cell tumors of unknown cellular origin. Histopathology revealed progressive hepatocellular necrosis, with nodular regeneration of the hepatic parenchyma, and extensive remodeling of the liver architecture. Acute lesions associated with DMN-induced hepatoxicity included degenerative changes in hepatocytes (cell swelling, cytoplasmic vacuolation, hyalinization), massive hepatocellular necrosis, multiloculated cystic degeneration of the hepatic parenchyma, and infiltration of mixed inflammatory cells. With progressive hepatotoxicity,

proliferation of biliary epithelial cells, HSCs, bile preductular epithelial cells (BPDECs), and intermediate cells was evident and accompanied by increased deposition of fibrillar collagen, hepatocellular dysplasia, and regeneration. BPDECs are the purported bi-potential liver stem cell in fish and "intermediate cells" are cells intermediate in differentiation between BPDECs and hepatocytes. BPDECs and intermediate cells were identified based on morphologic criteria described by Okihiro and Hinton (2000). Chronic hepatoxicity was associated with nodular accumulations of regenerative hepatocytes (regenerative nodules), occasionally surrounded by thin, irregular bands of collagenous connective tissue (forming cirrhotic-like nodules), and multi-lobulation of the medaka hepatic architecture. Neither neoplastic nor nonneoplastic lesions were apparent in DMN-exposed rats at 6 months post-exposure. IHC and HC staining of rat livers revealed no qualitative differences between DMN-treated rats and controls.

IHC and HC demonstrated increased staining of hepatocytes, biliary epithelial cells, BPDECs and/or intermediate cells for TGF-β1, and Smad3 to a lesser extent, in the medaka liver. Taken together, the possible association of TGF-β1 and Smad3 expression with DMN-induced hepatocellular necrosis; proliferation and migration of biliary epithelial cells, HSCs, and BPDECs; deposition of fibrillar collagenous matrix; and remodeling of the hepatic architecture; all suggest that the TGF-β1 pathway plays a similar role in the repair of hepatic injury for medaka as it does in mammals. BPDECs and intermediate cells present within neoplastic foci also demonstrated increased staining with TGF-β1, suggesting a possible stem cell origin for these neoplasms. Increased neoplastic cell TGF-β1 expression was

occasionally associated with decreased staining with Smad 3, implying a possible disruption of TGF-β1's growth inhibitory effects. Cytokeratin staining aided in the identification of BPDECs and intermediate cells, and the proliferation of these cells in response to hepatic injury supports their role in re-epithelialization of the denuded hepatic parenchyma. HSCs also stained for cytokeratin, and their apparent alignment around damaged hepatocytes indicates a possible structural role in maintaining the hepatic architecture. Although less evident, HSCs also stained with MSA, suggesting myofibroblast-like properties and implying epithelial-to-mesenchymal transdifferentiation. TGF-β1 staining coupled with transdifferentiated HSCs and increased collagen deposition supports a pro-fibrogenic role for this cytokine in medaka liver. Increased reticulin staining of basement membranes highlighted re-structuring of the hepatic architecture through hepatocellular regeneration as well as sprouting of new, small biliary and vascular branches.

Many of the morphologic changes described herein for DMN-induced toxicity in the medaka liver are similar to those described for rats treated with DMN, and positive correlation of these lesions with TGF-β1 suggests a similar dependence in medaka to that known for DMN-exposed rats (de Gouville et al., 2005). However, despite the similarities between DMN-induced hepatotoxicity in rats and medaka, specific differences are apparent in medaka that might limit the use of this model as a surrogate for the DMN rat model for human alcoholic cirrhosis. According to George et al. (2001), DMN-induced liver injury in rats is a valuable animal model for studying human hepatic cirrhosis, because the observable histopathological changes and biochemical abnormalities of this animal model correlate well

with the alterations observed in human alcoholic cirrhosis. Tissue pathological changes of DMN-induced rat liver fibrosis include centrilobular necrosis and hemorrhage, parenchymal collapse, regeneration, fibrillar septae formation and bridging fibrosis leading to marked lobular disarray and well-circumscribed cirrhotic nodules (George et al., 2001, 2004; He et al., 2007).

Although necrosis, collapse, collagen deposition, nodular regeneration, and re-modeling of the hepatic architecture occurred in medaka, the specific pattern of lesions frequently observed in human alcoholic cirrhosis and DMN-exposed rats (centrilobular necrosis and fibrosis bridging portal tracts and central veins) is absent (George et al., 2001). The mammalian liver is formed by numerous lobules that consist of several portal tracts around a central vein. Hepatocytes directly adjacent to the central vein have a higher concentration of P450s and are less oxygenated than their periportal counterparts, contributing to the overall pattern of lesions seen in mammalian cirrhosis (Schlenk and Benson, 2001). This concept of metabolic zonation is absent in the medaka liver. In comparison to mammals, the medaka liver is in the form of a single lobe (Hinton et al., 2008). Recent 3-dimensional reconstruction of the medaka liver has revealed it to be akin to a single mammalian lobule (Hardman et al., 2007). Despite this similarity, the distribution of biotransforming enzymes is more heterogeneous in the medaka liver, leading to a seemingly more random distribution of lesions (Wolf and Wolfe, 2005).

Another major difference apparent between medaka and rat models is the fibrotic response to DMN-induced hepatotoxicity. DMN-induced hepatoxicity in rats is

accompanied by abundant fibrosis similar to that seen in human alcoholic cirrhosis. Thick bands of fibrous connective tissue form septae that bridge between portal tracts and central veins and surround nodular accumulations of regenerative hepatocytes (George et al., 2004). Unlike mammals, in which significant damage to the liver parenchyma results in hepatic fibrosis during the reparative phase, hepatic parenchymal fibrosis as a sequel to hepatocellular necrosis is reported to be a rare occurrence in fish (Ferguson, 1989; Wolf and Wolfe, 2005). In the present study, formation of thick fibrous septae as a reparative response to hepatic necrosis was absent in DMN-exposed medaka. Instead, collagen deposition in medaka liver was apparent as a fine, fibrillar matrix along the reticular framework of the denuded hepatic parenchyma. This pattern of collagen deposition is similar to that seen [early] in mammalian hepatic fibrosis (Jin et al., 2003). Although Ferguson (1989) reports cirrhosis to be rare in fish, cirrhotic-like nodules characterized by thin strands of collagen surrounding regenerative hepatocytes were apparent in DMN-exposed fish. However, multinodular remodeling of the medaka hepatic architecture lacked the fibrous septae seen in cirrhotic mammalian livers.

Tumors described in the livers of DMN-exposed medaka were consistent with that previously reported by Peto et al. (1991) for 4080 rats chronically exposed to DMN in their drinking water, although variations in specific cell types were apparent between the two species. Peto et al. reported tumors of liver cells (hepatocytes), bile ducts, blood vessels, and Kupffer cells in DMN-exposed rats, whereas DMN-induced tumors in medaka included predominantly hepatocellular tumors, with fewer of biliary origin, mixed (hepatocellular and

biliary) origin, and spindle cell of unknown origin. This difference in tumor cell types between medaka and rats is in part due to some species-specific differences in liver cell constituents (Hinton et al., 2008). The medaka liver lacks Kupffer cells; therefore, tumors of Kupffer cell origin such as those described for DMN-exposed rats were not present in DMN-exposed medaka. Angiogenesis accompanied DMN-induced injury in medaka in our study; however, tumors of endothelial origin were absent. With regard to previous DMN carcinogenesis studies in fish, the spectrum of hepatic tumor types presented here is consistent with those previously reported by Khudoley (1984) for zebrafish and guppies exposed to DMN, as well as medaka exposed to DMN's homologue, DEN (Okihiro and Hinton, 1999).

Overall, results for the pathology study demonstrate that medaka respond in a similar fashion to DMN-exposure as that previously reported for DMN-exposed rats. For medaka and rats, DMN-induced hepatic neoplasia consists predominantly of malignant hepatocellular neoplasms, and response to DMN-induced hepatocellular necrosis includes repair of the denuded hepatic parenchyma through collagen deposition and hepatocyte regeneration. In addition, suggestion of increased TGF-β1 expression associated with DMN-induced hepatoxicity implies a similar TGF-β1 dependence for medaka as that reported for DMN-exposed rats (de Gouville et al., 2005). However, species-specific physiological and anatomical differences affected slight variations in the DMN-induced responses of medaka and rats, evident as an absence of some tumor cell types and the extent of fibrosis in DMN-exposed medaka. Despite these differences, medaka remain a good model for DMN-induced

hepatocarcinogenesis, and DMN-induced hepatoxicity in medaka may prove useful for studying the underlying molecular mechanisms of such lesions, as well as provide a means to investigate potential treatments for hepatic fibrosis and/or cancer. Further investigations of the role TGF-β1 plays in the progression of DMN-induced hepatic neoplasia and toxicity via RT-PCR and western blot should strengthen the DMN medaka model.

In Chapter 4, we asked the question, "Is the drinking water disinfection by-product, dibromonitromethane (DBNM), mutagenic in the medaka fish model?" In 1974, the U.S. Congress passed the Safe Water Drinking Act (SWDA) to protect public health through regulation of the nation's public water supply (EPA, 1999). With this act, the Environmental Protection Agency (EPA) set national standards for drinking water based on sound science and oversees all of the states, localities, and water suppliers who implement these standards. Disinfection of drinking water was a major public health improvement of the 20th century that significantly reduced the transmission of deadly waterborne diseases (Plewa et al., 2004). Drinking water disinfection byproducts (DBPs) are an unintended consequence of chemical disinfection that occur due to the reaction of chlorine, chloramine, and/or ozone with naturally occurring humic acids and dissolved organic matter in ground water (Plewa et al., 2004). Epidemiological studies have suggested an association between cancer in humans and the consumption of chlorination byproducts in drinking water (Kundu et al., 2004). The EPA prioritized approximately 600 DBPs for future health studies according to predicted adverse health effects, of which the halonitromethanes (HNMs), bromo-, dibromo-, and

tribromonitromethane, received the highest ranking (Plewa et al., 2004; Richardson, 2002). *In vitro* mutagenicity studies with the *Salmonella* plate-incorporation (Ames) assay demonstrated HNMs as a class to be weak mutagens (Kundu et al., 2004). Dibromonitromethane (DBNM) and bromochloronitromethane (BCNM) were the most mutagenic HNMs. Studies to determine the chronic cytotoxicity and genotoxicity of HNMs with Chinese Hamster Ovary (CHO) cells and single cell gel electrophoresis (Comet assay) revealed DBNM to be one of the most potent cytotoxins and genotoxins (Plewa et al., 2000, 2004). These *in vitro* studies would suggest that exposure to DBNM poses a threat to public health. However, the effects of DBNM *in vivo* would provide a better estimate of cancer risk because the results would account for variables such as individual uptake, distribution, bioactivation and/or detoxification of the compound.

Preliminary DNA adduct data obtained from DBNM-exposed rats via ^{32}P-postlabeling procedures indicated that DBNM interacted directly with hepatic DNA *in vivo* to form DBNM guanine and adenine adducts (DeAngelo and King, unpublished data). This direct acting mechanism of action for DBNM was confirmed by interaction of DBNM with calf thymus DNA, as well as adenine- and guanine-monophosphates, *in vitro*. Based on the adduct results for rats exposed to DBNM in their drinking water, it was hypothesized that (1) DBNM would adduct directly with medaka hepatic DNA, and (2) DBNM would be mutagenic in the livers of *λcII* transgenic medaka and Big Blue® rats exposed to DBNM via their ambient water and drinking water, respectively. If DBNM proved to be mutagenic *in vivo* as it was *in vitro*, using the Ames assay, then a molecular equivalent dose would be

determined from adduct and MF dose-response curves for rats and medaka exposed to DBNM.

Lambda cII transgenic medaka were exposed to 0, 10, 100, or 500 ppb DBNM, or to 50 ppb benzo[a]pyrene (B[a]P, positive control) for 96 hours. Medaka used for adduct isolation were euthanized and livers removed at 96 hours, whereas fish used for the cII assay and histopathology were grown out in clean water for 30 days and then euthanized. As with DBNM-exposed rats, butanol extraction and ^{32}P-postlabeling were used to isolate DBNM adducts from medaka liver. Due to the amount of DNA required to isolate DNA adducts (~50 μg of DNA from ~200 mg of liver tissue), medaka livers were pooled (on average, 1 medaka liver weighs about 10 mg). Despite successful DNA extraction, no adducts (DBNM or B[a]P) were isolated from medaka DNA. Isolation of B[a]P adducts, in the absence of DBNM adducts, would have suggested that (1) DBNM does not adduct with medaka hepatic DNA, or (2) DBNM did not make it to the medaka liver. However, because no adducts were isolated from medaka hepatic DNA, it was concluded that the integrity of the DNA had likely been compromised during the ^{32}P-postlabeling procedure. Results for λ transgenic medaka exposed to DBNM demonstrated that MFs for 0, 10, 100, or 500 ppb DMN were no different statistically from the background MF calculated for control medaka. MFs for medaka exposed to 50 ppb B[a]P as a positive control were consistent with MFs previously described by Winn and Norris (2005).

Contrary to the *in vitro* mutagenicity results obtained for DBNM with the *Salmonella* plate-incorporation assay, DBNM was not mutagenic in the livers of λ transgenic medaka.

Although this evidence suggests that DBNM is not mutagenic *in vivo*, mutant induction in tissues of initial contact (i.e. gills and skin) could not be ruled out. Successful isolation of DBNM adducts from medaka DNA would have helped elucidate if the lack of mutation induction in medaka hepatic DNA was due to DNA repair of DBNM adducted DNA or due to poor distribution of DBNM to the target tissue. Isolation of DBNM adducts from livers of rats would suggest that liver is a target organ for DBNM; however, this result may represent a species-specific response to DBNM exposure for rats. Due to the lack of mutant induction in λ transgenic medaka, DBNM was not used for the determination of a molecular equivalent dose. Disagreement in the mutagenic potential *in vitro* versus *in vivo,* such as reported here for DBNM with the Ames assay and λ *cII* mutagenesis assay, was also reported by Geter et al. (2004) for λ transgenic medaka exposed to MX [3-chloro-4-(dichloromethyl)-5-hydroxy-2[5*H*]-furanone]. Mutagenicity assays with Salmonella demonstrated MX to be a potent mutagen, whereas MX failed to induce mutations in livers of λ transgenic medaka exposed to MX. The data for both MX and DBNM stress the point of considering the effects of the chemical *in vivo* when determining potential carcinogenic risk in humans. However, the fact that DBNM was only weakly mutagenic in *Salmonella* should be considered when interpreting the *in vivo* mutagenicity results for DBNM in medaka. It is possible that the weak mutagenic potential of DBNM was not sufficient to overcome such factors as DNA repair in medaka and cause mutagenesis *in vivo*.

According to Law et al. (1998), "studies at different phyletic levels than rodents and humans can enhance our understanding not only of the basic mechanisms of carcinogenesis, but also of the hazards of environmental toxicants in recipient species." Fish models are useful in monitoring and assessing risks of exposure to chemicals in aquatic environments. Regarding the assessment of toxicity associated with exposures to complex chemical mixtures or in low dose chronic exposure regimens, they are recognized as test organisms with distinct and superior benefits in providing insights to disease processes (Powers, 1989; Winn, 2001). Fish models are cost-effective alternatives to more traditional animal models in genetics, developmental biology, and toxicology, and the advent of transgenic models can improve the assessment of realistic risks related to exposure to waterborne contaminants and address mechanistic questions for a variety of disease processes including carcinogenicity (Kissling, et al., 2006; Winn, 2001). However, Law (2001) states "a gap exists between the mechanistic information available for the more traditional rodent models for carcinogenicity testing and those for small fish models." More mechanistic data is needed for fish, if work with alternative animal models is to continue (Law, 2001).

The purpose of the present research was to strengthen the use of the medaka model in comparative risk assessment through (1) demonstration of a "molecular equivalent dose" for medaka and rats exposed to the known carcinogen, DMN; (2) demonstration of common morphologic and biochemical alterations for medaka and rats exposed to DMN; and (3) demonstrate the usefulness of the λ transgenic fish in evaluating the mutagenicity of an unknown chemical (DBNM). Although more head-to-head comparisons between rodent and

fish models will need to be performed before we can feel comfortable in expressing a precise molecular equivalent dose for small alkylating carcinogens, the data generated here did successfully demonstrate the usefulness of mechanistic data, such as DNA adducts and mutations, in interpreting individual dose-responses and conducting species-to-species dose comparisons. Despite inherent differences in physiology and anatomy, DMN-induced hepatopathology in medaka and rats showed remarkable similarities, and immunohistochemistry for TGF-β1 suggests that similar biochemical alterations contribute to lesion formation in both species. Lastly, use of the λ transgenic medaka demonstrated that DBNM was not mutagenic *in vivo*, despite *in vitro* evidence to the contrary.

Future work that may strengthen the medaka fish model for carcinogenicity testing and mechanistic research using small alkylating agents like DMN should include:

(1) DNA sequencing of the *cII* gene from DMN-treated λ transgenic medaka to further characterize the mutation spectra and determine if the mutant frequency was affected by clonal expansion.

(2) Use of proliferating cell nuclear antigen (PCNA) or bromodeoxyuridine (BrdU) to determine if cell proliferation contributed to the marked differences in DMN-induced MF for medaka versus rats.

(3) Measurement of levels of alkylguanine-alkyl transferase (AGT) to determine the contribution of DNA-repair to the DMN-induced MFs in medaka.

(4) Electron microscopy to characterize at the ultrastructural level the fibrotic response in DMN-exposed medaka.

(5) RT-PCR and Western blots for TGF β1 to determine the relative expression of this cytokine in medaka liver secondary to DMN exposure and to better characterize its role in DMN-induced hepatotoxicity in the medaka model.

(6) Regarding DBNM exposures in medaka, use of a different adduct detection method to confirm the presence or absence of DBNM adducts in medaka liver may produce different results. In addition, since DBNM is probably direct acting, determination of the MF in tissues of initial contact such as gill and skin would strengthen the data currently presented and provide more information about the potential risk of DBNM exposure to human health.

Despite the many positive contributions of the medaka model to cancer research, some concerns exist as to the usefulness of the model as a screen for compounds with target tissues other than liver (Kissling et al., 2006). The data presented here does not suggest the medaka model is a replacement for rodent models in carcinogenicity testing. With regard to the use of trout in carcinogenicity testing, Bailey et al. (1996) states, "there should be no expectation that [trout] will supplant traditional rodent models in carcinogen bioassays or human cancer research." Rather, with further research, small fish models may prove useful for presumptive (stage one or tier one) carcinogen testing or as augments to current rodent models of human disease (Law, 2001). Regardless, much insight into human health and safety can be gained

through research involving various aquatic species (Hinton et al., 2009). However, as with translation of research results from any animal model system to humans, careful analysis of similarities and differences from molecular to organismal levels must be conducted before proposing the use of a particular model system (Hinton et al., 2009).

In conclusion, interspecies dose extrapolation factors (such as that determined for DMN-exposed medaka and F344 rats) have important implications for risk assessment in that they will 1) help regulatory agencies to choose the appropriate animal model and dosing regimens for an unknown agent of similar pharmacokinetics, 2) validate the use of alternative animal models such as fish in risk assessment by equalizing the data at the molecular level, and 3) provide a means for extending the range of statistical data orders of magnitude lower than that which can normally be obtained from rodent tumor data. In addition, correlation of DMN hepatopathology data with molecular dosimetry data in the medaka strengthened the dose extrapolation factor determined for DMN-exposed medaka and F344 rats. As stated in Hobbie et al. (2009), "future work with other [carcinogenic] compounds will generate a more complete picture of comparative dose responses between different phyletic levels and will help guide risk assessors using "alternative" models."

REFERENCES

Bailey GS, Williams DE, Hendricks JD, 1996. Fish models for environmental carcinogenesis: the rainbow trout. Environmental Health Perspectives 104 (Suppl 1), 5-21.

Bailey GS, Dashwood R, Loveland PM, Pereira C, Hendricks JD, 1998. Molecular dosimetry in fish: quantitative target organ DNA adduction and hepatocarcinogenicity for four aflatoxins by two exposure routes in rainbow trout. Mutation Research 339, 233-244.

Begg CB, 2001. The search for cancer risk factors: when can we stop looking. American Journal of Public Health 91, 360-364.

Bissell DM, Roulot D, George J, 2001. Transforming growth factor β and the liver. Hepatology 34, 859-867.

Boorman GA, Botts S, Bunton TE, Fournie JW, Harshbarger JC, Hawkins WE, Hinton DE, Jokinen MP, Okihiro MS, Wolfe MJ, 1997. Diagnostic criteria for degenerative, inflammatory, proliferative nonneoplastic and neoplastic liver lesions in medaka (*Oryzias latipes*): consensus of a National Toxicology Program pathology working group. Toxicol Pathol 25, 202-210.

Brown-Peterson NJ, Krol RM, Zhu Y, Hawkins WE, 1999. N-Nitrosodiethylamine Initiation of Carcinogenesis in Japanese Medaka (*Oryzias latipes*): Hepatocellular Proliferation, Toxicity, and Neoplastic Lesions Resulting from Short Term, Low Level Exposure. Toxicological Sciences 50, 186-194.

Bunton TE, 1990. Hepatopathology of Diethylnitrosamine in the Medaka (*Oryzias latipes*) Following Short-Term Exposure. Toxicologic Pathology 18, 313-323

Bunton TE: Expression of actin and desmin in experimentally induced hepatic lesions and neoplasms from medaka (*Oryzias latipes*), 1995. Carcinogenesis 16, 1059-1063.

Choi K, Lehman DW, Harms CA, Law JM, 2007. Acute hypoxia reperfusion triggers immunocompromise in Nile tilapia. Journal of Aquatic Animal Health 19, 128-140.

Clapp R, 2000. Environment and health: 4. Cancer. Canadian Medical Association Journal. 163, 1009-1012.

Csänady GA, Bond JA, 1991. Species differences in the biotransformation of 1,3 butadiene to DNA-reactive epoxides: role in cancer risk assessment. CIIT 11, 1-8.

De Gouville A-C, Boullay V, Krysa G, Pilot J, Brusq J-M, Loriolle F, Gauthier J-M, Papworth SA, Laroze A, Gellibert F, Huet S, 2005. Inhibition of TGF- β signaling by an ALK 5 inhibitor protects rats from dimethylnitrosamine-induced liver fibrosis. British Journal of Pharmacology 145, 166-177.

Doll R and Peto R, 1981. The causes of cancer: quantitative estimates of avoidable risks of cancer in the United States today. J Natl Cancer Inst 66, 1191-1308.

Dick A, Mayr T, Hermann B, Meier A, Hammerschmidt M, 2000. Cloning and characterization of zebrafish *smad2*, *smad3* and *smad4*. Gene 246, 69-80.

Elliot EL, Blobe GC, 2005. Role of transforming growth factor beta in human cancer. Journal of Clinical Oncology 23, 2078-2093.

Environmental Protection Agency, 1999. Understanding the Safe Drinking Water Act, U.S. Environmental Protection Agency.

Ferguson HW, 1989. Systemic Pathology of Fish: A Text and Atlas of Comparative Tissue Responses in Diseases of Teleosts. Iowa State University Press, Ames, IA, 263 pp.

Friedman SL, 2000. Molecular regulation of hepatic fibrosis, an integrated cellular response to injury. The Journal of Biological Chemistry 275, 2247-2250.

George J, Roa KR, Stern R, Chandrakasan G, 2001. Dimethylnitrosamine-induced liver injury in rats: the early deposition of collagen. Toxicology 156, 129-138.

George J, Tsutsumi M, Takase S, 2004. Expression of hyaluronic acid in *N*-nitrosodimethylamine induced hepatic fibrosis in rats. The International Journal of Biochemistry & Cell Biology 36, 307-319.

Geter DR, Winn RN, Fournie JW, Norris MB, DeAngelo AB, Hawkins WE, 2004. MX [3-Chloro-4-(Dichloromethyl)-5-Hydroxy-2[5H]-Furanone], A Drinking-Water Carcinogen, Does Not Induce Mutations in the Liver of cII Transgenic Medaka (*Oryzias latipes*). Journal of Toxicology and Environmental Health, Part A 67, 373-383.

Gollapudi BB, Jackson KM, Stott WT, 1998. Hepatic lacI and cII mutation in transgenic (λ LIZ) rats treated with dimethylnitrosamine. Mutat. Res. 419, 131-135.

Grisham JW, 1996: Interspecies comparison of liver carcinogenesis: implications for cancer risk assessment. Carcinogenesis 18, 59-81.

Hardman RC, Volz DC, Kullman SW, Hinton DE, 2007. An in vivo look at vertebrate liver architecture: three-dimensional reconstructions from medaka (*Oryzias latipes*). The Anatomical Record 290, 770-782.

Harms CA, Kennedy-Stoskopf S, Horne WA, Fuller FJ, Tompkins WAF, 2000. Cloning and sequencing hybrid striped bass (*Morone saxatilis x M. chrysops*) transforming growth factor-β (TGF- β), and development of a reverse transcription quantitative competitive polymerase chain reaction (RT-qcPCR) assay to measure TGF- β mRNA of teleost fish. Fish & Shellfish Immunology 10, 61-85.

Harms CA, Ottinger CA, Kennedy-Stoskopf S, 2000. Correlation of Transforming Growth Factor- β Messenger RNA (TGF- β mRNA) Expression with Cellular Immunoassays in Triamcinolone-Treated Captive Hybrid Striped Bass. Journal of Aquatic Animal Health 12, 9-17.

Harvard University (no authors listed), 1996. Harvard report on cancer prevention. Volume 1: Causes of human cancer. Cancer Causes and Control 7 (Suppl) 53-59.

He J-Y, Ge W-H, Chen Y, 2007. Iron deposition and fat accumulation in dimethylnitrosamine-induced liver fibrosis in rat. World J Gastroenterol 13, 2061-2065.

Himmelstein MW, Asgharian B, Turner MJ, Medinsky MA, Bond JA, 1994. Interspecies Differences in 1,3-Butadiene Metabolism. Challenging Default Assumptions Used to Estimate Human Cancer Risks. CIIT 14, 1-8.

Hinton DE, Hardman RC, Kullman SW, Law JM, Schmale MC, Walter RB, Winn RN, Yoder JA, 2009. Aquatic animal models of human disease: Selected papers and recommendations from the 4th conference. Comparative Biochemistry and Physiology, Part C 149, 121-128.

Hinton DE, Kullman SW, Hardman RC, Volz DC, Chen P-J, Carney M, Bencic DC, 2005. Resolving mechanisms of toxicity while pursuing ecotoxicological relevance? Marine Pollution Bulletin 51, 635-648.

Hinton DE, Segner H, and Braunbeck T: Toxic responses of the liver. In: Target Organ Toxicity in Marine and Freshwater Teleosts, ed. Schlenk D and Benson WH, 1st ed., pp. 224-261. Taylor & Francis, New York, NY, 2001.

Hinton DE, Segner H, Au DWT, Kullman SW, Hardman RC: Liver Toxicity. In: Toxicology of Fishes, ed. Giulio RT and Hinton DE, 1st ed., 328-368. Taylor & Francis, Boca Raton, FL, 2008.

Hobbie KR, DeAngelo AB, King LC, Winn RN, Law JM, 2009. Toward a molecular equivalent dose: use of the medaka model in comparative risk assessment. Comparative Biochemistry and Physiology, Part C 149, 141-151.

Jin Y-L, Enzan H, Kuroda N, Hayashi Y, Nakayama H, Zhang Y-H, Toi M, Miyazaki E, Hiroi M, Guo L-M, Saibara T, 2003. Tissue remodeling following submassive hemorrhagic necrosis in rat livers induced by an intraperitoneal injection of dimethylnitrosamine. Virchows Arch 442, 39-47.

Johnson AK, Harms CA, Levine JF, Law JM, 2006. A quantitative real-time RT-PCR assay to measure TGF-β mRNA and its correlation with hematologic, plasma chemistry and organo-somatic indices responses in triamcinolone-treated Atlantic menhaden, Brevoortia tyrannus. Developmental and Comparative Immunology 30, 473-484.

Khudoley, VV, 1984. Use of Small Fish Species in Carcinogenicity Testing, National Cancer Institute Monograph 65, NIH Publication No 84-2653. National Cancer Institute, Bethesda, MD.

Kissling GE, Bernheim NJ, Hawkins WE, Wolfe MJ, Jokinen MP, Smith CS, Herbert RA, Boorman GA, 2006. The Utility of the Guppy (*Poecilia reticulata*) and Medaka (*Oryzias latipes*) in Evaluation of Chemicals for Carcinogenicity. Toxicological Sciences 92, 143-156.

Kundu B, Richardson SD, Swartz PD, Matthews PP, Richard AM, DeMarini DM, 2004. Mutagenicity in Salmonella of halonitromethanes: a recently recognized class of disinfection by-products in drinking water. Mutation Research 562, 39-65.

Kyrtopoulos SA, 1998. DNA Adducts in Humans After Exposure to Methylating Agents. Mutat. Res. 405, 135-143.

La DK and Swenberg JA, 1996. DNA adducts: biological markers of exposure and potential applications to risk assessment. Mutat. Res. 365, 129-146.

Laurén DJ, The SJ, Hinton DE, 1990. Cytotoxicity phase of diethylnitrosamine-induced hepatic neoplasia in medaka. Cancer Research 50, 5504-5514.

Law JM, Bull M, Nakamura J, Swenberg JA, 1998. Molecular dosimetry of DNA adducts in the medaka small fish model. Carcinogenesis 19, 515-518.

Law JM, 2001. Mechanistic considerations in small fish carcinogenicity testing. ILAR Journal 42, 274-284.

Maronpot RR, Flake G, and Huff J, 2004: Relevance of Animal Carcinogenesis Findings to Human Cancer Predictions and Prevention. Toxicologic Pathology 32, 40-48.

Mirsalis JC, Provost GS, Matthews CD, Hamner RT, Schindler JE, O'Loughlin KG, MacGregor JT, Short JM, 1993. Induction of hepatic mutations in lacI transgenic mice. Mutagenesis 8, 265-271.

Okihiro MS, Hinton DE, 1999. Progression of hepatic neoplasia in medaka (*Oryzias latipes*) exposed to diethylnitrosamine. Carcinogenesis 20, 933-940.

Okihiro MS, Hinton DE, 2000. Partial hepatectomy and bile duct ligation in rainbow trout (Oncorhynchus mykiss): Histologic, immunohistochemical and enzyme histochemical characterization of hepatic regeneration and biliary hyperplasia. Toxicologic Pathology 28, 342-356.

Peto R, Gray R, Brantom P, Grasso P, 1991a. Effects on 4080 rats of chronic ingestion of *N*-nitrosodiethylamine or *N*-nitrosodimethylamine: a detailed dose-response study. Cancer Res. 51, 6415-6451.

Peto R, Gray R, Brantom P, Grasso P, 1991b. Dose and time relationships for tumor induction in the liver and esophagus of 4080 inbred rats by chronic ingestion of *N*-nitrosodiethylamine or *N*-nitrosodimethylamine. Cancer Res. 51, 6452-6459.

Plewa MJ, Wagner ED, Jazwierska P, 2004. Halonitromethane Drinking Water Disinfection Byproducts: Chemical Characterization and Mammalian Cell Cytotoxicity and Genotoxicity. Environ. Sci. Technol. 38, 62-68.

Powers DA, 1989. Fish as model systems. Science 246, 352-358.

Preston RJ, 2002. Quantitation of molecular endpoints for the dose-response component of cancer risk assessment. Toxicol. Pathol. 30, 112-116.

Rall DP, Hogan MD, Huff JE, Schwetz BA, Tennant RW, 1987. Alternatives to using human experience in assessing health risks. Annu Rev Public Health 8, 355-385.

Recio L, Steen A-M, Bond JA, 1997. Linking Dosimetry of Butadiene with Mutational Spectra to Assess the Roles of Epoxybutene and Diepoxybutane in the Genotoxicity of Butadiene. CIIT 17, 1-9.

Richardson SD, Simmons JE, Rice G, 2002. Disinfection Byproducts: The next generation. Environmental Science and Technology 36, 198A-205A.

Rossmanith W, Schulte-Hermann R, 2001. Biology of transforming growth factor β in hepatocarcinogenesis. Microscopy Research and Technique 52, 430-436.

Souliotis VL, Chhabra S, Anderson LM, Kyrtopoulos SA, 1995. Dosimetry of O^6-methylguanine in rat DNA after low-dose, chronic exposure to N-nitrosodimethylamine (NDMA). Implications for the mechanism of NDMA hepatocarcinogenesis. Carcinogenesis 16, 2381-2387.

Souliotis VL, Henneman JR, Reed CD, Chhabra S, Diwan BA, Anderson LM, Kyrtopoulos SA, 2002. DNA adducts and liver DNA replication in rats during chronic exposure to N-nitrosodimethylamine (NDMA) and their relationships to the dose-dependence of NDMA hepatocarcinogenesis. Mutat. Res. 500, 75-87.

Weisburger JH and Williams GM, 1981. Carcinogen Testing: Current Problems and New Approaches. Science 214, 401-407.

Winn RN, 2001. Transgenic fish as models in environmental toxicology. ILAR Journal 42, 322-329.

Winn RN, Norris MB, 2005: Techniques in Aquatic Toxicology (Volume 2). Boca Raton, FL: Taylor and Francis.

Winn RN, Norris MB, Brayer KJ, Torres C, Muller SL, 2000. Detection of mutations in transgenic fish carrying a bacteriophage λcII transgene target. Proc. Natl. Acad. Sci. USA 97, 12655-12660.

Wolf JC and Wolfe MJ, 2005. A brief overview of nonneoplastic hepatic toxicity in fish. Toxicologic Pathology 33: 75-85.